



## Copyright Undertaking

This thesis is protected by copyright, with all rights reserved.

**By reading and using the thesis, the reader understands and agrees to the following terms:**

1. The reader will abide by the rules and legal ordinances governing copyright regarding the use of the thesis.
2. The reader will use the thesis for the purpose of research or private study only and not for distribution or further reproduction or any other purpose.
3. The reader agrees to indemnify and hold the University harmless from and against any loss, damage, cost, liability or expenses arising from copyright infringement or unauthorized usage.

### IMPORTANT

If you have reasons to believe that any materials in this thesis are deemed not suitable to be distributed in this form, or a copyright owner having difficulty with the material being included in our database, please contact [lbsys@polyu.edu.hk](mailto:lbsys@polyu.edu.hk) providing details. The Library will look into your claim and consider taking remedial action upon receipt of the written requests.

EFFICACY AND MECHANISTIC STUDY OF POSTURE  
CORRECTION GIRDLE ON ADOLESCENTS WITH  
EARLY SCOLIOSIS

LIU PAK YIU

PhD

The Hong Kong Polytechnic University

2025

The Hong Kong Polytechnic University  
School of Fashion and Textiles

Efficacy and Mechanistic Study of Posture Correction Girdle  
on Adolescents with Early Scoliosis

Liu Pak Yiu

A thesis submitted in partial fulfilment of the requirements for the  
degree of Doctor of Philosophy

July 2024

## **CERTIFICATE OF ORIGINALITY**

I hereby declare that this thesis is my own work and that, to the best of my knowledge and belief, it reproduces no material previously published or written, nor material that has been accepted for the award of any other degree or diploma, except where due acknowledgement has been made in the text.

\_\_\_\_\_ (Signed)

LIU PAK YIU (Name of student)

## ABSTRACT

In Hong Kong, 2-3% of all adolescents suffer from adolescent idiopathic scoliosis (AIS), one of the most common conditions related to their growth spurt (Student Health Service - Department of Health 2022; Chan, 2019; Lam, 2010). Cases of scoliosis with a lateral curvature larger than or equal to a Cobb angle of  $10^\circ$  are typically considered as a medical issue (Hresko, 2013). The likelihood of spinal progression in girls is 3.6 times higher than in boys (Kubat & Ovadia, 2020; Weinstein, 1994). Patients with a spinal curvature larger than  $25^\circ$  are recommended to undergo therapy with a hard brace, while surgery may be required if the curvature progresses to  $40-50^\circ$  (Spoonamore, 2024, Hresko, 2013). However, the usual course of action for those whose spinal curvature is less than  $25^\circ$  is typically only observation with periodic examinations (Yip et al., 2016). To address the issues of the lack of appropriate orthosis products for early scoliosis treatment and the problems with existing orthosis products for scoliosis treatment in the market, Liu et al. (2015) developed a posture correction girdle (PCG) for adolescents with early scoliosis (i.e. Cobb angle  $10-20^\circ$ ) with the aim to reduce posture imbalance and, consequently, the likelihood that the spinal curvature will continue to advance. Patients with AIS are more likely to experience scoliosis progression due to changes in posture and asymmetry (Kouwenhoven and Castelein, 2008; Fortin et al., 2012). They may also experience painful symptoms that worsen as a result of poor posture and insufficient control over their postural stability, according to Wong and Wong (2008) and Chen et al. (1998). In view of this, using a posture training device could be a feasible and suitable way to help AIS patients (Wong and Wong, 2008; Lenssinck et al., 2005). This is also the reason behind the development of the PCG in Liu et al. (2015).

According to the initial findings, the PCG may be able to control the progression of spinal curvature and contribute to reducing posture imbalance in the frontal, horizontal, and sagittal planes (Liu et al., 2015; Yip et al., 2016). Yet, the PCG is custom-made, so that there is a long production lead time. Limitations are also found with the girdle design which affects the exertion of corrective forces and wear comfort. In order to optimise the exertion and effectiveness of the corrective forces, as well as enhance wear comfort, this study modifies the PCG by refining the design features and replacing materials with those that have better properties. This study also develops a sizing system for the modified posture correction girdle (mPCG) so that the girdle can be mass produced and customised, and thus reduce production cost and wait time of patients. Furthermore, this study examines the corrective mechanism and

performance of the mPCG through finite element (FE) modelling, as well as facilitate and streamline the girdle prescription and fitting processes by building an intelligent prescription system. It is then anticipated that the mPCG can be considered as a personalised orthosis treatment to help adolescents with early scoliosis or posture issues. Therefore, enhancement of the effectiveness of treatment, reduced treatment costs, and promotion of the use of the mPCG could be realised.

A school screening programme has been carried out to understand the prevalence of AIS in Hong Kong and approach potential subjects for the wear trial in this study. Of the 1747 participants, 487 (27.88%) are suspected to have scoliosis and 247 of the 487 accepted the offer for a radiographic examination. That is, 6.07%, 5.6% and 2.46% of the school-screened participants are diagnosed with a spinal curvature less than 10°, between 10°-20° and more than 20° respectively. After modifications are made to the girdle and the sizing system is developed, 10 subjects are recruited for the 9-month wear trial but 2 withdrew in the early stages of the study. Scientific experiments are conducted at the beginning of the wear trial (0 M), and after three (3 M), six (6 M) and nine (9 M) months. The test results including changes in spinal curvature (radiographic examination and comparison of Cobb angle), improvements in posture balance (3D body scanning and posture angle), and the effects on proprioception deficit (Vicon Nexus 3D motion capture system) are analysed to evaluate the efficacy of the girdle. It is found that the girdling treatment shows a good performance for posture correction except correcting the alignment in the horizontal plane, while improvements in proprioception deficits are not apparent. In regard to controlling the spinal curvature, 6 of the subjects show a significant and immediate reduction (which ranges from a reduction of 5° to 11°) after donning the girdle for 2 hours. On the other hand, 4 of the 8 subjects show an apparent reduction for the long-term after completion of the 9-month intervention even when the girdle is doffed (curve reduction ranges from 5.2° to 8°). The ability of the mPCG to control the progression of the spinal curvature is more apparent for those with an S curve.

Aside from the experiments mentioned above, the compliance rate with the girdling treatment and the questionnaire results related to quality-of-life evaluation during the wear trial are also discussed. It is found that the average compliance rate with the mPCG is 95%, which is 1.75% higher than that with the original PCG in Liu (2015). The increase in compliance might be due to the modified girdle design and use of other fabric materials, which improve the girdle both aesthetically and functionally (i.e. wear comfort, convenience, effectiveness of corrective

mechanism). Besides, it is found that the subjects who show an apparent reduction in their spinal curvature after the 9-month wear trial tend to comply more with the treatment. The data collected by the temperature logger also indicate that the level of thermal comfort of the girdling treatment is acceptable, and none of the subjects reported any issues during the intervention period. In regard to the quality-of-life questionnaire results, the subjects indicate concerns with their “self-perceived image” and “stress level”, but the level of satisfaction with the girdling treatment in this study is comparable or excels that of other studies (Wong, 2021; Weiss et al., 2007). The results show that the subjects might need more time to become accustomed to the girdling treatment. Since the mPCG is not yet commercially available, the general public might be curious about this device, which might cause the subjects in this study to feel uncomfortable.

On the other hand, an FE model is developed in this study for simulating and predicting the corrective effects of the mPCG. The pressure distribution on the skeletal model and the displacement of each vertebral body can be calculated by simulating the use of the mPCG. Modifications made to the wear parameters make it possible to improve the efficacy of the mPCG in terms of the spinal adjustment and optimise the pressure distribution on the skeletal model. The corrective mechanism of the mPCG is examined by using the developed FE model.

Finally, an intelligent system that consists of a decision tree and a trained neural network (NN) is developed to identify target patients who are suitable for the girdling treatment with the mPCG, as well as choosing the appropriate wear parameters (e.g. placement of padding to produce the points of pressure) for patients according to their needs and spinal conditions without the need to undergo a trial-and-error process. The rate of accuracy of the final model of the decision tree is 100%., which means that the model is highly reliable. The trained NN is also highly accurate in predicting the curvatures, with Curve 1 at 96.36%, Curve 2 at 96.97%, and Curve 3 at 93.94%

## LIST OF PUBLICATIONS

### Journal paper

**Liu, P.Y.**, Zhang, J., Wan, K. W., Yu, H. T., Lau, K. L., Cheung, M. C., Chen, B., Yip, J. (2024). Evaluating the Impact of Soft Bracing and Textile Engineering in Enhancing Postural Control and Proprioception in Adolescent Idiopathic Scoliosis. *Journal of Industrial Textiles*. [Under review]

### Book chapter

**Liu, P.Y.**, Cheung, H.Y. & Yip, J. (2023). Chapter 10 – Current state of using soft braces. Cheung, J.P.Y., Sakai, D.& Shetty, A.P. (ed.) *Insights and Innovations from AO Spine Asia Pacific*. Thieme: pp. 123-140 [ISBN: 9789395390620]

### Conference paper

**Liu, P. Y.**, Yip, J., Chen, B., He, L., Cheung, J., Yick, K., Ng, S. (2022). Immediate Effects of Posture Correction Girdle on Adolescents with Early Scoliosis. In: Jay Kalra and Nancy Lightner (eds) *Healthcare and Medical Devices*. AHFE (2022) International Conference. AHFE Open Access, vol 51. AHFE International, USA. <http://doi.org/10.54941/ahfe1002104> [The paper was selected as Best Student Paper Award at the AHFE conference 2022 (Date: 24-28 July 2022)]

### Patent

Active Biotechnology (Hong Kong) Company Ltd., Yip, Y. W. J. **Liu, P. Y.** (2023). *Chinese Design Patent No. ZL 2023 3 0553931.4. & CN 308501086 S*. China National Intellectual Property Administration.

## ACKNOWLEDGEMENTS

First, I would like to express my deepest thanks to Prof Joanne Yip, my chief supervisor and Associate Dean of the School of Fashion and Textile, The Hong Kong Polytechnic University, for her vast knowledge and immense patience throughout my PhD study and research. Her passion for the work is inspiring, and her advice helpful to me throughout the entire research and thesis writing process.

In addition, I would like to sincerely thank my co-supervisor, Dr Brian Y. Chen, Associate Professor of Computer Science and Engineering, Lehigh University, for his valuable guidance and insightful advice.

Besides, I must express my appreciation to Dr Alice Zhang for sharing her experience with the statistical analysis in this study, helping with the interpretation of proprioception data and assisting with the wear trial experiments.

I would also like to express my special thanks to Mr Alex Mak for sharing his valuable experience with the construction of neural networks as well as to Dr Frances Wan and Ms Hallie Cheung for supporting the wear trial experiments.

Furthermore, I would like to express my gratitude to Dr Cynthia Liang, Ms Emma Lei, Ms Ida Chan, Ms Sabrina Lui, Ms Harriet Yu, Ms Jinjin Chen, Ms Xiaolu Li, Ms Mia Ma, and Mr John Wong for their support and help with the different aspects of the research.

My appreciation is extended to my colleagues in the different laboratories, especially Ms Suki Siu and Ms Rachel Ng for their help.

Moreover, I must express my utmost gratitude to my family members and dearest friends for their love, warm encouragement and unconditional support in reaching my goals.

Last but not least, I would like to acknowledge the Laboratory for Artificial Intelligence in Design and Lee Hysan Foundation for the funding support of this research project.

# TABLE OF CONTENTS

	<b>Page</b>
<b>ABSTRACT</b>	<b>i</b>
<b>LIST OF PUBLICATIONS</b>	<b>iv</b>
<b>ACKNOWLEDGEMENTS</b>	<b>v</b>
<b>TABLE OF CONTENTS</b>	<b>vi</b>
<b>LIST OF FIGURES</b>	<b>xiv</b>
<b>LIST OF TABLES</b>	<b>xvii</b>
<b>LIST OF ABBREVIATIONS</b>	<b>xix</b>

## CHAPTER 1 - INTRODUCTION

1.1 Research background .....	1
1.2 Problem statement .....	3
1.3 Aim and research objectives .....	4
1.4 Project originality and significance .....	5
1.5 Report outline.....	6

## CHAPTER 2 - LITERATURE REVIEW

2.1 Introduction .....	7
------------------------	---

2.2 General review of scoliosis.....	7
2.2.1 Definition and types of scoliosis .....	7
2.2.2 Possible effects of scoliosis .....	9
2.2.3 Detection methods and signs of scoliosis .....	10
2.2.4 Classifications of scoliosis .....	19
2.2.5 Prevalence of Adolescents Idiopathic Scoliosis .....	25
2.2.6 Treatment options for AIS .....	26
2.3 Existing orthosis products for scoliosis .....	27
2.3.1 Hard braces .....	27
2.3.2 Semi-rigid braces .....	31
2.3.3 Flexible braces .....	32
2.3.4 Problems of existing orthosis for AIS .....	35
2.4 Overview of posture .....	38
2.4.1 Definition of posture .....	38
2.4.2 Importance of proper posture .....	39
2.4.3 Poor posture and consequences .....	40
2.4.4 Prevalence of poor posture .....	40
2.4.5 Posture correction methods .....	41
2.5 Posture Correction Girdle .....	48
2.5.1 Design and garment components of PCG .....	48
2.5.2 Corrective mechanism of PCG .....	49
2.5.3 Previous wear trial studies of PCG – effectiveness and limitations .....	51
2.5.4 Effectiveness evaluation methods for the PCG .....	54
2.6 Finite element modelling .....	58
2.6.1 Finite element modelling of bracing treatment .....	58
2.6.2 Process of building FE model .....	58

2.7 Computer-aided models .....	59
2.7.1 Application examples in garment industry .....	59
2.7.2 Application examples in spinal deformity assessment .....	61
2.8 Chapter Summary .....	62

## **CHAPTER 3 - METHODOLOGY**

3.1 Introduction .....	63
3.2 Experiment design overview .....	63
3.3 Modification to PCG .....	65
3.3.1 Identifying limits and possible modifications .....	65
3.3.1.1 Fitting and sizing .....	65
3.3.1.2 Placement and magnitude of corrective forces .....	67
3.3.1.3 Level of wear comfort and durability .....	67
3.3.1.4 Aesthetics .....	68
3.3.2 Material selection and testing .....	69
3.3.2.1 Selection criteria .....	69
3.3.2.2 Elasticity and recovery test .....	71
3.3.2.3 Repeated stretching test .....	72
3.3.2.4 Washing test (dimensional changes of fabrics after home laundering test) .....	72
3.3.2.5 Air permeability test .....	73
3.3.2.6 Water vapor / Moisture permeability test .....	74
3.3.2.7 Pilling resistance test .....	75
3.3.2.8 Hand feel .....	76
3.4 Subject recruitment .....	76
3.4.1 Inclusion and exclusion criteria .....	77
3.4.2 School-screening programme .....	77

3.5 Wear trial and effectiveness evaluation .....	79
3.5.1 Girdle fitting and prescription .....	79
3.5.2 Interface pressure measurement (Pliance®-xf 16 system) .....	80
3.5.3 Wear trial instruction and evaluation time point .....	81
3.5.4 Evaluation methods .....	81
3.5.4.1 Radiographic examination and Cobb angle comparison ...	81
3.5.4.2 Posture balance evaluation	
(3D body scanning and posture angle) .....	84
3.5.4.3 Proprioception deficits test	
(Vicon Nexus 3D motion capture system) .....	88
3.5.4.4 Questionnaires for QoL evaluation .....	92
3.5.4.4.1 SRS-22 Questionnaire .....	93
3.5.4.4.2 Brace Questionnaire .....	93
3.5.4.4.3 Bad Sobernheim Stress Questionnaire	
(BSSQ)-Brace .....	93
3.5.4.5 Compliance and thermal comfort monitoring .....	93
3.6 Chapter summary .....	94

**CHAPTER 4 – MODIFICATION OF POSTURE CORRECTION  
GIRDLE**

4.1 Introduction .....	96
4.2 Design feature refinements .....	96
4.3 Specific sizing system of mPCG .....	101
4.4 Material testing results and selection .....	103
4.4.1 Basic information of the sourced fabrics and elastic straps .....	103
4.4.2 Results of elasticity and recovery testing .....	105

4.4.3 Results of repeated stretching test .....	106
4.4.4 Results of washing test (dimensional changes of fabrics after home laundering test) .....	107
4.4.5 Results of air permeability test .....	109
4.4.6 Results of water vapor / moisture permeability test .....	111
4.4.7 Results of pilling resistance test .....	112
4.4.8 Results of hand feel test .....	113
4.4.9 Material selection .....	114
4.5 Pattern development and garment assembling .....	115
4.6 Donning of Modified Posture Correction Girdle .....	118
4.7 Chapter summary .....	118

**CHAPTER 5 – RESULTS OF GIRDLE PRESCRIPTION AND  
WEAR TRIAL**

5.1 Introduction .....	120
5.2 Subject recruitment .....	120
5.2.1 Results of the school-screening programme .....	120
5.2.2 Demographics of recruited subjects .....	121
5.3 Girdle prescription for the recruited subjects .....	122
5.4 Interface pressure measurement .....	123
5.5 Changes in spinal curvature .....	124
5.5.1 Immediate effects on spinal curvature (after 2 h) .....	126
5.5.2 Long-term effects on controlling spinal curvature (after 9 M) .....	128
5.5.3 Spinal condition after 3 months out-orthosis .....	130

5.5.4 Maintenance of the effectiveness of mPCG on controlling progression of spinal curvature .....	131
5.5.5 Discussion of effects of mPCG on controlling progression of spinal curvature .....	132
5.6 Improvements on posture balance (3D body scanning and posture angle) .....	133
5.6.1 Posture balance in frontal plane during habitual standing .....	133
5.6.2 Posture balance in horizontal plane during habitual standing .....	136
5.6.3 Posture balance in sagittal plane during habitual standing .....	140
5.6.4 Posture balance in sagittal plane during habitual sitting .....	142
5.6.5 Discussion of effects on posture correction .....	144
5.7 Effects on Proprioception deficit (Vicon Nexus 3D motion capture system) .....	145
5.7.1 Results of NRZ test .....	146
5.7.2 Results of EFY test .....	147
5.7.3 Results of the KEY test .....	149
5.7.4 Results of STP test .....	151
5.7.5 Discussion of effects on proprioception deficit .....	153
5.8 Quality-of-life evaluation .....	154
5.8.1 Results of SRS-22 questionnaire .....	154
5.8.2 Results of the BrQ .....	155
5.8.3 Results of (BSSQ)-Brace .....	156
5.9 Compliance and thermal comfort monitoring .....	157
5.10 Chapter summary .....	160

**CHAPTER 6 - FINITE ELEMENT MODELING AND  
DEVELOPMENT OF INTELLIGENT SYSTEM FOR GIRDLE  
PRESCRIPTION**

6.1 Introduction .....	162
6.2 Finite element modelling .....	162
6.2.1 Construction of finite element model .....	162
6.2.1.1 Geometric model .....	163
6.2.1.2 Material properties .....	164
6.2.1.3 Defining type of mesh element .....	165
6.2.1.4 Boundary conditions .....	166
6.2.1.5 Analysis girdle-body interactions .....	167
6.2.1.6 Effect of the mPCG .....	168
6.2.1.7 Validation .....	170
6.3 Development of the intelligent system for girdle prescription .....	172
6.3.1 Development of decision tree in this study.....	172
6.3.1.1 Using decision tree to group subjects into different treatment groups .....	172
6.3.1.2 Structure and construction of decision tree .....	173
6.3.1.3 Validation of decision tree .....	176
6.3.2 Construction of neural network .....	176
6.3.2.1 Using trained neural network for suggesting padding placement .....	176
6.3.2.2 Neural network architecture and model training process .....	176
6.3.2.3 Training result and accuracy of developed neural network model .....	181
6.4 Chapter summary .....	181

**CHAPTER 7 - CONCLUSIONS AND RECOMMENDATIONS FOR  
FUTURE WORK**

7.1 Conclusions ..... 183

7.2 Limitations and recommendations for future work ..... 188

**APPENDICES** **190**

**BIBLIOGRAPHY** **217**

## LIST OF FIGURES

		Page
Figure 2.1	Normal vs. scoliotic spine (Pittsburgh Physical Medicine, 2023) .....	8
Figure 2.2	Walter Reed Visual Assessment Scale for determining Scoliosis (McCathy, 2001) .....	11
Figure 2.3	a) Adam’s forward-bending test (Patias et al.,2010) and b) measurement of ATR by using scoliometer.(Hresko, 2013) .....	12
Figure 2.4	Moiré topography (Adair et al., 1977) .....	13
Figure 2.5	Moiré fringe images of spine: (a) without curvature, and (b) with curvature (Adair et al., 1977) .....	13
Figure 2.6	Greyscale infrared image of an AIS patient (Cooke et al., 1980) .....	14
Figure 2.7	EOS™ imaging system (EOS imaging, 2020) .....	16
Figure 2.8	Procedure of the Cobb angle measurement (Vrtovec et al., 2009; Zhang et al., 2010) .....	17
Figure 2.9	(a) Initial and (b) modified Risser system (Kotwicki, 2008) .....	18
Figure 2.10	Nash-Moe grading system for vertebral rotation (Anitha & Prabhu, 2012) .....	19
Figure 2.11	Visual of five types of scoliosis based on King classification (King et al., 1983) .....	20
Figure 2.12	Three-point pressure system of thoracic-lumbo-sacral orthosis (Seymour, 2002) .....	28
Figure 2.13	a) Proper standing and (b) sitting postures (Kwok, 2017) .....	40
Figure 2.14	Schroth’s three-dimensional exercise .....	42
Figure 2.15	Two nylon loops of Micro Straight (Wong et al., 2001) .....	44
Figure 2.16	Front, back and inside views of posture correction girdle (Liu et al.,2015) .....	49
Figure 2.17	Corrective forces exerted by elastic components of PCG (Liu et al., 2015) .....	51
Figure 2.18	Example of points of pressure created by EVA foam pads for different spinal conditions (Liu, 2015) .....	51
Figure 3.1	Research plan and flow of current study .....	63
Figure 3.2	Limitations and possible modifications of original design of PCG .....	65
Figure 3.3	Centre front zipper of the original design .....	66
Figure 3.4	Squared ends and curling of shoulder straps .....	66
Figure 3.5	Six partitions with lined pockets on original design .....	67
Figure 3.6	Figure 3.6 Pilling on tricot fabric of original design .....	68
Figure 3.7	Stitch lines on the surface of the girdle .....	69
Figure 3.8	Instron 4411 tensile strength tester .....	71
Figure 3.9	Washer and dryer .....	72
Figure 3.10	KES-F8 Air Permeability Tester .....	73
Figure 3.11	Set up of water vapor permeability test .....	74
Figure 3.12	Martindale abrasion tester .....	75
Figure 3.13	Pilling Scope .....	76
Figure 3.14	KESFB4-AUTO-A Automatic Surface Tester .....	76
Figure 3.15	Form used for the school screening programme .....	78

Figure 3.16	Measurement of ATR with scoliometer in Adam’s forward bend test .....	78
Figure 3.17	Spine length from C7 to pelvis level .....	80
Figure 3.18	Pliance®-xf 16 system (Novel, Munich, Germany) a single sensor .....	80
Figure 3.19	EOS™ imaging system (EOS imaging, 2020) .....	82
Figure 3.20	Sample of EOS™ low dosage image .....	82
Figure 3.21	Anthroscan body scanning system .....	85
Figure 3.22	Body landmarks for posture angle measurement (Liu et al., 2022) .....	86
Figure 3.23	Standing posture during 3D body scanning .....	87
Figure 3.24	Sitting posture during 3D body scanning .....	87
Figure 3.25	Posture angles measured .....	88
Figure 3.26	Placement of reflective markers for proprioception experiment ...	89
Figure 3.27	Placement of the reflective markers for the proprioception experiment .....	90
Figure 4.1	Design sketch of mPCG: (a) front and (b) back views .....	96
Figure 4.2	Design sketch of mPCG (inner view) .....	97
Figure 4.3	Design sketch of mPCG (outer view) .....	97
Figure 4.4	Three zippers at centre front of mPCG .....	98
Figure 4.5	Newly added Velcro hook tape underneath straps .....	99
Figure 4.6	Newly added markings on shoulder straps and waistband .....	100
Figure 4.7	Elimination of stitch lines on the surface of mPCG .....	101
Figure 4.8	Force applied to elastic strap samples during repeated stretching test .....	107
Figure 4.9	Dimensional changes of fabric samples after laundering .....	108
Figure 4.10	Dimensional changes of elastic strap samples after laundering ....	109
Figure 4.11	Air resistance of fabric samples .....	110
Figure 4.12	Air resistance of elastic strap samples .....	110
Figure 4.13	Water vapor transmission rate of fabric samples .....	111
Figure 4.14	Water vapor transmission rate of elastic strap samples .....	112
Figure 4.15	Pilling resistance of fabric samples .....	113
Figure 4.16	Fuzzing resistance of fabric samples .....	113
Figure 4.17	New pattern block for mPCG .....	116
Figure 4.18	Completed mPCG on subject: (a) front, (b), side, and (c) back views .....	119
Figure 5.1	Changes in spinal curvature of Subjects 1, 4, 6, 8, 9 and 10 after 2 h .....	128
Figure 5.2	Changes in spinal curvature of Subjects 7, 8, 9 and 10 after 9 M .....	130
Figure 5.3	Results of asymmetry of acromion in frontal plane during habitual standing .....	134
Figure 5.4	Results of pelvis asymmetry in frontal plane during habitual standing .....	135
Figure 5.5	Results of asymmetry of acromion/pelvis in frontal plane during habitual standing .....	136
Figure 5.6	Results of asymmetry of acromion in horizontal plane during habitual standing .....	137
Figure 5.7	Results of pelvis asymmetry in horizontal plane during habitual standing .....	137
Figure 5.8	Results of scapula asymmetry in horizontal plane during habitual standing .....	138

Figure 5.9	Results of acromion/scapula asymmetry in horizontal plane during habitual standing .....	139
Figure 5.10	Results of acromion/pelvis asymmetry in horizontal plane during habitual standing .....	140
Figure 5.11	Results of thoracic imbalance in sagittal plane during habitual standing .....	141
Figure 5.12	Results of lumbar imbalance in sagittal plane during habitual standing .....	142
Figure 5.13	Results of thoracic imbalance in sagittal plane during habitual sitting .....	143
Figure 5.14	Results of lumbar imbalance in sagittal plane during habitual sitting .....	144
Figure 5.15	Results of NRZ test (concave side) .....	146
Figure 5.16	Results of NRZ test (convex side) .....	147
Figure 5.17	Results of EFY test (dominant side) .....	148
Figure 5.18	Results of EFY test (non-dominant side) .....	149
Figure 5.19	Results of KEY test (dominant side) .....	150
Figure 5.20	Results of KEY test (non-dominant side) .....	151
Figure 5.21	Results of STP test (displacement) .....	152
Figure 5.22	Results of STP test (rotation) .....	153
Figure 5.23	Mean scores of SRS-22 questionnaire .....	155
Figure 5.24	Results (mean scores) of BrQ .....	156
Figure 5.25	Results of BSSQ-Brace .....	157
Figure 5.26	Hours mPCG worn throughout 9 month-wear trial .....	158
Figure 6.1	Geometric models to build FE model .....	164
Figure 6.2	4-node quadratic tetrahedral element .....	165
Figure 6.3	Mesh models in this study .....	166
Figure 6.4	Boundary conditions on workpiece to simulate the condition .....	167
Figure 6.5	Effects of initial status (“without padding”) on ribs and spine .....	168
Figure 6.6	Effects of pressure exertion (“with padding”) on ribs and spine .....	169
Figure 6.7	Displacement results of spine and body with use of different magnitudes of exerted force through padding and locations of inserted padding .....	170
Figure 6.8	Comparison of spinal curvatures between actual and simulated curves .....	171
Figure 6.9	Concept behind a decision tree in this study .....	173
Figure 6.10	Decision tree structure .....	175
Figure 6.11	Weight of each feature in the decision tree .....	176
Figure 6.12	Eight padding placement options of mPCG .....	178
Figure 6.13	Neural network architecture for prescription of mPCG .....	179
Figure 6.14	Input and output for training neural network .....	180

## LIST OF TABLES

		Page
Table 2.1	Five King classifications of scoliosis (King et al., 1983) .....	20
Table 2.2	Six Lenke classifications of scoliosis and criteria (Lenke et al., 2001) .....	21
Table 2.3	Lumbar spine modifier in Lenke Classification System (Lenke et al., 2001) .....	22
Table 2.4	PUMC Classification System (Qiu et al., 2008) .....	23
Table 2.5	Commonly prescribed traditional hard braces .....	28
Table 2.6	Examples of semi-rigid braces .....	31
Table 2.7	Examples of flexible braces .....	33
Table 2.8	Examples of posture corrective garments .....	45
Table 3.1	Material laboratory tests for fabric and elastic strap materials ....	70
Table 3.2	X-ray timetable .....	83
Table 3.3	Comparison of inclusion criteria, definition of curve progression and progression rates of idiopathic scoliosis .....	84
Table 3.4	Marker set for data collection and calculation in each test .....	90
Table 3.5	Questionnaire survey conducted at different time points in the wear trial .....	92
Table 4.1	Sample size, mean and standard deviations for weight, height, BMI, WC and WHTR (Sung et al., 2008) .....	102
Table 4.2	Age- and sex-specific waist circumference percentile values (cm) (Sung et al., 2008) .....	102
Table 4.3	Spine length (from C7 to pelvis level) .....	102
Table 4.4	Range of measurements of mPCG .....	103
Table 4.5	Basic information of sourced fabrics and elastic straps .....	104
Table 4.6	Results of elasticity and recovery tests of sourced fabrics and elastic straps .....	105
Table 4.7	Hand feel test results of the sourced fabric and elastic strap samples .....	114
Table 4.8	Details of pattern pieces and material applications of mPCG ....	117
Table 5.1	School-screening results .....	121
Table 5.2	Demographic data of recruited subjects .....	121
Table 5.3	Details of prescribed girdle for recruited subjects .....	123
Table 5.4	Results of interface pressure measurements .....	124
Table 5.5	Cobb angle comparison and purpose .....	125
Table 5.6	Cobb angle results at different points of time .....	126
Table 5.7	Cobb angle changes at 0 M before and after 2 h (immediate effects) .....	127
Table 5.8	Cobb angle changes from 0 M pre-intervention to 9 M (long-term effects) .....	129
Table 5.9	Cobb angle changes from 0 M pre-intervention to 3 M (out-orthosis) .....	131
Table 5.10	Changes of Cobb angle from 0 M to 6 M (in-orthosis) .....	132
Table 5.11	Standards extracted from Lau et al. (2022) to determine repositioning error .....	145
Table 5.12	Wear practices and compliance rate up to 9 M .....	158

Table 6.1	Information of subject for FE model .....	163
Table 6.2	Material properties for different components in FE model .....	165
Table 6.3	Summary of information for decision tree classification .....	174

## LIST OF ABBREVIATIONS

### A

AATCC	American Association of Textile Chemists and Colorists
AI	artificial intelligence
AIS	adolescent idiopathic scoliosis
ALV	apical lumbar vertebrae
ANNs	artificial neural networks
AP	anterior-posterior
ASIS	anterior superior iliac spine
ATB	anisotropic textile brace
ATI	angle of trunk inclination
ATR	angle of trunk rotation
ATR	angle of trunk rotation

### B

BMI	body mass index
BrQ	Brace questionnaire
BSSQ	Bad Sobernheim Stress Questionnaire

### C

C7	the 7 <sup>th</sup> spinous process of Cervical Spine
CART	Classification and Regression Trees
CFHD	center front of the forehead
CNNs	convolutional neural networks
CSVL	center sacral vertical line
CT	computer tomography
CTLSSO	cervico-thoraco-lumbo-sacral orthosis

**E**

EC exercise capacity

EFY Elbow flexion

EVA ethylene vinyl acetate

**F**

FE finite element

FEM finite element modelling

FITS Functional Individual Therapy of Scoliosis

**H**

HKAI Hong Kong Advanced Imaging

**I**

IS idiopathic scoliosis

**K**

KEY knee extension

**L**

L3 the 3<sup>rd</sup> spinous process of lumbar spine

L4 the 4<sup>th</sup> spinous process of lumbar spine ...

LASI left anterior superior iliac spine

LPSI left posterior superior iliac spine

LSHO left acromion

LSPL left inferior angle of scapula

LUM lumbar

**M**

MIU coefficient of friction

MMD	deviation of MIU
mPCG	modified posture correction girdle
MRI	Magnetic Resonance Imaging
MT	main thoracic
<b>N</b>	
NN	neural network
NRZ	neck rotation
NTRBs	night time rigid braces
<b>P</b>	
P & O	prosthetist and orthotist
PCG	posture correction girdle
PA	posterior-anterior
PT	proximal thoracic
PUMC	The Peking Union Medical College Classification System
<b>Q</b>	
QoL	quality of life
<b>R</b>	
RASI	right anterior superior iliac spine
RPSI	right posterior superior iliac spine
RSHO	right acromion
RSPL	right inferior angle of scapula
<b>S</b>	
SACR	sacrum
sEMG	surface electromyography
SMA <sub>s</sub>	shape memory alloys

SMD	geometric roughness
SNCH	sternal notch
SOSORT	Scoliosis Orthopedic and Rehabilitation Treatment
STP	Unterberger stepping
STRN	sternum
<b>T</b>	
T6	the 6 <sup>th</sup> spinous process of thoracic spine
T7	the 7 <sup>th</sup> spinous process of thoracic spine
T8	the 8 <sup>th</sup> spinous process of thoracic spine
T9	the 9 <sup>th</sup> spinous process of thoracic spine
T10	the 10 <sup>th</sup> spinous process of thoracic spine
T11	the 11 <sup>th</sup> spinous process of thoracic spine
T12	the 12 <sup>th</sup> spinous process of thoracic spine
TAPS	Trunk Appearance Perception Scale
THOR	thoracic
TL/L	thoracolumbar/ lumbar
TLSO	thoraco-lumbar-sacral-orthoses
<b>W</b>	
WVT	water vapor transmission
<b>V</b>	
VC	vital capacity

# Chapter 1 – Introduction

## 1.1 Research Background

Adolescent idiopathic scoliosis (AIS) affects 2-3% of all adolescents in Hong Kong, which is one of the common health problems related to growth among adolescents (Student Health Service - Department of Health 2022; Chan, 2019; Lam, 2010). Richards and Vitale (2008) also reported that a certain degree of spinal curvature or deformity is found in about 10% of all adolescents after reaching 10 years old. AIS is a complex three-dimensional (3D) spinal deformity found among adolescents between 10 years old and skeletal maturity (Dobbs & Weinstein, 1999). The condition involves lateral curvature and sometimes rotation of the spine, which can be measured and the severity and stage determined by using the Cobb's method on radiographic images (Kane, 1997; Cobb, 1948). Generally, scoliosis cases with a lateral curvature greater than or equal to 10° in the Cobb angle are regarded as medical conditions (Hresko, 2013). Girls are 3.6 times more likely than boys to experience progression of their spinal curvature (Kubat & Ovadia, 2020; Weinstein, 1994). Bracing treatments are recommended for patients with a spinal curvature that is more than 25°, while surgery is considered for patients with a spinal curvature that has progressed to 40 to 50°. Only observation with periodical examination is suggested to patients with a spinal curvature less than 25° (Spoonamore, 2024, Hresko, 2013). However, it is believed that more treatment options can be offered to patients with early scoliosis, i.e., those with a Cobb angle that ranges from 10 to 20° (Yip et al., 2016).

For those who need to undergo bracing treatment, there are several different types of hard and flexible braces available for treatment, but none are specifically designed for those with mild scoliosis. Hard braces like the Boston and Milwaukee Braces have a “rigid frame” that compresses and nearly constrains with high tension, thus restricting movement of the covered area of the body (Liu et al., 2014). Flexible braces like the SpineCor has questionable efficacy and a rather low compliance rate due to the inconvenience during toileting (Wong et al., 2008). To address the limitations of existing hard and flexible braces in the market and the problem of the absence of suitable orthosis products for early scoliosis treatment, Liu et al. (2015) developed a posture correction girdle (PCG) with the aim to reduce posture imbalance and thus reduce the likelihood that the curvature of the spine will continue to progress in severity.

The 3D deformities of the spine and rib cages affect the posture balance of AIS patients by changing the body segment relationship (Masso et al., 2000). The posture imbalance problems related to the head, shoulders, scapular and pelvis are commonly found in the frontal, horizontal and sagittal planes (Nault et al., 2002). The risk of scoliosis progression in AIS patients might be related to posture asymmetry and changes (Kouwenhoven and Castelein, 2008; Fortin et al., 2012). Improper posture and poor posture stability control may further worsen spinal deformity problems and the related painful symptoms in patients (Wong and Wong, 2008; Chen et al., 1998). Therefore, using a posture training device may be one of the possible and acceptable ways to help AIS patients (Wong and Wong, 2008; Lenssinck et al., 2005). This is also the intention behind the development of the PCG in Liu et al (2015).

The PCG in Liu et al. (2015) which was subsequently modified by Fok et al. (2018) uses a point pressure system to provide lateral corrective forces that prevent progression of the spinal curvature in female adolescents who are 10-13 years old in the early stage of scoliosis (i.e. Cobb angle between  $10^{\circ}$  and  $20^{\circ}$ ). The preliminary result showed that the PCG helps to improve the imbalance in posture in the frontal, horizontal and sagittal planes, as well as control the progression of the spinal curvature (Liu et al., 2015; Yip et al., 2016). However, the PCG was tailor-made for the subjects in the study. This made to measure process is time consuming and leads to a longer production lead time. Patients may need to wait for weeks before the girdle/orthosis is ready for use. The trial and error fitting process during the prescription of the girdle also takes time. Finally, the girdle design has some limitations which affect the corrective force exertion and the level of wear comfort. Therefore, this research project aims to develop a sizing system for the PCG, so the girdle can be mass produced and customised which may reduce the production cost and wait time of the patient. The girdle design is also modified and refined to work better with the newly developed sizing system, optimise the corrective force exertion and effectiveness, as well as enhance the level of wear comfort. In addition, this research project also aims to study the corrective mechanism and performance of the PCG by using finite element modelling (FEM) and construct an intelligent PCG prescription system to facilitate the prescription and fitting process. With modifications to the girdle design, establishment of the corresponding sizing system, corrective mechanism study, and application of the intelligent PCG prescription system, it is anticipated that the PCG can be personalised as a treatment for scoliosis,

increase the efficacy of the bracing process, reduce the cost of treatment, and popularise the use of the PCG as an orthosis, which could benefit adolescents with early scoliosis or posture problems.

## 1.2 Problem Statements

There are four issues that need to be examined. They are as follows:

**1. *It is time consuming to produce the PCG in a made-to-measure manner***

In traditional AIS bracing treatment, the orthoses are produced by using a made-to-measure method. The PCG in previous studies were also produced by using a tailored method. These production methods result in a longer lead time for patients. Patients may need to wait for weeks before the orthoses are ready for use (Fung et al., 2020). More comprehensive research work needs to be done to address the spinal biomechanics through clothing design. In this research project, PCGs are mass customised to reduce production lead time and production costs.

**2. *Girdle design modification for mass customisation, optimisation of effectiveness and enhancement of wear comfort***

To facilitate the implementation of the newly developed sizing system and mass customisation method, some modifications are needed to be done to the PCG (e.g. the size adjustment system/girdle fastener). By doing so, the girdle might accommodate a larger range of different body sizes. Under the mass customisation of the PCG, the main body of the girdle and padding for point pressure creation could be pre-fabricated by following the measurement specifications in the sizing system. With flexibility in padding insertion and placement as well as strap tension adjustment, corrective forces can be exerted according to different needs. Besides, other girdle design features (e.g. inside pocket dividers) can also be modified to optimise the exertion and effectiveness of the corrective forces. Furthermore, less than optimal fabric and elastic materials are replaced by those with a better performance so as to enhance the level of wear comfort and durability of the girdle. Human subjects are then recruited for a 9-month wear trial and scientific experiments so as to evaluate the effectiveness of the girdle.

### **3. *Subjects for wear trial***

It is always not easy to identify and then recruit participants for a wear trial, especially for a longer period of time with a target group of adolescents. They might not be mature enough to understand the reason behind the wear trial nor patient enough to withstand the long bracing/treatment hours throughout the day. Therefore, FEM is a good method to further simulate the corrective performance and understand the corrective mechanism of the PCG.

### **4. *Computerised prescription system for AIS brace treatment***

The “trial and error” fitting process during the prescription of the girdle is an inefficient process. However, computer-aided models that are specially designed and developed for prescribing the PCG are limited in the market. Related research or journal papers are also limited. To address this research gap, this project aims to construct an intelligent system to facilitate the prescription process. Academics, clinicians and patients will benefit from the project, and the project outputs can be extended to the application of machine learning in biomechanical research in which the generated automated solutions can increase the accuracy and repeatability of the execution of critical tasks.

## **1.3 Aim and Objectives**

The PCG targets to help female adolescents who are 10-13 years old and diagnosed with early scoliosis, i.e., a Cobb angle of  $10^{\circ}$  to  $20^{\circ}$  (Liu et al., 2014; Liu, 2015). This project aims to develop a sizing system for the mass customisation of the PCG, modify the design of the PCG to optimise its effectiveness and level of wear comfort, study the corrective mechanisms and performance of the PCG, as well as develop an intelligent system to facilitate the prescription and fitting process of the PCG. By doing so, the PCG can serve as a personalised girdle treatment with optimised treatment efficacy but lower production and treatment costs, which could benefit adolescents with early scoliosis or posture problems. Also, the use of the PCG is anticipated to be popularised for health care. Since AIS is more commonly found in females, this research project focuses on preteen and teenage girls in the early stages of scoliosis.

The principal objectives of this project are as follows:

1. To understand the theory behind existing orthosis products for AIS treatment and investigate the prevalence of AIS in Hong Kong.
2. To modify the design of the PCG and select suitable materials that optimise its treatment efficacy and level of wear comfort, as well as enhance garment durability.
3. To develop a specific sizing system for the modified PCG for adolescents with early scoliosis to facilitate mass customisation.
4. To recruit subjects who can meet the inclusion criteria for a wear trial in order to evaluate the efficacy of the modified PCG with scientific tests.
5. To study the corrective mechanism of the PCG by using FEM.
6. To construct and validate an intelligent system that facilitates the prescription of the PCG.

#### **1.4 Project Originality and Significance**

The purpose of this project is to develop a specific sizing system for the mass customisation of the PCG, modify the design of the PCG to optimise effectiveness and level of wear comfort, study the corrective mechanism and performance of the PCG, and develop an intelligent prescription system for the PCG. As a result, the modified PCG can serve as personalised health care treatment at a lower price. With a more affordable treatment price, shorter waiting time before receiving the girdle treatment and more scientific proof on the treatment efficacy, treatment with the PCG could be popularised and more adolescents with early scoliosis could benefit. In addition, with the application of the intelligent prescription system for the PCG, orthopaedic clinicians can easily fit the modified PCG to each AIS patient according to recommendations. Thus, the medical/orthotists and prosthetists (P&O) consultation and prescription process could be done more efficiently and accurately. Furthermore, the findings of this project will provide useful information to academics and orthopaedic clinicians on the engineered design of flexible braces.

## **1.5 Report Outline**

There are 7 chapters in this thesis. Chapter 1 includes the background information, rationale, concept, problem statement and objectives of this study, together with details on the project originality and significance. Chapter 2 is the literature review which includes a brief review of scoliosis information, common types of treatments used for scoliosis, associated problems of existing products for the related treatments, methods used to improve posture, research related to posture correction through interventions on adolescents and the use of computer-aided models in the garment industry. Chapter 3 describes the research plan and methodology of this study including development of a specific sizing system for the PCG, development of the modified PCG, subject recruitment, prototype production, wear trial and evaluation tests. Chapter 4 presents the research results with a discussion on the establishment of a specific sizing system, PCG modifications and physical tests of the main materials. Chapter 5 presents the research results with discussion on the subject recruitment, prototype production, evaluation tests and analysis of wear trial. Chapter 6 discusses the corrective mechanism of the PCG with the use of FEM and describes the construction of an intelligent system for prescribing the PCG through the integration of decision trees and convolutional neural networks (CNNs). Finally, Chapter 7 provides a conclusion of the study.

## **Chapter 2 – Literature Review**

### **2.1 Introduction**

This chapter begins with an overview of scoliosis as an introduction on the definition, types and possible effects of scoliosis. This is followed by a discussion on the different methods of identifying this condition, including both physical and radiographic assessments, signs of scoliosis, as well as the common classification methods. In addition, the prevalence of AIS, possible treatment options, and problems of existing orthosis products for AIS are also reviewed. An overview of posture is also included in the discussion. For instance, the importance of proper posture, consequences and prevalence of poor posture, and the different posture correction methods are elaborated. Besides, the design features and garment components of the PCG are also described. The corrective mechanism of the PCG, and previous wear trial results with respect to its effectiveness and limitations are discussed. Evaluation methods of the PCG on its effectiveness are also outlined. Finally, the use of FEM to predict the efficacy of bracing treatment as well as the potential use of computer-aided models in the garment industry for spinal deformity assessment are investigated.

### **2.2 General review of scoliosis**

#### **2.2.1 Definition and types of scoliosis**

Scoliosis, as defined by The International Society on Scoliosis Orthopedic and Rehabilitation Treatment (SOSORT), is a 3D deformity found in the spine and trunk (Negrini et al., 2012). The condition includes the lateral displacement and axial rotation of the vertebra (Chan et al., 2013). Figure 2.1 shows the difference between a normal and scoliotic spine (Pittsburgh Physical Medicine, 2023). Patients are diagnosed with scoliosis when their Cobb angle is greater than  $10^{\circ}$  in the anterior plane of a standard radiography (Kubat & Ovadia, 2020).

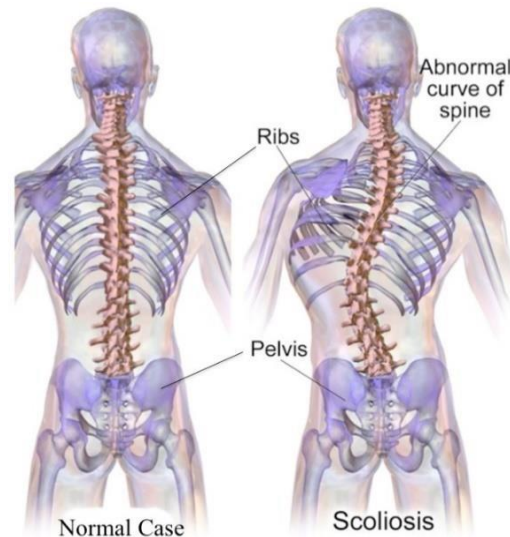


Figure 2.1 Normal vs. scoliotic spine (Pittsburgh Physical Medicine, 2023)

Scoliosis is generally differentiated as three main types depending on its aetiology, which includes idiopathic, congenital and neuromuscular scoliosis (Lonstein & Carlson, 1984). Idiopathic scoliosis (IS), which comprises more than 80% of the scoliosis cases, has no documented etiopathogenesis even with a number of clinical studies conducted in the literature (Reamy & Slakey, 2001; Negrini et al., 2012). Congenital scoliosis is an innate condition caused during the development of the vertebrae, and possibly linked to the deformity of other organs such as the heart. Finally, neuromuscular scoliosis is caused by brain disorders which affect the nerves and muscles, such as in the case of cerebral palsy or muscular dystrophy.

IS is further categorised into three types based on the age of the initial onset, which comprises infantile (under 3 years old), juvenile (between 3 and 10 years old), and adolescent (older than 10) idiopathic scoliosis (Horne et al., 2014; Aulisa et al., 2014). Among them, the latter is the most prevalent type of scoliosis, as AIS has been diagnosed in 0.9 to 12 percent of the general public, even among those who appear to be physically healthy without a medical history of scoliosis (Negrini et al., 2012; Grivas et al., 2006). A number of research studies have concluded that rapid growth, and hormonal and muscle imbalances during puberty are all likely to contribute to spinal curvature (Mackenzie, 1922; Lonstein & Carlson, 1984). Apart from these factors, there is the assumption of a relationship between heredity and scoliosis since about 30% of AIS patients are found to have a related family history of scoliosis (Kim et al., 2009). Kesling et al. (1997) conducted a systematic review of AIS cases with identical and fraternal twins and found that 73% of identical twins and 36% of fraternal twins show

concordance of scoliosis, respectively. The hereditary factors in scoliosis include dominance or multiple inheritance, maternal effect, X-linked dominance gene, etc. (Miller, 2007; Yamada et al., 1984).

AIS usually occurs in youths between 10 and 17 years old during skeletal immaturity (Negrini et al., 2018). Negrini et al. (2018) added that the most appreciable progression of scoliosis occurs when puberty starts, but this progression gradually decreases in the later period of puberty and after female patients have their first menstruation period. With skeletal maturity, the progression of scoliosis is reduced to the smallest risk.

### **2.2.2 Possible effects of scoliosis**

An ‘‘S’’ or ‘‘C’’-shaped curve can be observed in the spine of scoliosis patients due to torso rotation and deformity of the spine (Harvard Medical School, 2023). A large Cobb angle of the spine will give rise to negative feelings as there is back pain, especially in the lower back, owing to weak abdominal and back muscles, loss of leg flexibility, and the demands of everyday life activities. In Ramirez et al. (1997), 23% of the 2442 patients in their study experienced back pain at the beginning of the study while 9% continued to experience back pain problems throughout the study.

Since the progression of scoliosis is high during puberty, specifically among girls, the condition may cause severe torso deformity and further damages their joints, limits their mobility, affects their pulmonary functions and changes the appearance of their chest (Negrini et al., 2018). These give rise to a lower exercise capacity (EC) and vital capacity (VC) (DiRocco et al., 1988; Szeinberg et al., 1988). The effect on pulmonary functions will continue even if the progression of this condition slows down as the core functions of the body are already negatively affected. As for the influence on the chest, the function and strength will erode as the patients mature (Branthwaite, 1986; Pehrsson et al., 1992).

The influence of scoliosis may further continue into adulthood so that serious health issues emerge, such as back pain; fatigue; trunk deformity; asymmetric shoulders, waist, hips and trunk; twisted rib cage; and other ventilatory functional restrictions. For serious cases, respiratory and lung disorders may occur (Hresko, 2013). According to Lonstein (2006), patients with a spinal curvature that exceeds the threshold limit (30° to 50°) will have a higher

possibility of serious health issues in adulthood, which affects quality of life (QoL). Moreover, the physical deformity and features of disability may erode their self-confidence (Parent et al., 2004; Lonstein, 2006; Negrini et al., 2006). Ascani et al. (1986) stated that about 20% of AIS patients, especially those with more severe scoliosis, have psychological problems. To reduce the risk of further health issues like back pain in adulthood due to scoliosis, it is highly recommended that spinal curvature is diagnosed in the early stages, and treatment prescribed as early as possible during puberty to minimise the effects.

### **2.2.3 Detection methods and signs of scoliosis**

To examine the signs of scoliosis which will contribute to a timely diagnosis and treatment, several detection methods are available, including those that are physical and radiographic assessments.

#### ***Physical assessment***

Physical assessment is a basic checkup of the subjects that involve their height, walking posture, skin, pubertal growth, sensing organs, shoulder balance and ilium asymmetry, and back outline (Janicki & Alman, 2007). To better assess scoliosis, previous studies have summarised several noticeable signs of scoliosis. It is proposed that asymmetric shoulders, unbalanced hips and curved spine are the main symptoms for identifying scoliosis at the onset (Lau, 2011). Sanders et al. (2003) developed the Walter Reed Visual Assessment Scale to comprehensively determine the presence of scoliosis as shown in Figure 2.2, which measures the subjective perception of the deformity, and involves: (1) a twisted body, (2) protruding rib on one side of the body, (3) protruding flank on one side of the body, (4) twisting along the head, rib and pelvis, (5) pelvis leaning to one side of the body, (6) misalignment of the head and pelvis, (7) protruding scapula on one side of the body, (8) twisted scapula, and (9) protruding and asymmetrical hips (Zaina et al. 2009; Bago et al. 2007). The scale defines the severity of scoliosis as five grades, with (1) being the least serious and (5) being the most serious. The scores calculated based on the scoliosis signs are highly related to the extent of the spinal curvature. Pineda et al. (2006) found that this assessment scale is effective and has high internal consistency and reliability in determining scoliosis.

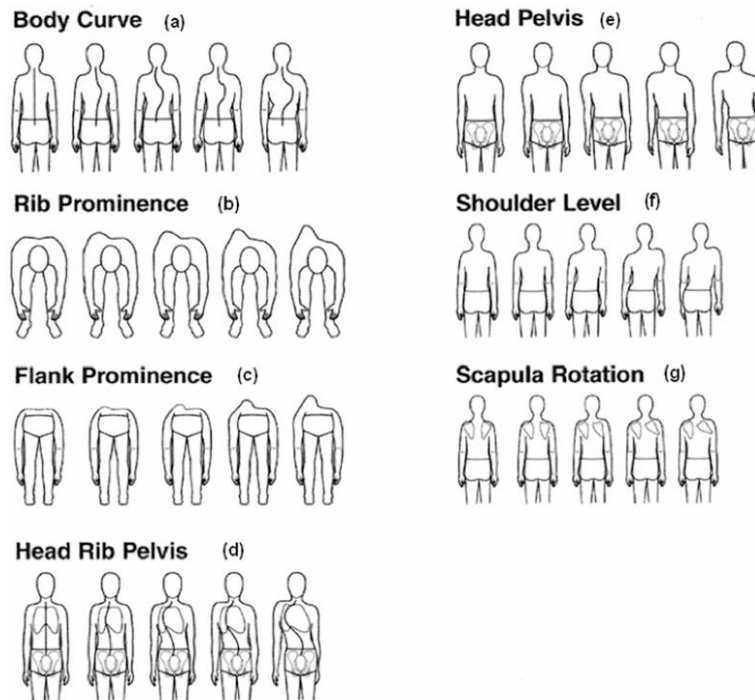


Figure 2.2 Walter Reed Visual Assessment Scale for determining scoliosis (McCathy, 2001)

The Adam's forward bend test is the main clinical examination practice used to measure scoliosis with the use of a scoliometer (Horne et al., 2014; Negrini et al., 2012). Patients are required to remove their top to allow clear observation of their spine (Reamy & Slakey, 2001). They need to bend forwards at the waist until their spine is parallel to the surface of the ground. During this process, their legs need to be in a straight upright position and placed together while their arms are pointing to the ground. After that, the technician will measure the angle of trunk rotation (ATR) at the axial plane of the thoracic, thoracolumbar and lumbar areas and evaluate whether the outline is balanced or there is a 'rib bulge' as shown in Figure 2.3 (Horne et al., 2014; Hresko, 2013). A rib bulge represents a Cobb angle that is greater than  $10^{\circ}$  and a standard radiography is needed according to Reamy and Slakey (2001). As shown in Figure 2.3, a scoliometer is used to determine the angle of trunk inclination (ATI) or angle of trunk rotation (ATR) which ranges from  $0^{\circ}$  to  $30^{\circ}$  (Hresko, 201 ; Patias et al., 2010). The ATR is an objective measurement of the size of the hump of the trunk (Horne et al., 2014; Kotwicki, 2008).

Recommendations provided by the SOSORT Guidelines 2016 indicate that patients with an ATR of  $5^{\circ}$  are advised to undergo a more detailed evaluation and possibly adopt more conservative therapy (Adams, 1882; Patias et al., 2010) while those with an ATR of  $7^{\circ}$  should undergo surgery since this is a sign of scoliosis (Negrini et al., 2018). Even though the Adam's

forward bend test is used for most scoliosis assessments, it is debatable as to whether this test produces false positive or negative results (Soucacos et al., 1997; Wong et al., 2005). In addition, there are two other tools that are commonly used to measure the back profile of patients, which are the hump-meter and level protractor (Tajima et al., 1981; D'Oswaldo et al., 2000). The hump-meter can measure the differences in height between the curve apex and bottom of apex, but cannot be used to determine the ATR. As stated by the SOSORT Guidelines 2016, a 5 mm difference could point to different severity of the back bulge, as the bulge size can be a symptom of scoliosis in children (Negrini et al., 2018; Ferraro et al., 2016). To enhance a better clinical assessment of AIS, a hump-meter is used together with radiography in this study.

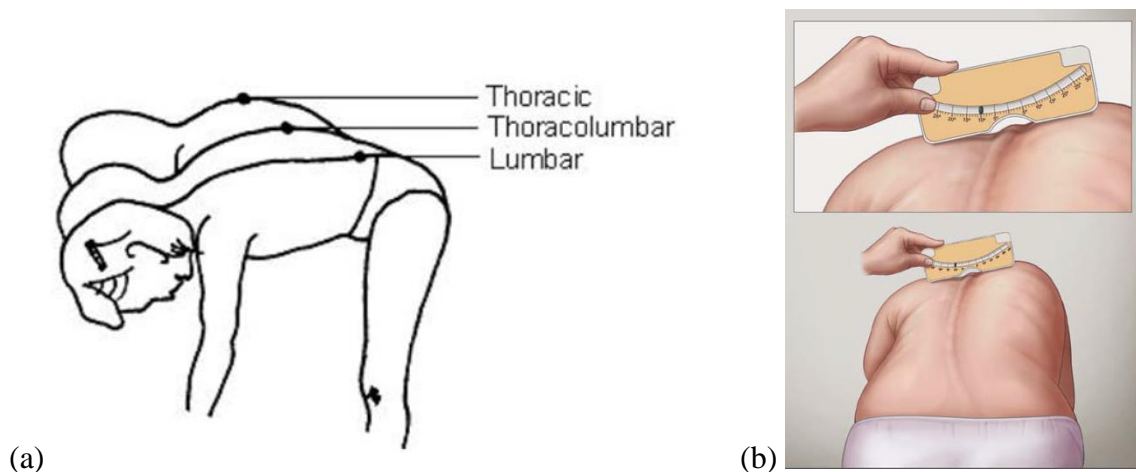


Figure 2.3 a) Adam's forward-bend test (Patias et al., 2010) and b) measurement of ATR by using scoliometer (Hresko, 2013)

Apart from the Adam's forward-bend test, Moiré topography is another method to examine the body contours and a more acceptable method because it is more accurate and does not expose the subject to radiation (Ueno et al., 2011; Adair et al., 1977; Willner, 1979). Moiré topography is mainly used for evaluating the 3D plane and determining whether the target has asymmetric contours. Figure 2.4 shows the Moiré topography setup which comprises a Moiré frame, light source and single-lens camera that is used to project dark and bright fringes onto the back of the patient. If the individual has a curved spine, the pattern or fringes curve away from the reference line, which is used to determine the severity of the scoliosis (Adair et al., 1977). Conversely, if the fringes are straight, this indicates a normal spine. Figure 2.5 shows the Moiré fringes of subjects with and without scoliosis.

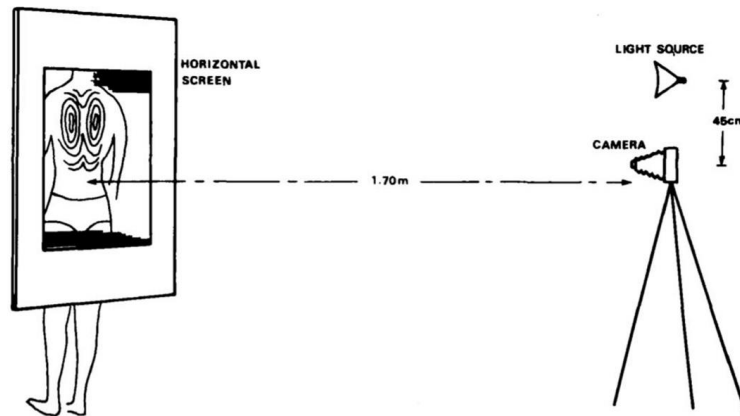


Figure 2.4 Moiré topography (Adair et al., 1977)

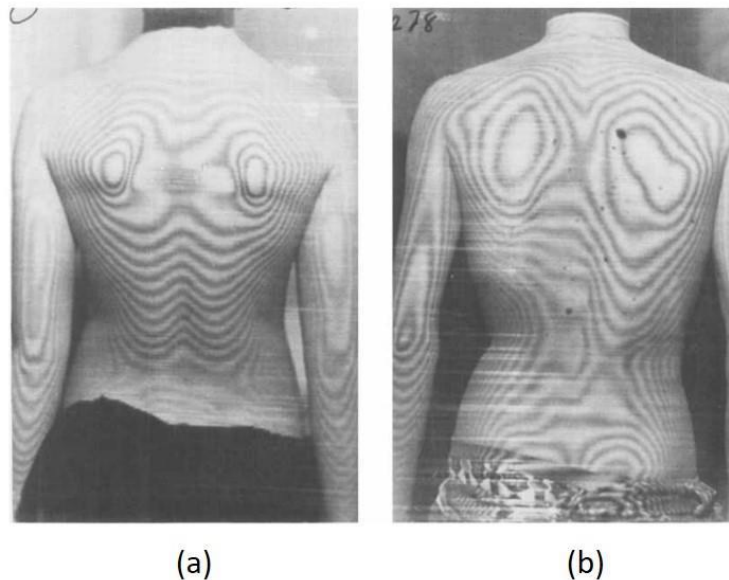


Figure 2.5 Moiré fringe images of spine: (a) without curvature, and (b) with curvature (Adair et al., 1977)

To determine the different ATRs, the following screening tests are carried out in Hong Kong. The Hong Kong Department of Health carries out an annual health screening programme for students in Primary 5 or those who are 10 years old. They use the Adam's forward bend test to determine the presence of scoliosis and screen out those without symptoms. Moiré topography applies to students who have an angle of rotation between  $5^\circ$  and  $15^\circ$ . Finally, those who are found to have an ATR of over  $15^\circ$  or more than Moiré lines need further radiographic screening at a specialist clinic (Luk et al., 2010).

Other than the Adam's forward bend test and Moiré topography, some of the newly developed

surface topography methods like thermography and 3D surface imaging are now being used to screen for scoliosis. Thermography uses an infrared camera to measure the paraspinal skin surface temperature and amount of infrared emitted. Figure 2.6 shows an infrared image produced by using thermography (Cooke et al., 1980). The concave side of the spine shows more infrared and therefore a higher temperature while the reverse can be observed for the convex side (Cooke et al., 1980). For 3D surface imaging, the images captured by multiple cameras are joined to form a complete 3D profile of the spine. The profile of the body is evaluated by using a computer to determine the spinal curvature of patients (Lee et al., 2010). These physical assessments are non-invasive and time-efficient. They are also considered to be reliable and effective (Pearsall et al., 1992). However, they are designed to observe external symptoms of scoliosis and cannot determine the actual scoliosis situation.



Figure 2.6 Greyscale infrared image of an AIS patient (Cooke et al., 1980)

### **Radiographic assessment**

Since the above screening methods cannot provide the exact information of the curvature profile, they are used as a preliminary measure for determining scoliosis. A standard radiographic investigation is needed if the technician considers that the patient indeed has scoliosis according to the ATI value or back bulge (Cobb, 1948). As suggested by the SOSORT Guidelines 2016, the efficacy of bracing treatment should be based on in-brace radiographic imaging (Negrini et al., 2018). In a normal radiography, the 7<sup>th</sup> cervical vertebra (C7) to ilium should be x-rayed and a side image is also important to observe the deformity in the sagittal plane (Hresko, 2013). Besides, posterior-anterior (PA) imaging is commonly used instead of

anterior-posterior (AP) imaging to eliminate the radiation risk to the thyroid and chest glands and reduce the risk of thyroid problems (Hresko, 2013; Kotwicki, 2008).

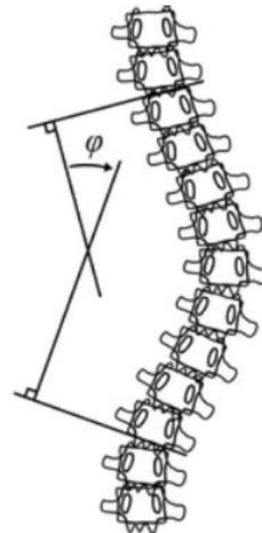
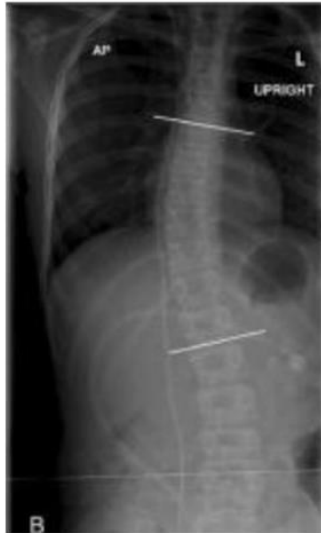
Apart from conventional radiography, there are more recent medical scanning techniques in recent years designed for scoliosis. For instance, there is computer tomography (CT) which is computerised and can capture and take images of specific body parts at different angles by using multiple cameras. This will provide 3D images of the lateral profile or images of the inside of the body (Kalender, 2011). These 3D images allow examination of the spinal curvature more comprehensively by turning the body to different angles (Hewitt, 2011).

One of the latest technologies is EOS™ x-ray imaging which has a comparatively low emitted radiation. This weight-bearing system will trace the body while the subject is standing and take the AP and cross section images. During the scanning process, patients need to stand inside the EOS™ cabin for about 10 to 25 seconds and take dual-plane images as shown in Figure 2.7 (Dubousset et al., 2005). Radiation emitted from using the EOS™ system is minimised to 1/10 of that of traditional radiographic imaging and 1/100 to 1/1000 of CT scanning (Illés & Somoskeöy, 2012; Wybier & Bossard, 2013). Moreover, the images generated by the EOS™ system have a better quality, contrast and resolution than traditional radiographic images. EOS™ dual-plane images are available in greyscale from 30 to 50,000 dpi and pixel resolution of 254 µm while traditional radiography can only offer greyscale of hundreds of dpi. In spite of the fact that more scoliosis imaging methods like the EOS™ system offers reduced radiation exposure along with more rapid X-ray imaging or 3-phase x-ray equipment, Knott et al. (2014) argued that there are still health repercussions and even carcinogenic risk. A number of studies, such as Ron (2003) show correlation between radiation and cancer, especially lung and breast cancers. For that reason, the potential risk of cancer with the use of radiography is an important factor to consider in scoliosis diagnosis and examination.



Figure 2.7 EOS™ imaging system (EOS imaging, 2020)

The **Cobb angle** is recognised as the benchmark of spinal curve measurement for AIS via radiography and can be used to measure both the major and minor vertebrae curves (Cobb, 1948). Figure 2.8 shows the procedure of measuring the Cobb angle. The first step is to determine the vertebrae with the highest inclination above and under the highest point of the curve. Then, vertical lines are drawn upright between the superior endplate of the upper vertebra and inferior endplate of the lower vertebrae, in which the lines extend to intersect each other and form the Cobb angle (Cobb, 1948; Patias et al., 2010; Vrtovec et al., 2009; Zhang et al., 2010). Malfair et al. (2010) indicated that the boundaries of the radix arcus vertebrae can be used to replace the endplates which affects the measurement. Regardless of the measurement methods used, the total difference between the actual Cobb angle and calculated angle may range from  $2^{\circ}$  to  $7^{\circ}$  due to the endplates chosen (Malfair et al., 2010). Through X-ray observations, technicians can evaluate the spinal condition, determine the classification and degree of frontal plane deformity, as well as more easily calculate the Cobb angle at the frontal or sagittal plane (Cobb, 1948).



(1) Vertebrae with the highest inclination above and under the highest point of the curve for radiographic imaging

(2) Cobb angle represents angle formed between the intersecting point of upright vertical line between superior endplate of upper end vertebra and inferior endplate of lower end vertebra

Figure 2.8 Procedure of Cobb angle measurement (Vrtovec et al., 2009; Zhang et al., 2010)

Horne et al. (2014) pointed out skeletal immaturity is the core factor for the severity of scoliosis. Therefore, in addition to the Cobb angle, Risser (1957) created the **Risser sign**, a measure of skeletal maturity, to pinpoint the skeletal development and maturity of patients. The Risser sign classifies spinal curvatures into six stages, i.e., Risser 0 to 5 (Malfair et al., 2010). No signs of the ossification of the triradiate cartilage are found in Risser 0, which is usually the start of puberty. Risser 1 to 5 represent different levels of ossification of the apophysis where Risser 1 means a 25% apophysis of the iliac crest or when the growth spurt during puberty starts to slow down. Risser 2 means a 50% apophysis of the iliac crest, in which the bone age of girls is 14 and that of boys is 16. Risser 3 means a 75% apophysis of the iliac crest when the bone age of girls is 14.5 and that of boys is 16.6, which means that there is one year left to their pubertal growth period. Risser 4 represents a 100% apophysis of the iliac crest or almost cessation of growth in which the bone age of girls is 15 and that of the boys is 17. Finally, Risser 5 is the complete fusion of the apophysis and iliac crest and also represents the end of pubertal growth (Dimeglio, 2001). Sun et al. (2013) showed that the development of the spinal curvature of patients with Risser 0 to 1 is more rapid than patients with Risser 2 to 4. This suggests that corrective therapy like bracing is necessary for AIS patients with Risser 0 and 1. Then, French researchers Brand (2008) and Kotwicki (2008) modified the Risser system, in

which Rissers 3 and 4 have the most apparent changes with complete ossification taking place in Risser 4. Figure 2.9 shows the initial and modified Risser system.

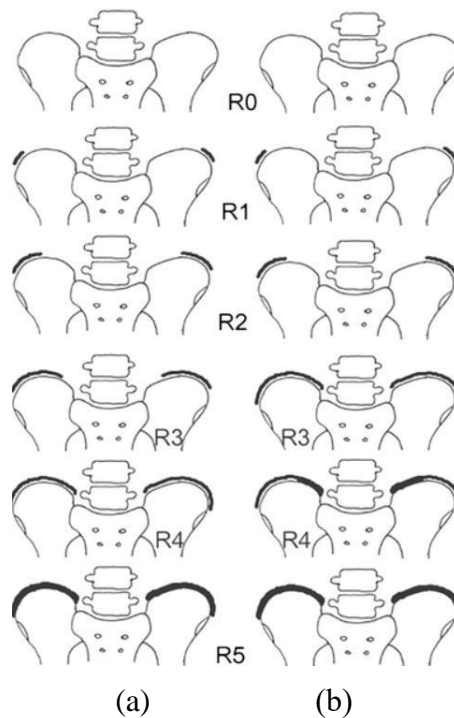


Figure 2.9 (a) Initial and (b) modified Risser system (Kotwicki, 2008)

There is also the **Nash-Moe method**, which is a grading system of spinal rotation. The method divides vertebral rotation into five grades in conformity with the location of the pedicles on the highest point of the spinal curvature (Anitha & Prabhu, 2012). Figure 2.10 illustrates the Nash-Moe system. Grade Normal (0) shows symmetric pedicles without any vertebrae rotation. Grade I means the pedicle in the inward curve is on the edges of the vertebrae while that in the outward curve is positioned towards the midline of the spine. Grade II means the pedicle in the inward curve is not quite visible while that in the outward curve is closer to the midline of the spine. Grade III denotes that the pedicle in the inward curve cannot be seen, while that in the outward curve is located on the midline of the spine. Grade IV means that the pedicle in the inward curve is not visible while that in the outward curve has moved beyond the midline of the spine and is closer to the inward curve (Anitha & Prabhu, 2012). Upadhyay et al. (1995) pointed out that vertebral rotation contributes to the progression of the lateral spinal curvature so that an increase in the rotation will reduce therapy success. Therefore, lateral spinal curvature not only needs to be controlled but also vertebral rotation.

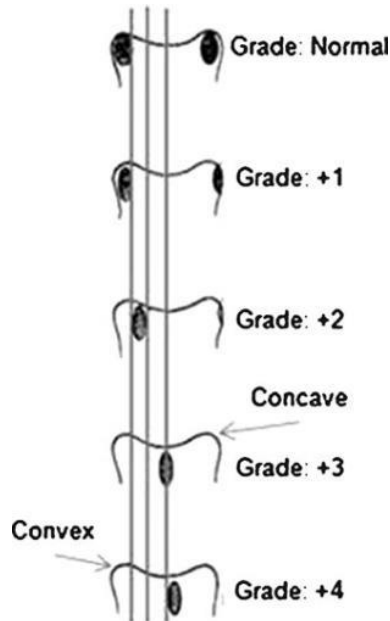


Figure 2.10 Nash-Moe grading system for vertebral rotation (Anitha & Prabhu, 2012)

#### 2.2.4 Classifications of scoliosis

A proper classification system is necessary to standardise the terms in clinical discussions and provide the criteria to group similar patterns of scoliosis (Alam et al., 2013). The King and Lenke classifications are two commonly used systems to classify scoliosis (Zhang et al., 2013). Qiu et al. (2003) also developed the Peking Union Medical College (PUMC) Classification System to offer more detail guidelines for classifying scoliosis.

##### **King Classification System**

The King classification system (King et al., 1983) divided idiopathic scoliosis into five types of curves according to the Cobb angle calculated by using standard radiography and the flexibility ratio obtained through a bending radiograph. In the 1980s, this system was widely used as the criterion along with the Harrington distraction device (Helenius et al., 2002; Padua et al., 2001). Figure 2.1 illustrates the five types of scoliosis based on the King classification system. Table 2.1 lists the five King classifications of scoliosis and their criteria (King et al., 1983).

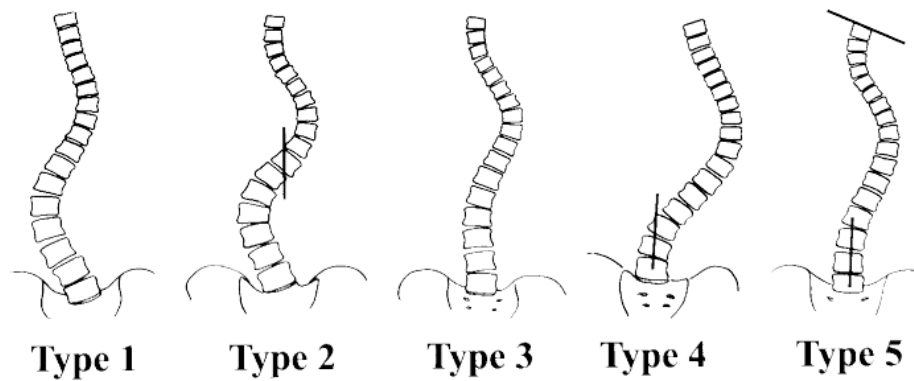


Figure 2.11 Visual of five types of scoliosis based on King classification (King et al., 1983)

Table 2.1 Five King classifications of scoliosis (King et al., 1983)

Classification	Criteria
Type I	<ul style="list-style-type: none"> <li>- S-shaped curve in which both thoracic and lumbar curves cross midline</li> <li>- Lumbar curve larger than thoracic curve in standing radiograph</li> <li>- Negative flexibility index (thoracic curve <math>\geq</math> lumbar curve in standing radiograph, but more flexible on side-bending)</li> </ul>
Type II	<ul style="list-style-type: none"> <li>- S-shaped curve in which thoracic and lumbar curves cross midline</li> <li>- Thoracic curve <math>\geq</math> lumbar curve</li> <li>- Flexibility index <math>\geq 0</math></li> </ul>
Type III	<ul style="list-style-type: none"> <li>- Thoracic curve in which lumbar curve does not cross midline (so-called overhang)</li> </ul>
Type IV	<ul style="list-style-type: none"> <li>- Long thoracic curve in which L5 is centered over sacrum but L4 tilts into long thoracic curve</li> </ul>
Type V	<ul style="list-style-type: none"> <li>- Double thoracic curve with T1 tilted into convexity of upper curve</li> <li>- Upper curve structural on side-bending</li> </ul>

### **Lenke Classification System**

Lenke et al. (2001) developed an advanced method that includes both the frontal and sagittal planes in standing AP radiographs of the spinal column, which was named the Lenke classification system. This system is commonly used to give surgeons information to communicate treatment for scoliosis (Rigo et al., 2009; Ogon et al., 2002). Table 2.2 lists the six Lenke classifications of scoliosis and their criteria (Lenke et al., 2001). There are three different steps that involve: (1) six types of spinal curvatures, numbered 1 to 6, (2) three lumbar

spine modifiers (A, B, and C), and (3) three thoracic sagittal modifiers (-/ N/ +). These three components will be discussed first and then incorporated, like Lenke Type 1A+ and Type 2A- for the final diagnosis.

The six different types of curves characterise the position of the structural and non-structural curves in the proximal thoracic (PT), main thoracic (MT) and thoracolumbar/ lumbar (TL/L) curves, and the region where the most tilted curve is found can be located. A curve over 25° in the coronal plane, more than 25° in a forward bend image or more than 20° in the sagittal plane is recognised as a structural curve. The curve with the largest Cobb angle is defined as the major structural curve in this system.

Table 2.2 Six Lenke classifications of scoliosis and criteria (Lenke et al., 2001)

<b>Classification</b>	<b>Criteria</b>
Type I	Main thoracic (MT) curve with positioning of major structural curve in MT area and minor non-structural curve in PT and TL/L
Type II	Double thoracic (DT) curve with positioning of major structural curve in MT, minor structural curve in PT and minor non-structural curve in TL/L
Type III	Double major (DM) curve with positioning of major structural curve in MT, minor non-structural curve in PT and minor structural curve in TL/L
Type IV	Triple major (TM) curve with positioning of major structural curve in MT or TL/L, and minor structural curve in PT
Type V	Thoracolumbar/ lumbar (TL/L) curve with positioning of major structural curve in TL/L and minor structural curve in PT and MT
Type VI	Double thoracolumbar/ lumbar (TL/L-MT) curve with positioning of major structural curve in TL/L, minor non-structural curve in PT and minor structural curve in MT

Besides, the lumbar spine modifier defines the symmetry of the lumbar and spine according to the relationship between the centre sacral vertical line (CSVL) and the apical lumbar vertebrae (ALV) with the curve group as reference, see Table 2.3. CSVL is marked as an upright straight line that crosses over the medial sacrum while the stable lumbar vertebra that is the nearest to the CSVL is used for comparison (Lenke et al., 2001). In this process, a vertical frontal radiography is taken to allow clear imaging of the CSVL and lumbar pedicle. The final data can also be used for later evaluation of postoperative location of the lumbar spine. Modifier A is the case where the CSVL is found between the pedicles and stable vertebrae without any lateral abnormality or rotation in the lumbar spine, and usually features Types 1 to 4 curvatures. Modifier B is used for Types 1 to 4 curvatures as well when the CSVL is lying in the lumbar

apex amidst the inner boundaries of the lumbar pedicle at the concave side of the body and lateral edge of the vertebrae apex. It is found to have a thoracic apex with low to moderate degrees of deformity in the lumbar spine. Modifier C is used for Types 5 and 6 curvatures when the CSVL is located entirely in the inner side of the concave vertebrae apex and no contact is found between the CSVL and vertebrae apex (Lenke et al., 2001).

As for the thoracic sagittal profile, this profile can determine the symmetry of the thoracic spine in accordance with the sagittal curve index between the 5<sup>th</sup> to 12<sup>th</sup> thoracic levels to prepare for medical intervention of scoliosis (Lenke et al., 2001). An angle smaller than 10° is classified as a hypokyphosis (-) case. Those with an angle between 11° to 40° are a normal (N) case. A hyperkyphosis (+) case is assigned when the angle is larger than 40° (Lenke et al., 2001).

Table 2.3 Lumbar spine modifier in Lenke Classification System (Lenke et al., 2001)

Curve Type				
Type	Proximal Thoracic	Main Thoracic	Thoracolumbar/Lumbar	Curve Type
1	Non-Structural	Structural (Major*)	Non-Structural	Main Thoracic (MT)
2	Structural	Structural (Major*)	Non-Structural	Double Thoracic (DT)
3	Non-Structural	Structural (Major*)	Structural	Double Major (DM)
4	Structural	Structural (Major*)	Structural	Triple Major (TM)
5	Non-Structural	Non-Structural	Structural (Major*)	Thoracolumbar/Lumbar (TL/L)
6	Non-Structural	Structural	Structural (Major*)	Thoracolumbar/Lumbar – Main Thoracic (TL/L–MT)

<p><b>STRUCTURAL CRITERIA</b> (Minor Curves)</p> <p><i>Proximal Thoracic:</i> –Side Bending Cobb <math>\geq</math> 25° –T2–T5 Kyphosis <math>\geq</math> +20°</p> <p><i>Main Thoracic:</i> –Side Bending Cobb <math>\geq</math> 25° –T10–L2 Kyphosis <math>\geq</math> +20°</p> <p><i>Thoracolumbar/Lumbar:</i> –Side Bending Cobb <math>\geq</math> 25° –T10–L2 Kyphosis <math>\geq</math> +20°</p>	<p>*Major = Largest Cobb Measurement, always structural Minor = all other curves with structural criteria applied</p> <p><b>LOCATION OF APEX</b> (SRS definition)</p> <table border="0"> <tr> <td><b>CURVE</b></td> <td><b>APEX</b></td> </tr> <tr> <td>THORACIC</td> <td>T2–T11-12 DISC</td> </tr> <tr> <td>THORACOLUMBAR</td> <td>T12–L1</td> </tr> <tr> <td>LUMBAR</td> <td>L1-2 DISC–L4</td> </tr> </table>	<b>CURVE</b>	<b>APEX</b>	THORACIC	T2–T11-12 DISC	THORACOLUMBAR	T12–L1	LUMBAR	L1-2 DISC–L4
<b>CURVE</b>	<b>APEX</b>								
THORACIC	T2–T11-12 DISC								
THORACOLUMBAR	T12–L1								
LUMBAR	L1-2 DISC–L4								

Modifiers		
Lumbar Spine Modifier	CSVL to Lumbar Apex	Thoracic Sagittal Profile T5–T12
A	CSVL Between Pedicles	- (Hypo) <10°
B	CSVL Touches Apical Body(ies)	N (Normal) 10°–40°
C	CSVL Completely Medial	+ (Hyper) >40°

Curve Type (1–6) + Lumbar Spine Modifier (A, B, or C) + Thoracic Sagittal Modifier (–, N, or +)  
Classification (e.g. 1B+): \_\_\_\_\_

### The Peking Union Medical College Classification System

The PUMC classification system is a broader and more inclusive system developed by Qiu et al. (2003). The system offers more detailed guidelines for patients with a thoracic lumbar double curve or those with lumbar curve smaller than 45° with a flexibility higher than 70%

while they are carrying out selective thoracic fusion (STF) (Qiu et al., 2005). The PUMC system includes every pattern of curvature found in scoliosis and divides them into three categories (PUMC Types I, II and III) according to the number of curves in the scoliotic spine. PUMC Type 1 denotes a single curve. PUMC Type 2 represents double curves while Type 3 is triple curves. After defining the type of curve, the system then classifies them into 13 subtypes with a more detailed criteria. Table 2.4 shows the types and subtypes of the PUMC classification system (Qiu et al., 2008).

Table 2.4 PUMC Classification System (Qiu et al., 2008)

PUMC Type I	Single Curve
Subtype Ia	Thoracic curve, apex between T2 and T11–T12 disc
Subtype Ib	Thoracolumbar curve, apex at T12, T12–L1 disc, and L1
Subtype Ic	Lumbar curve, apex between L1–L2 and L4–L5 disc
PUMC Type II	Double Curves
Subtype IIa	Double thoracic curves
Subtype IIb	Thoracic curve plus thoracolumbar/lumbar curve, the former is at least 10° higher than the latter. It is further divided into 2 subtypes
Subtype IIb1	Fulfill all 4 criteria: (1) Without thoracolumbar/lumbar kyphosis (2) The Cobb angle of thoracolumbar/lumbar curve is $\leq 45^\circ$ (3) Apical rotation of thoracolumbar/lumbar curve $< 2^\circ$ (4) Flexibility of thoracolumbar/lumbar curve $\geq 70\%$
Subtype IIb2	Not meet any of the aforementioned criteria
Subtype IIc	Thoracic curve plus thoracolumbar/lumbar curve, the curve magnitude difference is $< 10^\circ$ . It is further divided into 3 subtypes by comparing the curve flexibility
Subtype IIc1	Meet both the following 2 criteria: (1) Flexibility of thoracic curve is more than the thoracolumbar/lumbar curve (2) The Cobb angle of the thoracic curve on convex bending radiograph is $\leq 25^\circ$
Subtype IIc2	Meet both the following 2 criteria: (1) Flexibility of thoracic curve $>$ thoracolumbar/lumbar curve (2) The Cobb angle of the thoracic curve on convex bending radiograph is $> 25^\circ$
Subtype IIc3	Flexibility of thoracic curve $<$ thoracolumbar/lumbar curve
Subtype IId	Thoracic curve plus thoracolumbar/lumbar curve, the former is at least 10° smaller than the latter. It is further divided into 2 subtypes according to the flexibility of the thoracic curve
Subtype IId1	Cobb angle of the thoracic curve on convex bending radiograph is $\leq 25^\circ$
Subtype IId2	Cobb angle of the thoracic curve on convex bending radiograph is $> 25^\circ$
PUMC Type III	Triple Curves
Subtype IIIa	Distal curve meets IIb1 lumbar curve criteria
Subtype IIIb	Distal curve meets IIb2 lumbar curve criteria

### **Comparison of classification systems**

A number of studies in the literature have assessed and compared the effectiveness and

limitations of the currently available classification systems of scoliosis. For example, Ward et al. (2008) suggested that the King classification system is more comprehensive with a longer history compared to the Lenke classification system. Nevertheless, there are several arguments that the former is limited, and its effectiveness, reliability and duplicability are ambiguous, due to the inadequate information provided (Alam et al., 2013; Edgar, 2002; Lenke et al., 2001; Rigo et al., 2010; Zhang et al., 2013). Hannes et al. (2002) stated that the King classification system only has a medium degree of reliability. It is concluded that this system has low intra- and inter-observer reliabilities, together with a limited coverage of curvature patterns since it only emphasises the frontal radiography of the spine column and neglects the symmetry of the sagittal plane (Cummings et al., 1998; Lenke et al., 1998; 2001; Smith et al., 2008).

Comparatively, the Lenke classification system classifies the frontal plane first and hence differentiate the thoracic, lumbar, double or triple major curve (Richards et al., 2003). The system has higher inter- and intra-observer reliabilities as it requires both frontal and sagittal x-ray screenings (Ogon et al., 2002; Richards et al., 2003). Phan et al. (2010) stated that the step-by-step schema enhances the reliability of this system. The Lenke system is considered to be more unbiased with a wider and more comprehensive coverage of the different types of spinal curvatures, in which the two modifiers are conducive to the treatment arrangements (Puno et al., 2003). Despite that, Negrini et al. (2018) stated that the objective indicator in the Lenke classification system is not appropriate for scoliosis cases when the patient does not need to undergo surgery. This shows that scoliotic patients who are prescribed bracing or corrective exercises rarely need side bending radiography. Furthermore, the Lenke system cannot identify the minor structural curve in patients with a minor curve smaller than  $30^\circ$  while they are standing for the side bending radiography. Ogon et al. (2002) also mentioned that the system is not effective in finding the upper thoracic and lumbar curves. Besides, the radiographic images may not be able to clearly show the location of the CSVL, especially for smaller spinal curvatures.

As for the PUMC classification system, its reliability is equal to or higher than the Lenke Classification System due to fewer measurements of the curve angle and hence fewer subjective errors (Qiu et al., 2008). It is also found that the inter and intra-observer reliabilities of the PUMC system is higher compared to the Lenke system (Qiu et al., 2008). Moreover, the PUMC system has more distinct guidelines but no high technical requirements for conducting a radiography is needed.

### **2.2.5 Prevalence of Adolescents Idiopathic Scoliosis**

The Student Health Service of the Department of Health (2022) in Hong Kong stated that scoliosis affects 2-3% of adolescents. The spinal curvature of adolescent girls progresses more quickly than that of boys and hence they have a greater need for AIS treatment (Kubat & Ovadia, 2020; Raggio, 2006; Parent et al., 2004; Roach 1999; Weinstein, 1994; Pehrsson et al. 1992). Parent et al. (2005) indicated that the girl to boy ratio of those who suffer from spinal curvature with a Cobb angle of 10 to 20° is 1.3:1 while those with a Cobb angle of more than 30° is 7:1. This shows that the progression of spinal curvature is more serious among female children.

There is the assumption in previous research that topography is one of the factors that affect the morbidity rate of AIS patients (Grivas et al., 2006; Grivas, Vasiliadis, Savvidou, et al., 2006). In Hong Kong, the Department of Health organises an annual comprehensive health check with the assistance of the Student Health Service Centres and Special Assessment Centres and all primary and secondary school students are invited to participate in the health check. In the school screening system, students who are diagnosed with a Cobb angle of over 20° will be provided with a follow-up examination or treatment (Luk et al. 2010). It is generally assumed that the progression of AIS can be controlled and slowed down since the scoliosis can be addressed in the early stages (The University of Hong Kong- Faculty of Medicine, 2012). In the Department of Health 2013/2014 Annual Report, 6% are diagnosed with AIS out of 661,201 students who participated in the screening. Besides, the Department of Health 2009/2010 Annual Report indicated that scoliosis is the third most prevalent condition with 4.5% of the 737,922 students identified with AID in the screening programme during 2008/ 2009. This is higher than the 3.08% identified in 1998/1999 or an increase of 1.42%, which shows a trend of increase of AIS in Hong Kong. A number of research studies make assumptions about the progression of scoliosis including the use of a heavy schoolbag and incorrect posture during standing or sitting (Wong & Wong 2008; Bessette & Rousseau 2012). Chow et al. (2006) pointed out that girls with AIS have difficulties controlling their standing posture in comparison to those without AIS when they are carrying their schoolbag and are more prone to falls due to their asymmetric trunk.

Statistics on AIS in previous studies show that about 10% of those with AIS are prescribed conservative therapy like wearing a brace while 0.1 to 0.3% need surgery on their spine

(Negrini et al., 2018) Charles et al. (2006) conducted a study with 205 IS patients and found that the likelihood of surgery is 16% with a Cobb angle of about 20° at the beginning of puberty which is increased to 100% with a Cobb angle of more than 30°.

### **2.2.6 Treatment options for AIS**

The degree of the spinal deformity and skeletal maturity are used to classify the type of scoliosis, so that different treatment methods are prescribed accordingly. Negrini et al. (2012) stated that the fundamental goals of corrective treatments are to reduce the progression of scoliosis, and prevent respiratory problems and related pain as well as correct posture and the body contours. As such, patients are categorised as having a mild, moderate or severe Cobb angle.

Those who are considered to have mild AIS have a Cobb angle between 6° and 20°. As such, they are only recommended to regularly visit their physician every 6 to 12 months. Inpatient rehabilitation, respiratory care, rehabilitation exercise or physiotherapy are also conventional options for those with mild scoliosis (Weiss & Goodall 2008). In some cases, only simple observation is provided for patients diagnosed with a spinal curvature of 20° to 30° if they do not have other apparent health issues like back pain.

AIS patients with a Cobb angle between 21° and 40° are classified as moderate cases and generally recommended to undergo non-invasive therapy like bracing. Bracing is a common non-invasive method to reduce the progression of the spinal curvature for moderate AIS cases; that is, those with a Cobb angle of 20°-30° and Risser's 0-3 (Hresko, 2013; Trobisch et al., 2010; Lonstein, 2006; Negrini et al., 2006; Richards et al., 2005). The brace prevents the further deterioration of the spine in the early stages of scoliosis before skeletal growth is finished, so the need for spinal surgery is minimised (Bettijane, 1999). According to CareAllies (2007), the targets of bracing include: (1) patients with a Cobb angle of over 25° before skeletal maturity; (2) patients who have a Cobb angle between 20° and 29° and 2-years of growth left or girls who have not had their first menstruation; (3) patients with a Cobb angle between 20° and 29° and a deteriorating curve during their growth period. During bracing treatment, corrective pressure is applied onto the spine and torso to inhibit the progression of the curvature (Negrini et al., 2015). Patients need to wear the brace for about 23 hours daily in the early stages of treatment (Negrini et al., 2009). After the growth spurt, the bracing time can then be reduced. Sometimes, physiotherapy or rehabilitation exercises are used together with bracing to enhance

the corrective effect. Existing braces are classified into hard, semi-rigid and flexible braces, all of which share a common principal on correcting the spinal curvature by enhancing the spinal symmetry and arrangement through corrective mechanical forces like the three-point pressure system (Weinstein et al., 2013; Coillard et al., 2002).

Patients with a spinal curvature that is greater than  $45^\circ$  are considered to have severe scoliosis and spinal fusion surgery is recommended (USC Center for Spinal Surgery, 2005; Dolan et al., 2007). During surgery, the surgeon will add bone graft to the vertebrae and the bones in the spine will grow and connect together into one straight and solid structure. This surgery is considered to have a permanent effect. Yet, there are arguments on the restriction of skeletal growth since failure of spinal fusion may occur (Morgan & Scott, 1956). After corrective therapy, patients need to conduct follow-up visits that range from 2-3 months to 36-60 months along with X-ray imaging, in which the length of the follow-up time is based on the level of skeletal maturity as graded by the Risser system (Scoliosis Research Society, 2023).

### **2.3 Existing orthosis products for scoliosis**

As stated earlier, braces that have been developed for treating scoliosis are categorised as hard, semi-rigid, and flexible braces. The different types of existing braces are reviewed in the following section.

#### **2.3.1 Hard braces**

Hard braces are the conventional type of brace usually provided to patients with a Cobb angle between  $21^\circ$  and  $45^\circ$  (Liu, 2015). These braces are constructed with solid plastic material and inner paddings. The biomechanism used by most hard braces is the three-point pressure system, see Figure 2.12, which is considered to be the most effective way of treating scoliosis and provides a corrective effect by applying external forces to a specific point on the spine (Qian et al., 2010). Traditional hard braces are categorised based on the length of use each day. Full time rigid braces (FTRBs) require patients to wear the brace for 20 to 24 hours every day. Night time rigid braces (NTRBs) need to be worn for 8 to 12 hours while sleeping. Part time rigid braces (PTRBs) require a wear time of 12 to 20 hours after school and at night. Examples of some commonly prescribed traditional hard braces are shown and described in Table 2.5.

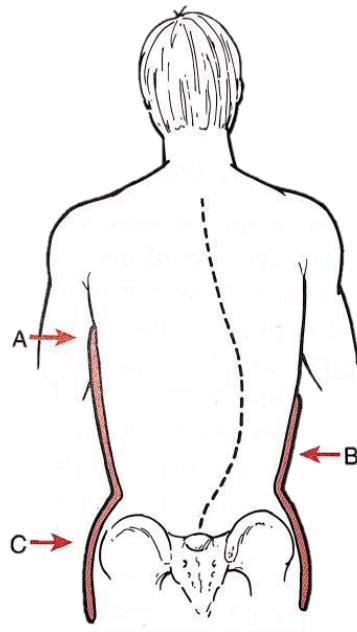


Figure 2.12 Three-point pressure system of thoracic-lumbo-sacral orthosis (Seymour, 2002)

Table 2.5 Commonly prescribed traditional hard braces

 <p><b><u>Boston Brace</u></b> (Medical Expo, 2023; Fayssoux et al., 2010)</p>	 <p><b><u>Dynamic derotation brace</u></b> (Grivas et al., 2010)</p>	 <p><b><u>Chêneau Brace</u></b> (Pham et al., 2008)</p>
 <p><b><u>Lyon Brace</u></b> (de Mauroy et al., 2011)</p>	 <p><b><u>Milwaukee Brace</u></b> (Optec USA, 2020; Maruyama et al., 2011)</p>	 <p><b><u>Charleston Bending Brace</u></b> (Fayssoux et al., 2010)</p>

The **Boston brace** is one of the most well-known thoracic-lumbo-sacral-orthoses (TLSOs) in

the North American market (Medical Expo, 2023). It is constructed by using a pre-made polypropylene outer shell and soft polyethylene foam as the inner lining. The plaster model is customised for each patient based on his/her body contours. The brace accommodates 15° of lumbar lordosis in the pelvic module, with straps fixed at the waist. The straps are pulled to fasten them and pressure is exerted onto the abdomen at the front and the trunk from the side (Chase et al., 1989). Besides, non-detachable pads are inserted to apply corrective forces at a particular location after determining the degree of the spinal curvature and curve apex through a standing radiography (Chase et al., 1989). Passive forces are exerted onto the convex side of the curvature through the upper pads while active forces exerted onto the concave side of the curvature through the pads fixed close to the open space zone in the top part of the brace (Dolan et al., 2007; Wiley et al., 2000; Lonstein, 2003).

The **dynamic derotation brace** is a modified version of the Boston Brace. It is developed specifically for patients with spinal rotation issues. This brace has aluminium blades that rotate in opposite directions at the back of the brace. Forward pressure is applied in the lateral side and backward pressure is applied to the other side, so the two parts of the brace move towards each other laterally (Grivas et al., 2010). The brace applies passive and active forces, with the former exerted by the brace itself and the latter by the wearers themselves when they pull away from the pressure (Grivas et al., 2010).

The **Chêneau brace** is a thermoplastic TLSO developed by Jacques Chêneau in 1979 for scoliosis and thoracic hypokyphosis patients (Federico & André, 2011). The three-point pressure system is the main corrective mechanism of this brace. The Chêneau brace can be used to treat all levels of spinal curvatures. Rigo et al. (2009) stated that the Chêneau brace applies torsional force for corrective purposes, which would not affect the sagittal structure of the spine. The brace has multiple pressure zones and expansion chambers to apply corrective forces (Giorgi et al., 2013). The convex part of the curvature is pulled towards the centre while the concave part of the curvature will shift from the centre due to the natural movement of the soft tissues. Free space is provided by the convex anterior and concave posterior so that the rib cage can expand towards the concavity which facilitates normal deep breathing as well as accommodates irregular breathing patterns during exercise (Kotwicki & Cheneau, 2008).

The **Lyon brace** is a type of TLSO that also uses the three-point pressure system, and designed by Pierre Stagnara in 1947. This brace is mainly prescribed for patients in Europe with a

thoracic curvature (Aulisa et al., 2015). The Lyon brace is composed of two upright steel bars with joints in the front and back and an outer shell connected to the bars. The outer shell is constructed from Plexidur™, which is a thermoplastic or poly(methyl methacrylate), and separated into multiple parts with different functions, including (1) a shell that balances the shoulders and convex side of the chest, (2) two thoracic shells with one placed at the convex side of the chest and the other at the opposite side to create a counter force, (3) a lumbar shell at the abdominal ribs, and (4) a pelvic belt that is made up of two half shells. The position of the shells in the upright bars can be adjusted based on the spinal situation while the pelvic belt can hold the brace firmly. Force is exerted onto the convex side of the body with some room for expansion in the concave part. de Mauroy et al. (2011) stated that spinal elongation is possible with the Lyon brace since the brace can be casted with continuous traction, which can reduce any constraints of the vertebra discs and correct the spinal curvature. The brace has flexibility, so that it can be modified as patients grow during puberty. The Lyon brace can accommodate a maximum increase of 7 cm in height and 7 kg in weight (de Mauroy et al., 2011).

The **Milwaukee brace** is also known as a cervical-thoracic-lumbo-sacral orthosis (CTLSO), which covers the entire body from the neck to the pelvis (Federico & André, 2011). It is supposed to target a curve apex above or at the 8th thoracic (Canavese & Kaelin, 2011). The most common version of the Milwaukee brace is that developed in 1946 by Walter Blount and Albert Schmidt (Optec USA, 2020). The brace includes a pelvic section which is made of plastic, one front and two back bars that are linked with a neck ring, auxiliary bands, and chest and lumbar pads (Maruyama et al., 2008). Attached together with the neck ring are a pad at the throat in the front and two pads at the back. The neck ring can help to fix the head so that it is in the midline of the pelvis while the metal bars can lengthen the trunk (Lonstein, 2003; Mac-Thiong et al., 2004; Wiley et al., 2000). The bracing mechanism is based on a two-point pressure system and force is actively exerted onto the anterior and lateral sides of the body by the patients themselves during elongation, which can keep the trunk and neck in the right posture (Blount & Moe, 1973). Corrective pressure is exerted through non-detachable pads and metal bars with bands onto a particular area based on the spinal situation (Qian et al., 2010).

The **Charleston Bending Brace** is an NTRB for patients to wear during sleeping, which can increase their compliance to bracing (Price et al., 1990). This brace uses a customised plaster model with solid plastic material. Price et al. (1990) indicated that this orthosis is designed to

stretch the spine to an over-corrected position, which results in a greater extension of the soft tissues that releases the stress of the endplates on the concave side of the spine. Owing to the overcorrected position, higher corrective forces are exerted so that the brace does not need to be worn during the day which removes or reduces the inconveniences brought about by bracing on daily life activities and thus increases compliance with treatment.

### 2.3.2 Semi-rigid braces

Comparing to hard braces, semi-rigid braces are constructed with both hard and soft materials and can provide greater wear comfort and flexibility. Again, the three-point pressure system is used as the main mechanism. Examples of semi-rigid braces include the TriaC Brace and the DonJoy® Back Brace II TLSO as shown in Table 2.6.

Table 2.6 Examples of semi-rigid braces

 <p><b>TriaC Brace</b> (Veldhuizen et al., 2002)</p>	 <p><b>DonJoy® Back Brace II TLSO</b> (DJO Global, 2023)</p>
--	---

The **TriaC Brace** can accommodate every curve pattern except when the apex of the curve is at the 12th thoracic and 1st lumbar vertebra. The aim of this brace is to provide treatment with good wear comfort and aesthetics but also can be easily used. The brace has three core design components, including the: (1) frame, (2) flexible components (springs or elastics) and (3) pelottes (Veldhuizen et al., 2002). The components of this brace are usually softer materials so the brace is lighter and gives a more natural profile so that younger patients are more receptive to its use as there is less impact on their self-esteem (Veldhuizen et al., 2002). Again, the brace uses the three-point pressure system. Corrective pressure is applied at the anterior plane and thoracic area in the sagittal plane (Veldhuizen et al., 2002). Bulthuis et al. (2008) conducted a

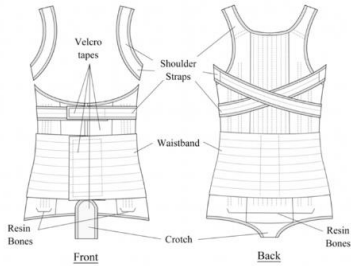
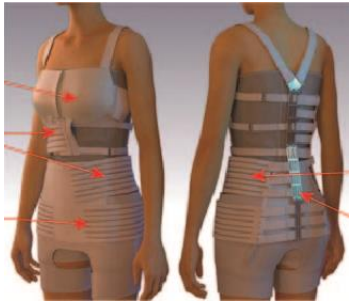
wear study, and found that the Cobb angle is reduced from 30.2° to 22° with the use of this brace.

The **DonJoy® Back Brace II-TLSO** is a brace that also uses the three-point pressure system. It is produced by DJO which is an international producer of orthopaedic equipment for recovery or rehabilitation ( DJO Global, 2023). Solid panels are installed in the front and back to prevent the trunk from buckling or rotating, and provide comprehensive and stable support from the shoulder blade-thoracic area to the intersecting point of the sacrum and tailbone. The solid overlapping side panels offer transverse stability, and the solid frontal panel restricts flexion. They can be easily unfastened and thermally manipulated for customisation based on the body contours of different patients. Besides, a telescoping sternal Y-bar is installed which can be adjusted and fixed at a specific height or angle to restrict movement and apply suitable forces. To facilitate three-points of pressure, the pads in the sternum and pelvis apply backward forces while the pads on the thoracic vertebrae apply forward forces onto the spine. This system limits forward flexion while extending the lumbar spine, which can thus fix the spine firmly to withstand lateral rotation. To improve the wear experience of patients, the brace is composed of flexible shoulder straps with soft pads inside, which enhance wear comfort and restrict the brace from sliding up during sitting. The brace is designed to be light, air-permeable and comfortable due to the spacer fabric used for the lining. In addition, the patented mechanical advantage pulley system facilitates modifications easily as desired.

### **2.3.3 Flexible braces**

Even though rigid braces are considered to be the traditional means of correcting scoliosis by stabilising the body and minimising any further progression of the spinal curvature, more and more flexible braces are being developed as a new form of therapy for scoliosis as they are more comfortable to wear and less bulky underneath clothing, and therefore increase treatment compliance. Examples of flexible braces include the Dynamic SpineCor Brace, Spinealite™, Dynamic Movement Orthosis (DMO) Structural Scoliosis Suit, Ergonomic Brace, and anisotropic textile brace as shown in Table 2.7. The soft orthosis of interest in this research study is the PCG in Liu et al. (2015), which will be elaborated in detail in Section 2.5.

Table 2.7 Examples of flexible braces

 <p><b>SpineCor Brace</b> (The SpineCorporation Limited, 2018)</p>	 <p><b>Spinealite™</b> (Issuu Inc., 2023)</p>	 <p><b>Posture Correction Girdle</b> (Liu, 2015)</p>
 <p><b>DMO Structural Scoliosis Suit</b> (DMO Orthotics, 2023)</p>	 <p><b>Ergonomic Brace</b> (Fung, 2020)</p>	 <p><b>Anisotropic Textile Brace</b> (Fok et al., 2021)</p>

The **SpineCor Brace** is a dynamic brace that was developed at Sainte-Justine Hospital in Quebec, Canada during 1992-1993 (Coillard et al., 2003). This is a flexible brace with a vest-like appearance. There is a pelvic base that comprises a belt and three soft thermoplastic pieces, two bands at the crotch and thighs respectively for stabilisation, a cotton bolero and four flexible bands that range from 0.2 m to 1 m for curve correction (ScoliCare, 2023; Coillard et al., 2003). The components of the SpineCor brace have a thickness that is less than 1.5 mm (Hasler et al., 2010). By adjusting the position of the elastic bands, the brace can be arranged in different configurations that offer targeted corrective movements to address different types of spinal curvatures (Coillard et al., 2003). The core principle of the corrective mechanism is the spinal coupling mechanism, which is meant to address the spinal curvature and increase symmetry of the trunk by pushing, rotating or pulling the trunk to improve the position of the spine with the use of the corrective bands (Coillard et al., 2003). Wong et al. (2008) indicated that the brace will inhibit the progression of the deformity and correct the profile in different postures by monitoring the shoulders, chest and pelvic girdle. The corrective mechanism

depends on active force rather than passive force, which is the opposite of traditional hard braces. The active corrective forces can inhibit curve progression, align and strengthen biofeedback of the muscles and nervous system, and correct the posture of patients (The SpineCorporation Limited, 2018). Coillard et al. (2008) recommended that scoliosis patients participate in the SpineCor® Exercise Program that is customised to every patient to enhance the bracing effect.

**Spinealite™** is a soft brace developed by GmbH & Co KG, a German company based on the SpineCor brace with the aim to reduce the inconvenience of toileting while wearing the brace. The brace can be more easily adjusted which means it is easier to use. A 3D system for correction is used to correct posture with the use of pelvic and spiral shoulder girdles. The sagittal plane profile is also corrected. Spinealite™ uses elastic bands, but their elasticity is lower than that of the bands used in the SpineCor brace in order to retain tension force and optimise the corrective forces. Nevertheless, the brace restricts movement, is less comfortable to wear, and affects daily activities (Issuu Inc., 2023).

The **DMO Structural Scoliosis Suit** is developed by DM Orthotics (2023) to address severe spinal deformity. This brace provides counter rotation with the strategic placement of different panels, which compresses the curved part of the spine. Since the panels are installed in specific parts of the body, the balance, stability, and mobility of the user can be strengthened. The DMO Structural Scoliosis Suit is a suit that tightly fits over the upper body and lower torso (Matthew, 2017). A reinforcement strap is attached to the torso, extended over the front or rear of the torso, crosses over one side of the shoulder and down to the underside of the armpits, and then through to the end at the hip (Matthew, 2017). The panel around the bottom front and back part of the trunk provides a bracing function that can resist rotation and apply compression. As for the two panels around the pelvis, they enhance the stability and balance of the users. Beyond the arrangement of panels, the DMO Structural Scoliosis Suit is fabricated with compression textile (i.e. Lycra® blend) for greater wear comfort and ease of mobility. As a custom-tailored suit, users can choose their preferred fasteners, openings plus reinforcements.

The **Ergonomic Brace** is a recently developed soft brace (Fung et al., 2020), specifically for scoliosis patients with a Cobb angle between 25° to 40°. The brace resolves the main problems of hard braces including low treatment compliance and a long manufacturing period (Fung et

al., 2020). With the aim to increase treatment compliance while retaining efficacy, the Ergonomic Brace contains soft elements for greater wear comfort and a hard component to ensure adequate corrective ability during treatment. The Ergonomic Brace consists of a compact knitted bodice supported by plastic resin bones, rigid pads, rigid straps with adjusters, pad holders, and pelvic belt. The plastic resin bones are placed uniformly along the sides of the bodice to straighten the posture and prevent the bodice from sliding upward. As for the rigid pads inside the pad holders, they create the corrective pressure exerted onto the spine. The pad holders are hot pressed onto the bodice. Layered and single layer pads are placed to treat the spinal condition; that is, the former provides the main corrective force while the latter is used as a counter corrective force or to correct a smaller curve. Rigid straps on the Boa® closure system are tightened to create and apply pressure for correcting the spinal curvature. Finally, the pelvic girdle is used to stabilise the pelvis to enhance spinal correction.

The **anisotropic textile brace** is created specifically for female scoliosis patients with a spinal curve of 20 to 30° (Fok et al., 2021). The aim of this brace is to provide a more comfortable user experience and allow patients to move more conveniently as opposed to wearing a hard brace thus anticipating to resolve the common problem of low treatment compliance. The anisotropic textile brace uses both the three-point pressure system and flexible fabric as its core design features. It is designed to be a customised garment that exerts corrective forces to treat scoliosis, with a bra top, corrective bands, pelvis belt, shorts and artificial backbone. The framework of the brace is based on the bra top and shorts, in which Velcro is stitched in the centre of the shorts in the front to attach the corrective bands. These corrective bands are made of two wide and flexible textiles of high elasticity. A bulging silicon pad is put in the middle of the two elastic straps to exert corrective forces at the convex part of the spine and reduce the spinal curvature. Besides, two wide elastic straps make up the pelvis belt which are fixed around the pelvis to maintain alignment at the base of the spine as well as keep the hinged backbone in the right position. The artificial backbone is constructed from hinges of different lengths, and it is the core element of the back of the brace, which helps to support the corrective bands. Its special structure can inhibit torso rotation and loss of suspension of the brace without limiting the forward-bending of patients (Fok et al., 2021).

#### **2.3.4 Problems of existing orthoses for AIS**

The following section discusses some of the problems of existing orthoses (hard, semi-rigid

and soft braces) in the treatment of AIS.

### **Hard braces**

Most scoliosis patients are required to wear a hard brace for 23 hours every day as their treatment regimen. Their trunk including chest and abdomen are compressed owing to wearing the tightly fitting and rigid brace for long periods of time. This gives rise to feelings of discomfort, breathing issues and even skin irritation (Canavese & Kaelin, 2011). The low breathability of the hard plastic and metal materials used for the brace trap heat and sweat, which intensifies the negative perception of hard braces, especially in the summer (Negrini et al., 2010; Refsum et al., 1990; Pehresson et al., 2001). Some users may find that wearing a hard brace can escalate to sleep disorders, headaches, poor sleep quality, psychological disorders like anxiety, and cognitive deficit (Climent & Sánchez, 1999). Physically, the limitations on body movement may lead to muscular dystrophy and lower flexibility of the spine if patients greatly depend on the brace to support their body because they can barely use their muscles to control or balance their trunk (Berger et al., 1983). The soft tissues and sternum may be damaged permanently and patients may also suffer from ulcers, skin indentation, irritation, or mobility problems under the prolonged compression of the brace (Frontera et al., 2008).

Moreover, traditional hard braces are usually made of thermoplastic material that is white in colour or skin tone, so that they resemble traditional medical prosthetic devices. Since hard braces are usually aesthetically unappealing and its profile can be easily noticed by others, young patients resist their use as they are usually very concerned about their image and want to conform to their peers (An & Lee, 2015; Liu & McClure, 2001). The hard brace is visible underneath clothing, and patients consider the brace as a negative reminder of their condition which differentiates them from normal people. AIS patients may thus suffer from low self-confidence (Stokes & Black, 2012). Bracing treatment with a hard brace also causes mental health issues and lowers self-esteem (Weiss et al., 2010; Bunge et al., 2009; Asher & Burton, 2006). AIS patients also suffer from feelings of awkwardness, depression, and shame.

Since the hard brace causes discomfort, is aesthetically unappealing, limits movement and is emotionally difficult to accept, the compliance with this type of treatment is lower. According to Landauer et al. (2003), patients who comply more with treatment experience less progression of their spinal curvature, while those who have a lower rate of compliance will experience a greater progression of their spinal curvature. If patients do not wear their brace for the

prescribed amount of time, the effectiveness of the brace will be reduced so that the efficacy of the treatment cannot be realised (Negrini et al., 2015; Climent & Sánchez, 1999). Treatment failure is also plausible when compliance is very low (Dworkin et al., 1985).

### **Semi-rigid braces**

Some of the hard material used in hard braces are replaced with softer and more flexible material in semi-rigid braces, which can allow more movement and improve the physical profile (Veldhuizen et al., 2002). Compared to hard braces, the compliance rate of patients who wear a semi-rigid brace is higher. Yet, the compression from these braces can also cause skin irritation and sores just like hard braces (Bulthuis et al., 2008). In addition, few research studies have shown the effectiveness of semi-rigid braces in correcting scoliosis, which limits its usage in bracing therapy.

### **Flexible braces**

Since AIS patients need to wear a compressive brace for a long period of time to correct their spinal condition but show low compliance with treatment that requires use of a hard or semi-rigid brace, more flexible braces have been developed to enhance treatment compliance and wear comfort. However, Wong et al. (2008) stated that the discomfort, low breathability, skin irritation, sores, and restriction of movement and breathing are still found with the use of flexible braces even though the issues are less severe comparatively speaking. It was observed that some patients will remove their brace or detach the bands or straps if they feel uncomfortable while eating, which will delay the corrective process. In addition, some flexible braces cause inconvenience during donning and doffing, or toileting. Much effort is required to don and doff the garment. Then there is also its bulky appearance, which affects QoL (Wong et al., 2008). For example, the plastic shell of the dynamic SpineCor brace covers the pelvis, which prevents patients from bending when they go to the toilet. The outcome in terms of user-friendliness of flexible braces falls below expectations, which gives rise to the same limited results with compliance to the hard brace (Hasler et al., 2010).

Apart from the factors that influence compliance with bracing treatment, the effectiveness of flexible braces has been the subject of criticism due to the insufficient number of subjects and incomplete criteria for the target subjects compared with the vast experiences and achievements of hard braces according to Gutman et al. (2016). Some of the information in the wear trial of flexible braces like the DMO Structural Scoliosis Suit is not clearly expressed with missing

accurate data on the subject matter, which reduces the reliability and validity. Besides, the long-term outcomes of flexible orthoses have not been demonstrated. The size of the sample in past research is found to be too small, which is not enough to assess the effectiveness of the flexible brace (DMO Orthotics, 2023). Due to the limited number of studies on the performance of soft braces, it is important to conduct more wear trials on different flexible braces with a large sample over a longer period of time.

Besides, the actual ability of flexible braces to correct spinal deformity is considered to be low compared to hard braces. A number of studies in the literature have indicated that soft braces cannot replace hard braces due to the limitations found (Weiss & Werkmann, 2012). Costa et al. (2021) further showed evidence that the corrective outcomes of hard braces excel those of soft braces.

## **2.4 Overview of posture**

### **2.4.1 Definition of posture**

Raine and Twomey (1994) defined posture as the attitude or position of the body, the arrangement of the body parts, or the manner in which people uphold and keep the body in balance. Posture is made up of various factors including gravity, muscle tension, sense of wholeness and bone strength (Raine & Twomey, 1994; Newton & Neal, 1994). Posture can be commonly categorised as static and dynamic postures. The former is known as the state when muscles and skeleton are balanced which keep the body stable through the alignment of the body components. Dynamic posture is how body components are aligned during movement (Eston & Reilly, 2008). The gravity line, which is distinguished by drawing an imaginary vertical line that crosses the point where gravity force is acting on the body, is the key factor to determine proper alignment for upright postures (Eston & Reilly, 2008; Penha et al., 2009). Good posture is when the muscles and skeleton maintain balance to avoid damage or continued disfiguration in the body regardless whether the body is resting or active (Penha et al., 2005). Poor posture, in contrast, represents a long-term situation in which the body is not positioned with a “neutral spine” (Wong & Wong, 2008; Dworkin et al., 1985, Birbaumer et al., 1994). Postural issues are easily found in AIS patients since their spinal curvature affects the trunk outline and the association between body divisions (Goldberg et al., 2001; Masso & Gorton, 2000). Poor posture further changes the attitude of the body and position of the head, shoulders, shoulder blades and pelvis in the frontal, sagittal and transverse planes during different postures,

and increases the rotations of the body in the transverse plane (LeBlanc, 1997).

#### **2.4.2 Importance of proper posture**

The right posture involves coordination and mobilisation of all parts of the body instead of a few parts of the body. It is essential to adhere to good postural patterns and balance in order to prevent trunk deformity during adolescent growth spurt. To determine whether a posture is proper, Lau (2011) recommended two easy and efficient tests: the Wall Test and Mirror Test. In the Wall Test, patients need to stand with their back against a wall with their head and feet coming into contact with the wall but 6 inches should be retained between the heels of the feet and the wall. If there are 1-2 inches between the neck or lower back and the wall, this signifies that the posture is correct. As for the Mirror Test, patients can observe the alignment and position of their body segments in the correct posture with the use of a full-length mirror and adjust their posture based on five checkpoints, which range from confirming that the shoulders are level to whether the ankles are straight. Through these simple tests, patients can determine whether their posture is correct and train themselves to adopt a proper posture independently or with the help of family members or therapists to halt the progression of spinal curvature.

The standard for a correct standing posture is to stand straight by making use of the thorax, abdomen and butt muscles as defined in McKenzie and Van Wijmen (1988). Both the posterior and anterior muscles are used to keep the body upright. Figure 2.13(a) shows a proper standing posture (Kwok, 2017). The lumbar lordosis is reduced accordingly (McKenzie & Van Wijmen, 1988). Joel Goldthwait (1915, cited from Zacharkow, 1988), Chief of Orthopaedic Surgery in Boston in the 1900s who found that many physical issues are attributed to body misalignment, added that improper standing posture is detrimental to health in that the lungs may expand less when inhaling, and the diaphragm will be flattened thus limiting mobility so that respiratory capacity is reduced.

McKenzie and Van Wijmen (1988) further suggested that a proper sitting posture is identified with the alignment of the head and ankles in a vertical line, balanced shoulders and hips, jaw that is in parallel with the ground surface and symmetric to the ears, and kneecaps that are pointing forwards. Figure 2.13(b) shows the alignment of a proper sitting posture (Kwok, 2017). A forward-leaning lumbar spine in small degrees is required to support the trunk without adding to the load on the spine. Lumbar lordosis results, so the trunk is supported by the lumbar

muscles and the spine as the head is kept upright.

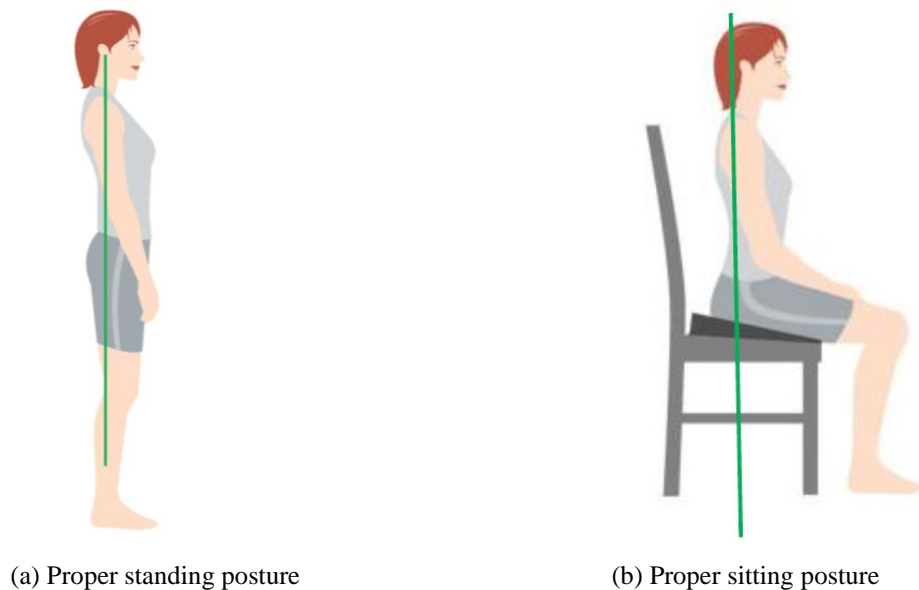


Figure 2.13 (a) Proper standing and (b) sitting postures (Kwok, 2017)

### 2.4.3 Poor posture and consequences

Incorrect posture and poor control of body position will intensify pain and trunk deformity, especially for AIS patients. AIS patients are found in general to have posture issues associated with the alignment of the head, shoulders, shoulder blades and pelvis (Sevastik & Diab, 1997). Studies have noted that an asymmetric posture and unstable posture control lead to spinal curvature and pain (Wong & Wong, 2008; Chen et al., 1998). Poor posture will distribute body weight on the spine unevenly, which gives rise to asymmetrical spinal development and wedged vertebrae. Those with poor posture patterns are more inclined to fall, especially if they carry heavy objects due to inadequate balance of the trunk (Chow et al., 2006). This results in spinal curvature and intensifies the progression of scoliosis. As the spinal curvature increases in size, the distribution of loads will be more irregular, and higher loads will be exerted onto specific parts of the spine. Muscle and skeletal balance is reduced. This creates a vicious cycle with poor posture which leads to spinal curvature before skeletal maturity (Burwell et al., 2006).

### 2.4.4 Prevalence of poor posture

Improper posture is a common phenomenon among adolescents. Juskeliene et al. (1996) measured the distance from the 7th cervical vertebra (C7) to the lower angles of the left and

right shoulder blades of 791 children and found that 46.9% of them have an unbalanced torso due to incorrect posture. Besides, an examination of the sitting posture of 95 children between 8 and 12 years old resulted in the finding of no correct posture (Oates et al., 1999). Furthermore, Marschall et al. (1995) found that 22.8% of primary school students suffer from back pain which is even more common among secondary school students (33.3%). The improper posture caused by the design of school desks is the main reason for the research outcome. In addition, Hong et al. (2011) found that the style and weight of schoolbags are associated with spinal alignment. Students who use shoulder bags have inclined spinal postures when they walk up the stairs. Children whose schoolbags are more than 15% of their weight are observed to have inclined spinal posture. To prevent the progression of spinal curvature caused by poor posture, it is essential to undertake measures that correct the posture during the growth spurt of adolescents.

#### **2.4.5 Posture correction methods**

There are different types of posture correction methods, such as exercise training, biofeedback postural training, posture correction garments, etc. Some of these are reviewed in the following section.

##### **Exercise training**

The **Schroth method** was founded by Katharina Schroth in 1921, which aims to treat scoliosis by correcting the position and alignment of the body segments. The Schroth method separates the trunk into four segments, which are the shoulders, chest, lumbar, and hip and pelvis. The segments are misaligned so they change the shape of the trunk from rectangular to trapezoid in people with scoliosis. The Schroth system shows the sideways orientation of the physical abnormality and rotating segments for therapy planning. It is a more active option for AIS patients to prevent the progression of their spinal curvature before it increases in severity and requires surgery. Schroth's three-dimensional exercise is designed specifically for scoliosis patients on the basis of the sensory-motor and tactile-motor theories (Negrini et al., 2008). Figure 2.14 shows the Schroth's three-dimensional exercise method. The core principle of the exercise is to correct the posture and respiration mode through rotational breathing (Lehnert-Schroth, 1979). Patients participate in the exercise to activate the sensory-motor system with internal or external stimuli depending on the type of curvature while a mirror will be used for monitoring purposes. This allows patients to identify the difference between the shape of a

normal spine and a scoliotic spine, and further adjust the structure (Kim & Park, 2017). A one-year experiment was conducted by Otman et al. (2005) to evaluate the effectiveness of the Schroth exercise among fifty scoliosis patients. The findings show an average decrease of  $8.25^\circ$  of the Cobb angle and an increase in lung capacity and muscle tension at the end of the study. Later, Park et al. (2018) carried out a systematic review of Schroth exercises and their effectiveness on scoliosis. They concluded that Schroth exercises can effectively treat scoliosis, especially for patients with a Cobb angle between  $10^\circ$  and  $30^\circ$ .



Figure 2.14 Schroth's three-dimensional exercise

Besides, **core stabilisation training** is designed to improve the alignment of posture and prevent motorial compensation. Figure 4.4 shows the process of core stabilisation training. The torso is maintained in the proper position for static or dynamic posture (Akuthota & Nadler, 2004; Ayhan et al., 2014; Muthukrishnan et al., 2010). The key spinal muscle is thus strengthened and becomes more stable in controlling and adjusting the spinal arrangement (Emery et al., 2010).

Other than the above methods, Marianna Bialek and Andrzej M'hango developed the **Functional Individual Therapy of Scoliosis (FITS)** method, which aims to treat scoliosis through self-correction and implementing proper posture. The treatment combines various therapy concepts and comprise three parts, including (1) evaluation of scoliosis cases, (2)

identification and reduction of myofascial triggers through myofascial release therapy, and (3) improvement and stabilisation of the posture. The reduction in myofascial triggers can lower the limitations of 3D self-corrective exercises while posture exercises allow patients to use corrective foot loading and facilitate a proper posture pattern (Berdishevsky et al., 2016). According to a study conducted by Bettany-Saltikov et al. (2012) for nearly 3 years, 8.9% of the patients who have slight scoliosis and practice FITS only experience an increase in their Cobb angle by over 5° while 21.6% of the patients who have moderate scoliosis and undergo FITS and bracing have an increase in their Cobb angle by over 5° after the treatment. This shows the effectiveness of the FITS method, together with bracing treatment. Still, the method is complicated and need patients to precisely follow the instruction with the help of therapists or parents (Bettany-Saltikov et al., 2012).

### **Biofeedback postural training**

Biofeedback can help to correct poor posture, that is, coaching users to control their muscles or other involuntary body movements with the use of an electronic apparatus (Kappes, 2008; Bray, 1998). Biofeedback therapy was first developed by Russian psychologist Maia Lisina in 1958 who used an electronic device to train subjects to regulate their vasoconstriction and vasodilation and further addressed various physical and mental issues (Lehrer et al., 2000; Nestoriuc et al., 2008; Ahmed et al., 2011; Gatchel & Price, 1979). In biofeedback treatment, signals from different body functions including brainwave activity, blood pressure, heart beat, temperature of the skin, sweat gland activity and muscle tension are collected, transformed into data and sent to the user immediately in real-time (Kappes, 2008). A number of studies in the literature have shown the effectiveness of biofeedback, especially for muscle training. Surface electromyography (sEMG) biofeedback, which is one of the methods that target muscle recovery, can activate the muscles of the upper limb and an optimum outcome can be obtained together with physical therapy (Lyons et al., 2003). Schleenbaker and Muinous (1993) obtained a similar finding in their systematic review of sEMG biofeedback in that it is able to increase the activity of the higher and lower limbs. This shows that biofeedback can be applied to users with muscular issues like poor posture.

Biofeedback can be adapted the in postural training of patients with spinal deformity as well (Wong et al., 2001). Micro Straight is one such postural training device, which involves an audio-biofeedback system, and was developed to inhibit the spinal progression of AIS patients via postural correction. The device is composed of two nylon loops that circle the trunk

vertically and horizontally, see Figure 2.15. They are used to inspect the trunk girth length and thoracic girth for breathing. Incorrect posture is recognised with a distinct trunk girth compared to the dimensions that are measured under a standard posture before. A warning is emitted when the wearer has an incorrect posture for over 20 seconds continuously. The sound will gradually increase until the wearer corrects the posture. This device can help to monitor the posture as well as progression of spinal deformity. A study conducted by Wong et al. (2001) found that about 60% of the patients experience an increase of  $5^\circ$  in their Cobb angle with the use of only this device and its controlled rate on spinal curvature progression is calculated to be 69% (Wong et al., 2001). The post-treatment effect of training is long-lasting, and most patients can maintain a proper posture.

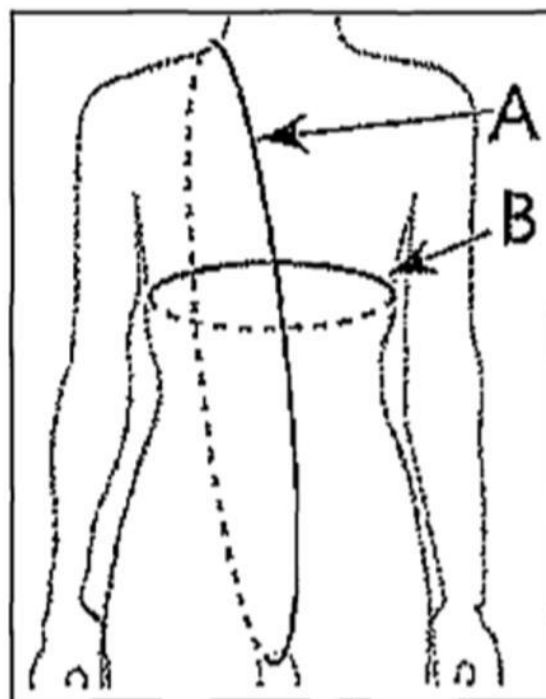


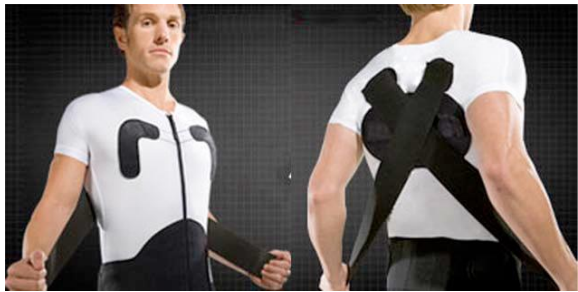
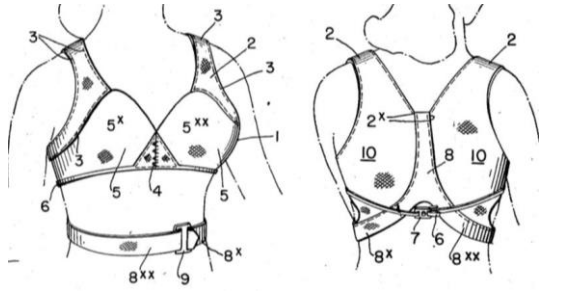
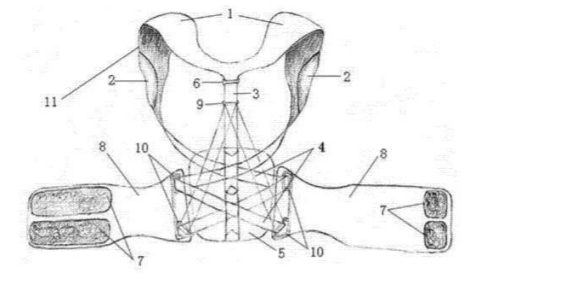
Figure 2.15 Two nylon loops of Micro Straight (Wong et al., 2001)

### **Posture correction garments**

Apart from posture correction via active training (exercise), there are other methods that can also train the body passively. Posture correction outfits or various supporting garments have been developed to train posture by exerting corrective forces through the elasticity of various components. The garments are mainly composed of semi-rigid or soft material with elements like wide elastic bands, abdominal belts, back straps, etc. These posture correction garments can enhance awareness of good posture and prevent trunk deformity before spinal problems

become severe. They reduce the need for bracing treatment or surgery, and also prevent related psychological issues like lack of self-confidence from using a hard brace (Sapountzi-Krepia et al., 2000). The greater flexibility and more natural profile of the posture correction garments enhance their receptivity. Several different types of posture correction garments are shown in Table 2.8, including the Babaka Corset Posture Corrector, Women’s Posture Corrector and Trainer, S3® Scapular Stabilization Brace, posture corrective brassiere, posture correcting garment, and posture corrector wireless back support bra. Their design principles are then discussed.

Table 2.8 Examples of posture corrective garments

 <p><b><u>Babaka Corset Posture Corrector</u></b> (Babaka, 2020)</p>	 <p><b><u>Women’s Posture Corrector and Trainer</u></b> (Underworks® 2024)</p>
 <p><b><u>S3® Scapular Stabilization Brace</u></b> (Mair et al., 2013)</p>	 <p><b><u>Posture corrective brassiere</u></b> (Mungo, 1952)</p>
 <p><b><u>Posture correcting garment</u></b> (Wang, 2013)</p>	 <p><b><u>Posture corrector wireless back support bra</u></b> (Leonisa Inc., 2017)</p>

The **Babaka Corset Posture Corrector** was developed by Babaka (2020) to adjust the improper posture of the upper trunk. This garment can align the trunk, reduce kyphosis, relieve back pressure and support the waist (Babaka 2020). The product is designed like a girdle and vest, and constructed of fabric with small holes to enhance air-permeability. The shoulder straps are in a double-Y shape to pull the shoulder blades to the proper location while Velcro tape is attached in the front for adjustments after the shoulder straps contrarily pass through the back and sides. Resin bones are inserted inside the garment to offer support. Besides, a set of Velcro tape can be found in the front waist, which is used to change the fit of the corset based on the body dimensions of the user (Babaka, 2020). Yet, there are arguments on its actual capability in that it can only change moderate posture issues such as kyphosis, but not severe cases like trunk disfiguration owing to its structure and the type of fabric used (Tainfu Morning Post, 2006). The double-Y shape of the shoulder straps is not custom-fitted to accommodate different body contours, especially thin individuals. Gaps are found between the straps and shoulders, which reduce the corrective strength. The corrective strength is further eroded by the short resin bones in the lumbar area as well as the textiles and elastic bands with low durability and resilience (Tainfu Morning Post, 2006). Besides, the length of the garment is not extended to the pelvis region which can affect the amount of corrective strength on the upper torso. These result in effectiveness in correcting trunk deformity and a shorter lifespan of the outfit although they are not ideal ways.

The goal of the **Women's Posture Corrector and Trainer** is to adjust the posture of the upper trunk. Sturdy brace straps can force the shoulders back to straighten the body and maintain an upright position. It can relieve the pressure on the spine and activate muscle biofeedback in stabilising and holding the upper trunk (Underworks®, 2024). The brace is designed as a vest and fabricated with long-lasting Lycra® spandex and nylon. The middle part of the torso is compressed by dual reinforced bands, which can encourage the muscles of the abdomen to contract. The bands are fastened through three rows of hooks and eyes at the front, which allows personalisation of the compactness of the bands. Metal is installed in the back brace to support the back of the trunk and resist pressure (Underworks®, 2024). Still, the shoulder straps cannot be modified which affect the fit of the garments to distinct body contours and prevent corrective strength on the shoulders. The tightness of the straps is possibly reduced after wearing them several times and the corrective forces will be weakened irreversibly due to the strap design. Moreover, the bonds only extend down below the breast and there are no resin bones to support

the lumbar and waist regions. The garment does not cover the pelvis region, so the amount of corrective strength on the upper torso is inadequate as well.

The **S3® Scapular Stabilisation Brace** is a corrective garment that looks like a short-sleeved jacket. The aim is to correct posture, strengthen the muscles, promote joint movement, relieve pain and increase the movement of the shoulders and spine (Maire et al., 2013). In addition, this brace prevents chest osteoporosis and provides therapy for the shoulders and shoulder blades. The S3® Scapular Stabilization Brace is composed of narrow flexible bands that offer good sweat management and uses Touch-Tension Neuroband™ Technology. Together with the straps, the outfit can train and readjust the order of muscle contraction. The brace completely surrounds the upper torso and elastic straps are used for adjustments. They extend to the back and sides, and are secured with the use of Velcro tape in the front. As for the opening, a zipper is found at the front. Since the zipper is the only adjustable component that is used to tighten the brace, it may not fit everyone, and the user cannot adjust the brace for optimum corrective forces if the brace becomes loose. Furthermore, it is questionable whether the corrective strength can only be exerted by using Velcro tape. Cole (2008) assessed the effectiveness of this brace for forward head and rounded shoulder posture (FHRSP) or electromyography movement on the muscles and found that the corrective forces applied by the strap design are inadequate to change posture. Therefore, the actual function of the brace is still controversial and requires more studies to determine its effectiveness.

On the other hand, there are functional intimate apparel that are designed to support the trunk and monitor posture by exerting forces that pull the shoulders back with the use of elastic bands, straps and resin bones. They realign the trunk contours and spinal structure. For instance, Mungo (1952) developed a **posture corrective brassiere**, which is a vest bra with a belt fastened from the front waist to the back of the bra. The belt can correct the posture by exerting forces that pull the back panel down and the shoulder straps towards the back. Besides, Wang (2013) developed a **posture-correcting garment** that aims to reduce kyphosis. The garment is composed of cushioned shoulder straps that are crossed twice and connected to the back panel, a wide waist belt and two back straps. The shoulder straps apply force to pull the shoulders back, and thus hold the posture upright. This mechanism is similar to that of the posture corrective brassiere (Mungo, 1952). Leonisa Inc. (2017) recently developed a **posture corrector wireless back support bra**, a vest-like garment that is closed by using hooks and eyes in the front. An X-shaped reinforcement can be found in the back to hold the trunk and

correct the posture.

## **2.5 Posture Correction Girdle**

To halt the progression of the spinal curvature and resolve the commonly found issues with braces or other orthotic products, Liu et al. (2014) developed the PCG with the use of warp knitted fabric and resin fastenings to control and train the posture of patients in the early stages of AIS who have a Cobb angle between 6° and 20° during their growth spurt. Both function and psychological state of the patients are taken into consideration during the design process.

### **2.5.1 Design and garment components of PCG**

The PCG is a flexible, symmetrical and custom-made garment that looks like intimate apparel, uses a vest-like design for the shoulders, and has a zipper at the front for the opening (Liu et al., 2014, 2015). The PCG fits the wearer tightly and stretches from the shoulder to the hip for supporting and maintaining the trunk. The girdle is fabricated by warp knitted fabric and elastic bands to improve the wear comfort. This brace uses tricot, satinette and powernet, all of which have high strength and recovery and good air-permeability. The main part of the PCG comprises three layers, in which tricot is utilised as the shell layer for a soft hand and good aesthetics. The middle layer is formed by using satinette to stabilise the girdle. The back and side panels are embedded with semi-rigid resin bones to support the spine along an upright plane and maintain trunk movement along a horizontal plane. For the inner layer, the inner lining of pockets uses powernet to allow placement of semi-rigid EVA foam pads. The PCG also has a pair of shoulder straps and a waistband, which are both made of elastic with high modulus and recovery. The shoulder straps extend to connect the back panel and surround the shoulders while Velcro tape is used as the opening at the centre of the front of the brace. The straps are adjustable for a better fit. The waistband cover the thoracic vertebrae to the lumbar areas and can be unfastened by using Velcro tape in the front. For convenience of toileting, a Velcro opening is created in the crotch part. The Velcro tape and zippers are used together to allow patients to more easily don and doff the PCG. Figure 2.16 shows the front, back and inside of the PCG.

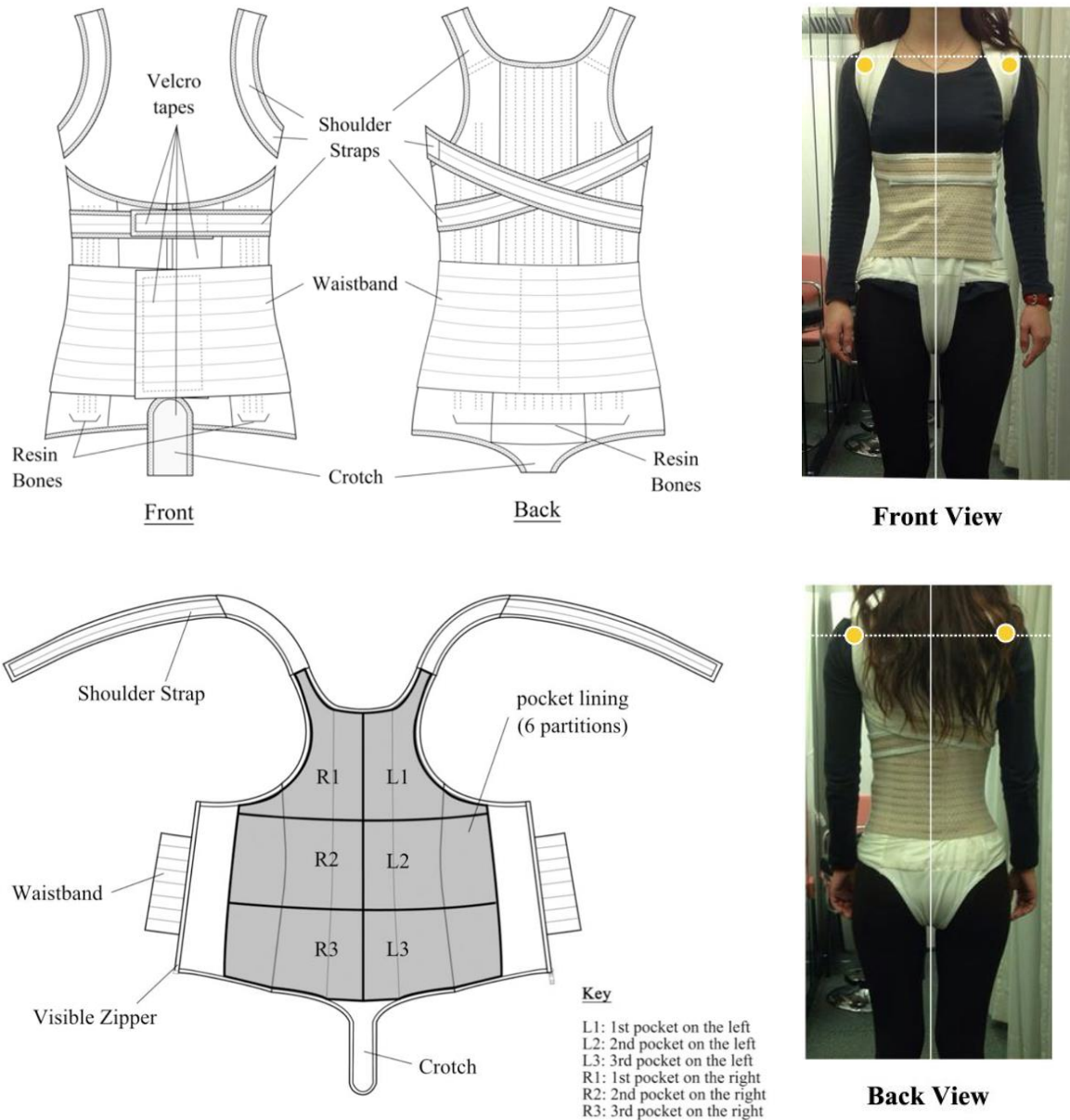


Figure 2.16 Front, back and inside views of posture correction girdle (Liu et al., 2015)

### 2.5.2 Corrective mechanism of PCG

Liu et al. (2015) indicated that the principles behind the corrective mechanism of the PCG is to reduce the severity of the spinal curvature by promoting better balance through posture. Instead of using passive corrective forces exerted by an external means like a traditional rigid brace, the PCG involves both active and passive training of the posture (Liu et al., 2014). The user is trained to maintain the spine into its natural curve and balance his or her posture through self-awareness. Patients are required to wear the girdle for eight hours daily, which is much shorter than the time required for a rigid brace (Liu et al., 2014; 2015, Yip et al., 2016). Figure 2.17 shows the primary corrective pressure applied by the PCG (Liu, 2015). Apart from the

primary corrective forces, secondary corrective forces are exerted through the three point-pressure system with the supporting system. Moderate compression exerted by the girdle can reduce leaning of the trunk with less restriction on body movement compared to a rigid brace, which allows patients to continue their daily activities and thus result in better treatment compliance.

Semi-rigid ethylene vinyl acetate (EVA) foam pads are inserted in pockets that are distributed throughout the PCG to allow adjustment of the pressure points based on the scoliosis condition. X-ray imaging is also used to determine the location of the curve apex and subsequently, the arrangement of the foam pads. Additional semi-rigid EVA foam pads are inserted into the pockets progressively from the lower to the upper part of the PCG to push the convex side of the curve to the concave side which balances the posture as long as the forces are exerted in the bottom part of the PCG. EVA foam is used for the padding due to its high elasticity, flexibility and resistance to pressure. Since EVA foam has a closed-cell structure, it has adequate strength and can exert corrective forces that target the convex side of the curve and correct the posture through pressure points in a more comfortable way (George et al., 2011). As the spinal curvature changes during the treatment, the position and number of EVA foam pads can also be adjusted to maintain appropriate and adequate corrective force that takes the spinal situation into consideration. In general, two to three EVA pads are arranged in opposite direction to each other to exert the corrective forces while one or up to three pads are also possible based on the condition itself. Figure 2.18 illustrates two ways of placing the EVA foam pads in the girdle and the corresponding points of pressure (Liu, 2015).

Apart from EVA foam pads, the extension and recovery of the elastic components like the shoulder straps and waistband produce corrective forces and correct the position of the shoulder, thus preventing the trunk from bending forward and waist from twisting sideways and holding the back upright. A prosthetist-orthotist (P&O) evaluates the situation and may adjust the tension of the elastic components along with positioning of the pads accordingly to maximise the effect of the girdle (Liu et al., 2014). These corrective forces and compression provided by the different components of the girdle can reduce body asymmetry, trunk displacement and inclination of the waist and pelvis (Liu et al., 2014).

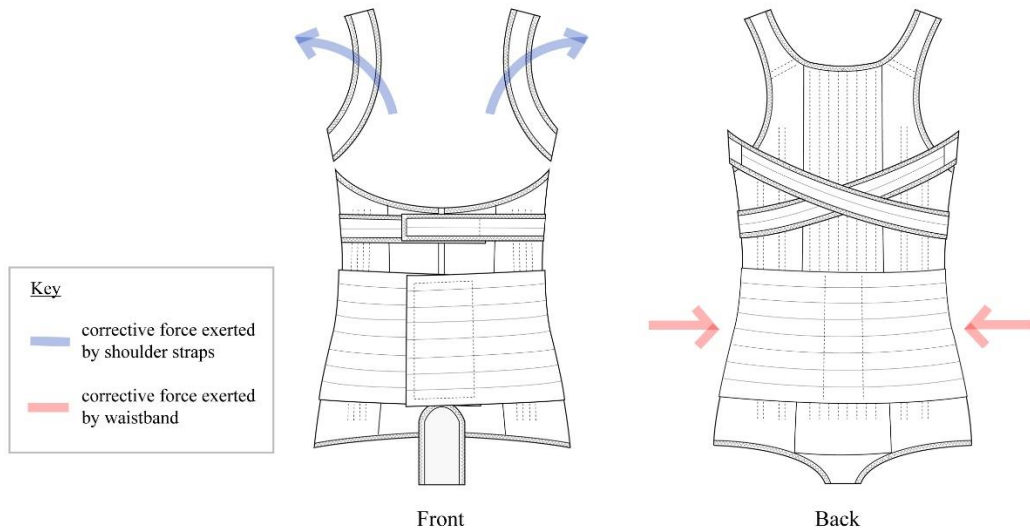


Figure 2.17 Corrective forces exerted by elastic components of PCG (Liu et al., 2015)

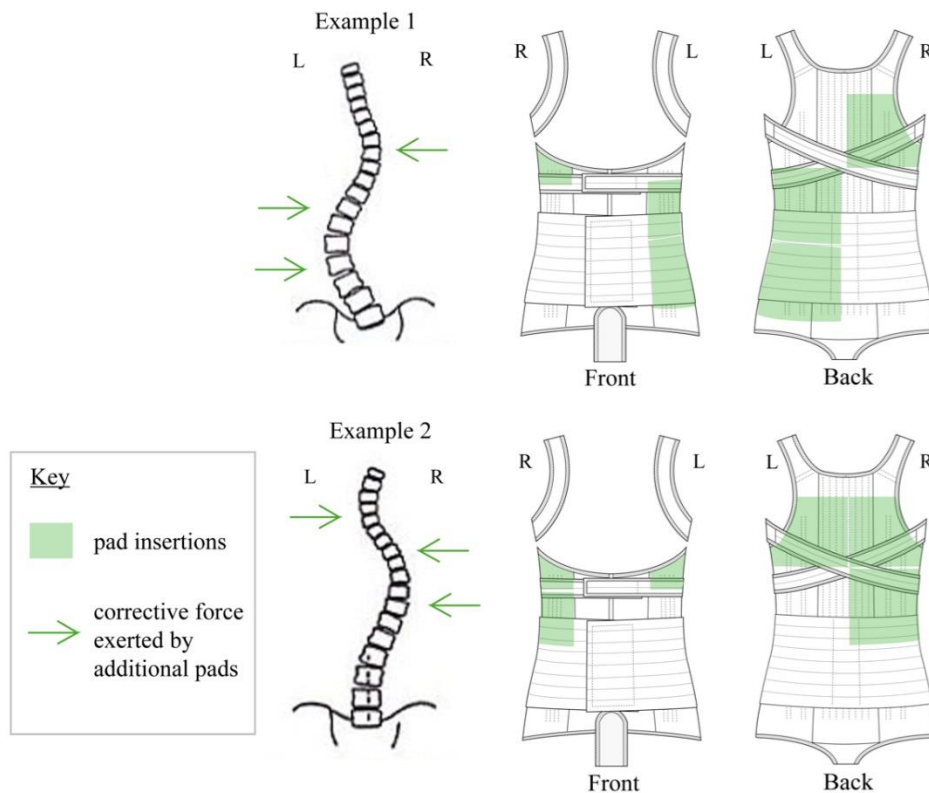


Figure 2.18 Example of points of pressure created by EVA foam pads for different spinal conditions (Liu, 2015)

### 2.5.3 Previous wear trial studies of PCG – effectiveness and limitations

Liu et al. (2014) carried out a wear trial to determine the corrective effects of the PCG. Seven female subjects between 10 and 13 years old with an increasing spinal curvature of 10° to 20°

and Risser 2 were recruited for the wear trial. Their body measurements and information on their spinal situation were collected by using different tools and a clinical analysis respectively. Health testing was carried out which measured the blood pressure, heartbeat, and peak expiratory flow both at the start and end of the wear trial to determine if there are any health impacts. No distinct impacts were observed during the wear trial, in which the three health parameters varied within an acceptable value. The effectiveness of the girdle was assessed based on the balance and alignment of the shoulders with the ground level as a reference. The findings revealed that the difference between the two sides of the shoulders is reduced, and the corrective effect on posture is enhanced with the inserted paddings. During the bending test, the PCG also showed that it could limit the flexion range of motion without affecting the movement of the subjects and thus their daily life activities.

To further assess the effectiveness of the PCG and the compliance rate with this treatment among AIS patients, Liu et al. (2014) conducted a six-month wear trial from spring to summer with 9 female patients between the age of 10 and 13 with mild scoliosis (Cobb angle less than  $20^{\circ}$ ). The results showed that the shoulder asymmetry in the frontal plane is reduced when EVA foam paddings were inserted based on the spinal conditions. Therefore, the EVA foam pads are the key factor in improving the spinal condition. As for compliance, the rate was reduced to 82.63% during the summer and two patients left the trial in the third month. The thermal discomfort caused by the multiple layers of textiles during the summer is assumed to be the main factor in the loss of compliance. These incidents further deteriorated the spinal corrective effects with the PCG. Concerns of the accuracy of the number of pads and efficacy of the exerted corrective forces were raised since the positioning of the pads was carried out visually based on the scoliosis case itself. The corrective forces exerted by the elastic components might have been insufficient as well.

After that, a 3-month wear trial of the effectiveness of the PCG was conducted by Liu et al. (2015) and 10 girls who are 10 to 13 years old with progressive scoliosis and a Cobb angle between  $6^{\circ}$  to  $20^{\circ}$  were recruited from a school screening programme. A Vicon motion capture system and temperature loggers (LogTag, OnSolution Pty Ltd) were used to monitor the wear trial. The former is a non-invasive means of determining the effectiveness of the PCG in changing the posture over a short period of time, and facilitates ease of repeating the evaluation while the latter record how long the girdle was worn. According to the results, both the standing posture in the coronal plane and walking posture in the coronal and horizontal planes are

improved. A relatively better outcome can be observed from the frontal plane of the acromion during standing, which means better balanced shoulders (Liu et al., 2015). The girdle shows effectiveness in limiting pelvis tilting during walking, and the front and side bending of the subjects. This shows that the girdle can enhance trunk symmetry, increasing control of the movement at the anterior and lateral levels while walking and flexing, and supporting a straighter back at the sagittal plane while sitting. As for the compliance rate, only one of the subjects withdrew from the wear trial as she decided to change her treatment method. It is reported that the compliance rate is 90% for 7 of the 10 subjects (Liu et al., 2015). Yet, the corrective effect is reduced three months after the wear trial due to repeated washing and extension of the girdle as well as skeletal growth. The fabric, elastic band and shoulder straps showed loss of elasticity which reduced the corrective effects of the girdle. As the subjects increased in height during the trial period, the girdle may not have been well fitting anymore. Regular adjustments are therefore essential to ensure that the trunk from the shoulders to hips are covered, and the optimal amount of corrective forces are exerted onto the scoliotic spine. The study also faced limitations with the small sample size and a small range of curvatures examined, so that further studies with a larger sample and different curvature size are needed.

Later, Yip et al. (2016) carried out a 6-month wear trial on the effectiveness of the PCG to control postural changes. Nine female subjects between 10 and 13 years old with mild scoliosis (Risser sign smaller or equal to 2 and Cobb angle between 10 to 20°) were recruited to wear the girdle for eight hours daily, like the previous wear trial carried out by Liu et al. (2015). In the study, a 3D motion capture device (Vicon system) was used to collect the statistics of both static and dynamic postures such as standing, sitting or flexing while 3D scanning equipment (Anthroscan system) was used to measure the angle of rotation of the shoulders and pelvis at the horizontal plane, and determine the actual improvement in posture. According to the 3D motion capture results, the alignment of the acromion and pelvis in the frontal plane with the standing posture as well as the angle of the back in the sagittal plane for sitting posture is greatly improved (Yip et al., 2016). The ability of the subjects to control the utmost extent of anterior and lateral bending is also improved. This study provides an optimistic outcome on the effectiveness of the PCG even though a random and controlled study at a larger scale would be helpful to enhance the study validity. Nevertheless, there are substantial differences among the subjects which show no statistically significant improvement in the angle of rotation at the horizontal plane with a larger standard deviation (Yip et al., 2016).

Fok et al. (2018) conducted a 6-month pretest-posttest wear trial to evaluate the ability of the PCG to slow the progression of spinal deformity. Sixteen patients who are between 10 and 16 years old with a Cobb angle between 10° to 30° and Rissers 0 to 4 are recruited from a school screening programme. They were to wear the girdle for a minimum of 8 hours daily during their active hours. Radiographic imaging was carried out at the frontal plane and back of the trunk to measure the change in the Cobb angle before and after wearing the girdle as well as during the bracing period. The result showed that the survival rate of the PCG is up to 90% and there is an obvious difference in the Cobb angle (8.4% reduction) before and after the treatment. The in-brace correction of the spinal curvature is reported to be 16%, which indicates a short-term corrective outcome resultant of wearing the girdle (Fok et al., 2018). As for the compliance rate, 10 of the subjects completed the wear trial while six left during the wear trial. In addition, Fok (2020) mentioned that the free-end elastic strap design of the PCG might not be able to control the tension and corrective forces well which might affect treatment effectiveness.

Furthermore, Chan et al. (2018) conducted a study on the use of smart materials for the PCG. The study evaluated and compared the corrective effects of the PCG when shape memory alloys (SMAs), resin bones and other materials are used as the girdle components. Two female AIS subjects who are between 10 and 14 years old with a Cobb angle between 25° to 40° were recruited for the wear trial. They were required to wear the PCG composed of SMAs or resin bone for two hours, after which radiography was carried out to identify the changes if any, of the spinal deformity with and without the girdle. The result indicated that SMAs have a good corrective effect on the thoracic vertebra due to their high elasticity and ability to exert repeated and manageable pressure for trunk correction. Yet, the lumbar curve is rarely corrected since the struts do not align to the body contours of the subjects to exert sufficient corrective forces. Even though this study shows a positive result of the use of SMAs in the PCG, the sample size is small so further investigations on the shape of the SMA struts are needed.

#### **2.5.4 Effective evaluation methods for the PCG**

The effectiveness of the PCG can be evaluated through different approaches. In-orthosis radiography exams are often performed to examine the effectiveness of interventions before and after they have taken place. According to Wong et al. (2000), the accuracy of the positioning and placement direction of the pressure pads of the PCG can impact the efficacy of

treatment when considering the anchoring of the orthosis. To investigate the quality of life of AIS patients when they don the orthosis, psychological variables are also crucial. Additionally, some researchers have hypothesised a connection between AIS (Cheng et al., 2015) and functional anomalies in the central nervous system, such as proprioceptive deficiency (Lao et al., 2008); that is, when the proprioceptors cannot send and receive information to the brain. This study also intends to determine if the PCG can alleviate proprioceptive impairment.

### **Radiographic examination**

Radiographs taken either with or without an orthosis need to be done frequently during the bracing therapy period to monitor the changes in spine curvature. Peltonen et al. (1988) and Upadhyay et al. (1995) claimed that the first in-brace result is essential for the success of the therapy over the long run. Meanwhile, the treatment should not just strive for higher in-brace correction as this would not result in good treatment results. Accordingly, treatment should aim to provide the best in-brace correction while maintaining the highest possible degree of comfort for patients so that they comply with the treatment (Borysov et al., 2013). Landauer et al. (2003) stated that girls with  $\geq 40\%$  in-brace correction in the early stages of treatment and good compliance achieve a  $7^\circ$  mean reduction in their spinal curvature until the final follow-up, while girls with  $< 40\%$  in-brace correction but good compliance with treatment can barely prevent deterioration of their Cobb angle. To obtain a successful outcome, the initial in-brace correction should aim for more than 40% correction.

To compare the outcomes of in-brace correction, Katz and Durrani (2001) stated that low-dose radiography exams in a standing position should be performed before the intervention. For at least two hours before the in-brace radiographic exams, the brace must be worn (Li et al., 2014). An in-brace correction of more than 25% has been deemed the threshold and is determined by using:

$$\text{In-brace correction(\%)} = \frac{(\text{Before bracing} - \text{In-brace}) \text{ Cobb angle}}{\text{Cobb angle before bracing}} \times 100\% \quad (1)$$

### **Interface pressure with padding**

Measuring the interface pressure with the pads on the brace is one of the possible ways of evaluating and explaining the effectiveness of the PCG. Wong et al. (2000) investigated the

efficiency and biomechanical aspects of spinal orthoses for treating patients with moderate AIS. The study showed that the strap tension, pressure distribution, and Cobb angle are all closely related. The standing Cobb angle is substantially related to the pressure of the padding (correlation coefficient=0.931,  $p < 0.05$ ), and the mean pressure of the pads used in the brace therapy was found to be  $7.09 \pm 1.77$  kPa. It is hypothesised that tightening the straps would create more pressure through the brace, which would help to correct the spinal deformity. In order to improve the efficacy of the therapy, independent standard tension test are recommended to be regularly done for each strap and monitor them closely. Mac-Thiong et al. (2004) suggested that higher strap tension in patients who have a single right thoracic curve can alleviate the interface pressure.

### **Posture angles**

Comparing the changes of the posture angles and examining improvements in body asymmetry can be considered as evaluation means to determine the effectiveness of the modified PCG on posture correction, since posture correction is one of the main aims of the development of this girdle. Some of the more commonly found posture asymmetries are related to the risk of scoliosis progression (Kouwenhoven & Castelein, 2008; Fortin et al., 2012). The common posture problems of AIS patients are left and right asymmetries of the shoulders, pelvis and scapula (Zabjek et al., 2008). Penha et al. (2017) suggested that both 2D and 3D photogrammetry can be used for assessing posture changes.

### **Compliance rate monitoring**

Monitoring compliance with treatment has also been considered for therapy with the PCG. Low treatment compliance with the brace is always a concern as it could greatly affect the bracing outcome, or even lead to further progression of the spinal curvature (Negrini et al., 2015). Katz et al. (2010) suggested that using a Boston brace for longer hours has a significantly positive impact on how well AIS patients are able to regulate the development of their condition. Younger patients will benefit more from wearing a brace. Patients who wear a brace for more than 12 hours each day will have a more ideal outcome. Thermosensors (Orthotimer, RollerwerkMedical, Germany) were used in Lin et al. (2022) to track the compliance of AIS patients with their orthosis treatment, and took into consideration the local daily maximum air temperature threshold. Thermochron™ iButton sensors and Hygrochron iButton sensors were used in Wong (2020) and Cheung (2024)'s study accordingly to monitor the compliance of recruited AIS patients with the Anisotropic Textile Brace treatment.

### **Quality-of-life questionnaires**

To determine the positive and negative effects of bracing on AIS patients, a number of questionnaires on the quality of life of the users have been used. In Lin et al. (2022), questionnaires including the Scoliosis Research Society (SRS)-22 questionnaire (SRS-22r), Trunk Appearance Perception Scale (TAPS), and Brace Questionnaire were given to AIS patients before the intervention and at the 3-month follow-up. The SRS-22r is primarily used to gain a better idea of the perceived deformation, load of the brace, and any symptoms that impact QoL (Cheung et al., 2007).

### **Proprioception deficits**

Idiopathic scoliosis is a spinal condition with no known aetiology, with uncertainty surrounding the etiopathogenesis of AIS patients. Some have suggested that the cause of AIS can be linked to functional anomalies in the central nervous system such as proprioceptive deficiency (Cheng et al., 2015). The brain relies on proprioceptive signals from different body parts to determine the relative locations and motions of body segments in order to maintain a proper spinal alignment and balance with different postures (Cignetti et al., 2013; Dietz, 2002). When performing various movements, the ability to rearrange body parts and movement might be impacted by abnormal proprioception (Hillier et al., 2015). According to the meta-analysis in Lau et al. (2022), AIS patients have proprioceptive deficiencies compared to non-AIS individuals, such as more repositioning mistakes and a higher motion detection threshold. Additionally, Lau et al. (2022) proposed that AIS is caused by proprioceptive impairment rather than as a result of it (i.e., the level of proprioception dysfunction may not be associated with the severity of the subsequent spinal curvature if the proprioceptive deficiency is the reason for AIS). On the other hand, larger Cobb angles and higher rate of progression of the spinal curvature may be linked to declined proprioceptive functions if proprioceptive deficiencies develop after a diagnosis of AIS. There is no significant correlation between the severity of AIS and the extent of proprioceptive deficits, severity of the spinal curvature, or the repositioning errors of the lower limbs in AIS patients, according to for example, Cheng et al., (1998) and Le Berre et al. (2017).

A number of studies have shown that proprioceptive abnormalities in various areas of the body of AIS patients may indicate systemic alterations in proprioception rather than a localised effect in a specific body part (Lau et al., 2022). The extent of spinal proprioceptive abnormalities in

AIS patients is still unclear because the majority of related research has primarily evaluated peripheral proprioception. Another potential cause is that spinal-related proprioception, particularly in the thoracic and lumbar regions, may be compromised. In addition, Guyot et al. (2016) found that age, sex, and Cobb angle do not differ between individuals with and without deficiencies as it is difficult for respondents to perform the repositioning test accurately. The conclusion drawn that there is no accepted norm for AIS clinical proprioception testing. Due to the knowledge gap, proprioception testing is carried out in this study to investigate if the proprioceptive abnormalities of patients with AIS would be affected by PCG therapy.

## **2.6 Finite element modelling**

The FE method is a viable and effective way of evaluating the pressure forces imposed by the flexible brace because it may offer a valuable reference for predicting the interface pressure without the need for repeated trials with volunteers and experimental testing. In order to establish approximations of solutions to boundary value issues in engineering analysis and design, the FE method entails building a numerical model (Dhatt et al., 2012; Bathe, 2006).

### **2.6.1 Finite element modelling of bracing treatment**

FE analysis is frequently used nowadays for simulation-based planning in the medical sector, including for treating cardiovascular disease (Wan et al., 2002), replacing joints (Dopico-González et al., 2010), and bone modelling (Poelert et al., 2013). The FE method is frequently used to model bracing for scoliosis (Vergari et al., 2015), assess the effectiveness of the brace and refine the design of the brace (Clin et al., 2010; Gignac et al., 2000), model stress distribution on the scoliotic spine (Wang et al., 2008; Yang et al., 2011), and evaluate the effectiveness of surgery (Huang et al., 2016). Abaqus software has often been used to investigate how corrective forces are applied during various scoliosis treatments and how the scoliotic spine moves (Perie et al., 2002; Yu et al., 2008; Lin et al., 2009; Berteau et al., 2011; Little et al., 2013). The amount of corrective pressure exerted by a flexible brace and the subsequent spinal corrective effects may thus be predicted by using the FE model built by the Abaqus programme.

### **2.6.2 Process of building FE model**

Four key phases are typically involved in creating an FE model: building a geometric model, specifying the material attributes, determining the types of elements and meshes, and defining

the boundaries and loading criteria for the biomechanical model. A number of FE programmes have been constructed to develop FE models, including the most popular systems like MSC NASTRAN, NX NASTRAN, ANSYS, Abaqus, ADINA, and MARC which are used for structural static and implicit dynamic studies. For explicit dynamic analyses, three programmes are used: LSDYNA, RADIOSS, and PAM-CRASH. Multiphysics issues may be solved with ADINA and ANSYS, particularly fluid-structure interactions (Bathe, 2008).

CT, MRI, or multiview radiographic reconstruction can be used to evaluate the 3D geometry of braces or human body (Clin et al., 2010; Perie et al., 2002; Wang et al., 2008). Conventional x-rays only produce 2D images, which makes creating 3D geometric models difficult. To reconstruct the 3D structure of the human body, multiview radiographic reconstruction and CT scanning can be utilised, however, they are relatively expensive and have radiation risk with repeated measurements owing to ionising exposure. Although MRI can provide 3D images with excellent resolution, the cost is not only high, but the scanning process takes time (Zheng et al., 2001). Moreover, reconstructing 3D geometric models of the body through 3D laser scanning is a less expensive option but this procedure can only record the contours of the surface of the body and cannot preserve the tissues or bone structures (Nebel, 2001; Kim et al., 2010; Yu et al., 2016). Therefore, a complete geometric model of the human body including bones can be created by using 3D body scanning, CT, MRI, and X-rays. Then, the FE programme can be used to specify the components and material characteristics, generate meshes, and configure the boundaries of the biomechanical model and loading parameters after the 3D images have been pre-processed.

## **2.7 Computer-aided models**

### **2.7.1 Application examples in garment industry**

Artificial intelligence (AI) is when machines complete tasks that would require human input. Reasoning, knowledge representation, planning, learning, prediction, and other elements are only a few of the many elements of AI. Artificial neural networks (ANNs), expert systems, genetic programming, searches, and optimisation are some of the technologies utilised in AI. Among them, expert systems and ANNs have been used in the engineering the design of textiles and clothing. A computer programme known as an expert system makes decisions based on knowledge of a certain specialised field to solve issues or provide guidance. The following are a few examples of its use in garment engineering.

An information processing system that shares several performance traits as those of the biological neural networks is known as an ANN. The goal of an ANN is to produce an output that is equal to, or as near to as possible, the target pattern. This is accomplished by training a model with experimental datasets such as modifying the weights or constants between the nodes in each layer. When mapping complex non-linear relationships between the component materials, constructional and processing variables, and the properties and performance of the garment, ANNs provide a significant advantage.

Meanwhile, Fan et al. (2001) proposed the use of a fuzzy-neural network system to anticipate and show the draped images of garments made with various fabrics and styles. This system assumes that the image database contains the standard drape images for garments produced from materials with a variety of characteristics and different feature dimensions. Finding the drape image that most closely matches the latest designed garment with the precise fabric qualities and feature dimensions is the target of the fuzzy-neural network system. As a result, the relevant fabric qualities and garment feature dimensions serve as the input units of the fuzzy-neural network system, and the output is the chosen drape picture that is most similar to the real drape image of the latest designed garment.

Furthermore, Gong and Chen (1999) used 19 fabric parameters assessed by the Kawabata evaluation system (KESF) and built an ANN to predict the performance of fabrics during the manufacture of garments. They showed that the ANNS can reasonably predict the issues with fabric performance in garment manufacture based on the mechanical parameters of the fabric. Since ANNS have a built-in learning capacity, they offer a substantial advantage over conventional analytical methodologies in that their prediction accuracy will increase with time.

Additionally, Liu et al. (2006) showed how an ANN model may be trained to determine the ideal level of clothing comfort for wearers of different sizes. The perceived body size is the output of the ANN in this work. The body or garment criteria that are most important to body image should be used as inputs. Body mass index, body chest circumference, and clothing ease were utilised and body chest girth minus garment chest girth was used to determine garment ease while computational experiments were used to estimate the number of hidden units.

Nevertheless, Liu et al. (2006) suggested a back propagation artificial neural network (BP-

ANN) model to predict pattern making-related body dimensions by entering a few critical human body measurements in lieu of the 3D body scanner, therefore greatly lowering the cost. The model can be used to create a computer-aided system that recommends the human body dimensions. Only the vital body measurements need to be entered into the suggested model for the pattern creators to quickly acquire exact body proportions for all potential patterns which can greatly boost pattern-making efficiency and enhance apparel fit. All of these cases show that AI has much potential for engineering garment design.

### **2.7.2 Application examples in spinal deformity assessment**

Scoliosis is a common spinal condition that features spinal curvatures on the side and deforms the spine. Deformation severity is generally evaluated by an index of curvature estimation. Traditionally, the angle of the spinal curvature is measured manually during the clinical diagnosis, which requires both time and effort. Horng et al. (2019) proposed a new Cobb angle measurement method by using convolutional neural networks. In the proposed method, the size of the anterior-posterior view images would be reduced first and then the horizontal and vertical intensity projected histograms would be used to define the region of interest of the spine for sequential processing. After that, intensity and gradient information of the region of interest are used to identify the boundaries of the spine, central spinal curve line, and spine foreground. The location of the vertebrae in the spine AP image would then be detected by using a progressive thresholding approach. Next, the deep learning convolutional neural network (CNN) approach would be employed to segment the vertebrae, so the influences of inconsistent intensity distribution of vertebrae in the spine AP image could be reduced. Finally, the segmentation results of the vertebrae would be reconstructed to form a complete segmented spine image which allows the spine curvature calculation based on the Cobb angle criterion.

On the other hand, machine learning was also applied to measure the axial vertebral rotation on radiographs (Logithasan et al., 2022). The team developed a machine learning algorithm to calculate AVR automatically on posteroanterior radiographs. The algorithm was developed based on CNNs. Three different body segments, which include the spinal column, individual vertebra, and pedicles, were used to carry out the AVR calculation. Each of the developed segmentation algorithms has its own separate labelling and training processes. The completed machine learning software was tested on 17 spinal radiographs. It was found that the automatic measurements calculated by the newly developed method are within the clinical acceptance

error ( $\pm 5^\circ$ ) compared with the traditional manual measurement method.

## **2.8 Chapter Summary**

This chapter provides an overview and background information on scoliosis and posture from an investigation on existing orthosis products for scoliosis and a study of the PCG. The consequences of poor posture have been discussed and some correction methods have been introduced. Although there are several treatment options for AIS, the orthosis products designed for them in the current market still have different problems. Patients in the early stages of AIS with a Cobb angle between  $6^\circ$  and  $20^\circ$  throughout their growth spurt can control and train their posture with the PCG in Liu et al. (2014). However, some of the design features need to be refined to enhance its effectiveness and wear comfort level. Previous wear trial studies suggest the effectiveness of PCG for these patients and also mentioned its limitations. The possible evaluation methods of the effectiveness of the PCG are also discussed in this chapter to prepare for a systematic evaluation on the modified version of the garment in this study. On the other hand, FEM and computer-aided modelling related to scoliotic brace treatment and assessment of spinal deformity are also reviewed in this chapter as a reference for the development of an intelligent PCG prescription system in this study. This chapter shows that the PCG still have its limitations, and there is the need to construct an intelligent system for prescribing this brace as a future advancement of the PCG.

# Chapter 3 – Methodology

## 3.1 Introduction

This chapter begins with a discussion of the methods for modifying the design of the PCG, which includes the fitting and sizing, placement and magnitude of the corrective forces, level of wear comfort and durability, as well as aesthetic aspects of the PCG. Then, the method for selecting the materials for the modified PCG (mPCG) is described, with details of the material selection criteria and laboratory tests. On the other hand, the details of the selection of the subjects such as the inclusion and exclusion criteria, and school-screening programme are also introduced. Furthermore, the wear trial experiments and evaluation methods to determine the effectiveness of the mPCG are elaborated. They include radiographic examination and comparison of the Cobb angle, 3D body scanning and evaluation of the posture balance, interface pressure measurement, testing for proprioception deficits, questionnaires to evaluate QoL, and monitoring compliance and thermal comfort.

## 3.2 Experimental design overview

A within-subject experimental design with 9 months of intervention is used in this study. Ethics approval was obtained from the Research and Innovation Office of the University. The research plan of this study is shown in the form of a flow chart diagram in Figure 3.1.

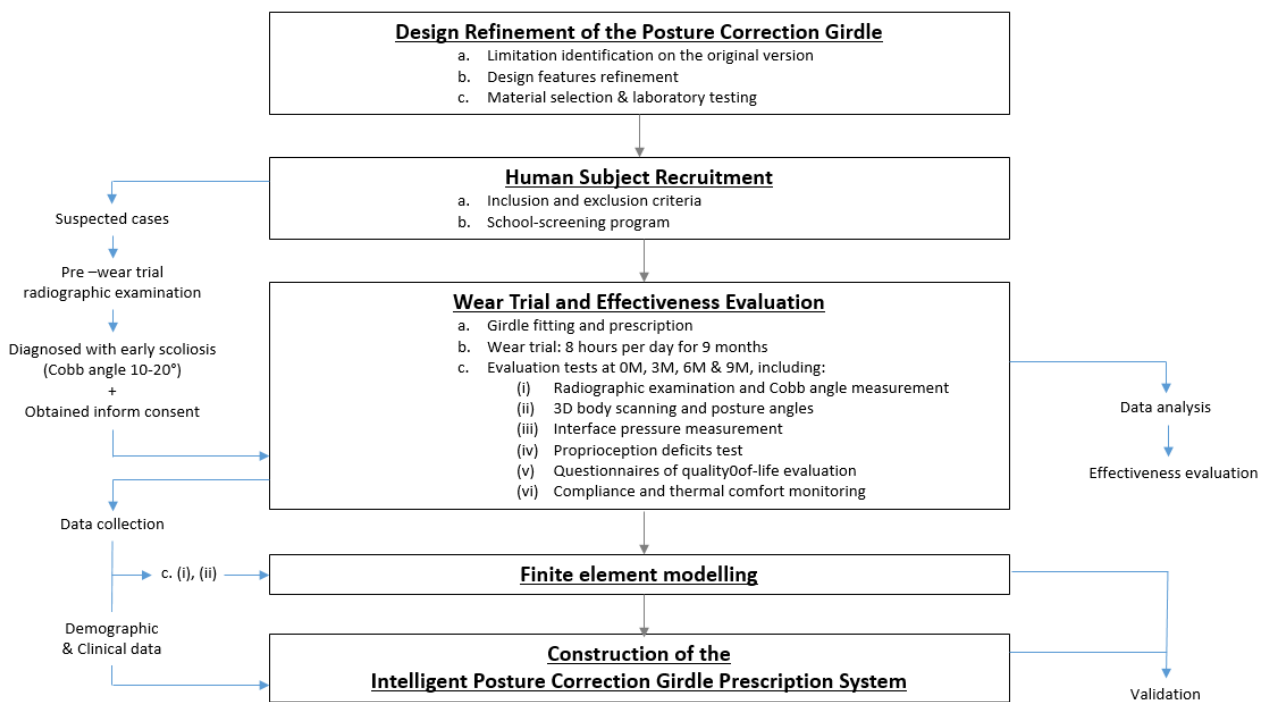


Figure 3.1 Research plan and flow of current study

After reviewing the original design of the PCG, different issues of the garment were found. Therefore, the effectiveness and wear comfort level of the girdle have to be refined, and changes were made to develop the mPCG. Laboratory tests were carried out to determine the materials used for producing the mPCG. A specific sizing system was developed to enhance the efficiency and accuracy of the fitting process. This system also translates into the development of an intelligent system to prescribe the mPCG and realise its mass customisation.

In this study, female adolescents between the ages of 10 and 13 years old who met the inclusion criteria were recruited as the subjects for a 9-month wear trial. Female adolescents were chosen because AIS is more common in females and usually increases in severity during puberty (Roach, 1999; Pehrsson et al., 1992; Mackenzie, 1922; Lonstein & Carlson, 1984). The subjects were recruited from a school-screening programme conducted in this study after a radiographic examination and giving informal consent. Since improper posture might be one of the possible factors that increases the severity of spinal deformities (Wong & Wong, 2008; Besette & Rousseau, 2012), each subject received an mPCG in her size with the appropriate placement of the padding after the fitting session as the intervention in the 9-month wear trial (8 hours of wear every day). To understand the amount of pressure exerted by the mPCG onto the wearer, interface pressure measurements were conducted right after the prescription of the mPCG.

Besides, some of the experiments were carried out progressively for monitoring purposes at the start of the experiments, and at the third, sixth and ninth months (0 M, 3 M, 6 M and 9 M, respectively) and to determine the effectiveness of the mPCG. The experiments included radiographic examination and comparison of the Cobb angle, 3D body scanning and evaluation of the posture balance, and testing for proprioception deficits. Besides, questionnaires for evaluating QoL and monitoring for compliance and thermal comfort were also carried out for a more comprehensive understanding of the intervention.

Since the number of subjects recruited for the physical wear trial in this study is limited, FE modelling is also carried out for simulating and predicting the efficacy of the mPCG. Thus, the corrective mechanism of the mPCG could be further investigated. Then, the girdle design parameters and collected data were used to train a prediction model with machine learning techniques. Finally, an intelligent system was developed to efficiently and accurately prescribe the effectiveness of the mPCG.

The method for the FE modelling and constructing the intelligent system (for prescribing the mPCG) is elaborated in Chapter 6 of this thesis.

### 3.3 Modification to PCG

#### 3.3.1 Identifying limits and possible modifications

Based on the literature review in Chapter 2 and a study of the PCG sample, limitations of the original design were identified that mainly involved four aspects: (i) fitting and sizing, (ii) placement and magnitude of corrective forces, (iii) level of wear comfort and durability, and (iv) aesthetics. The limitations and possible modifications are shown in Figure 3.2.

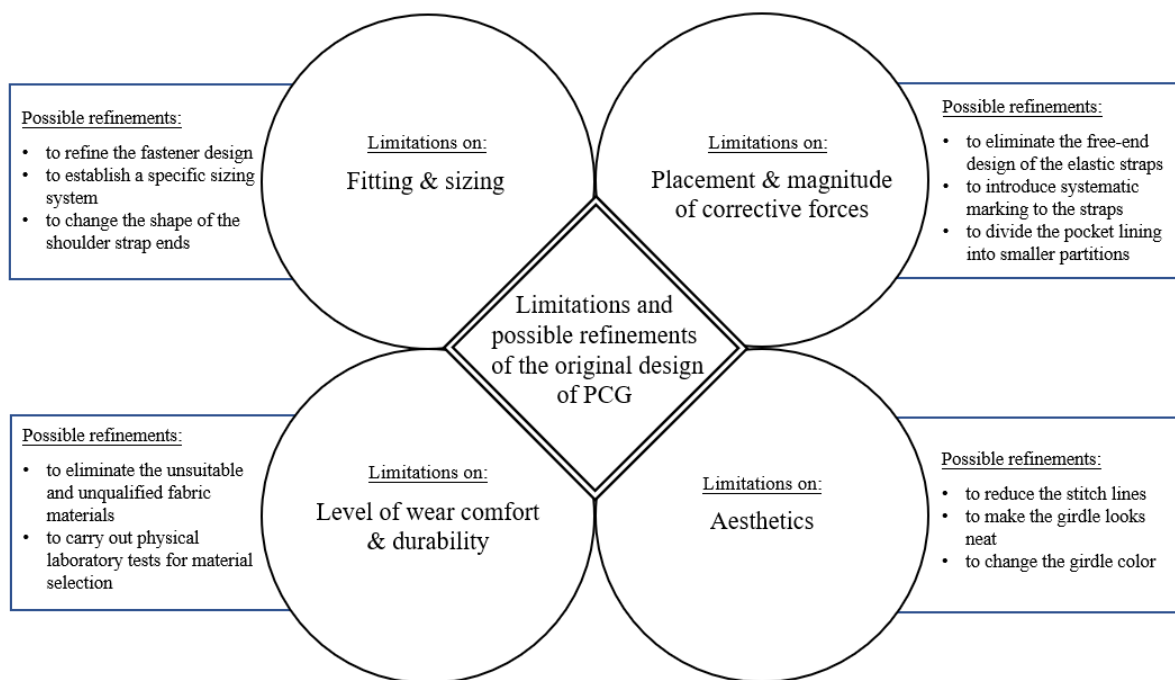


Figure 3.2 Limitations and possible modifications of original design of PCG

##### 3.3.1.1 Fitting and sizing

As for limitations in fitting and sizing, the PCG was tailor made for each subject in previous studies (Liu et al., 2015; Yip et al., 2016; Fok et al., 2018). Longer production lead time and waiting time before receiving the treatment with the PCG were attributed to the made to measure process. Moreover, the adjustment of the body of the PCG is limited as only one visible zipper is used at the centre front as the fastener (see Figure 3.3). This also limits the size range of each girdle. Besides, the ends of the shoulder straps are square in shape (see Figure 3.4). As such, the corners of the strap ends can easily curl upwards.



Figure 3.3 Centre front zipper of the original design



Figure 3.4 Squared ends and curling of shoulder straps

To address the issues, a decision was made to modify the fastener design at the centre front of the garment (i.e. adding more rows of zipper), which allows adjustment of the circumference. More rows of zipper at the centre front of the garment mean that the garment can accommodate a larger size range. In addition, a specific sizing system for the mPCG needs to be established to facilitate mass customisation, which may reduce the wait time of the patient before s/he receives the girdle as a treatment. On the other hand, the shoulder strap ends are modified so that they have rounded edges to eliminate curling of the strap ends.

### 3.3.1.2 Placement and magnitude of corrective forces

In terms of the exertion of the corrective forces, the free-end design of the elastic straps does not offer good control of the corrective forces (Fok, 2020). The strap can also easily shift which affects the accuracy of the corrective force exertion. Also, no systematic markings were found on the straps as a reference for strap tension adjustment. On the other hand, the size of each partition with the lined pockets for inserting the EVA foam pads to create the points of pressure is somewhat too big on the original design. There are only 6 partitions in total, see Figure 3.5. The corrective forces may be therefore weakened by this larger area covered and the padded areas also cover parts of the body that do not need the corrective forces.

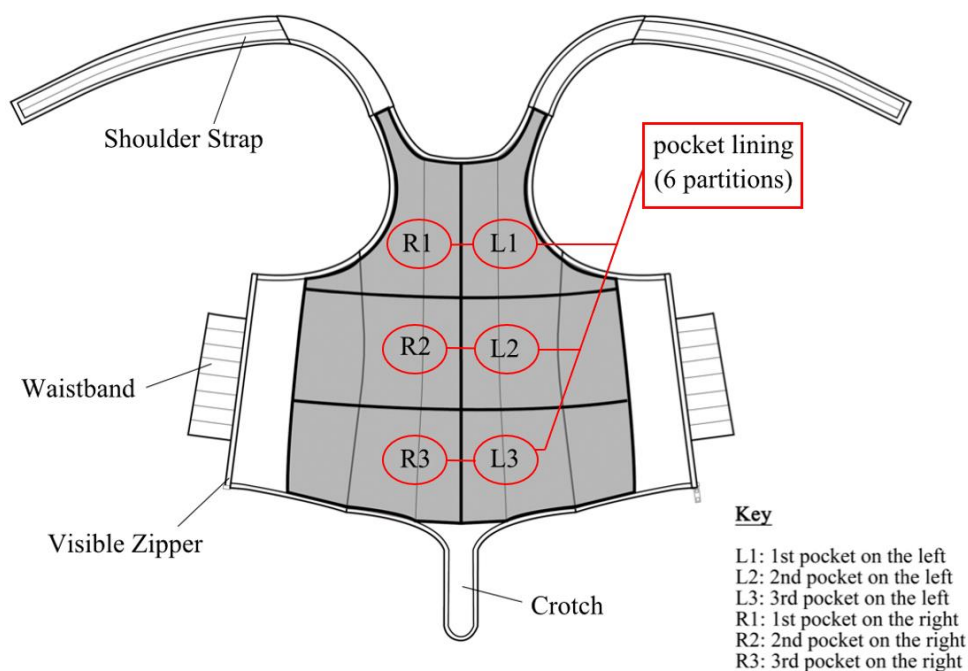


Figure 3.5 Six partitions with lined pockets on original design

In order to tackle the above problems, the free-end design of the elastic straps was eliminated and fasteners were added (e.g. Velcro hook tape) to fix the straps into position, so the corrective force can be controlled in a more precise way. Additionally, systematic marking was introduced on the straps as a reference for tension adjustment. Other than that, the pocket lining for EVA foam pad insertion should be divided into smaller areas so that sufficient corrective points of pressure could be exerted to the needed area.

### 3.3.1.3 Level of wear comfort and durability

In terms of the limitations related to the level of wear comfort on the original design, thermal

discomfort caused by multiple layers of fabric materials may be one of the reasons that resulted in a lower rate of compliance with the use of the garment during summer (Liu et al., 2014). The tricot fabric of the shell layer of the original design also has relatively low pilling resistance and is easily damaged by the Velcro hook tape attached to the elastic straps, which may affect the tactile comfort, see Figure 3.6. Other than that, Liu et al. (2015) stated that the corrective effect declines three months after the wear trial as a result of the repeated washing and extension of the girdle, which reflect the poor material strength and recovery of the original PCG.

To enhance the mPCG, materials that are unsuitable and inappropriate need to be eliminated and replaced by those with better performance in terms of breathability, pilling resistance ability, strength and recovery. To do so, several physical laboratory tests were carried out during the material selection process for the mPCG. Details of the material laboratory tests are described in Section 3.3.2.



Figure 3.6 Pilling on tricot fabric of original design

#### **3.3.1.4 Aesthetics**

In regard to the dissatisfaction with the original PCG in terms of its aesthetics, the primary reason is the excessive number of stitch lines on the surface of the girdle, which results in a ‘messy’ appearance (see Figure 3.7). The original PCG is beige in colour, which youths may consider to be outdated so they felt that the PCG is not aesthetically pleasing which reduces the treatment compliance.

To enhance the visual attractiveness of the girdle, it is recommended that the stitch lines should not be visible or as low in visibility as possible so that the girdle looks neat and tidy. Since the PCG is supposed to be worn as an undergarment by girls in the early stages of scoliosis, dark coloured fabric materials may not be a good idea as the girdle may be visible underneath the school uniform. Therefore, a white colour fabric is a better choice to create a cleaner look.

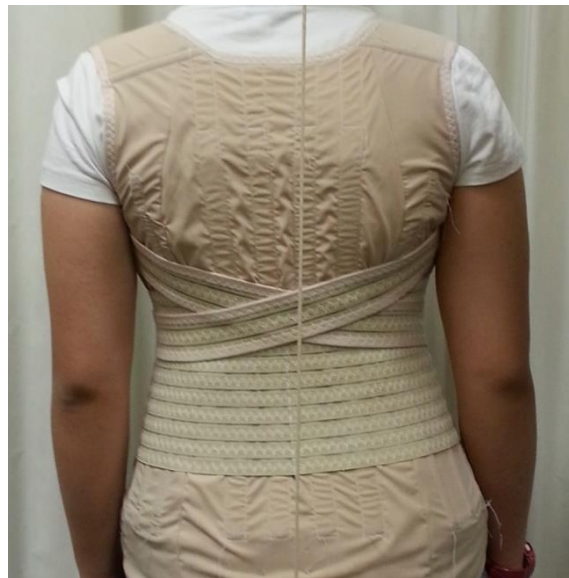


Figure 3.7 Stitch lines on the surface of the girdle

### **3.3.2 Material selection and testing**

#### **3.3.2.1 Selection criteria**

As mentioned earlier, the design of the original PCG used multiple layers of fabric materials which may lead to thermal discomfort and reduced compliance during summer (Liu et al., 2014). The tricot fabric of the shell layer of the original PCG also has poor pilling resistance, which may affect the tactile comfort and appearance. According to Yu (2016), powernet and satinette are common types of fabrics used for undergarment and shapewear. They provide aesthetics and enhance air permeability. Each layer of the PCG serves a purpose, so the multiple layers cannot be reduced; i.e., there is a shell layer for aesthetics, which also resists pilling and offers a good hand feel; middle layer to attach the resin bones and provide support, and inner layer for EVA foam pad insertion and good hand feel. Therefore, a different fabric material is the best option. The middle layer of the original PCG is a satinette with high strength and recovery that facilitates compressive force exertion as well as good air permeability, while the inner layer is made of a fine powernet with high air permeability and good hand feel. They performed well as expected. Therefore, only the fabric of the shell layer – the tricot fabric

would be replaced by another fabric material with better performance. Powernet was subsequently used as the shell layer of the mPGC to enhance its air permeability. However, the powernet for the shell and inner layers should not be the same since they have different purposes. Powernet with good elasticity and recovery, dimensional stability, air permeability, water vapor permeability, pilling resistance, and hand feel should be selected for the shell layer. Physical material laboratory tests were carried out to select the suitable fabric material for the shell layer. Details of the material laboratory tests are described in the following sections.

On the other hand, Liu et al. (2015) stated that repeated washing and extension of the girdle and straps reduce the corrective effect of the PCG after the third month of the wear trial. The elastic straps (shoulder straps and waist band) are key components that exert corrective forces for correcting the posture and spinal curvature. Therefore, apart from considering the performance of the fabric materials, the strap materials should also be selected carefully. Several physical material laboratory tests were conducted for selecting the elastic strap. The tests include those for elasticity and recovery, repeated stretching ability, dimensional stability, air and water vapor permeabilities, and hand feel. The material laboratory tests are summarised in Table 3.1 for the fabric and elastic strap materials.

Table 3.1 Material laboratory tests for fabric and elastic strap materials

	<b>Material test</b>	<b>Fabric</b>	<b>Elastic straps</b>
1	<u>Elasticity and recovery test</u> [Standard: ASTM D6614-07]	V	V
2	<u>Repeated stretching test</u> [Tensile Strength Tester Instron 4411]		V
3	<u>Washing test (dimensional changes of fabrics after home laundering test)</u> [Standard: AATCC 135]	V	V
4	<u>Air permeability test</u> [Standard: KES-F8]	V	V
5	<u>Water vapor permeability test/ Moisture permeability test</u> [Standard: ASTM E96]	V	V
6	<u>Pilling resistance test</u> [Standard: ASTM D4970]	V	
7	<u>Hand feel</u> [Standard: KESFB4-AUTO-A Automatic Surface Tester]	V	V

### 3.3.2.2 Elasticity and recovery test

Elasticity and recovery tests are designed to determine the stretch, growth, and recovery properties of the tested fabric. In this study, these tests are conducted on the selected fabric and elastic samples. In accordance with ASTM D6614-07 Standard Test Method, the Instron 4411 tensile strength tester (Figure 3.8) was used for the test.



Figure 3.8 Instron 4411 tensile strength tester

In the test, a specimen with dimensions of 35 x 5 cm was taken from each fabric and elastic sample. These specimens were stretched at a constant load (4 lbs) for 5 minutes respectively. After the end of cutting in tensile testing, the machine would be returned to its original position. The length of the sample was measured without slack. The length measurements were recorded before, during and after loading. Then, the material elongation and growth were calculated by using:

$$\text{Fabric stretches (\%)} = \frac{B - A}{A} \times 100 \quad (2)$$

$$\text{Fabric growth (\%)} = \frac{C - A}{A} \times 100 \quad (3)$$

where,

A= the initial length of specimen,

B= the length of specimen during loading (4 lb), and

C= the length of specimen after loading without slack.

### 3.3.2.3 Repeated stretching test

Repeated stretching is essential to assess the durability of the elastic bands in this study, which was done on select straps. The Instron 4411 tensile strength tester (Figure 3.8) was also used for this test.

Three 9 cm x 2 cm specimens were taken from each elastic strap sample with 2 cm markings made at the ends of the straps as the control. The specimens were fixed by using the clamps according to the markers. The distance between the two clamps was fixed as 5 cm. All the specimens were stretched 30% for 1000 times at 300 mm/min to simulate stretching during daily use. The forces exerted during the stretching of the specimens were recorded and plotted. The ideal elastic strap material to produce the mPCG should have good stretch properties.

### 3.3.2.4 Washing test (dimensional changes of fabrics after home laundering test)

Garments are expected to be laundered at home after being worn to maintain good hygiene. The washing test determines the changes in the length and width of the fabric after laundering. In this study, the washing test is conducted on the selected fabric and elastic straps based on the AATCC 135 Test Method for Dimensional Changes of Fabrics after the Home Laundering. Figure 3.9 shows the washer and dryer used in the test.



Figure 3.9 Washer and dryer

For each selected fabric material, three samples with dimensions of 38 cm x 38 cm were prepared for the test. Three sets of benchmarks were marked evenly on the fabric specimens

within 25 cm in the weft and warp directions, respectively. For the selected elastic straps, 38 cm specimens at their full width were prepared for the test. Three sets of benchmarks were marked evenly on the elastic strap specimens in the length direction of 25 cm. All of the specimens were washed in the washer using a normal cycle with warm water at 41°C and 66 g of AATCC 124 standard detergent. Apart from putting the fabric and elastic strap specimens into the laundering machine, dummy pieces were also added for a 1.8 kg load during the laundering process. After laundering, the specimens and dummy pieces were separated for tumble drying. Only the specimens were placed in the dryer at the delicate setting. Finally, the changes in the distance between the benchmarks on the specimens were measured and the percentage of their dimensional changes were calculated by using:

$$\%Dimensional\ Change = \frac{(B - A)}{A} \times 100\% \quad (4)$$

where,

A= original dimensions of the benchmark, and

B= dimensions of benchmark after laundering.

### 3.3.2.5 Air permeability test

The importance of air permeability in terms of the wear comfort of textiles was addressed by Kilinc-Balci (2011). In this study, an air permeability test is conducted on the selected fabric and elastic straps. The KES-F8 Air Permeability Tester (Figure 3.10) was used to measure the amount of the air passing through the specimens in accordance with the KES-F8 standard.



Figure 3.10 KES-F8 Air Permeability Tester

Five specimens with dimensions of 50 mm x 50 mm were obtained from the selected fabric and elastic strap samples. Each specimen was fixed between the pressure chamber and metal plate for the test. The vent area is  $2.8 \pi \text{ cm}^2$ . During the test, air was supplied at a constant flow rate and the amount of airflow resistance was calculated automatically. The findings were presented as a mean value and expressed in kPa s/m for each type of fabric and elastic strap material. A smaller mean value indicates higher permeability and breathability.

### 3.3.2.6 Water vapor / Moisture permeability test

The water vapor permeability test is used to evaluate the moisture permeation of fabric. Fabric with higher water vapor permeability always has better sweat-wicking ability. This is vital for the wear comfort of a fabric. In this study, the water vapor permeability test is conducted on the selected fabric and elastic straps by using the ASTM E96 standard test method to determine the WVT rate of the materials. The set up of the vapor permeability test is shown in Figure 3.11.



Figure 3.11 Set up of water vapor permeability test

Four specimens were prepared for each selected fabric and elastic strap sample. The specimens were cut to accommodate the outer edges of the test cup. The beaker was then filled with distilled water until 3/4 full. After that, the specimens were glued to the top of the test cup with a water-resistant adhesive. The back side of the specimens faced the water to simulate the moisture transfer from the skin to the environment. Each test cup (with the specimen) was weighed and the weight was recorded. After 24 hours, each test cup (with the specimen) were weighed and recorded again. Finally, the average water vapor transmission (WVT) rate was

calculated by using changes in weight with the balance which has an accuracy of 0.01 g as:

$$WVT = \frac{G}{TA} \quad (5)$$

where,

G= weight change in grams,

T= time duration when G occurred (hours), and

A= test area of testing cup in m<sup>2</sup>.

### 3.3.2.7 Pilling resistance test

Pilling is the formation of microfiber balls (pills) on the surface of fabric due to abrasion during wear. This study follows the ASTM D4970 Standard Test Method for Pilling Resistance and Other Related Surface Changes of Textile Fabrics to assess the resistance of the fabric samples to forming pills and other related surface changes. A Martindale abrasion tester (Figure 3.12) and the Pilling Scope for fabric evaluation (Figure 3.13) were used for the testing.



Figure 3.12 Martindale abrasion tester

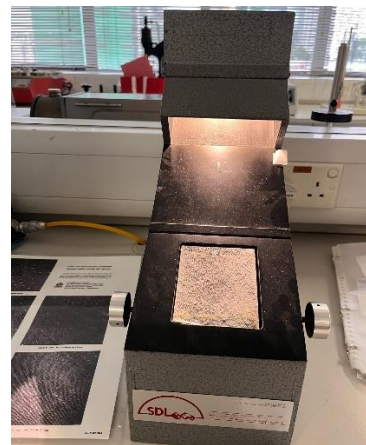


Figure 3.13 Pilling Scope

Since the design of the mPCG uses Velcro tape as fasteners, the hook side of the selected Velcro tape (hook tape) was also tested. Four pairs of each fabric sample and hook tape were cut into a circular shape with a diameter of 140 mm and 38 mm, respectively. During the test, the fabric specimens were placed onto the specimen holders of the Martindale abrasion tester and the hook tape was placed on a disk with 3 mm thick polyurethane foam. The spindle with the hook tape was then inserted into the tester holder to apply 3 kPa of pressure onto the fabric sample. The faces of both the fabric and hook tape came into contact. The specimen was subjected to 100

cycles to produce abrasion. After completing the test, the degree of pilling and fuzzing on the fabric specimens was determined by referring to the apparatus manual. The results obtained reflect the performance of each material sample in resisting pilling.

### 3.3.2.8 Hand feel

The hand feel test aims to determine the surface roughness of a material. A material with lower surface roughness gives a better hand feel. In this study, the hand feel test conducted on the selected fabric and elastic strap materials only examines their frictional properties and geometrical surface roughness. The KESFB4-AUTO-A Automatic Surface Tester (Figure 3.14) was employed to carry out the testing.



Figure 3.14 KESFB4-AUTO-A Automatic Surface Tester

A specimen of 20 cm x 20 cm in size was taken from each selected material. After the specimen was placed on the automatic surface tester, the roughness and friction sensors were positioned automatically, and the measurement process would then start. Three measurements of each required area were obtained. The sensors took the measurements at the required areas one by one. The mean coefficient of friction (MIU), variation of mean coefficient of friction (MMD) and surface roughness (SMD) were recorded during each measurement. Measurements were taken for both the technical face and technical back sides of the selected materials and in the vertical and horizontal directions.

### 3.4 Subject recruitment

In order to evaluate the effectiveness of the mPCG, subjects were recruited for a wear trial. The recruitment method and criteria are described below.

### **3.4.1 Inclusion and exclusion criteria**

Subjects were recruited based on inclusion criteria as follows: adolescent girls between 10 and 13 years old who are diagnosed with AIS (Cobb angle of 10 to 20°), iliac crest has a Risser grade equal to or less than 2 (indicates skeletal immaturity; however, individuals with a Risser 3 would also be considered and recruited), less than a year post-menarche or premenstrual, capable of following the entire routine both physically and intellectually, and able to read and speak English or Chinese. The participants agreed to engage in the study voluntarily and consented to the use of their personal information, including all measures taken and data obtained for data analysis and research purposes.

The exclusion criteria are: any subject who has a history of (1) previous surgical or orthotic treatment for AIS, (2) contraindications for x-ray exposure or pulmonary tests, (3) recent trauma, (4) mental disorder, (5) skin allergies, or (6) refusal to comply with wearing the mPCG.

### **3.4.2 School-screening programme**

In order to recruit subjects, school screenings were conducted in primary and secondary schools. The research group and a prosthetist-orthotist (P&O) carried out the spinal evaluation at the schools. Then after the subject was considered eligible, her parents gave signed consent for her participation and an information leaflet was provided to them. However, due to the COVID-19 pandemic restrictions at the time of this study, many local schools were conducting studies online. Even though there was a short period when classes resumed, the majority of schools focused on academics. Therefore, some of the school-screenings were carried out on-site at targeted schools, while others were carried out on university campus through invitation to the targeted group.

The standards used for scoliosis screening in California public schools (2007) are supposed to be comprehensive and repeatable. Consequently, these standards were referenced and used in this study. The P&O was tasked with conducting the Adam's forward bend test with a scoliometer to evaluate the curvature (Reamy & Slakey, 2001). The ATR was also determined by using the scoliometer. The ATR, also known as ATI, has a sensitivity of 84.37% for scoliosis detection (Karachalios et al., 1999). The posture alignment was also examined to see if there were any imbalance symptoms, particularly regarding shoulder balance, pelvis asymmetry, etc.

In addition, the name of the participant, age, body height, weight, indicators of poor posture, and contact method were also documented. The form used for the school screening is provided in Figure 3.15 (see Appendix I), while the Adam's forward bend test with the scoliometer is shown in Figure 3.16.

Figure 3.15 Form used for the school screening programme

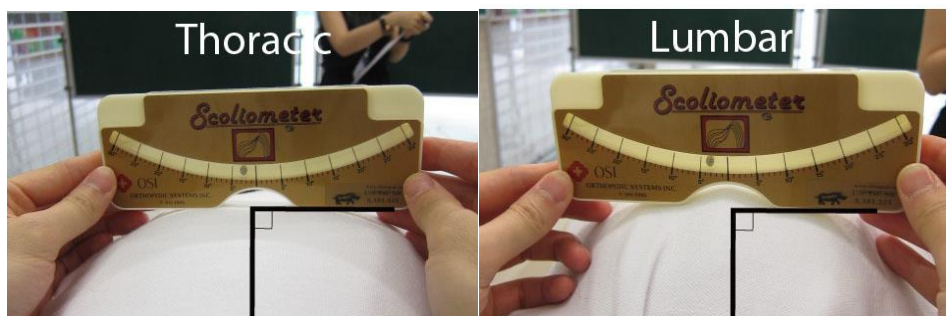


Figure 3.16 Measurement of ATR with scoliometer in Adam's forward bend test

An ATR of  $3^\circ$  may be an early symptom of the beginning of scoliosis, hence children who have an ATRs of  $3^\circ$ ,  $4^\circ$ , or larger based on a screening programme have to be rescreened more regularly and given extra attention (Bunnell 1984). As a result, participants who have an ATR of  $3^\circ$  or larger were considered potential research participants. All of these potential subjects were encouraged to undergo radiography after the school screening programme so that their

spinal conditions could be further appraised.

### **3.5. Wear trial and effectiveness evaluation**

#### **3.5.1 Girdle fitting and prescription**

After the participants of the school screening programme were diagnosed as having AIS in the early stages (Cobb angle 10 to 20°) based on a radiographic examination, they were invited to attend a fitting session of the mPCG on a voluntary basis. Prior to this, an information sheet of the current study was provided to them, and signed informed consent was sought from their parents (see Appendixes II and III for the information sheet and consent form, respectively). Apart from taking the body measurements of the potential subjects for an mPCG in their size, a 2-hour preliminary trial was conducted with each of them to determine if they are suitable for participating in the 9-month wear trial. When choosing a suitable girdle size for the recruited subjects, the measurement of the spine length from C7 to the pelvis level (see Figure 3.17) was critical apart from considering the circumference of the under bust, waist and high hip. More details of the girdle sizing system is provided in Chapter 4. During the preliminary trial, the potential subjects were prescribed an mPCG with inserted semi-rigid EVA foam padding based on their spinal curvature conditions to generate corrective forces onto different points of pressure. X-ray images were referenced to identify the location of the curve apex and determine the arrangement of the foam pads. Generally, two to three EVA foam pads were inserted into the inside pockets in opposite directions to each other and offer sufficient corrective forces while one or up to three pads were also possible based on the circumstances.

After prescribing the girdle, the potential subjects were required to take a low-dose X-ray after wearing the girdle for 2 hours to determine the immediate effects. If no negative effects are found, the participants were officially recruited as a subject for the 9-month wear trial. Additionally, evaluating the posture balance (by using 3D body scanning and posture angle measurements) and testing for proprioception deficits (by using the Vicon Nexus 3D motion capture system) were also conducted with and without the mPCG donned for data collection at 0 M, while the interface pressure measurements (by using the Pliance®-xf 16 system) were only conducted with the mPCG donned. The operation methods of these tests and measurements will be discussed in Section 3.5.3.

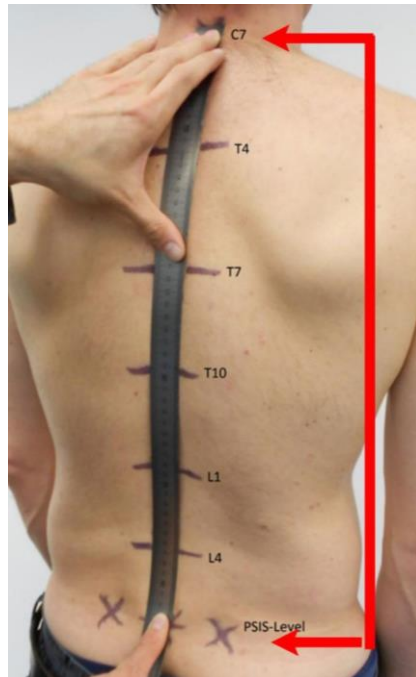


Figure 3.17 Spine length from C7 to pelvis level

### 3.5.2 Interface pressure measurement (Pliance®-xf 16 system)

In order to understand the pressure distribution of the mPCG, the interface pressure was measured after prescribing the girdle. A Pliance®-xf 16 system (Novel, Munich, Germany) with single sensors was employed for the interface pressure measurement (see Figure 3.18). The single sensor has a measurement range from 0 to 60 kPa and a measurement area of 78 mm<sup>2</sup>. Each sensor was placed between the girdle and skin based on the designated placement locations and curve apex for the interface pressure measurement.



Figure 3.18 Pliance®-xf 16 system (Novel, Munich, Germany) a single sensor

During the pressure measurement process, the subjects were required to wear a tightly-fitting bra top with shorts underneath the mPCG with the suggested inserted EVA foam pads and strap tension. The subjects were instructed to stand naturally with their hands at their sides for 3 minutes. To prevent data inconsistency and fluctuation, the pressure measurement recordings were not conducted for the first and last minutes. Only the measurements taken after the first minute were recorded and used for the evaluation.

### **3.5.3 Wear trial instruction and evaluation time point**

The officially recruited subjects participated in a 9-month wear trial with the mPCG and wore the girdle for the recommended 8 hours a day. Before the 9-month wear trial started, the recruited subjects were given a two-week adaptation period to become acclimatised to their girdle. The recommended amount of time to wear the girdle every day throughout the adaptation period was 2 hours during the first week and 4 hours during the second week. It was important to ensure that the participants understood the girdle-wearing method and did so appropriately before the wear experiment began. Apart from the evaluation tests taken before the start of the wear trial (0 M) under the conditions of both wearing and not wearing the girdle, evaluation tests were also conducted at 3 M, 6 M and 9 M to monitor the progress and compare the results. Questionnaires were also completed by the subjects to evaluate their QoL. Furthermore, data on the compliance with the bracing and skin temperature during the wear trial were collected and subsequently analysed.

### **3.5.4 Evaluation methods**

#### **3.5.4.1 Radiographic examination and Cobb angle comparison**

The radiographic approach has long been considered as the most accurate method for monitoring changes in bone structure. The golden standard for diagnosing scoliosis is the radiographic assessment of the Cobb angle (Patias et al., 2010). Radiological imaging is typically utilised to confirm the bone structure or spinal alignment (Fortin et al., 2011). Typically, during the evaluation, the specialist will measure the Cobb angle and note any changes in the spinal curvature. Nevertheless, this approach is intrusive due to cancer risks, and cannot be used to take repeated measurements frequently as a result (Fortin et al., 2011). Therefore, the Hong Kong Advanced Imaging (HKAI) now makes available a new x-ray imaging alternative dubbed the EOS<sup>TM</sup> imaging system which significantly reduces radiation

exposure (see Figure 3.19). The radiation of the EOS™ imaging system can be as low as 1:10 when compared to traditional radiography, and even as low as 1:100 to 1:1000 when compared to a CT scan (Wybier & Bossard, 2013). The resultant images with the use of the EOS™ have better clarity, contrast, and sharpness (see Figure 3.20). This low radiation technology allows the subjects to receive periodical radiographic examinations for their spinal condition and monitor their bone maturity with a lower degree of risk.



Figure 3.19 EOS™ imaging system (EOS imaging, 2020)



Figure 3.20 Sample of EOS™ low dosage image

During the radiographic scanning, the subjects had to stand in the imaging cabin with their hands placed on the front wall. After the radiographic image was taken, their Cobb angle was assessed by professionals. The Cobb angle was measured and validated by two well trained research team members by using RadiAnt DICOM Viewer (64-bit) software. Besides, their Risser sign was also determined at each time point (i.e., 0 M, 3 M, 6 M and 9 M).

Negrini et al. (2012) recommended taking an in-brace X-ray as one of the metrics to evaluate the effectiveness of the bracing treatment. To compare the prior and current changes due to the treatment, each patient was required to be X-rayed with the mPCG donned and doffed at different time points. The X-ray timetable is provided in Table 3.2.

Table 3.2 X-ray timetable

	<b>Prior to treatment (0 M)</b>	<b>After 2 hour preliminary wear trial at 0 M</b>	<b>3 M</b>	<b>6 M</b>	<b>9 M</b>
<b>X-ray without mPCG</b>	V		V		V
<b>X-ray with mPCG</b>		V		V	

Prior to the 9-month wear trial, the subjects were required to take an X-ray without the mPCG and then with the mPCG donned after a 2-hour preliminary trial in order to understand the pre-treatment spinal conditions and the immediate effects of the girdle. Equation 6 is used for the calculation of in-orthosis correction rate. The recruited subjects were also required to take an X-ray without the mPCG at 3 M, and with the mPCG donned at 6 M and 9 M for monitoring their spinal conditions and tracking the effect of the girdle.

$$\text{In-orthosis correction(\%)} = \frac{(\text{Pre-orthosis} - \text{In-orthosis}) \text{ Cobb angle}}{\text{Pre-orthosis Cobb angle}} \times 100\% \quad (6)$$

Studies conducted in the past have found that spinal curvatures progress further with an increase in the Cobb angle of 5° or 7° (Wong & Tan 2010; Brooks et al. 1975; Soucacos et al. 1998; Rogala et al. 1978). In these investigations, different inclusion criteria for the increase in Cobb angle led to different progression rates found, such as 5% with an increase in the Cobb angle of 5° or more, 14.7% with a Cobb angle of more than 10°, and 6.8% with a Cobb angle of 6° or more. The comparison of the inclusion criteria, definition of progression, and rates of progression reported by studies on the progression of idiopathic scoliosis curvatures are shown in Table 3.3. Additionally, adolescents between the ages of 10 to 12 and 13 to 15 show progression rates of 25% and 10%, respectively, with a curve magnitude of <19°.

Table 3.3 Comparison of inclusion criteria, definition of curve progression and progression rates of idiopathic scoliosis

Reference	Number of Subjects	Inclusion Criteria (Cobb angle °)	Definition of Progression (°)	Progression Rate (%)
Brooks et al. (1975)	474	5° or more	Average of 7°	5%
Soucacos et al. (1998)	839	More than 10°	5° or more	14.7%
Rogala et al. (1978)	603	6° or more	5° or more	6.8%

With reference to previous studies, the progression of the curvature in this study was determined to be an increase of 5° or more. If the Cobb angle increased by  $\leq 5^\circ$  following the 9-month wear trial, the spinal curvature was considered to be under control. In addition to comparing the Cobb angle at 0 M and 9 M, the Cobb angle with and without the mPCG donned would also be compared during the different time points.

#### 3.5.4.2 Posture balance evaluation (3D body scanning and posture angle)

Posture imbalance issues are commonly found in AIS patients (Goldberg et al., 2001; Masso & Gorton, 2000). One of the main functions that the mPCG is supposed to achieved is to improve the posture imbalance so as to control the spinal curve progression. In this study, the posture correction effectiveness of the mPCG is evaluated by carrying out 3D body scanning and posture angle measurement. The Anthroscan body scanning system (Figure 3.21) was employed to capture 3D images during the 3D body scanning process and Geomagic Design X Version 2019.0.2 software was used for the posture angle measurement on the 3D scanned images. The initial scanning was performed at the beginning of the wear trial (0 M) under two conditions: “without the girdle” (mPCG doffed) and “with the girdle” (mPCG donned) to investigate the immediate effect of the mPCG in correcting posture. Follow up scanning was also conducted at 3 M, 6 M and 9 M “without the girdle” and “with the girdle” to monitor posture changes.

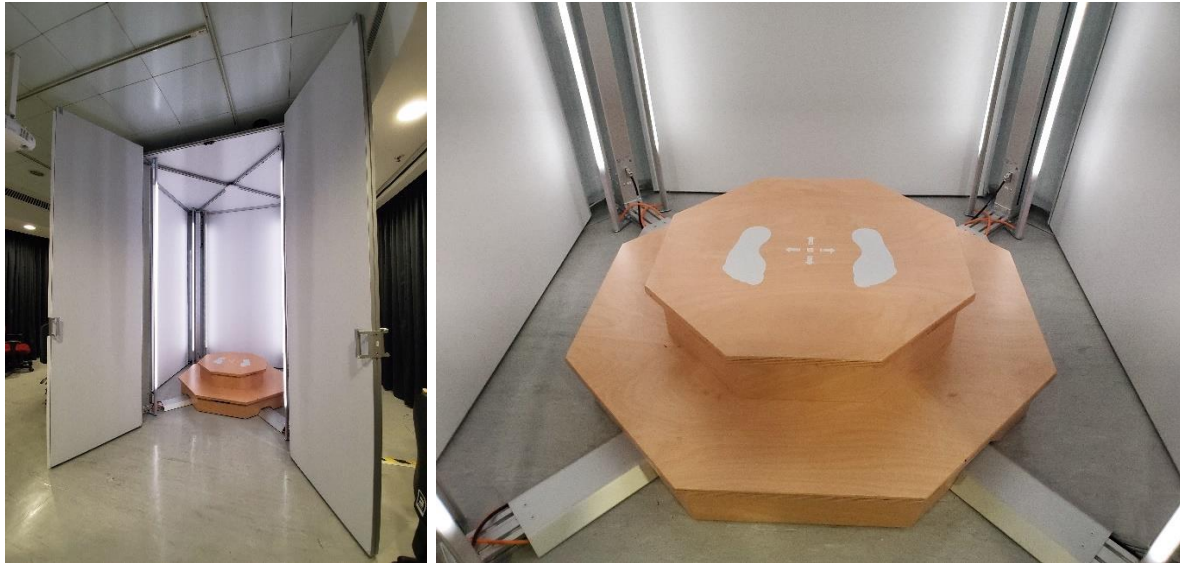
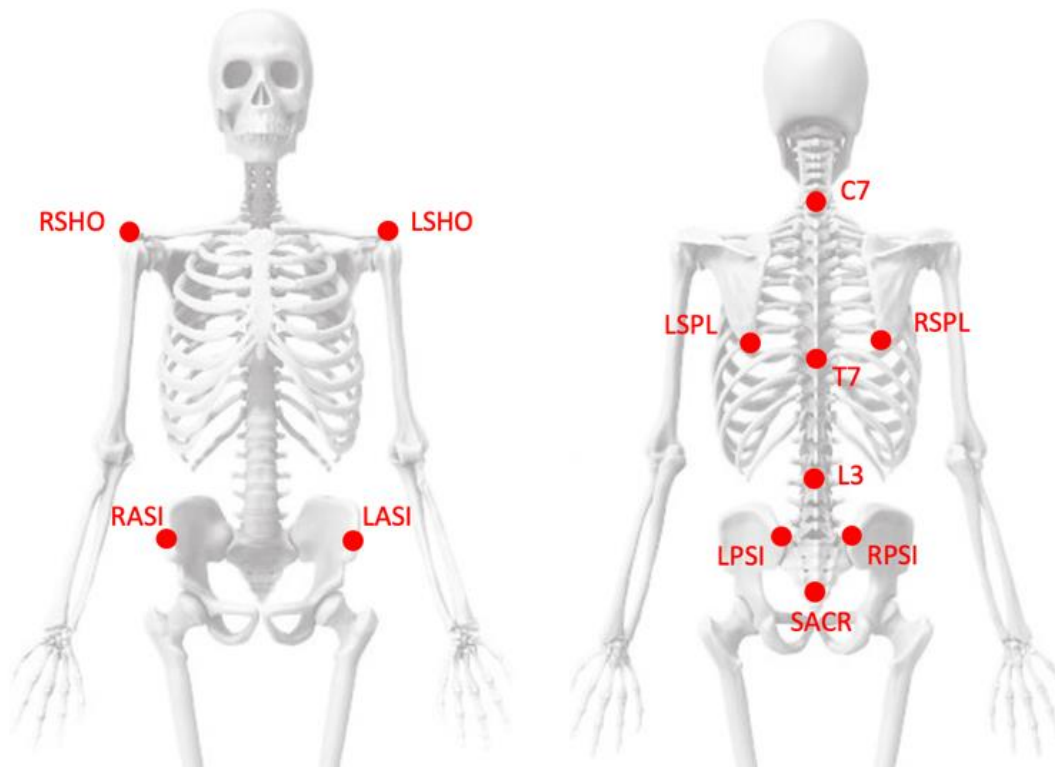


Figure 3.21 Anthroscan body scanning system

To ensure the accuracy of the data collected, calibration was performed in regard to the scanning process. The subjects were required to wear a tightly-fitting bra top with shorts in a plain light colour to obtain a better scanning outcome. Additionally, the subjects had to tie up their hair to prevent scanning interference, such as the hair covering the neck and back of the subject. Before scanning started, 12 markers of 15 mm in diameter were placed on the body of the subject according to the body landmarks shown in Figure 3.22 to facilitate the posture angle measurement (Liu et al., 2022). The 12 body landmarks include the: (i) left acromion (LSHO), (ii) right acromion (RSHO), (iii) left inferior angle of the scapula (LSPL), (iv) right inferior angle of the scapula (RSPL), (v) 7<sup>th</sup> cervical vertebra (C7), (vi) 7<sup>th</sup> thoracic vertebra (T7), (vii) 3rd lumbar spine vertebra (L3), (viii) sacrum (SACR), (ix) left anterior superior iliac spine (LASI), (x) right anterior superior iliac spine (RASI), (xi) left posterior superior iliac spine (LPSI), and (xii) right posterior superior iliac spine (RPSI). The subjects were required to perform standing and sitting postures for the scanning. When performing the standing posture, the subjects were instructed to stand up straight as they naturally would with their eyes open and looking forward. Also, their feet should be placed apart according to the footprint marker on the floor (see Figure 3.23). When performing the sitting posture, the subjects were asked to sit naturally on a chair with a proper height to make a 90° angle between the knee and calf. The subjects should also place their palms on their thigh with their eyes open and looking forward (see Figure 3.24).



1. left acromion (LSHO)
2. right acromion (RSHO)
3. left inferior angle of scapula (LSPL)
4. right inferior angle of scapula (RSPL)
5. the 7<sup>th</sup> spinous process cervical (C7)
6. the 7<sup>th</sup> spinous process of thoracic spine (T7)
7. the 3<sup>rd</sup> spinous process of lumbar spine (L3)
8. Sacrum (SACR)
9. left anterior superior iliac spine (LASI)
10. right anterior superior iliac spine (RASI)
11. left posterior superior iliac spine (LPSI)
12. right posterior superior iliac spine (RPSI)

Figure 3.22 Body landmarks for posture angle measurement (Liu et al., 2022)

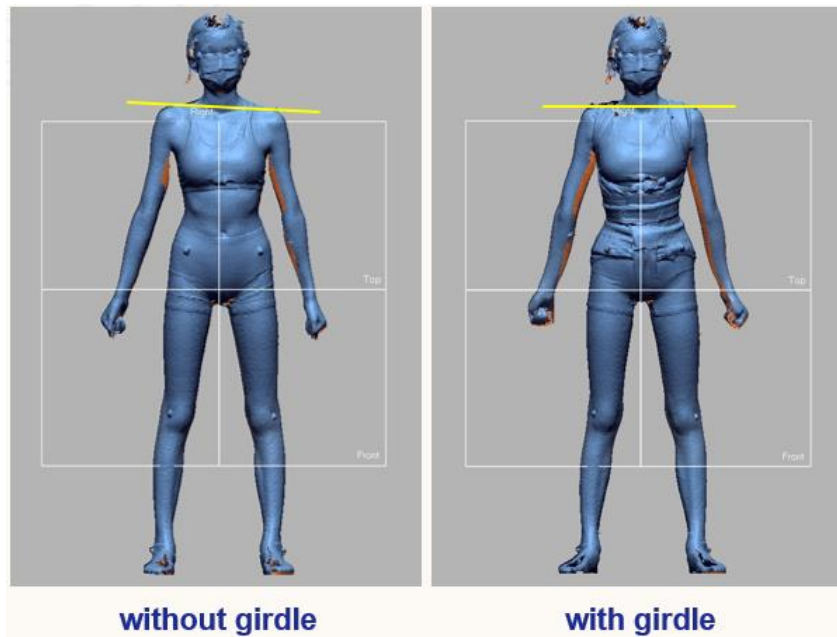


Figure 3.23 Standing posture during 3D body scanning

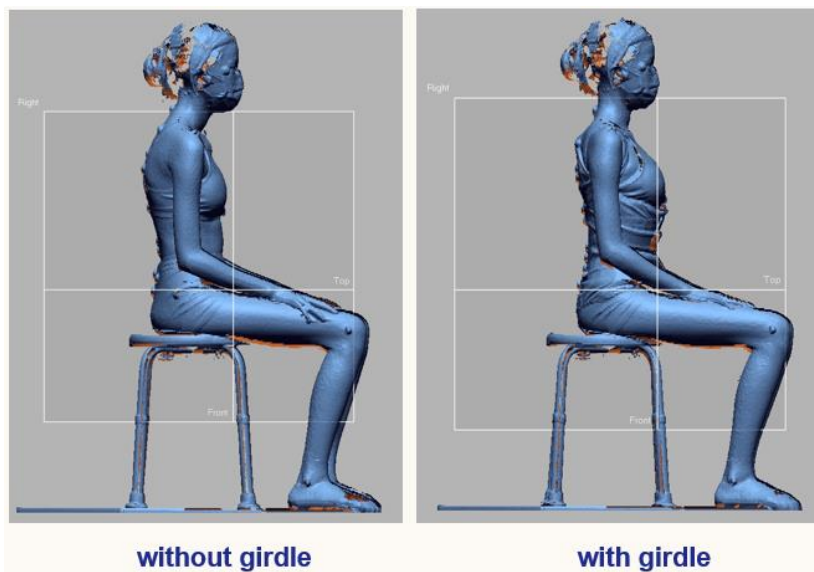


Figure 3.24 Sitting posture during 3D body scanning

For the standing posture, all of the posture angles shown in Figure 3.25 are measured for the posture evaluation. They include the acromion, pelvis, and acromion/pelvis angles in the frontal plane; acromion, pelvis, scapula, and acromion/scapula angles; and acromion/pelvis angle in the horizontal plane, as well as the thoracic and lumbar angles in the sagittal plane. As for the sitting posture, only the thoracic and lumbar angles in the sagittal plane were measured for the evaluation.

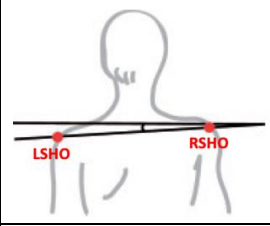
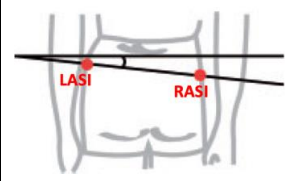
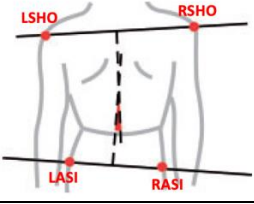
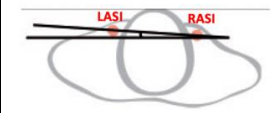
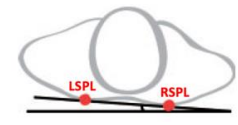
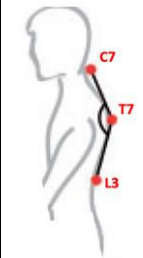
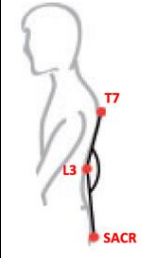
<p><u>Frontal</u> <b>Acromion</b></p> 	<p><u>Frontal</u> <b>Pelvis</b></p> 	<p><u>Frontal</u> <b>Acromion/ pelvis</b></p> 
<p><u>Horizontal</u> <b>Acromion</b></p> 	<p><u>Horizontal</u> <b>Pelvis</b></p> 	<p><u>Horizontal</u> <b>Scapula</b></p> 
<p><u>Sagittal</u> <b>Thoracic angle</b></p> 	<p><u>Sagittal</u> <b>Lumbar angle</b></p> 	<p><u>Horizontal</u> <b>Acromion/ scapula</b> (angle between the lines that pass through the markers on acromion and scapula in horizontal plane)</p> <hr/> <p><u>Horizontal</u> <b>Acromion/ pelvis</b> (angle between the lines that pass through the markers on acromion and pelvis in horizontal plane)</p>

Figure 3.25 Posture angles measured

### 3.5.4.3 Proprioception deficits test (Vicon Nexus 3D motion capture system)

Blecher et al. (2017) and Chesler et al. (2016) found an association between some of the proprioception-related gene mutations and idiopathic scoliosis development. Also, Lau et al. (2022) found proprioceptive deficits of the neck, elbow, and knee in participants with AIS in a comparison of participants without AIS in a meta-analysis. There is therefore a potential aetiological association between AIS and proprioception. Therefore, apart from looking at the effects of the mPCG on posture correction and spinal curvature control in this study, the consequential influence on proprioception deficit is also investigated.

The tests in the proprioception deficit experiment of this study include the: (i) neck rotation (NRZ), (ii) elbow flexion (EFY), (iii) knee extension (KEY) and (vi) Unterberger stepping (STP) tests. The tests were performed “without the girdle” and “with the girdle” at 0 M, 3 M, 6 M and 9 M for evaluation. During the tests, the subjects were instructed to perform specific movements with their eyes open and closed. A Vicon Nexus 3D motion capture system (Vicon

Motions Systems, Oxford, UK) operating at 120 Hz was employed for data collection. Before starting the tests, 39 reflective markers of 9 mm in diameter were placed on the body of the subject in accordance to the landmarks shown in Figure 3.26. A different set of reflective markers was needed for the data collection of each mentioned test (see Table 3.4), while some markers were used as reference. Once the reflective markers were placed onto the body, the subjects were asked to stand statically and hold a vertical position steadily at the centre of the detection area for 10 seconds. The purpose of this step was to let the motion capture system define each segment and detect the particular dimensions of the body parts. Then, the tests were performed one by one based on the sequence shown in Table 3.4. The tests “without the girdle” were conducted first, followed by those “with the girdle”.

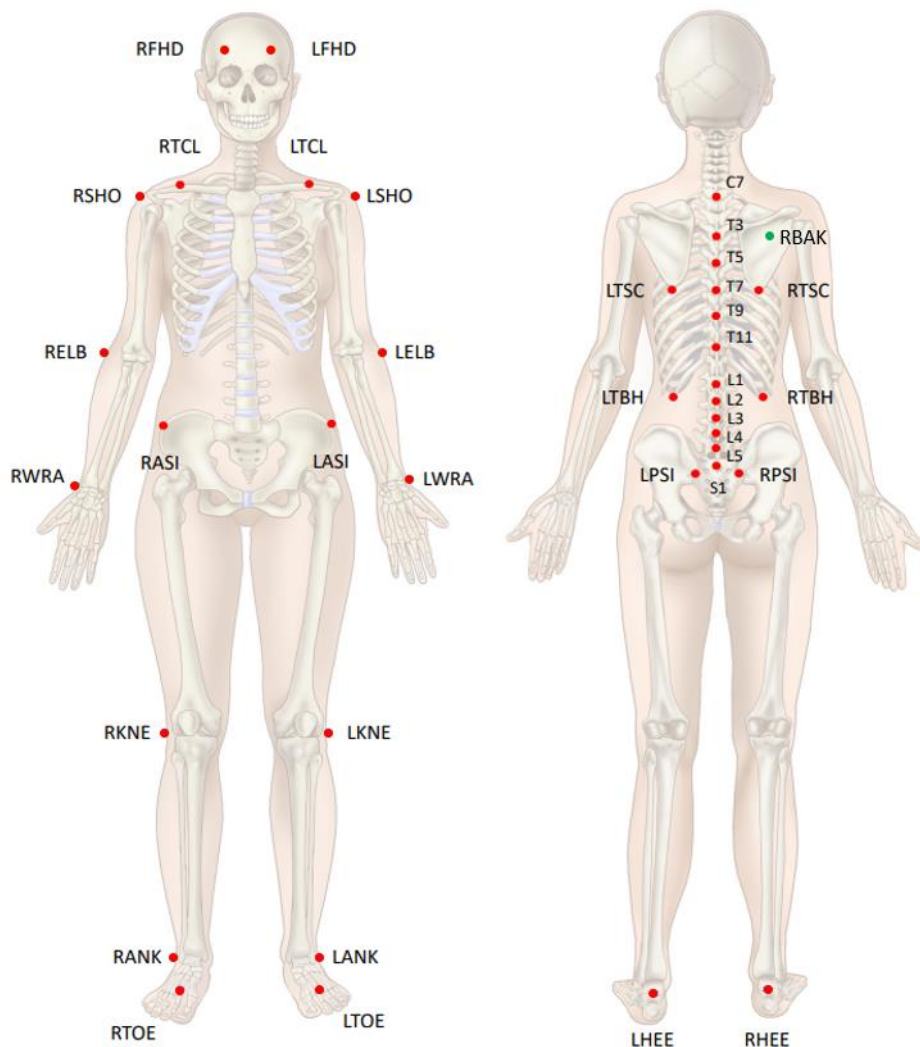
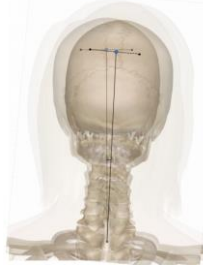
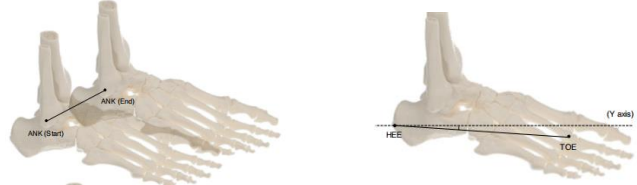


Figure 3.26 Placement of reflective markers for proprioception experiment

Table 3.4 Marker set for data collection and calculation in each test

Name of test	Marker set	Calculation formula & reference pictures (angle calculation)
<p>1. Neck Rotation (NRZ) – Left</p> <p>Neck Rotation (NRZ) – Right</p>	<p>RFHD, LFHD, C7</p>	 <p>Angle between the line of mid-head And C7 at start and the line of mid-head and C7 at end</p> <p><u>Calculation of the angle between vectors:</u>  <math>\tan(\theta) = \frac{\ u \times v\ }{(u \cdot v)}</math>                      [Rotation on traverse plane is needed before the calculation]                      Repositioning degree = <math>\theta_{end} - \theta_{start}</math></p>
<p>2. Elbow Flexion (EFY) – Left</p> <p>Elbow Flexion (EFY) – Right</p>	<p>LSHO, LELB, LWRA</p> <p>RSHO, RELB, RWRA</p>	 <p><math>\angle ELB: SHO-ELB-WRA</math></p> <p><u>Calculation of the angle between vectors:</u>  <math>\tan(\theta) = \frac{\ u \times v\ }{(u \cdot v)}</math>                      Repositioning degree = <math>\theta_{end} - \theta_{start}</math></p>
<p>3. Knee Extension (KEY) - Left</p> <p>Knee Extension (KEY) - Right</p>	<p>LASI, LKNE, LANE</p> <p>RASI, RKNE, RANE</p>	 <p><math>\angle KNE: ASI-KNE-ANK</math></p> <p><u>Calculation of the angle between vectors:</u>  <math>\tan(\theta) = \frac{\ u \times v\ }{(u \cdot v)}</math>                      Repositioning degree = <math>\theta_{end} - \theta_{start}</math></p>
<p>4. Unterberger Stepping (STP)</p>	<p>LANK, LTOE, LHEE, RANK, RTOE, RLEE</p>	 <p>ANK displacement</p> <p>TOE to HEE rotation (+ve angle indicates clock-wise rotation)</p>

		<p><u>Calculation of the displacement:</u> Ankle displacement= ANK_x_end - ANK_x_start (mm)</p> <p><u>Calculation of the angle between vectors:</u> <math>\tan(\theta) = \frac{\ u \times v\ }{(u \cdot v)}</math> Repositioning degree = <math>\theta_{end} - \theta_{start}</math></p>
<p><u>Notes:</u></p> <ul style="list-style-type: none"> <li>- RBAK is reference point for direction identification</li> <li>- T3, T5, T7, T9, T11, L1, L2, L3, L4, L5 and S1 are reference points to show the spine locations</li> <li>- LPSI and RPSI are reference points to show the location of superior posterior iliac spines</li> <li>- RTCL and LTCL are reference points to show clavicle locations</li> <li>- LTSC and RTSC are reference points to show scapula locations</li> <li>- LTBH and RTBH are reference points to show bottom rib locations</li> </ul>		

In the **NRZ** test, the subjects were asked to sit on a chair with a proper height to create a 90° angle between the knee and calf and place their hands by their sides, memorise the current position and hold the position for 3 seconds. The subjects were then instructed to memorise the current position in space and then close their eyes. Next, they were to turn their neck to the left, then to the neutral position and finally back to the memorised position and hold the position for 3 seconds. The test was repeated three times. After the completion of the tests for the left side, the tests for the right side were performed. The calculation of the angle between the line of the mid-head and C7 at the start, and line of the mid-head and C7 at the end was carried out for comparison and evaluation (see reference picture in Table 3.4).

In the **EBY** test, the subjects were asked to sit on a chair with a proper height to create a 90° angle between the knee and calf with their hands by their sides. The subjects were to lift their dominant hand to the middle position, memorise the position, hold it for 3 seconds, and then put down their dominant hand. Next, the subjects was instructed close their eyes, lift their dominant hand to the memorised position, hold it for 3 seconds and then put down their dominant hand. The test was repeated three times. After the completion of the tests for the dominant hand, the tests for the other hand were conducted. The calculation of the angle of the intersecting lines between shoulder-elbow and elbow-wrist was carried out for comparison and evaluation (see reference picture in Table 3.4).

In the **KEY** test, the subjects were asked to sit on a high chair and create a 90° angle with their legs hanging and feet. The subjects were instructed to lift their dominant leg, memorise the position, hold it for 3 seconds, and then put down their dominant leg. Next, they were to close their eyes, lift their dominant leg to the memorised position, hold the position for 3 seconds

and then put down their dominant leg. The test was repeated three times. After the completion of the test for the dominant leg, the test for the other leg was performed. The calculation of the angle of the intersecting lines between ASI-knee and knee-ankle was carried out for comparison and evaluation (see reference picture in Table 3.4).

In the **STP** test, the subjects were asked to stand at the centre of the detection area with lifted hands outstretched at 90° at the chest level and hold the start position for 3 seconds. Then, the subjects were to close their eyes, walk in place for 50 steps and hold the end position for 3 seconds. The start and end positions were recorded. Calculation of the ankle displacement and angle of the toe-heel rotation was carried out for comparison and evaluation (see reference picture in Table 3.4).

#### 3.5.4.4 Questionnaires for QoL evaluation

A good bracing or girdling treatment should be able to enhance the QoL and body image of the user (Wong, 2021). In this study, three questionnaires including the Scoliosis Research Society (SRS-22) questionnaire, the Brace Questionnaire (BrQ), and the Bad Sobernheim Stress Questionnaire (BSSQ)-Brace, were given to all of the recruited subjects to evaluate the treatment outcomes in terms of their QoL. Table 3.5 shows the questionnaire survey conducted at different time points throughout the wear trial period. At 0 M, the SRS-22 survey was conducted while the BrQ and BSSQ-Brace were conducted after the 2-hour preliminary wear trial. In the following session at 3 M and 6 M, as well as post-intervention at 9 M, the SRS-22 questionnaire, BrQ and BSSQ-Brace were all conducted. Since all of the recruited subjects could communicate effectively in Chinese/Cantonese, the Chinese version of the SRS-22 questionnaire, BrQ and BSSQ-Brace were used; see Appendixes IV, V and VI for details, respectively.

Table 3.5 Questionnaire survey conducted at different time points in the wear trial

	<b>SRS-22</b>	<b>BrQ</b>	<b>BSSQ</b>
Pre-intervention at 0 M	✓		
After 2-hour preliminary trial at 0 M		✓	✓
Follow up session at 3 M	✓	✓	✓
Follow up session at 6 M	✓	✓	✓
Post-intervention at 9 M	✓	✓	✓

#### **3.5.4.4.1 SRS-22 Questionnaire**

The main purpose of the SRS-22 questionnaire is to assess the outcome of health-related QoL (HRQoL) of patients with spinal deformity (Haher et al., 1999). The questionnaire contains 22 questions that are divided into 5 domains, including: (i) 5 questions about function/activity, (ii) 5 questions about pain, (iii) 5 questions about self-perceived body image, (iv) 5 questions about mental health, and (v) 2 questions about treatment satisfaction. A 5-point Likert scale is used from 1 (worst) to 5 (best). The average of each domain is calculated and the overall score will show the outcomes (Asher et al., 2006). The overall score is between 22 and 110; a higher score indicates a higher QoL.

#### **3.5.4.4.2 Brace Questionnaire**

The BrQ is a questionnaire developed specifically for children and teenagers who are receiving bracing treatment and are between 9 and 18 year old. Chan (2014) translated the questionnaire into Chinese. The questionnaire consists of 34 Likert scale questions based on the following 8 areas: (i) general health perception, (ii) physical functioning, (iii) emotional functioning, (iv) self-esteem and aesthetics, (v) vitality, (vi) school activities, (vii) physical pain, and (viii) social functioning. Total scores of the questions are multiplied by 20 and divided by 34 to obtain the final overall score of the questionnaire, which can range from 20 to 100. Higher BrQ scores indicate a better QoL (Aulisa et al., 2010).

#### **3.5.4.4.3 Bad Sobernheim Stress Questionnaire (BSSQ)-Brace**

The BSSQ-Brace is a questionnaire for evaluating the psychological and physical comfort of the brace. Eight questions in total with four option levels each make up the BSSQ-Brace. Each question can receive a maximum of three points and a minimum of zero. The total score can range from 0 to 24. The correlation between the stress level and sum of all question scores should be negative. The final scores can be 0-8 (high stress), 9-16 (medium stress), and 17-24 (little stress) (Botens-Helmus et al., 2006).

#### **3.5.4.5 Compliance and thermal comfort monitoring**

The success of an orthosis treatment throughout a long-term wear trial is closely related to the rate of treatment compliance. Temperature loggers are one of the possible tools for tracking the compliance rate (Hasler et al., 2010). In this study, one Hygrochron™ iButton sensor that is

16 mm in diameter (see Figure 3.27) was placed in the pocket lining of the mPCG for each subject in order to monitor treatment compliance. The placement location of the sensor was at the back and waist level.



Figure 3.27 Hygrochron™ iButton sensor

The data were collected by using a Blue Dot™ receptor. The sensor was set to record the data every 15 minutes. The sensor can only capture data for a maximum of 12 weeks at a time, therefore, the provided sensor was replaced with a new one every 3 months. On the other hand, a temperature of 30°C was set to indicate girdle wear because 30°C is the average normal skin temperature which gradually builds up under clothing (Benedict et al. 1919). Hence, when the captured temperature data exceed 30°C, it was considered that the subject was wearing the girdle. Besides, the captured temperature data may also provide information about the wear comfort level.

### 3.6 Conclusion

This chapter has provided the research flow plan of this study, from the design refinement of the PCG to the material selection for the mPCG, as well as details on subject recruitment, wear trial experiments and effectiveness evaluation, FE modelling to model the effects, and the development of an intelligent system for prescribing the mPCG. Each component of the research flow plan is interlinked. In the part where the design is modified, limitations of the original PCG are identified in terms of the fitting and sizing, placement and magnitude of the corrective forces, level of wear comfort and durability, as well as aesthetics with

recommendations for improvements. In the part on material selection, the criteria for selecting the materials and procedures of each laboratory test (i.e. elasticity and recovery, repeated stretching, washing, air permeability, water vapor permeability, pilling resistance, and hand feel tests) are clearly described. In terms of the subject recruitment, the inclusion and exclusion criteria, as well as the procedures of the school-screening programme are elaborated. As for the fitting of the mPCG and its prescription, wear trial experiments and girdle effectiveness evaluation methods, apart from the implementation plan, the steps and rationale for all the tests (i.e. interface pressure measurement, radiographic examination and Cobb angle comparison, 3D body scanning and posture balance evaluation, proprioception deficits test, questionnaires for QoL evaluation, and compliance and thermal comfort monitoring) are explained in detail. Finally, the method and development process of the FE modelling and constructing the intelligent system, will be discussed in Chapter 6 of this report.

## Chapter 4 – Modification of Posture Correction Girdle

### 4.1 Introduction

In this chapter, the mPCG is first discussed in terms of the (i) fitting and sizing, (ii) placement and magnitude of corrective forces, (iii) level of wear comfort and durability, and (iv) aesthetics aspects. Then, the details of the newly developed specific sizing system for the mPCG are given an introduction. After that, the material testing results of the sourced fabrics and elastic straps are reported, and the most suitable materials selected to produce the mPCG. Furthermore, the pattern development and garment assembling processes of the mPCG are described. Finally, photos of the finished prototype are shown.

### 4.2 Design feature modifications

In order to address the limitations of the original PCG in terms of the four aspects which include: (i) fitting and sizing, (ii) placement and magnitude of corrective forces, (iii) level of wear comfort and durability, and (iv) aesthetics aspects (see Section 3.3 for details), the girdle design and material use have been modified to fabricate a new prototype (mPCG) that enhances the corrective effectiveness and level of wear comfort. The design sketches of the mPCG (front and back, inner, and outer views) are shown in Figures 4.1, 4.2 and 4.3.

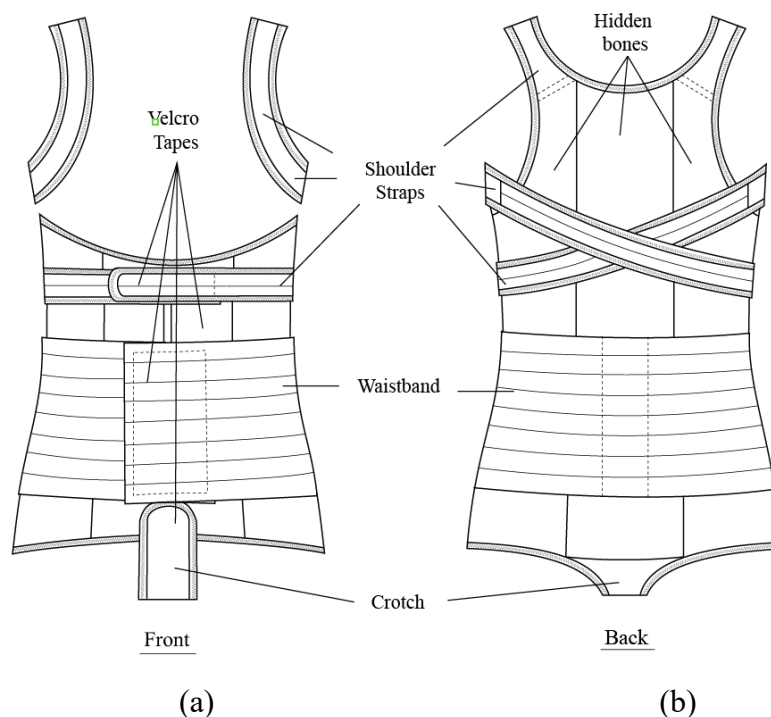
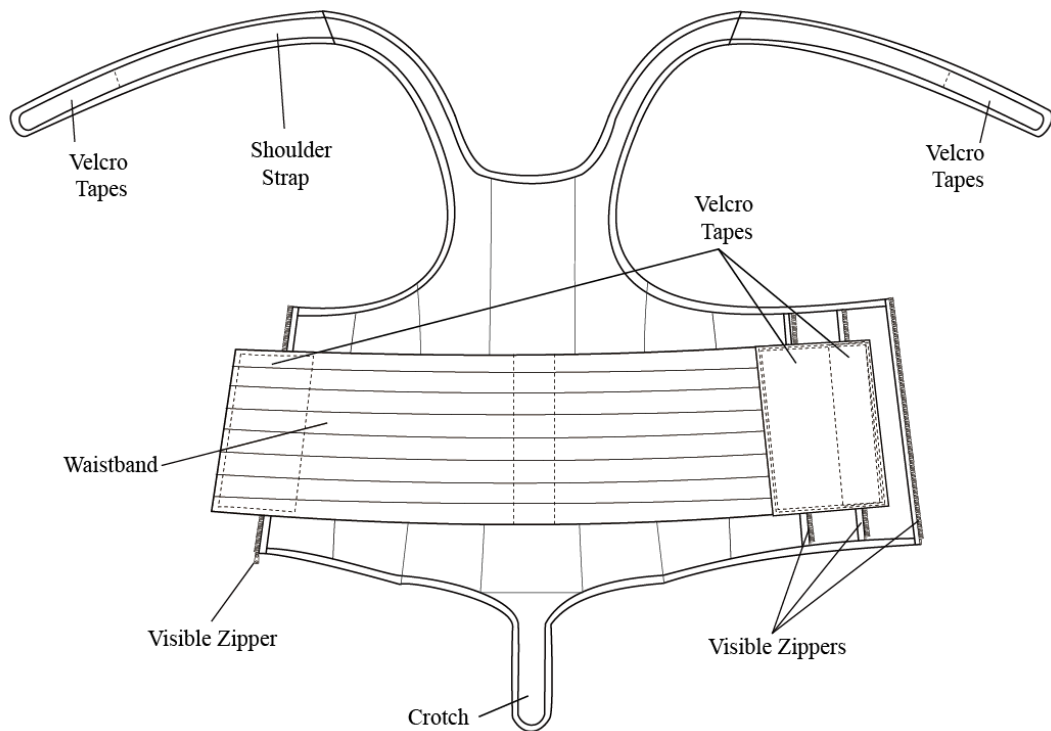
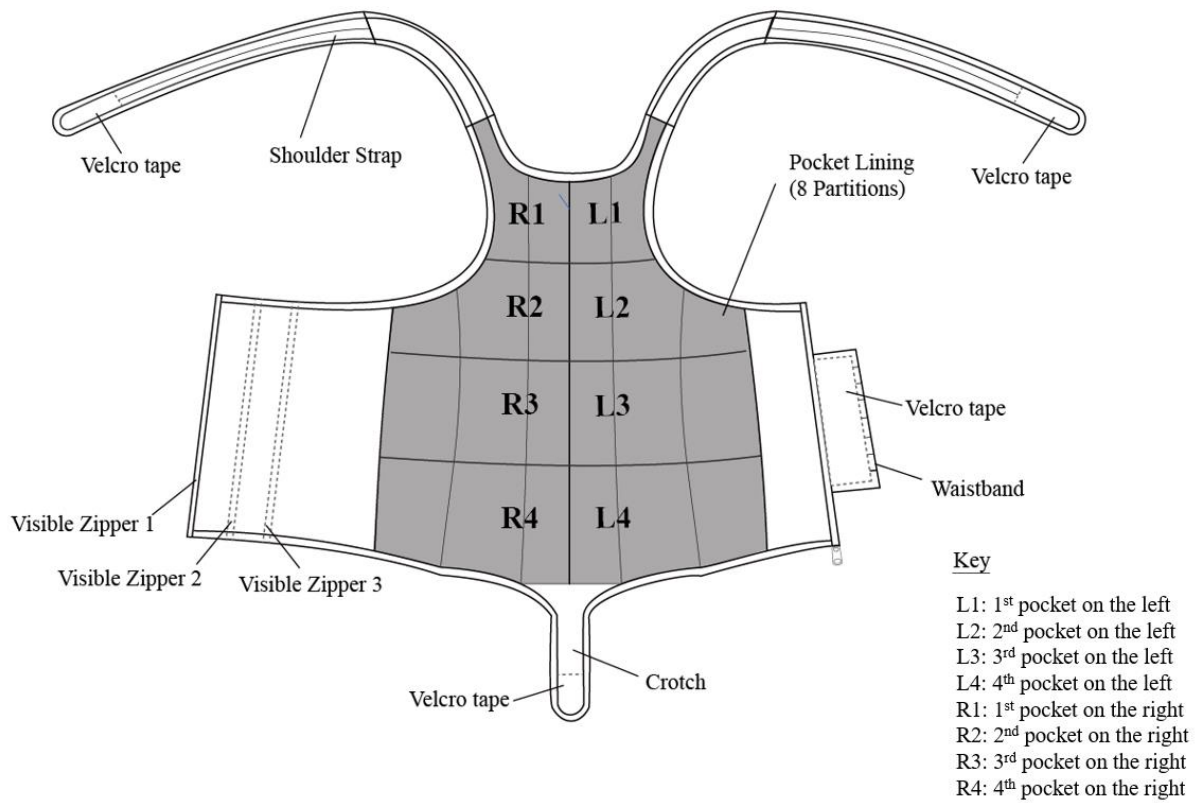


Figure 4.1 Design sketch of mPCG: (a) front and (b) back views



With respect to **fitting and sizing**, 2 more zippers were added to the centre front of the mPCG as the main closure of the girdle (in total, there are 3 zippers; see Figure 4.4). Therefore, a larger circumference range of the under bust, waist and high hips could be obtained with one girdle size. Adolescents grow rapidly during puberty, so if these three body parts change in circumference, the same girdle can still be used by making some fitting adjustments instead of ordering a new girdle within a short period of time. Thus, the mPCG is economical. Also, with a larger body circumference coverage, one girdle size can accommodate adolescents with different body shapes, which would facilitate the mass customisation of the mPCG. This might shorten the wait time of the patients by eliminating the long lead time spent during the made-to-measure process of the girdle. For mass customisation, a specific sizing system/size chart is needed, which will be described later in this chapter. On the other hand, the ends of the shoulder straps have been changed from a square shape into rounded edges. By doing so, the curling of the strap ends is eliminated.



Figure 4.4 Three zippers at centre front of mPCG

As for the **corrective forces**, the free-end design of the shoulder straps and waistband has been eliminated by adding Velcro hook tape underneath (see Figure 4.5), so the corrective forces could be exerted more accurately once the problem with the strap shifting has been remedied.

Moreover, the shoulder straps and waistband have been designed without free ends to allow different levels of corrective forces based on the imbalanced posture and spinal curvature condition, so the corrective forces could be exerted correspondingly. In addition, markings were added to the shoulder straps and waistband as a reference for tension adjustment. Each marking has a spacing of 2 cm from another marking (see Figure 4.6). By referring to the markings on the straps, the tension can be adjusted more systematically. On the other hand, the number of the pocket lining partitions were increased from 6 to 8 (see Figure 4.2). This allows the corrective forces from the points of pressure to be exerted onto the needed areas more precisely. Larger EVA foam pads in larger pockets means larger areas for the dissemination of corrective forces. When the forces are disseminated over a larger area, a smaller amount of exerted force would be the result. By increasing the number of partitions and making the partitioned area smaller, a larger amount of force could be exerted to a specific area that really requires the force. Also, with more pocket partitions, more padding insertion combinations are possible according to the different needs.



Figure 4.5 Newly added Velcro hook tape underneath straps



Figure 4.6 Newly added markings on shoulder straps and waistband

As for the **level of wear comfort and durability**, the objective is to increase the air-permeability and durability of the fabric, as well as reduce the likelihood of pilling. After studying the application of the fabric on the original girdle design, the decision was to change the shell fabric from a delicate tricot fabric to a powernet fabric which has high strength, recovery and air-permeability and ability to resist pilling. A number of powernet fabrics were sourced from the market for the shell fabric. Laboratory tests were carried out to evaluate the fabric properties and performances. The results are presented later in this chapter.

Regarding the **aesthetics** aspect, the mPCG should look neat and appear more aesthetically pleasing to adolescents. In order to eliminate the “messy” appearance of the original girdle design, the stitch lines for attaching the tape for bone insertion at the shoulder seams, and back and side panels were hidden (see Figure 4.7). Only the stitches on the V-fold elastic for finishing the edges and stitches to attach the waistband and fasteners (i.e. Velcro tape, zippers) can be seen on the surface. Besides, the colour of the main body of the girdle and the shoulder straps, waistband as well as fasteners was changed from beige to white, which help to create a more “cleaner” look and increase the consistency of the aesthetics of all the components. White is also a common colour for undergarments or bottoming garments for children and adolescents. The modified girdle in white can be undetectable underneath school uniforms. Therefore, the mPCG in white would be more acceptable to the users compared to the original design which used a beige (skin) colour.



Figure 4.7 Elimination of stitch lines on surface of mPCG

### 4.3 Specific sizing system of mPCG

One of the suggestions to optimise the PCG is to develop a specific sizing system so as to facilitate mass customisation. By doing so, the waiting time of the patient before undergoing treatment could be shortened and the production cost reduced. Besides, the newly developed specific sizing system for the mPCG is compatible with a computer-aided model (which is developed in this study after data collection) for prescribing the girdle, so the efficiency and accuracy of girdle size selection and the fitting process could be enhanced.

Sung et al. (2008) conducted a study with almost fifteen thousand children in Hong Kong to study their growth index including weight, height, body mass index (BMI), waist circumference (WC) and waist-to-height ratio (WHTR). Table 4.1 shows the extracted data from Sung et al. (2008), which include the sample size and mean and standard deviations (SDs) for weight, height, BMI, WC, and WHTR of Hong Kong Chinese children who are between 10 and 13 years old. The data show that the mean height of the girls is between 141 and 156 cm and their mean waist circumference is around 58 to 62 cm. Besides, Table 4.2 shows other extracted data from Sung et al. (2008), including age- and sex-specific waist circumference percentile values (cm). To exclude the extreme cases, only data between the 5<sup>th</sup> and 95<sup>th</sup> percentiles are considered for the establishment of the specific sizing system in this study.

Table 4.1 Sample size, mean and standard deviations for weight, height, BMI, WC and WHTR (Sung et al., 2008)

Sample	Age (years old)	N	Weight (kg)	Height (cm)	BMI	WC (cm)	WHTR
Girls (n=7370)	10	584	35.3±8.5	141.7±7.0	17.4±3.1	58.5±7.0	0.41±0.04
	11	599	40.1±9.3	148.9±7.0	19.0±3.2	60.2±6.9	0.40±0.04
	12	750	44.1±9.4	153.1±6.2	18.7±3.3	61.2±7.0	0.40±0.04
	13	637	47.8±8.5	156.2±5.4	19.6±3.1	62.2±6.5	0.40±0.04

Table 4.2 Age- and sex-specific waist circumference percentile values (cm) (Sung et al., 2008)

Sample	Age	n	Percentiles									Mean
			3 <sup>rd</sup>	5 <sup>th</sup>	10 <sup>th</sup>	25 <sup>th</sup>	50 <sup>th</sup>	75 <sup>th</sup>	90 <sup>th</sup>	95 <sup>th</sup>	97 <sup>th</sup>	
Girls	10	548	48.6	49.7	50.7	53.2	56.2	60.1	65.1	68.4	72.4	58.27
	11	599	50.0	51.1	52.2	54.7	57.8	61.7	66.9	70.1	74.3	59.87
	12	750	51.3	52.3	53.4	56	59.2	63.1	68.4	71.7	76	61.27
	13	637	52.3	53.4	54.5	57.1	60.3	64.3	69.7	72.9	77.4	62.43

Apart from considering the waist circumference data, the spine length (from C7 to pelvis level) for Hong Kong Chinese children who are 10 to 13 years old should also be considered when establishing the system. The spine length of the 10 tallest and 10 shortest participants who underwent a radiographic examination in the school screening programme was measured (results shown in Table 4.3). The spine length ranges from 34.0 to 46.1 cm.

Table 4.3 Spine length (from C7 to pelvis level)

Tallest participants	1	2	3	4	5	6	7	8	9	10
Height (cm)	178	175	172	169.5	168	168	168	168	167	166
Spine length from C7 to pelvis level (cm)	44.4	44.3	43.6	42.0	43.8	43.5	44.7	46.1	43.1	43.1
Shortest participants	1	2	3	4	5	6	7	8	9	10
Height (cm)	131	133.5	135	137	138	138.5	140	141	141	142
Spine length from C7 to pelvis level (cm)	34.5	34.2	34.0	36.1	35.0	35.3	36.6	34.9	36.1	35.8
Range of the spine length (cm)	34.0 to 46.1									

Based on the data and investigation, the range of measurements (i.e. spine length and waist circumference) that could be covered by each girdle size was determined, see Table 4.4. The mPCG is available in 3 standard sizes, which are small (S), medium (M) and large (L). S covers a spinal length from 33.1 cm to 38 cm, while M from 38.1 cm to 43 cm, and L from 43.1 cm to 48 cm. With reference to the age- and sex-specific waist circumference percentile values in Table 4.2, the percentile values range from 49.7 to 72.9 cm after excluding extreme cases (i.e. the 3<sup>rd</sup> and 97<sup>th</sup> percentiles). This means that the waist circumference range of the mPCG is 49.7 to 72.9 cm. Since the range is quite large, each size of the mPCG was further divided into 2 sub-sizes which are labelled as (I) and (II). Sub-size (I) covers a waist circumference from 50 to 59.9 cm, while Sub-size (II) covers a waist circumference from 60 to 74 cm.

Table 4.4 Range of measurements of mPCG

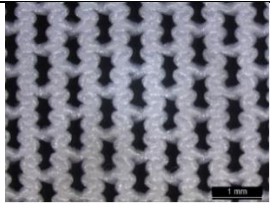
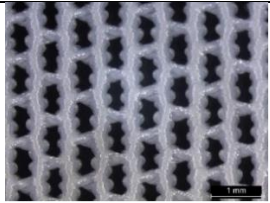
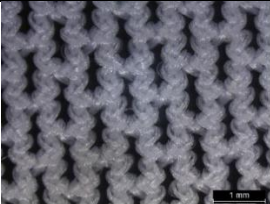
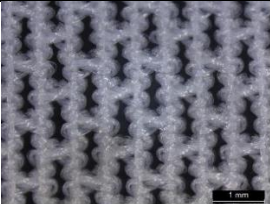
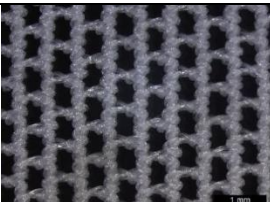
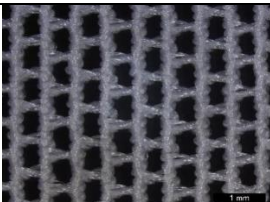
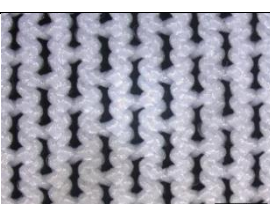
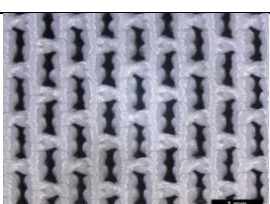
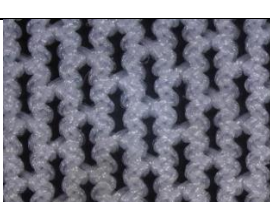
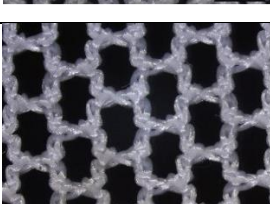
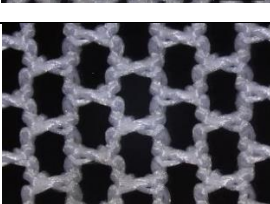
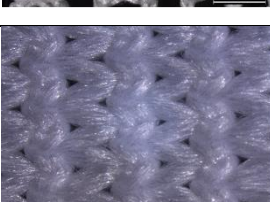
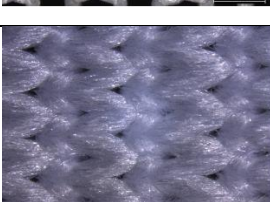
Standard size	Sub-size	Spine length from C7 to pelvis level (cm)	Waist circumference (cm)		
			Min.	Mid.	Max
S	(I)	33.1 - 38	50	55	59.9
	(II)	33.1 - 38	60	67	74
M	(I)	38.1 - 43	50	55	59.9
	(II)	38.1 - 43	60	67	74
L	(I)	43.1 - 48	50	55	59.9
	(II)	43.1 - 48	60	67	74

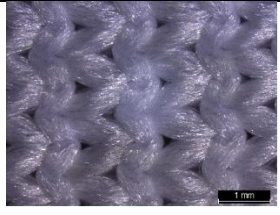
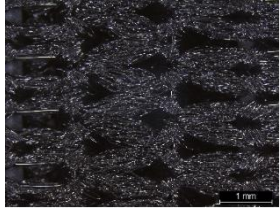
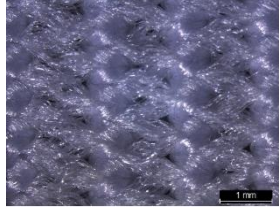
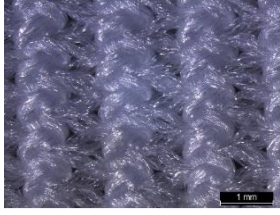
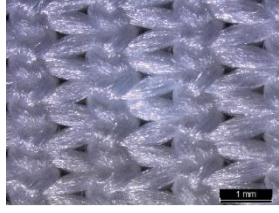
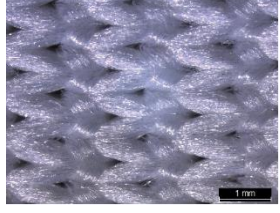
#### 4.4 Material testing results and selection

##### 4.1 Basic information of sourced fabrics and elastic straps

As mentioned in Chapter 3, powernet is the most suitable fabric to replace the shell fabric of the original girdle design, therefore 6 powernet fabrics were sourced from the market for laboratory testing. The powernet fabric with the best overall performance in elasticity and recovery, dimensional stability, air and water vapor permeabilities, pilling resistance, and hand feel would be used for the production of the mPCG. Besides, elastic straps (i.e. shoulder straps and waistband) of the girdle are suggested as the key elements for exerting corrective forces. Therefore, 5 elastic straps were also sourced from the market for laboratory testing. The elastic strap with the best overall performance in elasticity and recovery, repeated stretching ability, dimensional stability, air and water vapor permeabilities, and hand feel was selected for the production of the mPCG. Basic information of the sourced fabrics and elastic straps are shown in Table 4.5.

Table 4.5 Basic information of sourced fabrics and elastic straps

Type of	Name	Weight (g/m <sup>2</sup> )	Thickness (mm)	Microscopic View	
				Technical Face	Technical Back
Fabric	F1	1.66	0.36		
	F2	1.12	0.32		
	F3	0.65	0.24		
	F4	2.29	0.42		
	F5	0.93	0.30		
	F6	0.75	0.30		
Elastic straps	E1	5.81	1.24		

	E2	5.28	1.44		
	E3	4.61	1.08		
	E4	2.91	0.82		
	E5	6.39	1.26		

#### 4.4.2 Results of elasticity and recovery testing

According to Xiong and Tao (2018), the ability of elastic materials to stretch and recover affects the biomechanics of an orthosis. This means the elasticity and recovery of the elastic materials might influence the corrective effect of the mPCG in this study. Saville (1999) suggested that no more than 3% of the original dimensions should be lost during the wear of a form-fitting item. Table 4.6 shows the results of the elasticity and recovery tests of the sourced fabrics and elastic straps.

Table 4.6 Results of elasticity and recovery tests of sourced fabrics and elastic straps

Material Sample	Warp		Weft	
	Growth (avg.)	Recovery (avg.)	Growth (avg.)	Recovery (avg.)
F1	6.1%	95.0%	4.6%	94.7%
F2	15.2%	86.7%	22.0%	81.2%
F3	10.3%	94.6%	7.2%	90.0%
F4	2.4%	97.0%	4.6%	93.5%

<b>F5</b>	8.4%	92.1%	8.8%	90.6%
<b>F6</b>	12.7%	85.4%	5.3%	89.5%
<b>E1</b>	1.4%	97.5%	-	-
<b>E2</b>	1.8%	96.0%	-	-
<b>E3</b>	1.2%	96.6%	-	-
<b>E4</b>	2.7%	97.8%	-	-
<b>E5</b>	1.0%	97.8%	-	-

With reference to the results for the fabric samples, F2 shows the highest fabric growth in both the warp (15%) and weft (22%) directions, while F4 has the lowest fabric growth in both the warp (2.4%) and weft (4.6) directions. More fabric growth means lower dimensional stability of the fabric. Therefore, the results indicate that F4 has the highest dimensional stability among all of the fabric samples, in which its fabric growth is less than 5% in both directions. With reference to the recovery results, F1 and F4 show a better performance compared to the other fabric samples. F1 has 95% and 94.7% recovery in the warp and weft directions respectively, while F4 has 97% and 93.5% recovery in the warp and weft directions respectively. This indicates that F1 and F4 can revert back to their original shape more readily, thus preventing distortion and fatigue.

With reference to the results for the elastic strap samples, E4 is the thinnest strap and shows the highest warp-wise growth (2.7%), while E5, the thickest strap, shows the lowest warp-wise growth (1%). This shows how elastic thickness and growth are directly related. With regard to the elastic strap recovery results, both E4 and E5 have a high percentage of recovery or 97.8%. Aside from E4 and E5, E1 also shows a good recovery performance (97.6%). E1, E4, and E5 have less than a 3% dimension loss, therefore, they are suitable for making form-fitting items (Saville, 1999). However, E2 and E3 have relatively poorer recovery of 96% and 96.6% respectively. The results show that the thickness of the elastic straps and recovery have no direct relationship. However, E2 and E3 have a more extended monofilament lace structure in comparison to the other elastic strap samples which might be one of the factors that affect their recovery.

#### 4.4.3 Results of repeated stretching test

The elasticity of the elastic straps might deteriorate with repeated stretching and releasing during the daily use of the mPCG. Therefore, a repeated stretching test was conducted to investigate the robustness of the sourced elastic straps following multiple stretching bouts. In

the test, each elastic strap was stretched for 1000 cycles. Figure 4.8 graphically shows the force exerted onto each elastic sample during the repeated stretching test and the changes in force for every 100 cycles.

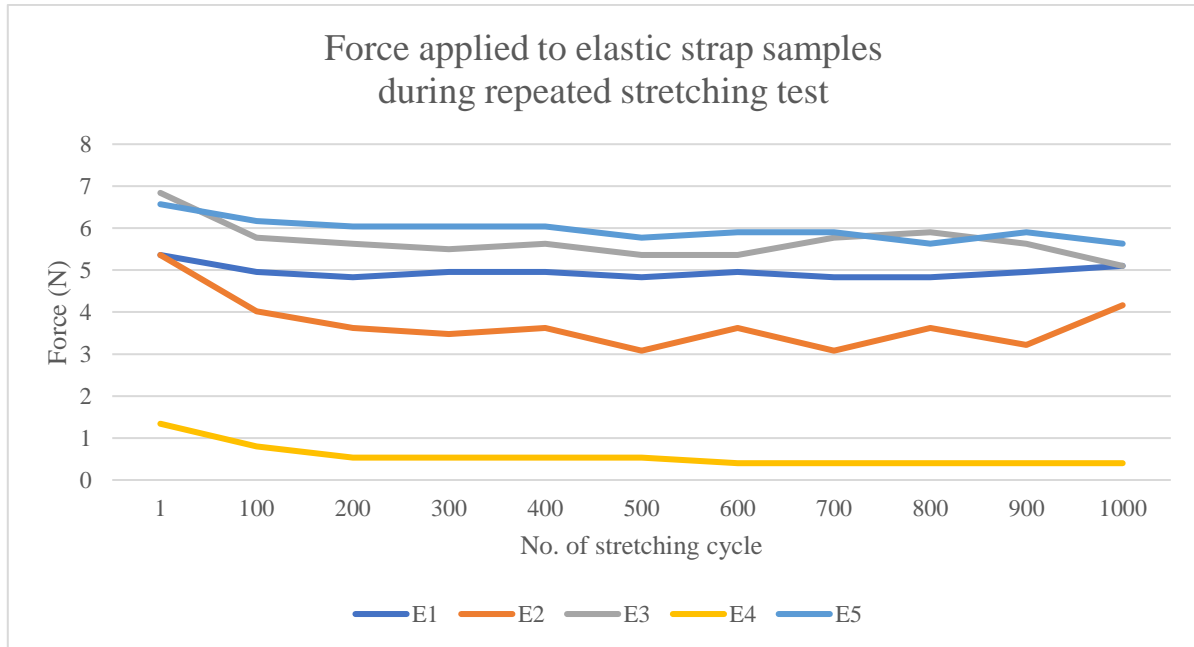


Figure 4.8 Force applied to elastic strap samples during repeated stretching test

The results show that the lowest load is used to stretch E4, while the highest load was used to stretch E5. Generally, elastic straps which require a higher load to stretch are preferred for constructing elements that exert corrective forces. Due to elastic fatigue, the effort to pull the elastic strap samples should be reduced progressively. However, the test results revealed elastic rigidity of some of the elastic strap samples (i.e., E2 and E3), which means that a larger force would be required after repeated stretching cycles since the elastic becomes more rigid. This is not an ideal scenario because the materials become stiffer and less flexible, so that it is potentially not possible for these elastics to stretch and apply corrective forces to the body. E1, E2 and E3 stiffened after 300 to 500 stretches so they are not ideal.

#### 4.4.4 Results of washing test (dimensional changes of fabrics after home laundering test)

A washing test (dimensional stability testing) is done in this study to determine whether the sourced fabric and elastic strap materials would maintain their dimensions when subjected to typical home laundering. The results are presented as the percentage difference between the original dimensions and the dimensions after washing. A dimensional change of 3% is

considered to be good dimensional stability. A measured value close to 0 would be considered high dimensional stability after laundering.

The dimensional changes of the fabric samples after laundering are shown in Figure 4.9. All of the fabric samples pass the washing test with dimensional changes of 3% or less. In the warp direction, the percentage of dimensional change ranges from -0.89% to -1.42%, and in the weft direction, from -0.47% to -1.91%. All of the fabric samples shrink after washing. F4 has a good performance in both the warp and weft directions, with dimensional changes of -0.89% and -0.71%, respectively. F4 is also the thickest fabric among all of the samples.

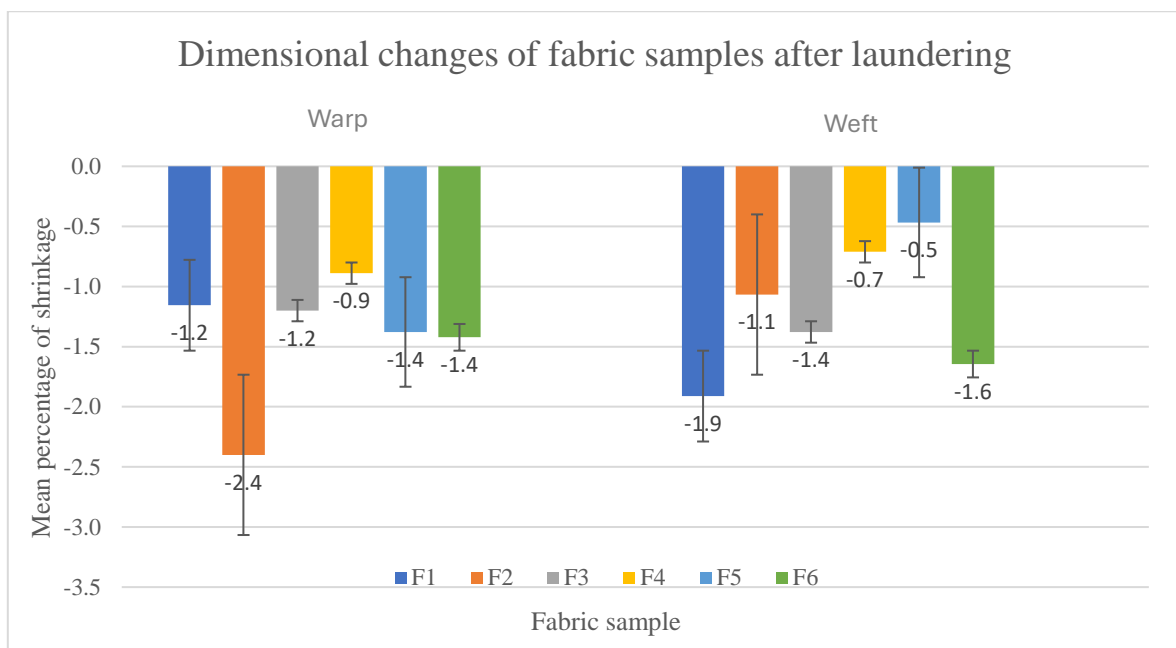


Figure 4.9 Dimensional changes of fabric samples after laundering

The results of the dimensional changes of the elastic strap samples after laundering are shown in Figure 4.10. All of the samples show a dimensional change of less than 3% after washing, therefore, none of the elastic band samples fail this test. However, shrinkage after washing could still be observed in all of the samples. E4 has the smallest shrinkage percentage and the lowest dimensional change among all of the samples.

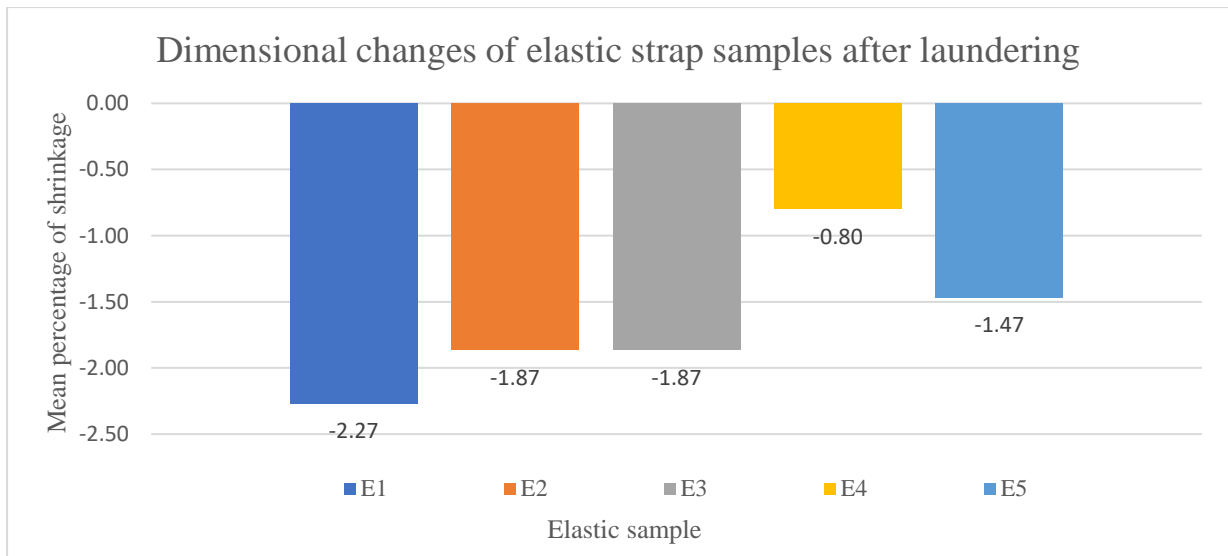


Figure 4.10 Dimensional changes of elastic strap samples after laundering

#### 4.4.5 Results of air permeability test

The air permeability of fabric varies depending on the fibre fineness and shape, fabric cross-section, shape, surface properties, thickness and density (Mukhopadhyay et al., 2011; Yip & Ng, 2008). In this study, the breathability of the sourced fabric and elastic strap samples is evaluated through an air permeability test. The test was conducted to determine the resistance to air flow from one side to the other of the textile materials. Poor air permeability, often reflected through a high air resistance value, means that it is difficult for air to flow through a fabric. The fabrics and elastic straps that are very air permeable are preferred for the mPCG so as to enhance its wear comfort.

The air resistance rate of the fabric samples is shown in Figure 4.11. The least air permeable fabric is F2 (0.02228 kPa s/m), while the most air permeable fabric is F6 (0.00062 kPa s/m). Fabric is more breathable with lower air resistance. Fabric thickness is one of the crucial parameters that influence air permeability (Kane et al., 2007). However, the fabric thickness of the samples in this study is comparable, so the fabric structure might be considered to have the most impact on the outcome—higher air permeability results from reduced density. Although F6 is the most air permeable fabric among the fabric samples, all of the fabric samples are actually air permeable according to their low air resistance values.

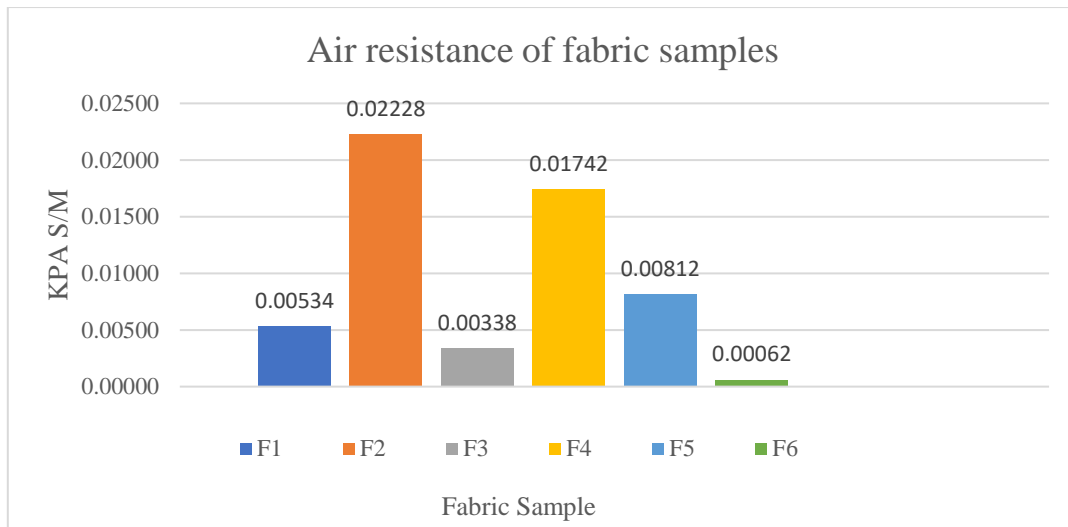


Figure 4.11 Air resistance of fabric samples

The results of the air resistance testing of the elastic strap samples are shown in Figure 4.12, in which it can be observed that the least air permeable elastic strap is E5 (0.27082 kPa s/m), while the most air permeable elastic strap is E4 (0.00266 kPa s/m). E1 and E5 have comparable high air resistance values among the elastic strap samples. E3 and E4 have comparable low air resistance values. Their relatively low air resistance might be due to their monofilament lace structure.

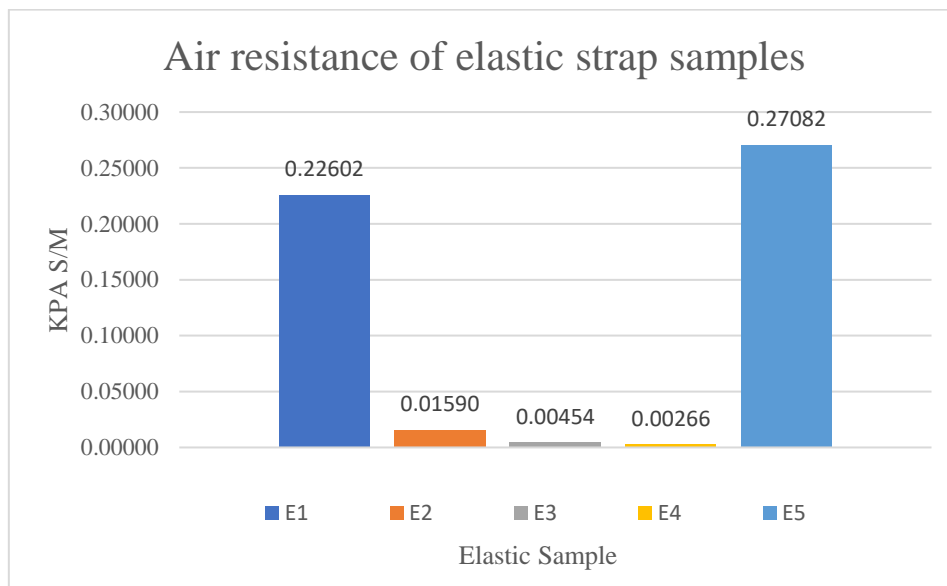


Figure 4.12 Air resistance of elastic strap samples

#### 4.4.6 Results of water vapor permeability/moisture permeability test

The amount of WVT can be used to show the water vapor permeability of a fabric, which means its capacity to transmit moisture vapor. The upright cup test is used in this study to simulate perspiration which passes through the fabric from the skin to the environment. Wear comfort is supposed to increase if the fabric quickly wicks sweat away and transfers moisture. A higher WVT rate means that the fabric can effectively wick moisture from the body.

Figure 4.13 presents the results of the WVT rate of the 6 sourced fabric samples in 4 days. Although F5 has the highest WVT rate (34.31 g/h.m<sup>2</sup>) and F4 has the lowest (32.11 g/h.m<sup>2</sup>), the difference in the WVT between them is small (i.e. only 2.2 g/h.m<sup>2</sup>). The findings show that all of the sourced fabrics have similar water vapor transmission properties since they are all constructed by using synthetic fibres, while their thickness may affect their WVT ability.

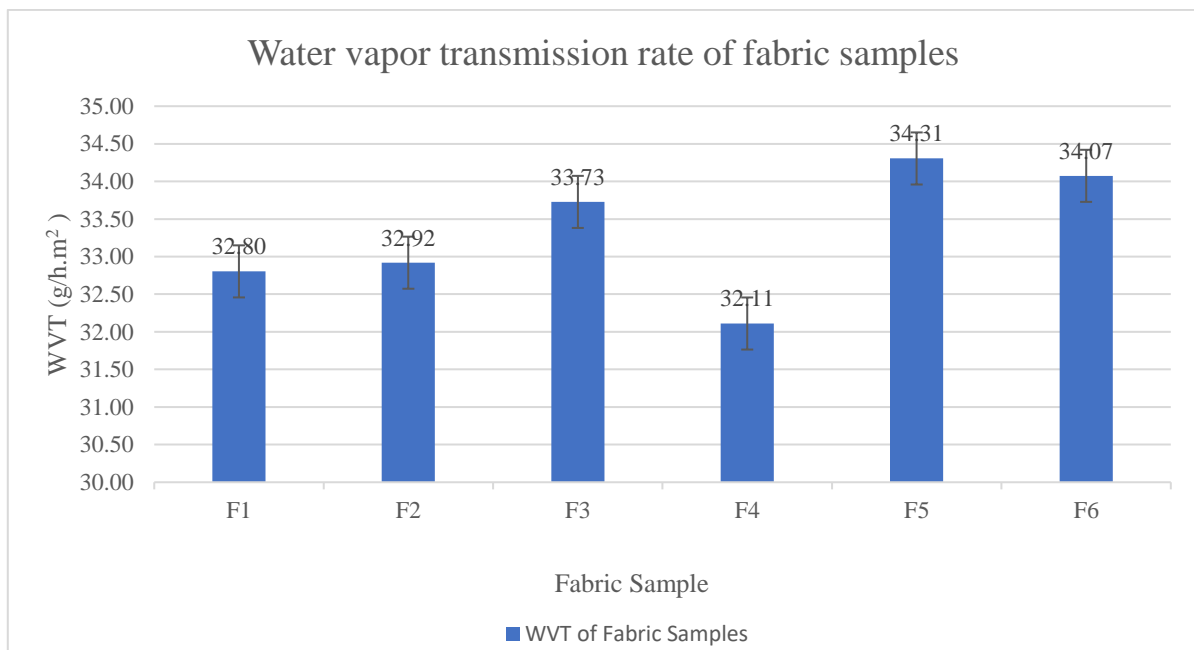


Figure 4.13 Water vapor transmission rate of fabric samples

Figure 4.14 presents the results of the WVT test of the 5 sourced elastic strap samples for a period of 4 days. E4 shows the highest WVT rate (31.53 g/h.m<sup>2</sup>) while E5 shows the lowest rate (28.76 g/h.m<sup>2</sup>). The difference is however small (i.e. 2.77 g/h.m<sup>2</sup>). The results indicate that there is no relationship between moisture permeability and the thickness of the elastic straps. For instance, E2 is the thickest strap but has the second highest WVT rate.

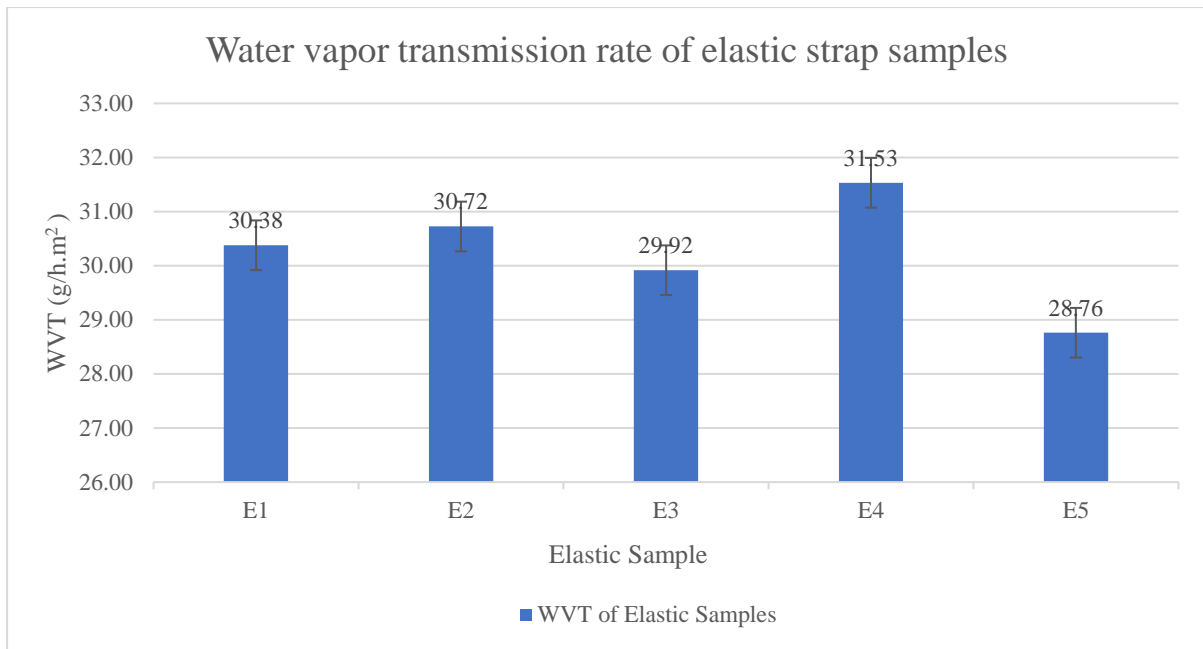


Figure 4.14 Water vapor transmission rate of elastic strap samples

#### 4.4.7 Results of pilling resistance test

A 5-scale rating system (from 1 to 5 with 1 being the lowest and 5 the highest) was used to evaluate the results of the pilling resistance test of the sourced fabric samples. The ratings were then compared to those of the ASTM D 3512 Photographic Standards which showed how well the fabrics samples performed in terms of pilling and fuzzing resistance. Higher resistance is indicated by a higher rating, and vice versa.

The results of the pilling and fuzzing resistance of the sourced fabric samples are shown in Figures 4.15 and 4.16 respectively. All of the fabric samples generally have a good performance in resisting pilling (i.e. rating between 3-5), while F1 and F4 have excellent resistance (5). F4 shows excellent resistance against fuzzing (5), while F1 has poor resistance (1).

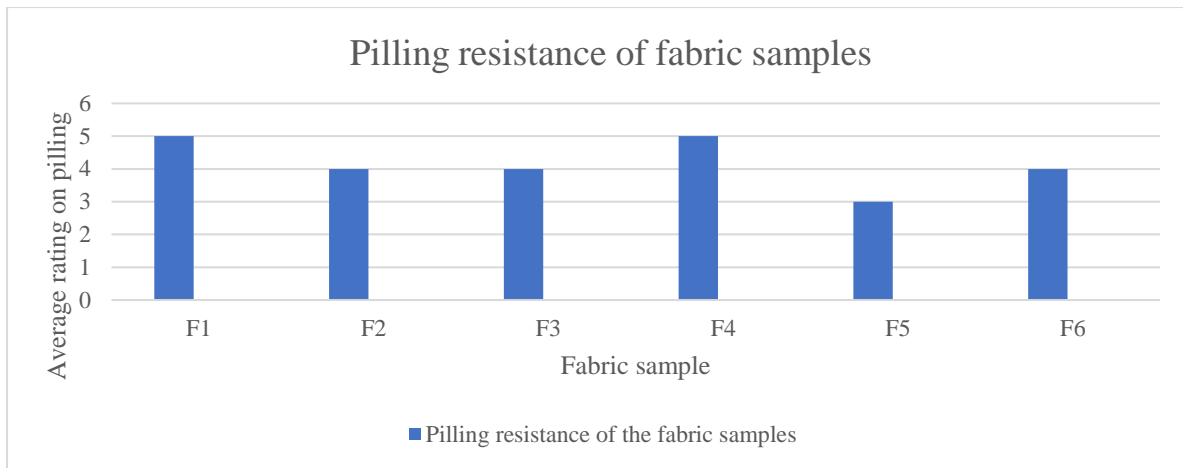


Figure 4.15 Pilling resistance of fabric samples

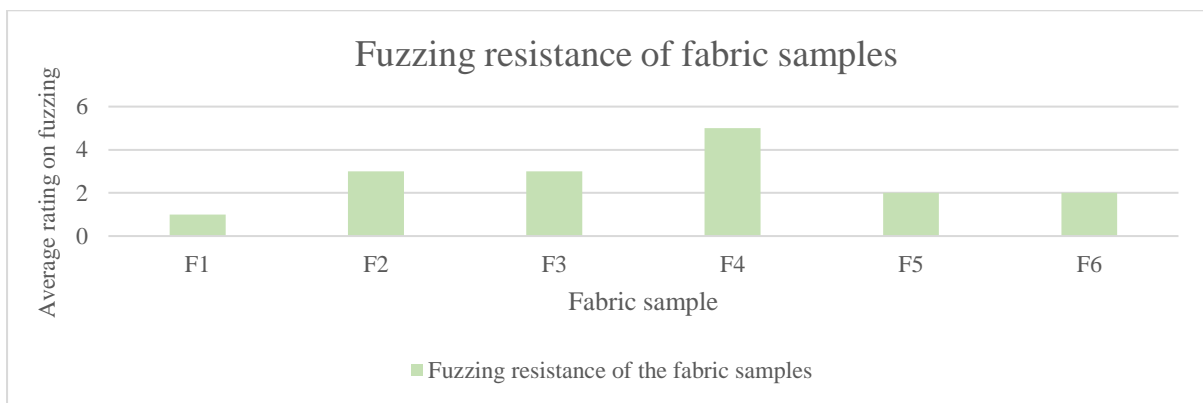


Figure 4.16 Fuzzing resistance of fabric samples

#### 4.4.8 Results of hand feel test

In order to ensure a good experience in tactile comfort for the girdle wearers, the surface characteristics of the sourced fabric and elastic strap samples were evaluated by using the hand feel test. In the test, the average coefficient of friction (MIU), average deviation of coefficient of friction (MMD), and average surface roughness (SMD) of the sourced samples were determined. Materials with a low MIU, MMD and SMD means a smooth hand feel and offers good tactile comfort. The test results are shown in Table 4.7. For the elastic strap samples, the data in the weft direction of E3 and E4 cannot be recorded since they have a substantial difference between the monofilament and elastic parts and the sensor could not penetrate the surface to provide a reading.

Table 4.7 Hand feel test results of the sourced fabric and elastic strap samples

Material Sample	Coefficient of friction (MIU)								Deviation of coefficient of friction (MMD)								Surface roughness (SMD)							
	Technical Face				Technical Back				Technical Face				Technical Back				Technical Face				Technical Back			
	Warp		Weft		Warp		Weft		Warp		Weft		Warp		Weft		Warp		Weft		Warp		Weft	
	Mean	SD	Mean	SD	Mean	SD	Mean	SD	Mean	SD	Mean	SD	Mean	SD	Mean	SD	Mean	SD	Mean	SD	Mean	SD	Mean	SD
F1	0.28	0.002	0.22	0.113	0.22	0.005	0.32	0.158	0.007	0.003	0.010	0.005	0.008	0.005	0.012	0.006	0.98	0.51	16.8	8.39	2.16	1.36	13.0	8.57
F2	0.22	0.008	0.29	0.147	0.29	0.012	0.23	0.113	0.014	0.007	0.007	0.003	0.032	0.037	0.005	0.002	4.23	2.14	6.88	3.44	3.83	1.92	5.75	2.87
F3	0.22	0.007	0.24	0.119	0.26	0.007	0.23	0.116	0.006	0.003	0.011	0.006	0.007	0.004	0.014	0.007	1.20	0.60	12.6	6.35	1.48	0.74	11.5	5.83
F4	0.20	0.004	0.16	0.080	0.16	0.003	0.17	0.087	0.009	0.005	0.015	0.008	0.007	0.003	0.009	0.004	1.49	0.78	10.7	5.43	0.96	0.50	6.71	3.36
F5	0.14	0.001	0.19	0.095	0.19	0.018	0.14	0.069	0.010	0.005	0.005	0.003	0.006	0.003	0.007	0.004	2.92	1.49	4.79	2.40	3.01	1.51	5.81	2.92
F6	0.13	0.002	0.17	0.087	0.13	0.002	0.15	0.075	0.009	0.005	0.007	0.004	0.006	0.003	0.009	0.004	5.03	2.56	13.2	6.58	4.49	2.29	13.6	6.84
E1	0.26	0.002	0.28	0.141	0.24	0.175	0.18	0.143	0.019	0.009	0.015	0.008	0.013	0.007	0.007	0.004	6.85	3.48	6.23	3.22	4.37	2.26	2.45	1.22
E2	0.32	0.009	0.41	0.207	0.29	0.019	0.24	0.122	0.011	0.005	0.019	0.009	0.025	0.014	0.017	0.008	8.98	4.71	11.4	5.74	8.27	4.18	9.32	4.67
E3	0.16	0.012	N/A	N/A	0.17	0.005	N/A	N/A	0.059	0.036	N/A	N/A	0.037	0.019	N/A	N/A	7.95	4.72	N/A	N/A	6.96	3.51	N/A	N/A
E4	0.23	0.007	N/A	N/A	0.29	0.012	N/A	N/A	0.010	0.005	N/A	N/A	0.013	0.007	N/A	N/A	6.01	6.56	N/A	N/A	2.36	1.41	N/A	N/A
E5	0.22	0.019	0.24	0.123	0.38	0.015	0.22	0.112	0.020	0.010	0.028	0.014	0.048	0.024	0.048	0.009	7.21	3.62	9.40	9.40	4.79	2.43	3.05	1.67

In terms of the fabric samples, the MIU of F4, F5 and F6 is relatively lower for both the technical face and back. The MMD of F1, F3 and F5 is relatively lower for the technical face, while that of F3, F4 and F5 is relatively lower for the technical back. The SMD of F2, F4 and F5 is relatively lower for both the technical face and back. As for the elastic samples, the MIU of E3 and E4 is relatively lower value for the technical face, while that of E1 and E3 is relatively lower for the technical back. The MMD of E2 and E4 is relatively lower for the technical face, while that of E1 and E4 is relatively lower for the technical back. The SMD of E1 and E4 is relatively lower for both the technical face and back. Although each sourced sample has its own advantage in specific areas for the hand feel test, F4, F5, E1 and E4 have a better overall performance.

#### 4.4.9 Material selection

As mentioned in Chapter 3, the shell fabric of the PCG is replaced with a new fabric in order to reduce pilling and at the same time, offer good strength and recovery, dimensional stability, durability, hand feel and thermal comfort. Based on the material test results, **F4** was selected as the shell fabric for the mPCG. F4 has an excellent performance. F4 is the most elastic with the highest recovery (2.4% and 4.6% growth in the warp and weft directions respectively; 97% and 93.5% recovery in the warp and weft directions respectively), has the lowest dimensional change after washing (-0.89% and -0.71% dimensional change in the warp and weft directions respectively), shows the least amount of pilling (with a rating of 5) and has the best hand feel test. Although F4 is not as air permeable or water vapour permeable as the other samples, the differences among all of the sourced fabric samples for the air permeability and water vapour permeability tests are very minimal (0.022 kPa s/m difference in air resistance rate and 2.2

g/h.m<sup>2</sup> difference in WVT rate). Therefore, in consideration of all the tested aspects, F4 was selected as the shell fabric.

Besides, as mentioned in Chapter 3, the material for fabricating the shoulder straps and waistband should also be replaced with a new type of elastic strap that offers good strength and recovery, dimensional stability, durability, hand feel and thermal comfort. Based on the material test results, **E5** was selected as the elastic strap to fabricate the shoulder straps and waistband of the mPCG. E5 has an excellent performance. E5 has the highest elasticity and recovers the most (1% growth and 97.8% recovery in the warp direction), and can withstand the highest force during stretching (average of 5.96 N for 1000 stretching cycles). This elastic strap material also has good performance and ranked second in lowest dimensional change (-1.47% dimensional change in the warp direction). Although E5 is not the most air permeable and water vapour permeable or has the best hand feel, the differences among all the sourced elastic strap samples in the air and water vapour permeability and hand feel tests are minimal (0.27 kPa s/m difference in air resistance rate, 2.77 g/h.m<sup>2</sup> difference in WVT rate).

#### **4.5 Pattern development and garment assembling**

Based on the method used to develop the pattern of the PCG in Liu (2015), a new pattern block for the mPCG is developed in this study (see Figure 4.17). The newly developed pattern block has a centre front, side front, centre back, side back, shoulder, crotch, and zipper panels. There are 32 pattern pieces for the entire girdle (excluding the 3 elastic straps for the waistband and shoulder straps). Details of the pattern pieces and material applications of the mPCG are shown in Table 4.8. Apart from the newly selected fabric (F4) for the shell and the newly selected elastic strap (E5) for the waistband and shoulder strap, other fabrics, elastic straps, and accessories used are the same as those of the original PCG (Liu, 2015).

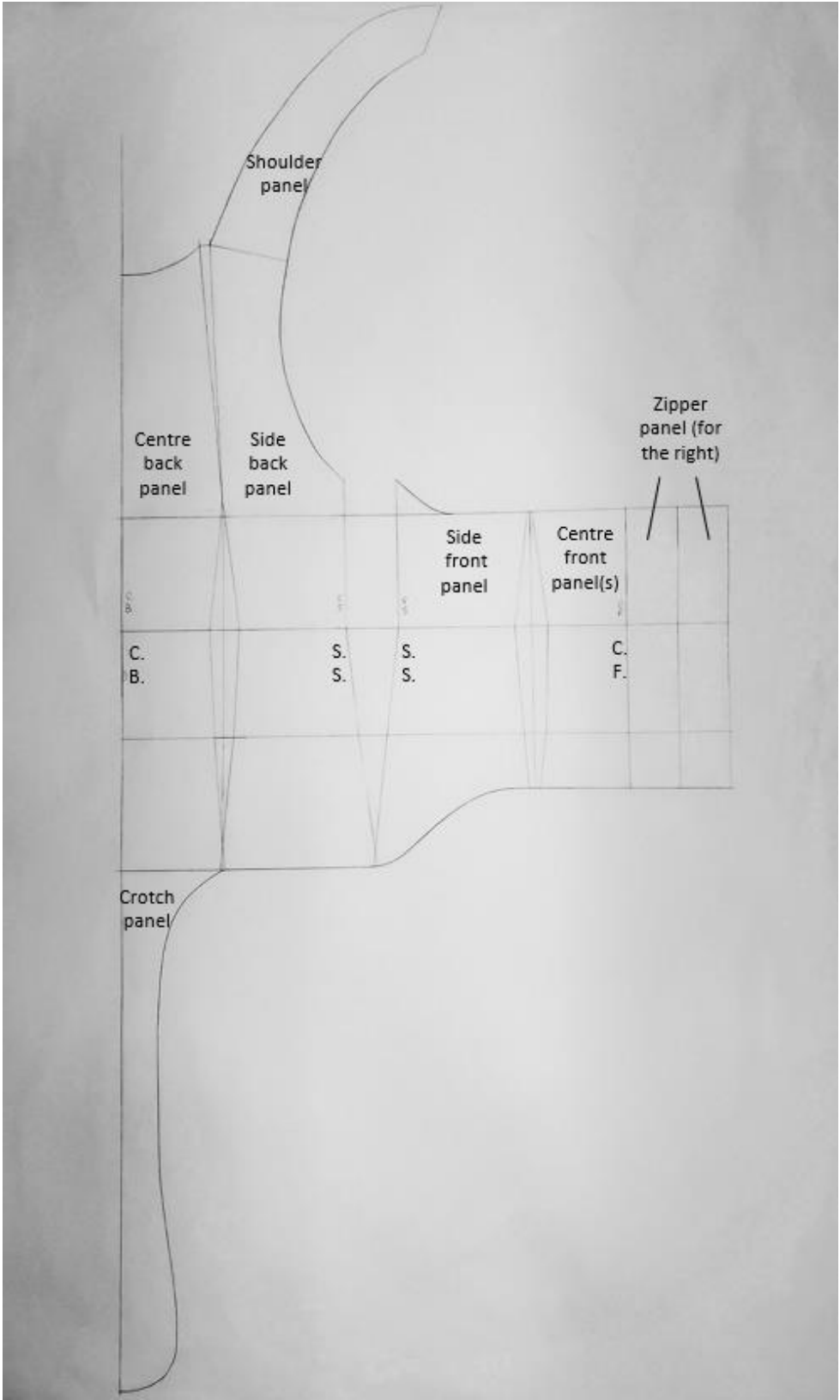


Figure 4.17 New pattern block for mPCG

Table 4.8 Details of pattern pieces and material applications of mPCG

Layer	Name of pattern panel	Number of pieces	Material	Remarks
Shell	1. Centre front panel	1 pair	Velcro (plush)	For attaching 1 zipper
	2. Zipper panel (for the right side)	2 pieces	Velcro (plush)	For attaching 2 more zippers
	3. Side front panel	1 pair	Powernet F4	/
	4. Side back panel continuous to the shoulder panel	1 pair	Powernet F4	/
	5. Centre back panel	1 piece	Powernet F4	
	6. Crotch panel	1 piece	Powernet F4	With Velcro tape (plush) attached as fasteners
Middle	7. Centre front panel	1 pair	Stabiliser	/
	8. Zipper panel (for the right)	2 pieces	Stabiliser	/
	9. Side front panel	1 pair	Satinette	For attaching 3 side bones
	10. Side back panel	1 pair	Satinette	For attaching 3 side bones
	11. Shoulder panel	1 pair	Foam sheet	Attaching bone at shoulder seam
	12. Centre back panel	1 piece	Stabiliser	For attaching 3 back bones
	13. Crotch panel	1 piece	Powernet F4	With Velcro tape (hook) attached as fasteners
Inner	14. Centre front panel (for the left)	1 piece	Soft Powernet	/
	15. Centre front panel continues to zipper panels (for the right)	1 piece	Soft Powernet	/
	16. Side front panel	2 pair	Soft Powernet	As pocket lining
	17. Side back panel continuous to the shoulder panel	1 pair	Soft Powernet	As pocket lining
	18. Narrow centre back panel	1 piece	Soft Powernet	As pocket lining
	19. Entire back panel	1 piece	Soft Powernet	As pocket lining
Elastic straps	20. Waist band	1 piece	Elastic strap E5	With Velcro tape (plush & hook) attached as fasteners
	21. Shoulder straps	1 pair	Elastic strap E5	With Velcro tape (plush & hook) attached as fasteners
	22. Edge finishing straps	Around 6 meters	V-fold elastic	/

As for girdle assembling process, a single needle lock stitch was mainly used to join the vertical seams, sew the Velcro tape for insertion of the resin bones and attach the fasteners. A one-point zigzag stitch was used to attach the V-fold elastic for the edge finishing. Seam allowances were hidden and sandwiched between the layers to create a smooth and clean look.

#### 4.6 Donning of Modified Posture Correction Girdle

The front, side and back views of a completed mPCG prototype are shown in Figure 4.18. After the confirmation of the girdle size, shoulder straps and waistband tension, as well as the EVA foam padding placement for exerting the points of pressure, the mPCG was given to the subject for a 9-month wear trial.

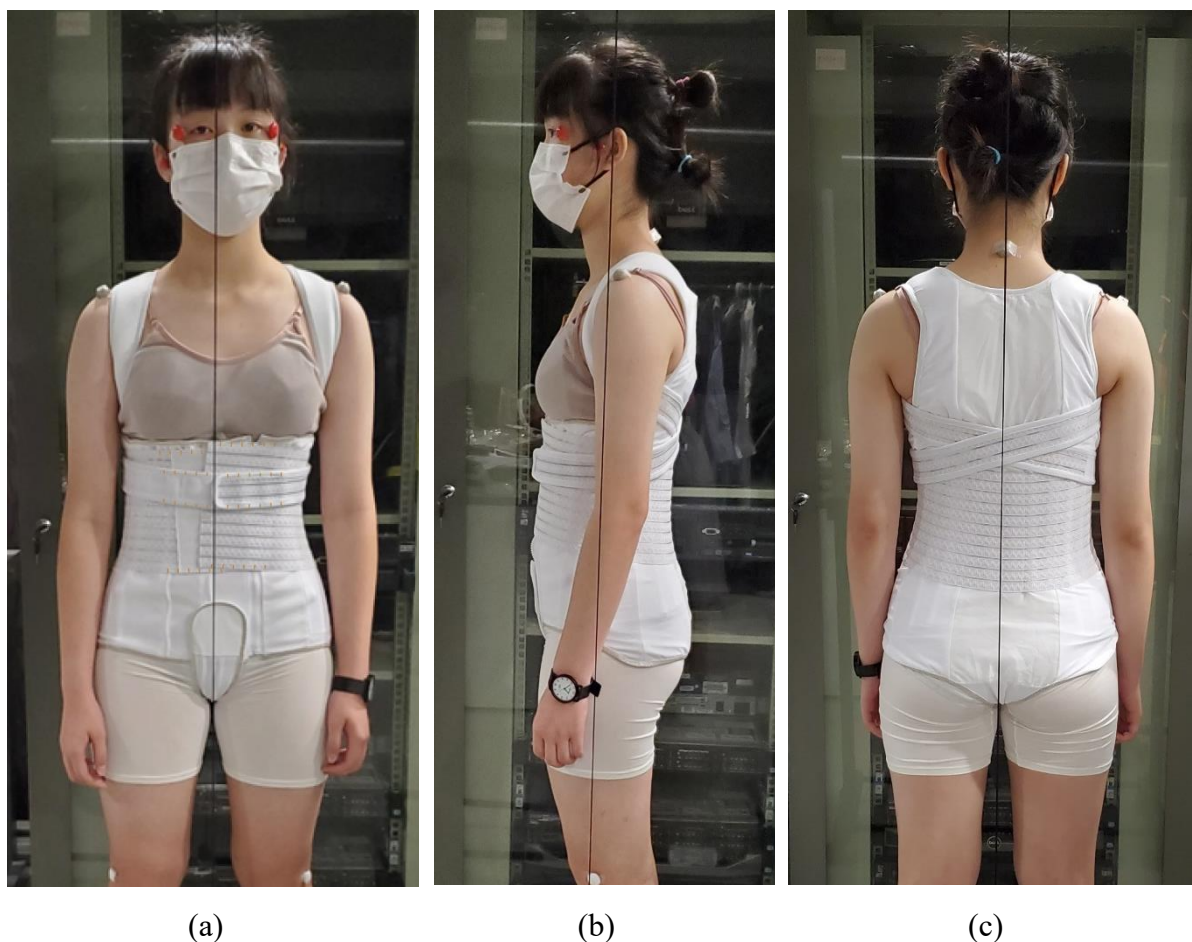


Figure 4.18 Completed mPCG on subject: (a) front, (b), side, and (c) back views

#### 4.7 Chapter summary

After modifying the girdle design, the limitations of the original PCG are eliminated. For instance, a systemic sizing system for the mPCG is developed based on the body measurement

review and investigation, which increases the efficiency of the girdle sizing and fitting processes, as well as realising mass customisation. Also, the use of 3 zippers at the centre front allows the same girdle to accommodate a wider range of different waist circumferences. In addition, the elimination of the free-end design of the shoulder straps and waistband facilitated different magnitude of corrective forces and the newly added markings offered better control and more clarity of the tension adjustment. Furthermore, the increased number of the pocket lining partitions enhanced the accuracy of exerting points of pressure to the necessary areas especially on the parts that need higher corrective forces. Moreover, the replacement of the shell fabric with F4, a powernet, improves the dimensional stability, durability, pilling resistance and wear comfort of the girdle. The newly selected elastic strap (E5) also shows a good performance in most of the material tests. Besides, the elimination of the stitches on the surface and change in girdle colour from a nude or beige colour to white increase the tidiness of the mPCG, giving it a clean look so that it is more attractive and acceptable to the users. Apart from these changes, the pattern development and girdle assembling details are also described. There are 32 pattern pieces in total. The types of stitches used for the girdle assembly are single needle lock stitch and one-point zigzag stitch. Finally, photos of the front, side and back views of the girdle donned by a subject are provided as a reference.

# CHAPTER 5 – RESULTS OF GIRDLE PRESCRIPTION AND WEAR TRIAL

## 5.1 Introduction

This chapter presents the results of the school-screening programme, subject recruitment (demographic data), prescription of the mPCG for the recruited subjects, and wear trial experiment to evaluate the effectiveness of the mPCG. The wear trial results include examining the changes in spinal curvature (through a radiographic examination and comparison of Cobb angle), improvements in posture balance (through 3D body scanning and measuring posture angle), and effects on proprioception deficit (by using the Vicon Nexus 3D motion capture system). Details on the rate of compliance with the girdling treatment in this study and the questionnaire results related to the evaluation of QoL during the wear trial are also included and discussed.

## 5.2 Subject recruitment

### 5.2.1 Results of school-screening programme

In order to investigate the presence of scoliosis of the targeted group and recruit subjects for this study, school screening was carried out at 6 primary schools and 3 secondary schools in February 2020. Apart from organising school screening activities at the primary and secondary schools, 15 screening activities were also held on PolyU campus, so that adolescents from other primary and secondary schools could participate. The total number of screened adolescents is 1747. The mean age of the participants is  $11.57 \pm 0.96$  years old, while the mean height, mean weight and BMI of the participants are  $152.78 \text{ cm} \pm 9.1$ ,  $44.2 \text{ kg} \pm 11.63$  and  $18.74 \pm 3.76$  respectively.

Among the 1747 screened individuals, 487 (27.88%) were suspected of having scoliosis. All 487 were offered a radiographic examination but only 247 of them accepted the offer. According to the radiographic examination results of the 247 individuals, 106 of them are diagnosed with a spinal curvature less than  $10^\circ$ , while 98 and 43 are diagnosed with a spinal curvature between  $10^\circ$ - $20^\circ$  and more than  $20^\circ$ , respectively. That is, among the 1747 screened participants, 6.07%, 5.6% and 2.46% are diagnosed with a spinal curvature less than  $10^\circ$ , between  $10^\circ$ - $20^\circ$  and more than  $20^\circ$  respectively. The school screening results are summarised in Table 5.1.

Table 5.1 School-screening results

	Number of screened individuals	%	Mean age	Mean height (cm)	Mean weight (kg)	Mean BMI
<b>Total screened</b>	1747	100	11.57±0.957	152.78±9.10	44.20±11.63	18.74±3.76
<b>Suspected to have scoliosis</b>	487	27.88	11.75±0.88	154.90±8.49	44.66±10.15	18.47±3.12
<b>Underwent radiographic examination</b>	247	14.14	11.83±1.01	154.82±8.67	42.62±8.02	17.67±2.30
<b>Diagnosed with spinal curvature less than 10°</b>	106	6.07	11.72±1.01	153.88±9.49	42.53±8.61	17.83±2.40
<b>Diagnosed with spinal curvature between 10°-20°</b>	98	5.60	11.87±1.03	155.31±8.74	42.77±8.04	17.62±2.34
<b>Diagnosed with spinal curvature more than 20°</b>	43	2.46	12.05±0.93	156.03±5.83	42.47±6.46	17.39±1.98

### 5.2.2 Demographics of recruited subjects

In this study, the mPCG is examined as an alternative treatment option for adolescents with early scoliosis (spinal curvature between 10°-20°). To recruit subjects for the wear trial in this study, invitations were sent to the 98 adolescents who were diagnosed with a spinal curvature between 10°-20° in the school screening programme. However, only 10 of them accepted the offer to voluntarily participate in the wear trial. Table 5.2 shows the demographic data of the recruited subjects.

Table 5.2 Demographic data of recruited subjects

Subject	Risser Grade	Type of curve (S/C)	PUMC Classification*	Cobb Angle of Upper Curve (°) & Spinal Level	Cobb Angle of Lower Curve (°) & Spinal Level	Age	Height (cm)	Weight (kg)	BMI
1	2	S	IIC	14.8 (T6-T11)	16.1 (T12-L3)	12	150	45.2	20
2	3	C	Ib	/	12 (T7-L3)	12	156	44.7	18.08
3	3	C	Ia	17 (T5-L1)	/	13	162.5	52.5	19.81
4	3	S	IIC	18 (T5-T11)	15 (T12-L3)	12	164	55.1	20.45
5	2	S	IIC	11.1 (T3-T9)	15.1 (T11-L3)	12	156.5	43.5	17.8
6	0	C	Ia	/	12.6 (T10-L2)	12	157	35.3	14.3
7	3	S	IIC	14.1 (T6-T9)	19.4 (T10-L2)	13	156	43.7	18
8	0	S	IIC	8.6 (T5-T10)	13 (T11-L4)	12	148.5	46.9	21.3
9	2	S	IIC	10.1 (T5-T10)	13.1 (T11-L4)	12	158.5	38	15.1
10	3	S	IIC	13.7 (T6-L1)	17.5 (L2-L5)	12	167	45	16.1

	<b>Mean</b>	12.2	157.6	44.99	18.09
	<b>SD</b>	0.42	5.79	5.86	2.35

\*Curve flexibility was not compared.

The mean age of the recruited subjects for the wear trial is  $12.2 \pm 0.42$  years old, while the mean height, weight and BMI are  $157.6 \text{ cm} \pm 5.79$ ,  $44.99 \text{ kg} \pm 5.86$  and  $18.09 \pm 2.35$ , respectively. Among the 10 recruited subjects, 7 of them are diagnosed with an S curve (Subjects 1, 4, 5, 7, 8, 9 and 10) while 3 of them (Subjects 2, 3 and 6) have a C curve. The details of the Cobb angle of each subject are listed in Table 5.2. The type of curve was classified by using the standards in the PUMC classification system, which showed that the 7 subjects with an S curve all fall under type IIc, while 2 of the subjects (Subjects 3 and 6) with a C curve fall under type Ia, and 1 of the subjects (Subject 2) with a C curve fall under type Ib (definitions of the type of curve in the PUMC classification system are provided in Chapter 2). As for the Risser grade, 2 of them (Subjects 6 and 8) are Grade 0, 3 of them (Subjects 1, 5 and 9) are Grade 2, and 5 of them (Subjects 2, 3, 4, 7 and 10) are Grade 3.

### 5.3 Girdle prescription for recruited subjects

As for the prescription of the mPCG, each subject was given her own mPCG for the 9-month wear trial based on her body measurements (see Appendix VII for body measurement details) and length of spine from C7 to the pelvis level. Of the 10 recruited subjects, 7 of them were fitted with an M size girdle, while 3 of them were fitted with an L size girdle. Then the subjects were to zip up the girdle by using 1 of the 3 zippers at the centre front with just the right amount of tension. Also, the subjects were to fasten the crotch panel to the bottom of the centre front panel by using just the right amount of tension. Next, padding was inserted in the pocket lining of the girdle according to the magnitude of the spinal curvature based on each individual case to create the points of pressure to exert the corrective forces. Generally, 1-3 paddings were inserted into the girdle. Then, the tension of the waistband was determined and followed by determining the tension of the shoulder straps. When determining the waistband tension, the left and right bands were wrapped around the left and right sides of the body towards the centre front first, and fixed with just the right amount of tension. Then, if the subject has a spinal curvature between the low thoracic and lumbar regions (between T10 to L5), the waistband at the side of the curve apex would be tightened. When the curve is between  $1-5^\circ$ ,  $6-10^\circ$ ,  $11-15^\circ$  and  $16-20^\circ$ , the band would be tightened to the first, second, third or fourth marked interval, respectively. When the shoulder strap tension was being determined, first, the left and right straps were wrapped around the left and right shoulders and passed through the underarms

towards the centre front and fixed there with just the right amount of tension. If the subject has a spinal curvature between the high thoracic and mid thoracic regions (between T1 to T9), the shoulder strap at the side of the curve apex would be tightened. When the curve is between 1-5°, 6-10°, 11-15° and 16-20°, the band would be tightened to the first, second, third or fourth marked interval, respectively.

Before starting the 2-hour preliminary trial and 9-month wear trial, the tension of the girdle, shoulder straps and waistband was confirmed with the subjects to ensure that the tension was acceptable. Details of the girdle size, location of the inserted padding, and tension of the shoulder straps and waistband for each recruited subject are shown in Table 5.3.

Table 5.3 Details of prescribed girdle for recruited subjects

Subject	Length of spine (cm)	Girdle size	Location of inserted padding		Tension of waistband*		Tension of shoulder straps*	
			Left	Right	Left	Right	Left	Right
1	40	M	L4	R2, R3	-4	0	0	-3
2	40.5	M	L3	/	-2	0	0	0
3	44.5	L	/	R2, R3	0	-4	0	-4
4	43.5	L	L3, L4	R2	-3	0	0	-4
5	41	M	L3, L4	R2	-3	0	0	-3
6	39.5	M	/	R3	0	-2	0	0
7	41.5	M	L2	R3, R4	0	-4	-3	0
8	40	M	L2	R3, R4	0	-3	-2	0
9	42.5	M	L3, L4	R2	-3	0	0	-2
10	45.5	L	L4	R2, R3	-4	0	0	-3

\*Notes: 0 = just the right amount of tension, -1 = tightened to the first marked interval, -2 = tightened to the second marked interval, etc.

#### 5.4 Interface pressure measurement

In order to investigate how much pressure the mPCG exerts, the interface pressure was measured after prescribing the girdle. The data can be used to compare the corrective forces exerted by the points of pressure between the original and modified versions of the PCG. The results of the mean interface pressure measurements at 0 M are shown in Table 5.4.

Table 5.4 Results of interface pressure measurements

Subject	Upper curve				Lower curve			
	Padding location 1	Mean interface pressure (kPa)	Padding location 2	Mean interface pressure (kPa)	Padding location 1	Mean interface pressure (kPa)	Padding location 2	Mean interface pressure (kPa)
1	R2	8.375	R3	8.875	L4	6.250	/	/
2	/	/	/	/	L3	5.375	/	/
3	R2	6.375	R3	6.875	/	/	/	/
4	R2	7.625	/	/	L3	6.875	L4	6.750
5	R2	6.500	/	/	L3	6.625	L4	5.750
6	/	/	/	/	R3	5.625	/	/
7	L2	5.625	/	/	R3	8.250	R4	6.875
8	L2	5.375	/	/	R3	5.875	R4	5.625
9	R2	4.625	/	/	L3	5.625	L4	4.875
10	R2	5.125	R3	5.75	L4	5.625	/	/

The mean interface pressure measurements range from 4.625 kPa to 8.875 kPa. Generally, the highest mean interface pressure is found in the thoracic of the spine after comparing the values of the same subject. For instance, the highest mean interface pressure for Subjects 1, 5, 7, 8, 9 and 10 was found at padding location R3 (i.e. 8.875 kPa), L3 (i.e. 5.525 kPa), R3 (i.e. 8.250 kPa), R3 (i.e. 5.875 kPa), L3 (i.e. 5.625 kPa) and R3 (i.e. 5.750 kPa), respectively. This might be due to the presence of the rib cage, which is the most protruding area near the thoracic or mid-level of the spine.

A comparison of the interface pressure measurements of the modified and the original versions of the PCG, higher pressure values were generally found with the mPCG. According to Liu (2015), the mean interface pressure measurements of the original PCG ranged from 3.667 kPa to 5.219 kPa. This means that the highest mean pressure exerted by the mPCG (i.e. 8.875 kPa) is 3.656 kPa (70%) higher than that of the original girdle. Higher mean interface pressure measurements might indicate higher corrective forces exerted onto the wearer.

The EVA foam pad material used in the two PCGs are the same. Therefore, the increase in the mean interface pressure exerted by the mPCG might be due to the elimination of the free end design of the waistband and shoulder straps, as well as the increase in the number of pocket lining partitions in the mPCG. Thus, corrective forces might be exerted more effectively and precisely to the needed area.

### 5.5 Changes in spinal curvature

The changes in the spinal curvature of the recruited subjects under the intervention of the girdling treatment were examined by using the radiographic method and Cobb angle comparison. In order to evaluate the effectiveness of the mPCG in terms of controlling the

spinal curvature, the recruited subjects were required to take x-rays at 0 M, 3 M, 6 M and 9 M as mentioned in Section 3.5.4.1. The Cobb angles are compared by using X-rays taken at different points of time; see Table 5.5. To investigate the immediate effects of the mPCG in reducing the spinal curvature, the Cobb angles measured on the x-rays taken at 0 M before the intervention (hereinafter pre-intervention) and 0 M after the 2-hour intervention with the use of the mPCG (hereinafter 0 M 2 h) were compared. To investigate the long-term effects of the mPCG in controlling the progression of the spinal curvature, the Cobb angles measured on the x-rays taken at 0 M pre-intervention and 9 M after the wear trial but without the mPCG donned (hereinafter 9 M out-orthosis) were compared. To monitor the spinal condition without the mPCG, the Cobb angles measured on the X-rays taken at 0 M pre-intervention and 3 M after using the mPCG for 3 months but without the mPCG donned (hereinafter 3 M out-orthosis) were compared. To examine whether the mPCG can sustain the results after 6 months of use, the Cobb angles measured on the X-rays that taken at 0 M after 2 h and after 6 M of using the mPCG with the mPCG donned (hereinafter 6 M in-orthosis) were compared.

Table 5.5 Cobb angle comparison and purpose

Comparison	X-rays taken at different points of time	Out-orthosis/ In-orthosis when taking the X-rays	Purpose
1	0 M - pre-intervention	Out-orthosis	To investigate the immediate effect on reducing spinal curvature
	0 M - after 2 hours of wearing mPCG	In-orthosis	
2	0 M - pre-intervention	Out-orthosis	To investigate the long-term effect on controlling the progression of the spinal curvature
	9 M - after 9 months of wearing mPCG	Out-orthosis	
3	0 M - pre-intervention	Out-orthosis	To monitor the spinal condition without the mPCG donned
	3 M – after 3 months of wearing mPCG	Out-orthosis	
4	0 M – after 2 hours of wearing mPCG	In-orthosis	To examine whether the mPCG can sustain changes after 6 months of use
	6 M – after 6 months of wearing mPCG	In-orthosis	

The Cobb angles measured on the X-rays at different points of time are summarised in Table 5.6 (the X-ray scans are available in Appendix VIII). When determining the effect of the mPCG in controlling the spinal curvature, a Cobb angle increase of more than 5° is considered to be an increase in the curvature, whereas the curvature is considered to be under control or progression halted if the increase is less than 5° or there is no increase. A Cobb angle that is

reduced by more than 5° is considered to be an improvement and a decrease in the curvature (Wong et al., 2008; Wong & Tan 2010; Brooks et al. 1975; Soucacos et al. 1998; Rogala et al. 1978).

Table 5.6 Cobb angle results at different points of time

Subject	0 M before girdling [Out-orthosis]		0 M after 2 hours girdling [In-orthosis]		3 M [Out-orthosis]		6 M [In-orthosis]		9 M [Out-orthosis]	
	Cobb angle (°) & spinal level		Cobb angle (°) & spinal level		Cobb angle (°) & spinal level		Cobb angle (°) & spinal level		Cobb angle (°) & spinal level	
	Upper curve	Upper curve	Lower curve	Upper curve	Lower curve	Upper curve	Lower curve	Upper curve	Lower curve	Upper curve
1	14.8 (T6-T11)	16.1 (T12-L3)	8 (T6-T11)	7 (T12-L3)	13.7 (T6-T11)	17.3 (L1-L4)	9.5 (T5-T11)	6.9 (T12-L4)	12.1 (T6-T11)	14 (T12-L4)
2	/	12 (T7-L3)	/	12 (T7-L3)		10.6 (T10-L3)	/	5.5 (T11-L4)	/	9 (T9-L4)
3	17 (T5-T11)	/	17 (T5-L1)	/	Withdrew		Withdrew		Withdrew	
4	18 (T3-T9)	15 (T12-L3)	7 (T5-T12)	/	Withdrew		Withdrew		Withdrew	
5	11.1 (T3-T9)	15.1 (T11-L3)	10.5 (T5-T9)	14.1 (T11-L2)	9.1 (T4-T10)	10 (T12-L4)	9.1 (T4-T10)	13 (T12-L4)	7.8 (T4-T10)	13.5 (T12-L4)
6	/	12.6 (T10-L2)	/	5.9 (T10-L2)	/	8.4 (T10-L2)	/	8.9 (T8-T12)	/	10.3 (T11-L2)
7	14.1 (T6-T9)	19.4 (T10-L2)	11.2 (T6-T9)	15.1 (T10-L2)	10.5 (T7-T10)	18.4 (T11-L3)	7.8 (T7-T10)	17.1 (T11-L3)	8.9 (T7-T10)	18 (T11-L3)
8	8.6 (T5-T10)	13 (T11-L4)	6 (T4-T10)	7.6 (T11-L4)	4.1 (T6-T11)	8.3 (T12-L5)	3.8 (T6-T11)	5.6 (T12-L5)	1.8 (T6-T11)	7 (T12-L5)
9	10.1 (T5-T10)	13.1 (T11-L4)	5.1 (T5-T10)	7.9 (T11-L4)	4.6 (T5-T10)	16 (T11-L4)	5.1 (T5-T10)	10 (T11-L4)	2.1 (T5-T10)	9 (T11-L4)
10	13.7 (T6-L1)	17.5 (L2-L5)	7.5 (T6-L1)	15.2 (L2-L5)	9.5 (T6-L1)	16.3 (L2-L5)	6 (T6-L1)	14.6 (L2-L5)	5.9 (T6-L1)	14.9 (L2-L5)

Remarks: T = Thoracic; L = Lumbar

### 5.5.1 Immediate effects on spinal curvature (after 2 h)

In determining immediate effects of the mPCG on controlling the progression of the spinal curvature, apart from a comparison of the changes in Cobb angle between 0 M pre-intervention and 0 M 2 h, the rate of change with the mPCG donned would also be considered. The results of the 10 recruited subjects are presented and discussed as follows.

Table 5.7 and Figure 5.1 show that there are apparent reductions in the spinal curvature with the use of the mPCG (i.e., Cobb angle reduction  $\geq 5^\circ$ ) immediately for 6 of the subjects (Subjects 1, 4, 6, 8, 9 and 10) or more than a half of the subjects after 2 h. The thoracic curve of Subject 1 is reduced from 14.8° to 8° and her lumbar curve is reduced from 16.1° to 7°, which means the correction with the mPCG donned is 45.95% and 56.52% for her thoracic and lumbar curves, respectively. The double curve of Subject 4 changes to a single curve; her Cobb angle is reduced from 18° to 7°, which means a correction of 61.11%. The Cobb angle of Subject 6

is reduced from 12.6° to 5.9°, which means a correction of 53.17%. The thoracic curve of Subject 8 is reduced from 8.6° to 6° and lumbar curve from 13° to 7.6°, which means a 30.23% and 41.54% correction, respectively. The thoracic curve of Subject 10 is reduced from 13.7° to 7.5° while her lumbar curve is reduced from 17.5° to 15.2°, which means a 45.26% and 13.14% reduction of her thoracic and lumbar curves, respectively. Apart from the apparent reduction in the Cobb angle of these 6 subjects, Subjects 5 and 7 also showed some reduction. The thoracic and lumbar curves of the former are reduced from 11.1° to 10.5° and 15.1° to 14.1°, respectively, or a 5.4% and 6.62% reduction. The thoracic and lumbar curves of the latter are reduced from 14.1° to 11.2° and 19.4° to 15.1°, respectively, or a 20.57% and 22.16% reduction.

Table 5.7 Cobb angle changes at 0 M before and after 2 h (immediate effects)

Subject	Cobb angle (°) & spinal level				Cobb angle changes (°)		In-orthosis correction rate (%)	
	0 M before girdling [Out-orthosis]		0 M after 2 hours girdling [In-orthosis]		Upper curve	Lower curve	Upper curve	Lower curve
	Upper curve	Lower curve	Upper curve	Lower curve				
1	14.8 (T6-T11)	16.1 (T12-L3)	8 (T6-T11)	7 (T12-L3)	-6.8	-9.1	45.95%	56.52%
2	/	12 (T7-L3)	/	12 (T7-L3)	/	0	/	0%
3	17 (T5-T11)	/	17 (T5-L1)	/	0	/	0%	/
4	18 (T3-T9)	15 (T12-L3)	7 (T5-T12)	/	-11	/	61.11%	100%
5	11.1 (T3-T9)	15.1 (T11-L3)	10.5 (T5-T9)	14.1 (T11-L2)	-0.6	-1	5.4%	6.62%
6	/	12.6 (T10-L2)	/	5.9 (T10-L2)	/	-6.7	/	53.17%
7	14.1 (T6-T9)	19.4 (T10-L2)	11.2 (T6-T9)	15.1 (T10-L2)	-2.9	-4.3	20.57%	22.16%
8	8.6 (T5-T10)	13 (T11-L4)	6 (T4-T10)	7.6 (T11-L4)	-2.6	-5.4	30.23%	41.54%
9	10.1 (T5-T10)	13.1 (T11-L4)	5.1 (T5-T10)	7.9 (T11-L4)	-5	-5.2	49.5%	39.69%
10	13.7 (T6-L1)	17.5 (L2-L5)	7.5 (T6-L1)	15.2 (L2-L5)	-6.2	-2.3	45.26%	13.14%

Remarks: T = Thoracic; L = Lumbar

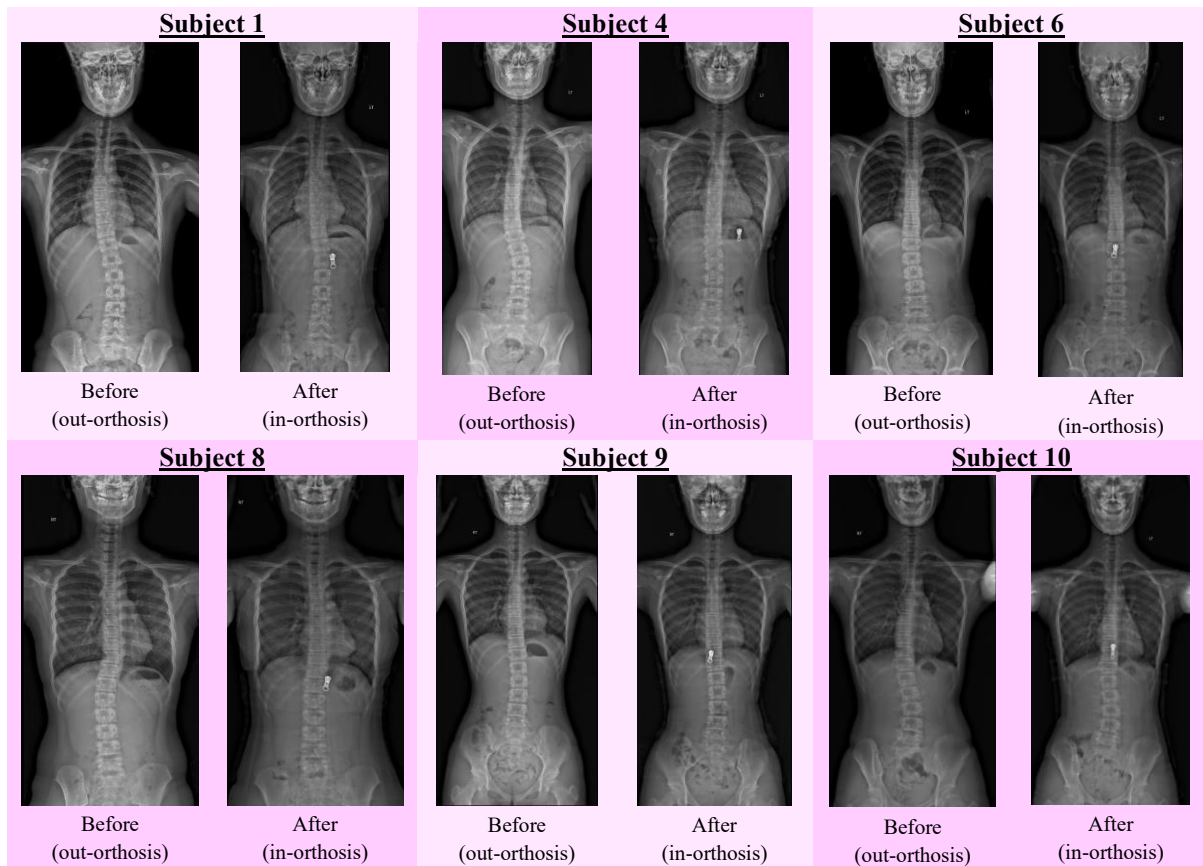


Figure 5.1 Changes in spinal curvature of Subjects 1, 4, 6, 8, 9 and 10 after 2 h

### 5.5.2 Long-term effects on controlling spinal curvature (after 9 M)

Regarding the long-term effects of the mPCG on controlling the progression of the spinal curvature, the rate of change before and after the intervention is also considered apart from the comparison of the Cobb angle changes between 0 M pre-intervention and 9 M. Since Subjects 3 and 4 withdrew and did not complete the 9-month wear trial, only 8 subjects underwent X-ray scanning at 9 M.

Table 5.8 and Figure 5.2 show apparent long-term reductions in the spinal curvature (i.e. Cobb angle reduction  $\geq 5^\circ$ ) of 4 (Subjects 7, 8, 9 and 10) of the 8 subjects after 9 M, or half of the subjects who underwent the 9-month wear trial. The thoracic and lumbar curves of Subject 7, are reduced from  $14.1^\circ$  to  $8.9^\circ$  and  $19.4^\circ$  to  $18^\circ$ , respectively, or a 36.88% and 7.22% reduction. The thoracic and lumbar curves of Subject 8 are significantly reduced from  $8.6^\circ$  to  $1.8^\circ$  and  $13^\circ$  to  $7^\circ$ , respectively, or a 79.07% and 46.15% reduction. The thoracic and lumbar curves of Subject 9 are greatly reduced from  $10.1^\circ$  to  $2.1^\circ$  and  $13.1^\circ$  to  $9^\circ$ , respectively, or a 79.21% and 31.3% reduction. The thoracic and lumbar curves of Subject 10 are also reduced, from  $13.7^\circ$  to  $5.9^\circ$  and  $17.5^\circ$  to  $14.9^\circ$ , respectively, or a 56.93% and 14.86% reduction. Apart from the

apparent reduction in the Cobb angles of Subjects 7 to 10, some reduction in spinal curvature was also in general, found in the remaining subjects (i.e., Subjects 1, 2, 4 and 5), whose reduction ranges from 10.6% to 29.73%.

Table 5.8 Cobb angle changes from 0 M pre-intervention to 9 M (long-term effects)

Subject	Cobb angle (°) & spinal level				Cobb angle changes (°)		Pre- and post-correction rate (%)	
	0 M before girdling [Out-orthosis]		9 M after 9 months girdling [Out-orthosis]		Upper curve	Lower curve	Upper curve	Lower curve
1	14.8 (T6-T11)	16.1 (T12-L3)	12.1 (T6-T11)	14 (T12-L4)	-2.7	-2.1	-18.24%	-13.04%
2	/	12 (T7-L3)	/	9 (T9-L4)	/	-3	/	-25%
3	17 (T5-T11)	/	Withdraw		N/A		N/A	
4	18 (T3-T9)	15 (T12-L3)	Withdraw		N/A		N/A	
5	11.1 (T3-T9)	15.1 (T11-L3)	7.8 (T4-T10)	13.5 (T12-L4)	-3.3	-0.6	-29.73%	-10.6%
6	/	12.6 (T10-L2)	/	10.3 (T11-L2)	/	-2.3	/	-18.25%
7	14.1 (T6-T9)	19.4 (T10-L2)	8.9 (T7-T10)	18 (T11-L3)	-5.2	-1.4	-36.88%	-7.22%
8	8.6 (T5-T10)	13 (T11-L4)	1.8 (T6-T11)	7 (T12-L5)	-6.8	-6	-79.07%	-46.15%
9	10.1 (T5-T10)	13.1 (T11-L4)	2.1 (T5-T10)	9 (T11-L4)	-8	-4.1	-79.21%	-31.30%
10	13.7 (T6-L1)	17.5 (L2-L5)	5.9 (T6-L1)	14.9 (L2-L5)	-7.8	-2.6	-56.93%	-14.86%

Remarks: T = Thoracic; L = Lumbar

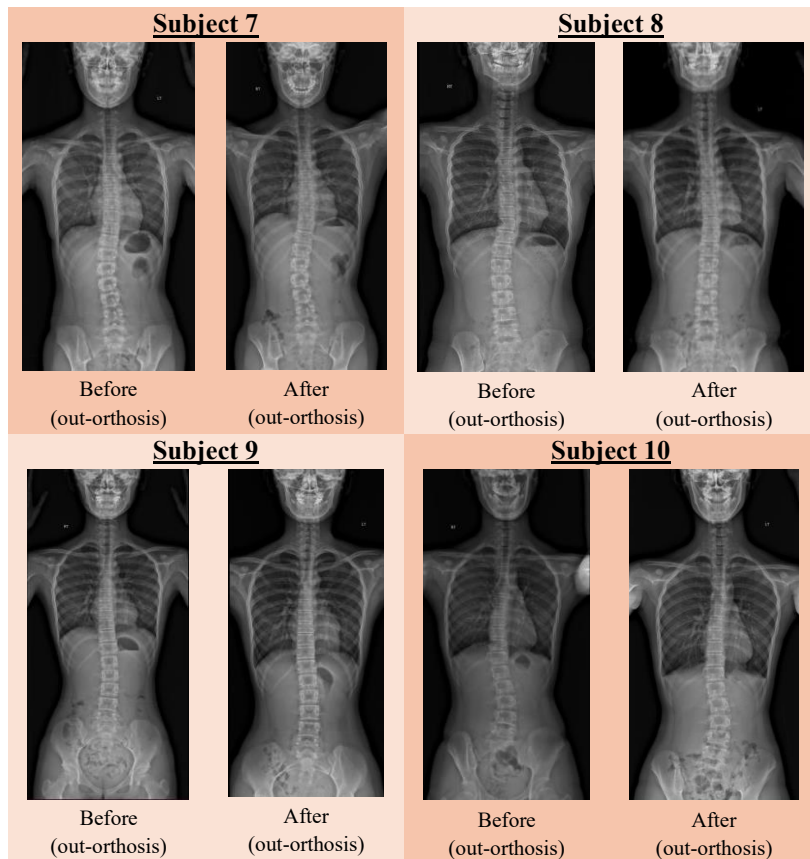


Figure 5.2 Changes in spinal curvature of Subjects 7, 8, 9 and 10 after 9 M

### 5.5.3 Spinal condition after 3 months out-orthosis

At 3 M out-orthosis, the rate of progression of the spinal curvature is considered aside from the Cobb angle changes between 0 M pre-intervention and 3 M. Since Subjects 3 and 4 withdrew before the evaluation session at 3 M, only the results of the remaining 8 subjects are presented; see Table 5.9.

The table shows that there is no apparent progression of the curvature (i.e., increase of Cobb angle  $\geq 5^\circ$ ) of any of the subjects. Only very small increases of the lumbar curve are found for Subjects 1 and 9 of  $1.2^\circ$  (+7.45%) and  $2.9^\circ$  (+22.14%), respectively, out-orthosis. Instead, the subjects in general have a smaller Cobb angle. The decrease ranges from  $-1^\circ$  (5.15%) to  $-5.5^\circ$  (54.46%). The subjects even show that their curvature is under control and reduced even with the mPCG doffed. This might indicate the effectiveness of the mPCG in controlling the progression of the curvature even though the subjects have just used the mPCG for a short period (3 months) of time.

Table 5.9 Cobb angle changes from 0 M pre-intervention to 3 M (out-orthosis)

Subject	Cobb angle (°) & spinal level				Cobb angle changes (°)		Curve progression rate (%)	
	0 M before girdling [Out-orthosis]		3 M after 3 months girdling [Out-orthosis]		Upper curve	Lower curve	Upper curve	Lower curve
	Upper curve	Lower curve	Upper curve	Lower curve				
1	14.8 (T6-T11)	16.1 (T12-L3)	13.7 (T6-T11)	17.3 (T12-L4)	-1.1	+1.2	-7.43%	+7.45%
2	/	12 (T7-L3)	/	10.6 (T10-L3)	/	-1.4	/	-11.67%
3	17 (T5-T11)	/	Withdraw		N/A		N/A	
4	18 (T3-T9)	15 (T12-L3)	Withdraw		N/A		N/A	
5	11.1 (T3-T9)	15.1 (T11-L3)	9.1 (T4-T10)	10 (T12-L4)	-2	-5.1	-18.02%	-33.77%
6	/	12.6 (T10-L2)	/	8.4 (T10-L2)	/	-4.2	/	-33.33%
7	14.1 (T6-T9)	19.4 (T10-L2)	10.5 (T7-T10)	18.4 (T11-L3)	-3.6	-1	-25.53%	-5.15%
8	8.6 (T5-T10)	13 (T11-L4)	4.1 (T6-T11)	8.3 (T12-L5)	-4.5	-4.7	-52.33%	-36.15%
9	10.1 (T5-T10)	13.1 (T11-L4)	4.6 (T5-T10)	16 (T11-L4)	-5.5	+2.9	-54.46%	+22.14%
10	13.7 (T6-L1)	17.5 (L2-L5)	9.5 (T6-L1)	16.3 (L2-L5)	-4.2	-1.2	-30.66%	-6.86%

Notes: T = Thoracic; L = Lumbar

#### 5.5.4 Maintenance of effectiveness of mPCG on controlling progression of spinal curvature

As for the ability of the mPCG in maintaining effectiveness in controlling the progression of the spinal curvature, this was determined by comparing the changes of the Cobb angle in the early stages of using the mPCG (i.e., 0 M) to the later stages (i.e., 6 M) of the girdling treatment. Since Subjects 3 and 4 withdrew during the wear trial, only the results of the remaining 8 subjects would be compared.

Table 5.10 shows that even though increases in the Cobb angle are found while using the mPCG on parts of the spinal curvatures of 3 subjects (i.e., Subjects 1, 6 and 9), the Cobb angles generally decrease from 0 M to 6 M in most of the spinal curvatures. The reductions range from 0.1° (1.43%) to 6.5° (54.17%). This shows that the use of the mPCG to slow the progression of the spinal curvature is still effective even though the mPCG has been used for 6 months already. However, this should only be used as a reference since other changes in spinal conditions might be a factor that affects curvature control performance.

Table 5.10 Changes of Cobb angle from 0 M to 6 M (in-orthosis)

Subject	Cobb angle (°) & spinal level				From 0 M to 6 M: in-orthosis Cobb angle changes (°)		From 0 M to 6 M: in-orthosis Cobb angle changes (%)	
	0 M after 2 hours girdling [In-orthosis]		6 M after 6 months girdling [In-orthosis]		Upper curve	Lower curve	Upper curve	Lower curve
	Upper curve	Lower curve	Upper curve	Lower curve				
1	8 (T6-T11)	7 (T12-L3)	9.5 (T5-T11)	6.9 (T12-L4)	+1.5	-0.1	+18.75%	-1.43%
2	/	12 (T7-L3)	/	5.5 (T11-L4)	/	-6.5	/	-54.17%
3	17 (T5-L1)	/	Withdrew		N/A		N/A	
4	7 (T5-T12)	/	Withdrew		N/A		N/A	
5	10.5 (T5-T9)	14.1 (T11-L2)	9.1 (T4-T10)	13 (T12-L4)	-1.4	-1.1	-13.33%	-7.8%
6	/	5.9 (T10-L2)	/	8.9 (T8-T12)	/	+2.2	/	+50.85%
7	11.2 (T6-T9)	15.1 (T10-L2)	7.8 (T7-T10)	17.1 (T11-L3)	-3.4	+2	-30.36%	-13.25%
8	6 (T4-T10)	7.6 (T11-L4)	3.8 (T6-T11)	5.6 (T12-L5)	-2.2	-2	-36.67%	-26.32%
9	5.1 (T5-T10)	7.9 (T11-L4)	5.1 (T5-T10)	10 (T11-L4)	0	+2.1	0%	+42.85%
10	7.5 (T6-L1)	15.2 (L2-L5)	6 (T6-L1)	14.6 (L2-L5)	-1.5	-0.6	-20%	-3.95%

Notes: T = Thoracic; L = Lumbar

### 5.5.5 Discussion of effects of mPCG on controlling progression of spinal curvature

#### Immediate effect

Most or 6 of the 10 subjects show a significant reduction in their spinal curvature in terms of the immediate effect after 2 h. As for the specific type of curve (Table 5.2), a higher immediate correction rate was generally found among the subjects with an S curve with the mPCG donned, or 5 of these 6 subjects while only 1 has a C curve. Also, when looking at all of the subjects who show a Cobb angle reduction after wearing the mPCG (total of 8 subjects), 7 of them are diagnosed with an S curve and only 1 with a C curve. This might indicate that the corrective mechanism of the mPCG is more effective for those with an S curve.

Besides, when looking at all of the subjects who have a significant and immediate reduction of their Cobb angle after the mPCG was donned for 2 hours (6 subjects in total), most of them have a Risser sign of 0-2, and only 2 of them have a Risser sign of 3. For the 4 subjects who do not show any apparent immediate changes, 3 of them have a Risser sign of 3 while 1 has a Risser sign of 2. This might imply that the mPCG may perform better in terms of immediate control of the curvature of adolescents with a Risser grade 2 or lower.

### **After 9 months**

After 9 M of treatment, 4 of the 8 subjects showed a significant reduction in their spinal curvature (excluding the 2 who withdrew). They all have an S curve, which might indicate that the corrective mechanism of the mPCG is more effective for this type of curve which is in agreement with the results for the immediate effects.

Among the 4 subjects who showed an apparent reduction after 9 M, 2 of them have a Risser sign of 0-2, while 2 of them have a Risser sign of 3. Unlike the immediate effects, when analysing the corrective effect after 9 M, the commitment of the subjects to the wear trial played an important role. For instance, those who have a higher compliance rate (i.e., Subjects 7, 8, 9 and 10) generally showed a larger reduction in their curvature when their X-rays without the use of the mPCG were examined. More results related to compliance with the mPCG in this study are presented in Section 5.9.

### **5.6 Improvements in posture balance (3D body scanning and posture angle)**

Improvements in the posture balance of the recruited subjects, if any, were determined by carrying out 3D body scanning and comparing the posture angle, so as to understand the effectiveness of the mPCG on posture correction. The subjects underwent 3D body scanning at 0 M, 3 M, 6 M and 9 M in both their habitual standing and sitting postures. As mentioned in Section 3.5.4.2, the initial scanning was performed at the beginning of the wear trial (0 M) “without the girdle” and “with the girdle” for the investigation of immediate posture correction. Three-dimensional body scanning was also conducted at 3 M, 6 M and 9 M “without the girdle” and “with the girdle” to monitor the posture changes. The results of the posture angles on the 12 items mentioned in Section 3.5.4.2 (Figure 3.35) are obtained as follows. The data collected were analysed by using SPSS with a paired t-test for non-parametric Wilcoxon rank-sum test. The level of significance was set at  $p=0.05$ . In this study, a total of 10 subjects are recruited for the 9-month wear trial ( $n=10$ ). Since Subjects 3 and 4 withdrew in the early days of the wear trial, their collected data would only be presented in the 0 M tests.

#### **5.6.1 Posture balance in frontal plane during habitual standing**

##### **Asymmetry of acromion**

The results of the asymmetry of the acromion in the frontal plane during habitual standing are shown in Figure 5.3 (details of the collected data are provided in Appendix IX). According to

the results, significant differences are found with: 0 M without girdle vs. 0 M with girdle ( $p=0.0078$ ), 3 M without girdle vs. 3 M with girdle ( $p=0.0156$ ), 6 M without girdle vs. 6 M with girdle ( $p=0.0234$ ), and 0 M without girdle vs. 9 M without girdle ( $p=0.0052$ ). In other words, by comparing the results “with the girdle” and “without the girdle” at the same time point, immediate and significant effects that reduce the asymmetry of the acromion in the frontal plane during habitual standing are found at 0 M, 3 M and 6 M when the girdle is donned. Besides, by comparing the results “without the girdle” between 0 M and 9 M, it was found that the 9-month treatment can significantly reduce the asymmetry of the acromion for the long term, even if the girdle is doffed.

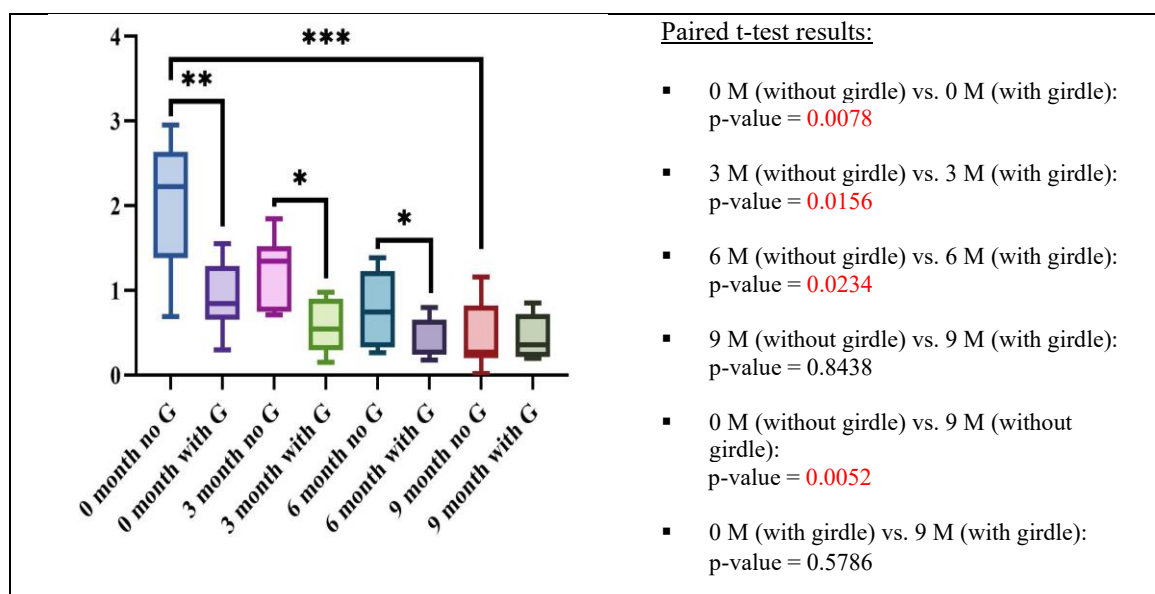


Figure 5.3 Results of asymmetry of acromion in frontal plane during habitual standing

### Pelvis asymmetry

The results of the asymmetry of the pelvis in the frontal plane during habitual standing are shown in Figure 5.4 (details of the collected data are available in Appendix IX). According to the results, significant differences are found with: 0 M without girdle vs. 0 M with girdle ( $p=0.0156$ ), 6 M without girdle vs. 6 M with girdle ( $p=0.0078$ ), and 0 M without girdle vs. 9 M without girdle ( $p=0.0078$ ). In other words, by comparing the results “with the girdle” and “without the girdle” at the same time point, immediate and significant effects that reduce the pelvis asymmetry in the frontal plane during habitual standing are found at 0 M and 6 M when the girdle is donned. Besides, by comparing the results “without the girdle” between 0 M and 9 M, it was found that the 9 months of treatment significantly reduces pelvis asymmetry for the long-term even if the girdle is doffed.

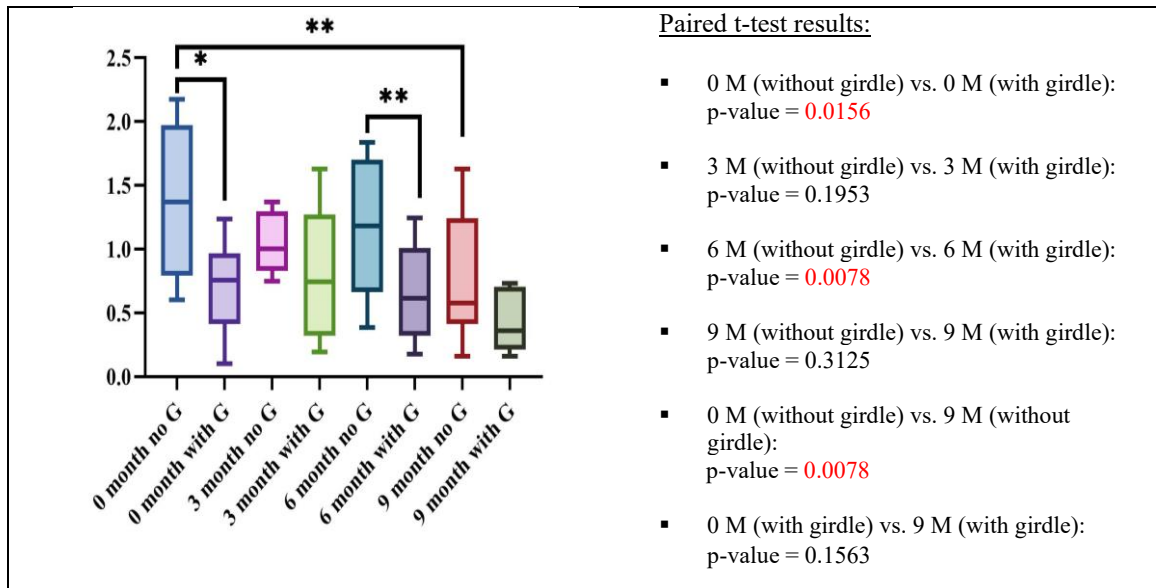


Figure 5.4 Results of pelvis asymmetry in frontal plane during habitual standing

### Asymmetry of acromion/pelvis

The results of the asymmetry of the acromion/pelvis in the frontal plane during habitual standing are shown in Figure 5.5 (details of the collected data are provided in Appendix IX). According to the results, significant differences are found at: 0 M without girdle vs. 0 M with girdle ( $p=0.0156$ ), 3 M without girdle vs. 3 M with girdle ( $p=0.0391$ ) and 6 M without girdle vs. 6 M with girdle ( $p=0.0234$ ). In other words, by comparing the results “with the girdle” and “without the girdle” at the same time point, immediate and significant effects that reduce the asymmetry of the acromion/pelvis in the frontal plane during habitual standing are found at 0 M, 3 M and 6 M when the girdle is donned.

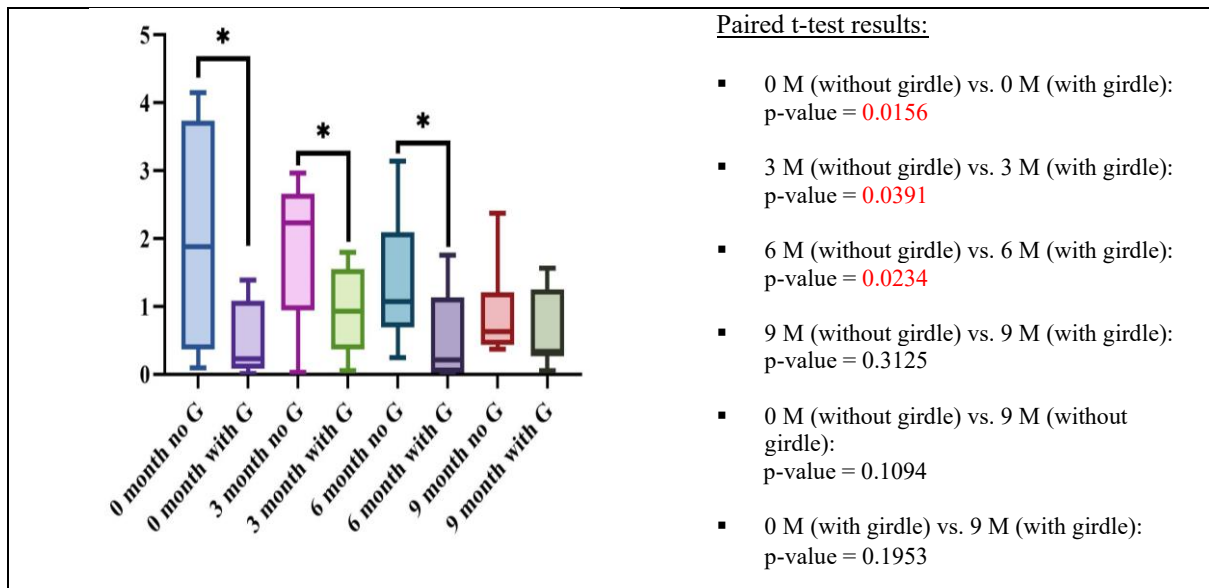


Figure 5.5 Results of asymmetry of acromion/pelvis in frontal plane during habitual standing

## 5.6.2 Posture balance in horizontal plane during habitual standing

### Asymmetry of acromion

The results of the asymmetry of the acromion in the horizontal plane during habitual standing are shown in Figure 5.6 (details of the collected data provided in Appendix IX). According to the results, significant differences are found in: 0 M without girdle vs. 9 M without girdle ( $p=0.0391$ ). In other words, by comparing the results “without the girdle” between 0 M and 9 M, it was found that the 9 months of treatment significantly reduce the asymmetry of the acromion in the horizontal plane during habitual standing for the long term even if the girdle is doffed.

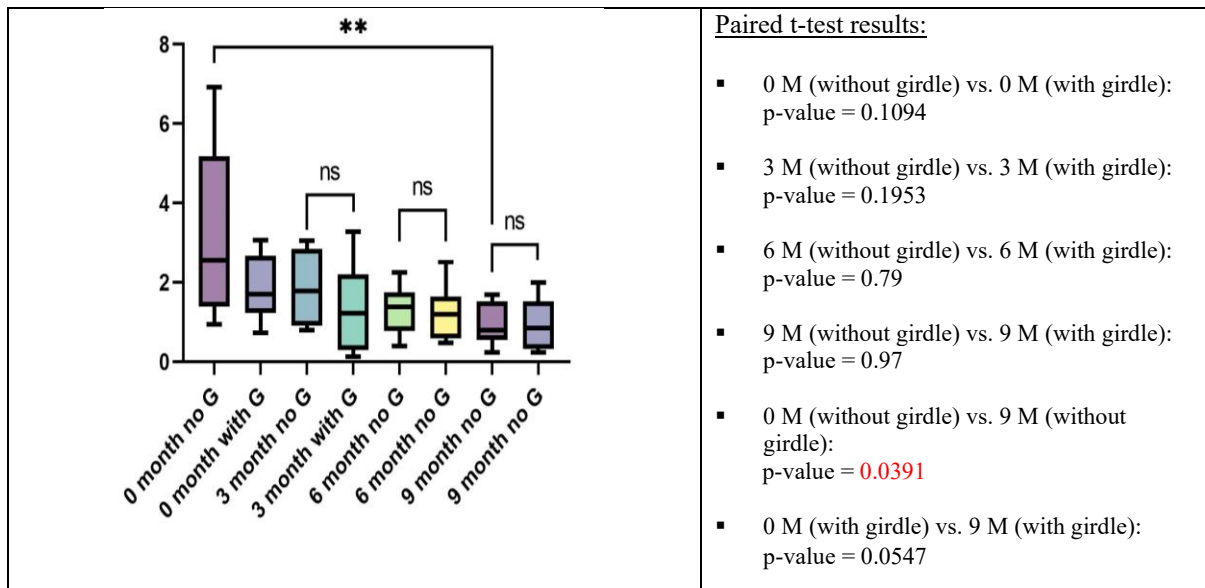


Figure 5.6 Results of asymmetry of acromion in horizontal plane during habitual standing

### Pelvis asymmetry

The results of the pelvis asymmetry in the horizontal plane during habitual standing are shown in Figure 5.7 (details of the collected data are provided in Appendix IX). According to the results, no significant differences are found on the tested items at 0 M, 3 M 6 M and 9 M. In other words, no immediate and significant effects can be found that reduce the pelvis asymmetry in the horizontal plane during habitual standing at all points of time. Also, no significant reduction in the pelvis asymmetry can be found in the horizontal plane for the long term during habitual standing after the completion of the 9-month wear trial.

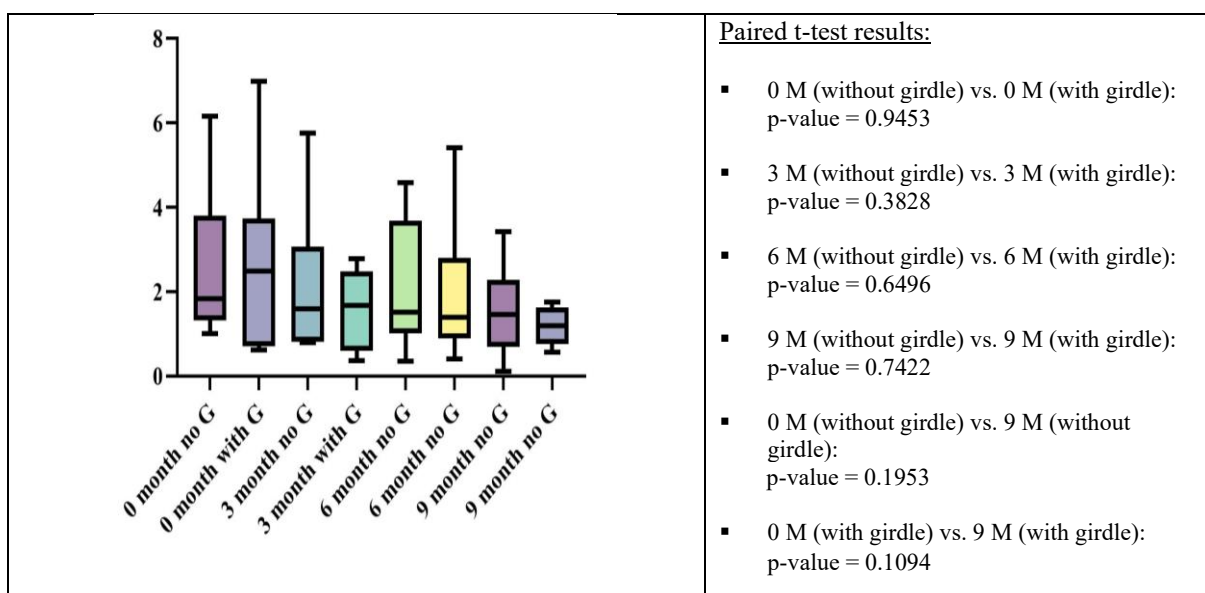


Figure 5.7 Results of pelvis asymmetry in horizontal plane during habitual standing

### Scapula asymmetry

The results of the scapula asymmetry in the horizontal plane during habitual standing are shown in Figure 5.8 (details of the collected data are provided in Appendix IX). According to the results, significant differences are found for: 0 M without girdle vs. 0 M with girdle ( $p=0.0078$ ), and 0 M without girdle vs. 9 M without girdle ( $p=0.0078$ ). In other words, by comparing the results “with the girdle” and “without the girdle” at the same time point, an immediate and significant effect that reduces the scapula asymmetry in the horizontal plane during habitual standing is found at 0 M when the girdle is donned. Besides, by comparing the results “without the girdle” between 0 M and 9 M, it can be found that the 9 months of mPCG use significantly reduce the scapula asymmetry for the long term, even if the mPCG is doffed.

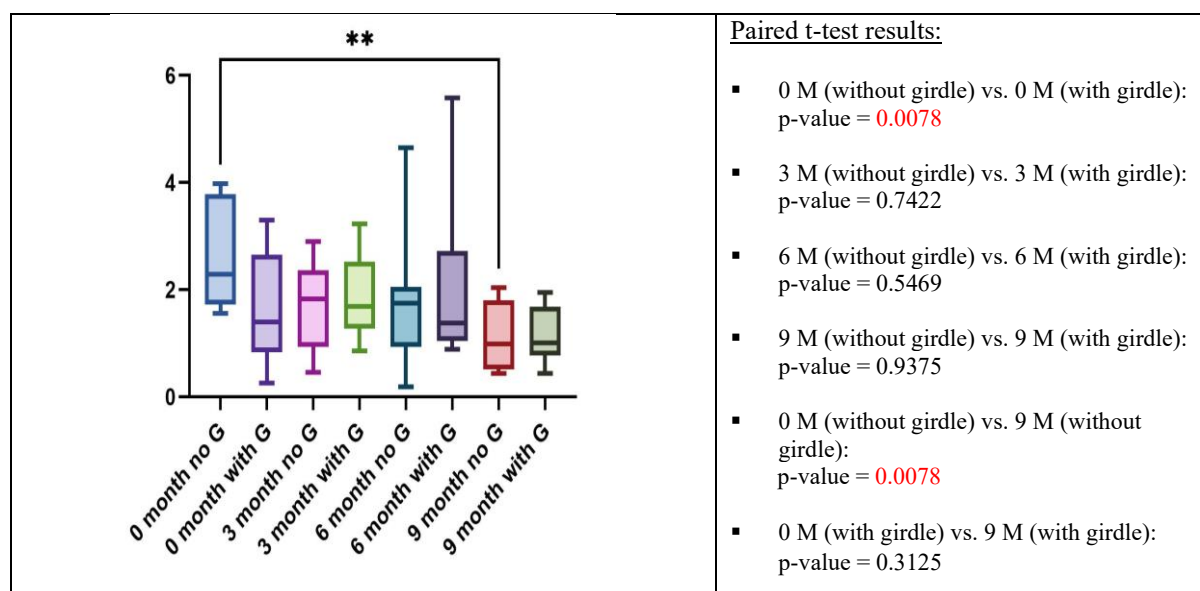


Figure 5.8 Results of scapula asymmetry in horizontal plane during habitual standing

### Acromion/scapula asymmetry

The results of the acromion/scapula asymmetry in the horizontal plane during habitual standing are shown in Figure 5.9 (details of the collected data are provided in Appendix IX). According to the results, no significant differences are found on the tested items at 0 M, 3 M 6 M and 9 M. In other words, no immediate and significant effects can be found that reduce the acromion/scapula asymmetry in the horizontal plane during habitual standing at all points of time. Also, no long-term significant improvement can be found that reduces the acromion/scapula asymmetry in the horizontal plane during habitual standing after the completion of the 9-month wear trial.

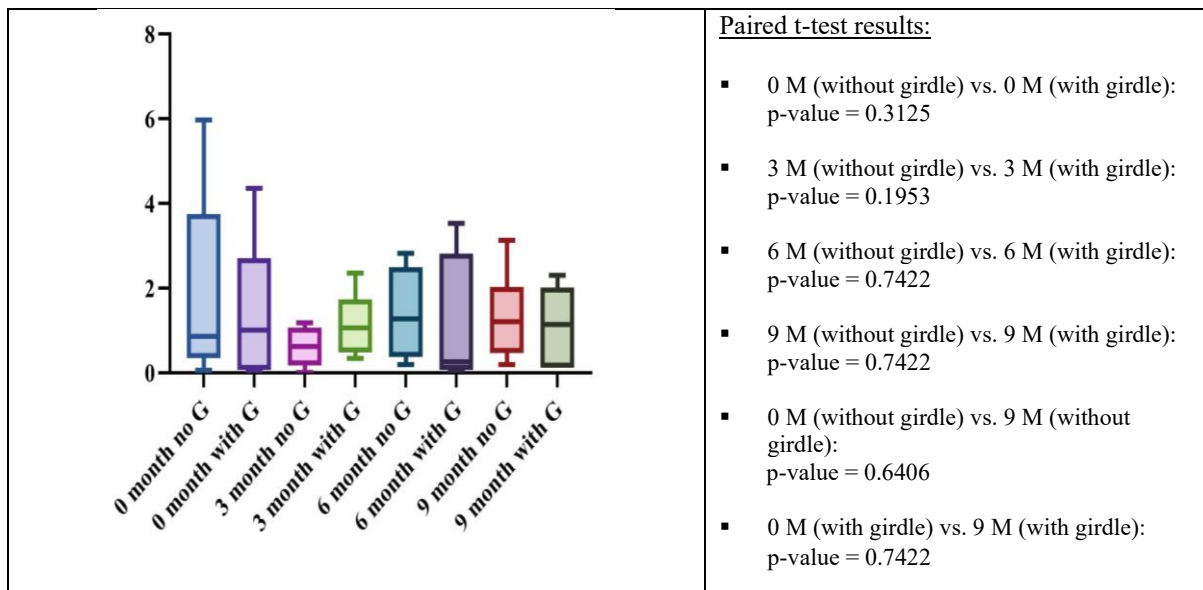


Figure 5.9 Results of acromion/scapula asymmetry in horizontal plane during habitual standing

### Acromion/pelvis asymmetry

The results of the acromion/pelvis asymmetry in the horizontal plane during habitual standing are shown in Figure 5.10 (details of the collected data are provided in Appendix IX). According to the results, a significant difference is found for: 3 M without girdle vs. 3 M with girdle ( $p=0.0156$ ), and 0 M without girdle vs. 9 M without girdle ( $p=0.0391$ ). In other words, by comparing the results “with the girdle” and “without the girdle” at the same time point, immediate and significant effects that reduce the acromion/pelvis asymmetry in the horizontal plane during habitual standing can be found at 3 M when the girdle is donned. Besides, by comparing the results “without the girdle” between 0 M and 9 M, it was found that the 9 months of treatment significantly reduce the acromion/pelvis asymmetry even if the mPCG is doffed.

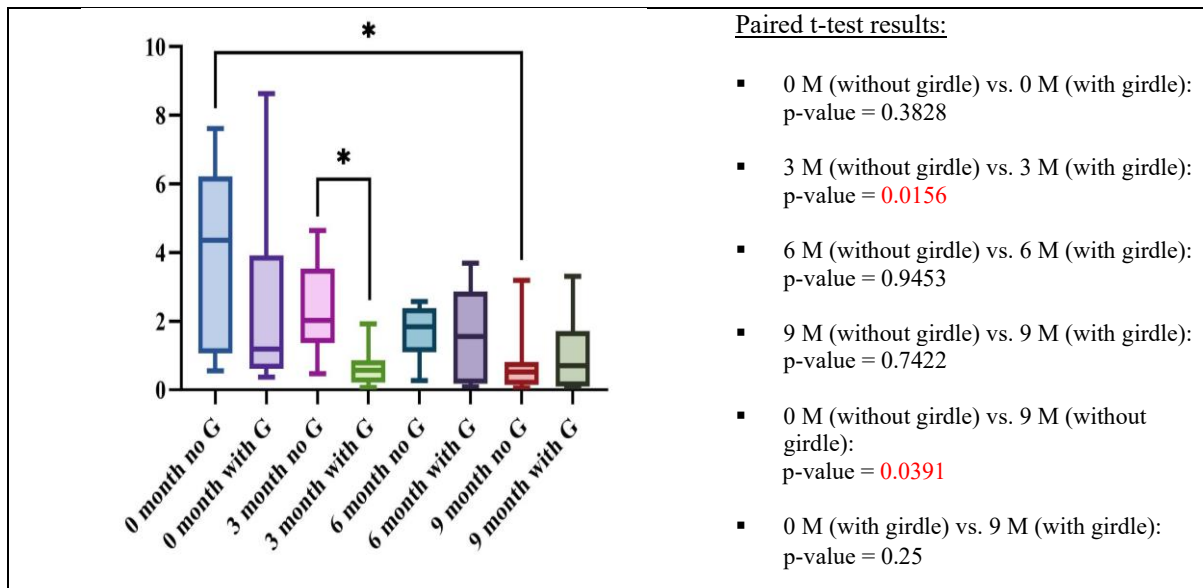


Figure 5.10 Results of acromion/pelvis asymmetry in horizontal plane during habitual standing

### 5.6.3 Posture balance in sagittal plane during habitual standing

#### Thoracic curve

The results of the thoracic imbalance in the sagittal plane during habitual standing are shown in Figure 5.11 (details of the collected data are provided in Appendix IX). According to the results, significant differences are found for: 0 M without girdle vs. 0 M with girdle ( $p=0.0078$ ), 3 M without girdle vs. 3 M with girdle ( $p=0.0078$ ), and 0 M without girdle vs. 9 M without girdle ( $p=0.0078$ ). In other words, by comparing the results “with the girdle” and “without the girdle” at the same time point, immediate and significant effects that reduce the thoracic imbalance in the sagittal plane during habitual standing are found at 0 M and 3 M when the girdle is donned. Besides, by comparing the results “without the girdle” between 0 M and 9 M, it was found that the 9 months of treatment significantly reduce the thoracic imbalance for the long term even if the girdle is doffed.

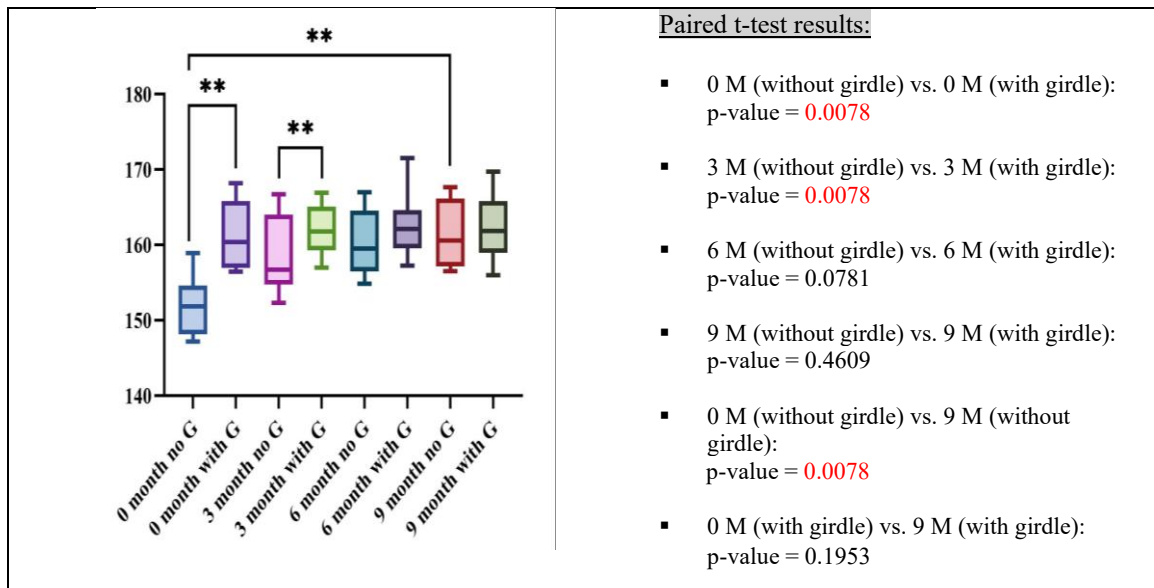


Figure 5.11 Results of thoracic imbalance in sagittal plane during habitual standing

### Lumbar curve

The results of the lumbar imbalance in the sagittal plane during habitual standing are shown in Figure 5.12 below (details of the collected data are provided in Appendix IX). According to the results, significant differences are found for: 0 M without girdle vs. 0 M with girdle ( $p=0.0078$ ), 3 M without girdle vs. 3 M with girdle ( $p=0.0078$ ), 6 M without girdle vs. 6 M with girdle ( $p=0.0078$ ), 9 M without girdle vs. 9 M with girdle ( $p=0.0078$ ), 0 M without girdle vs. 9 M without girdle ( $p=0.0078$ ), and 0 M with girdle vs. 9 M with girdle ( $p=0.0156$ ). In other words, by comparing the results “with the girdle” and “without the girdle” at the same time point, immediate and significant effects that reduce the lumbar imbalance in the sagittal plane during habitual standing are found at 0 M, 3 M, 6 M and 9 M when the girdle is donned. Besides, by comparing the results “without the girdle” between 0 M and 9 M, it was found that the 9 months of treatment significantly reduce lumbar imbalance for the long term even if the girdle is doffed. In addition, by comparing the results “with the girdle” between 0 M and 9 M, it was found that posture correction to reduce the lumbar curve is enhanced with the girdle donned after 9 months of treatment.

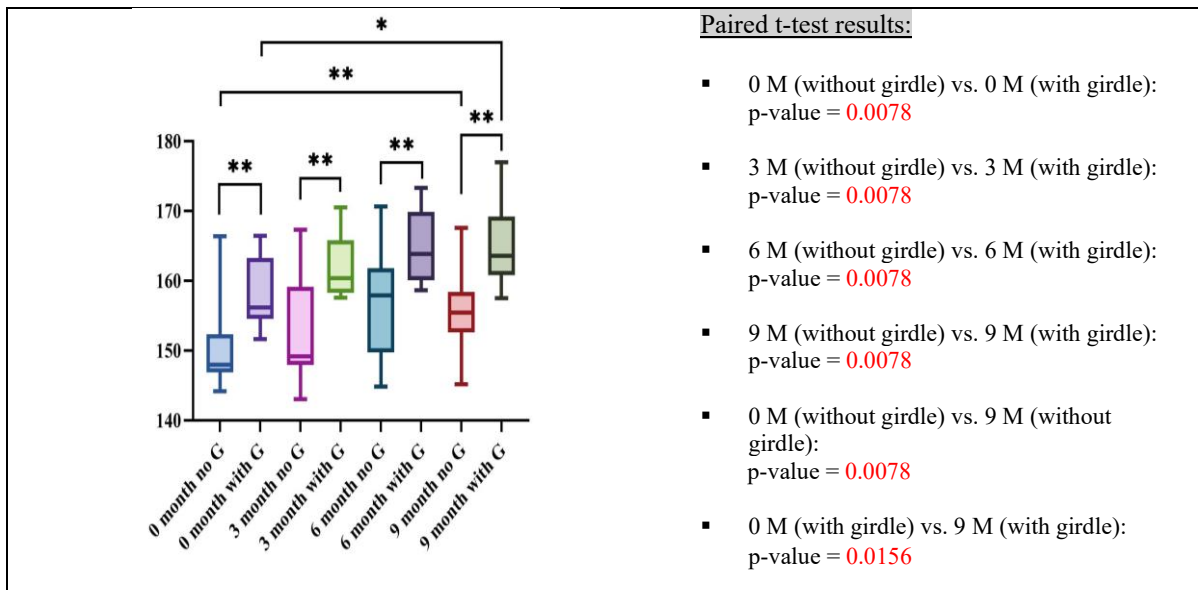


Figure 5.12 Results of lumbar imbalance in sagittal plane during habitual standing

### 5.6.4 Posture balance in sagittal plane during habitual sitting

#### Thoracic curve

The results of the thoracic imbalance in the sagittal plane during habitual sitting are shown in Figure 5.13 (details of the collected data are provided in Appendix IX). According to the results, significant differences are found for: 0 M without girdle vs. 0 M with girdle ( $p=0.0078$ ), 3 M without girdle vs. 3 M with girdle ( $p=0.0156$ ), 0 M without girdle vs. 9 M without girdle ( $p=0.0078$ ), and 0 M with girdle vs. 9 M with girdle ( $p=0.0156$ ). In other words, by comparing the results “with the girdle” and “without the girdle” at the same time point, immediate and significant effects that reduce the thoracic imbalance in the sagittal plane during habitual sitting are found at 0 M and 3 M when the girdle is donned. Besides, by comparing the results “without the girdle” between 0 M and 9 M, it was found that the 9 months of treatment significantly reduce thoracic imbalance even if the girdle is doffed. In addition, by comparing the results “with the girdle” between 0 M and 9 M, it was found that the posture correction to reduce the thoracic imbalance is enhanced after undergoing the 9 months of treatment.

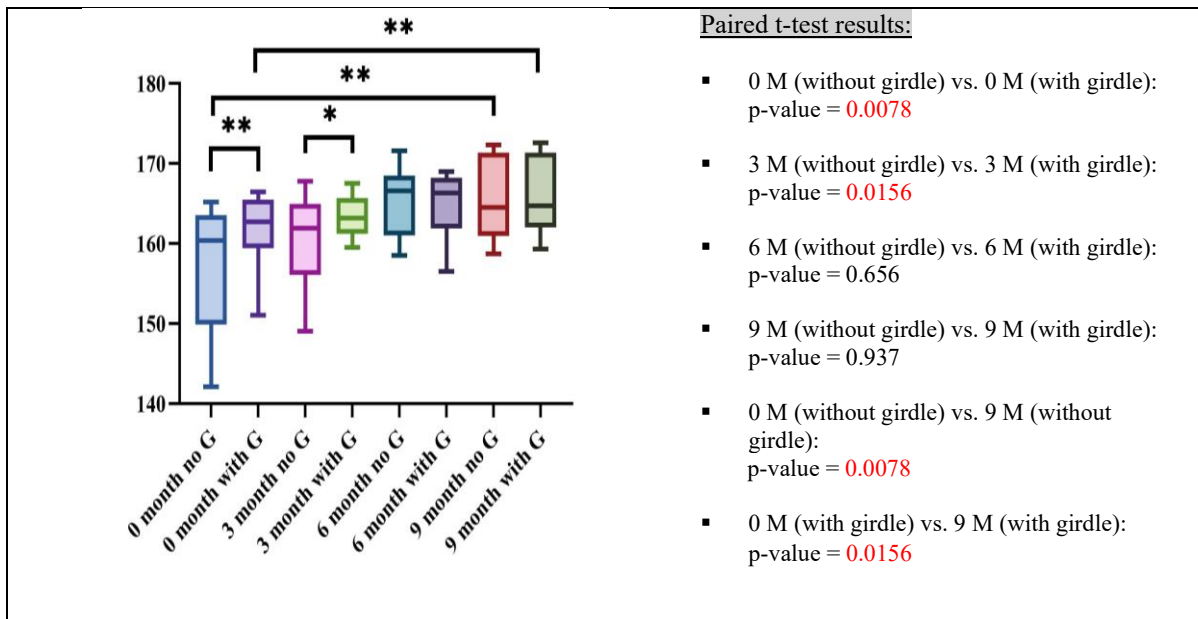


Figure 5.13 Results of thoracic imbalance in sagittal plane during habitual sitting

### Lumbar curve

The results of the lumbar imbalance in the sagittal plane during habitual sitting are shown in Figure 5.14 (details of the collected data are provided in Appendix IX). According to the results, significant differences are found for: 0 M without girdle vs. 0 M with girdle ( $p=0.0156$ ), 3 M without girdle vs. 3 M with girdle ( $p=0.0156$ ), 9 M without girdle vs. 9 M with girdle ( $p=0.0078$ ), and 0 M without girdle vs. 9 M without girdle ( $p=0.078$ ). In other words, by comparing the results “with the girdle” and “without the girdle” at the same time point, immediate and significant effects that reduce the lumbar imbalance in the sagittal plane during habitual sitting are found at 0 M, 3 M and 9 M when the girdle is donned. On the other hand, when comparing the results “without the girdle” between 0 M and 9 M, the p value is 0.089, which is marginally close to significance. This shows that there may be some changes that are worth further investigation to determine if the 9 months of treatment would significantly reduce lumbar imbalance even if the girdle is doffed.

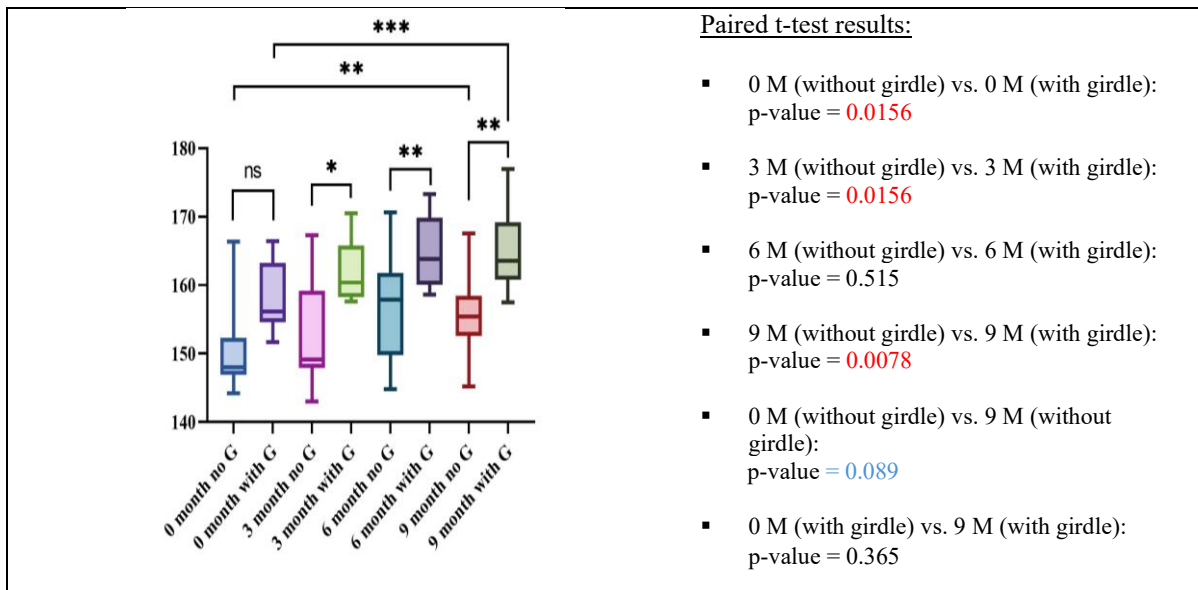


Figure 5.14 Results of lumbar imbalance in sagittal plane during habitual sitting

### 5.6.5 Discussion of effects on posture correction

Looking at the results of the treatment with the mPCG on posture correction during habitual standing, significant reductions can be found in the lumbar imbalance in the sagittal plane for all of the evaluated points of time (i.e., 0 M, 3 M, 6 M, 9 M) and when a comparison is made between 0 M and 9 M both “without the girdle” and “with the girdle”. This shows that the mPCG performs extremely well to provide both immediate and long-term reduction of the lumbar imbalance in the sagittal plane. In addition, significant reductions were found to the asymmetry of the acromion in the frontal plane at most of the evaluated points of time (i.e., 0 M, 3 M, and 6 M) and when a comparison is made between 0 M and 9 M “without the girdle”. This shows that the mPCG performs very well to reduce the immediate and long-term asymmetry of the acromion in the frontal plane. Besides, significant reductions can be found in the pelvis asymmetry in the frontal plane and thoracic imbalance in the sagittal plane for half of the evaluated points of time (i.e., 0 M and 6 M for pelvis asymmetry; 0 M and 3 M for thoracic asymmetry). This shows that the mPCG also performs well at immediately reducing the asymmetry of the pelvis in the frontal plane and thoracic imbalance in the sagittal plane. However, the mPCG does not really perform as well to correct the postures in the horizontal plane.

On the other hand, when looking at the results of the mPCG on posture correction during habitual sitting, significant reductions can be found in the lumbar imbalance in the sagittal plane at most of the evaluated points of time (i.e., 0 M, 3 M, and 9 M). This shows that the

mPCG is very good at immediately reducing the lumbar imbalance in the sagittal plane during sitting. Also, significant reductions were found in the thoracic imbalance in the sagittal plane for half of the evaluated points of time (i.e., 0 M and 3 M) and when 0 M and 9 M are compared both “without the girdle” and “with the girdle”. This shows that the mPCG can well reduce the thoracic imbalance in the sagittal plane both immediately and in the long-term.

### 5.7 Effects on Proprioception deficit (Vicon Nexus 3D motion capture system)

Studies have indicated that there might be a potential aetiological association between AIS and proprioception (Blecher et al., 2017 & Chesler et al., 2016). The proprioception deficit tests in this study include the (i) NRZ, (ii) EFY, (iii) KEY and (vi) STP tests. The tests were performed both “without the girdle” and “with the girdle” for comparison and evaluation purposes, so as to investigate the consequential influence of the treatment with the mPCG on proprioception deficit. Table 5.11 lists the standards extracted from Lau et al. (2022) to determine the repositioning error which would be used for the comparison in this study.

Table 5.11 Standards extracted from Lau et al. (2022) to determine repositioning error

Tests	Grouping	Value for determining repositioning error
<b>Neck Rotation (NRZ)</b>	AIS with left or right curvature and AIS with kyphosis or lordosis	4.5°
<b>Elbow Flexion (EFY)</b>	Better side and poor side on repositioning performance	3.2° (AIS: 3.61 ± 1.65; Control: 3.21 ± 1.68)
<b>Knee Extension (KEY)</b>	Better side and poor side on repositioning performance	4.4° (AIS: 5.1 ± 2.5; Control: 2.6 ± 1.8)
<b>Unterberger Stepping (STP) - displacement</b>	AIS and control	41.8° (AIS: 41.8 ± 25.6; Control: 31.2 ± 22.7)
<b>Unterberger Stepping (STP) - rotation</b>	AIS and control	25° (AIS: 24.5 ± 21.9; Control: 13.1 ± 14.5)

Referring to the standards listed in Table 5.11, the calculated results for the NRZ test larger than 4.5°, EFY test larger than 3.2°, KEY test larger than 4.4° and STP tests displacement and rotation larger than 41.8° and 25°, respectively, would be considered as repositioning error respectively.

The results of the 4 mentioned proprioception tests at 0 M, 3 M, 6 M and 9 M both “without the girdle” and “with the girdle” are presented in the following. Originally, there were 10 subjects but since Subjects 3 and 4 withdrew, their data are only used in the 0 M tests. Details of the collected data are available in Appendix X. The data collected were analysed by using SPSS with a paired t-test for non-parametric Wilcoxon rank-sum test. The level of significance was set at  $p=0.05$ .

### 5.7.1 Results of NRZ test

#### NRZ (concave side)

The results of the NRZ test for the concave side are shown in Figure 5.15 (details of the collected data are provided in Appendix X). According to the results, no significant differences are found for the tested items at 0 M, 3 M 6 M and 9 M. In other words, no immediate and significant reduction can be found for proprioception deficit (NRZ) at all points of time. Also, no long-term significant reduction can be found for proprioception deficit (NRZ) after the completion of the 9-month wear trial regardless whether girdle is donned or doffed.

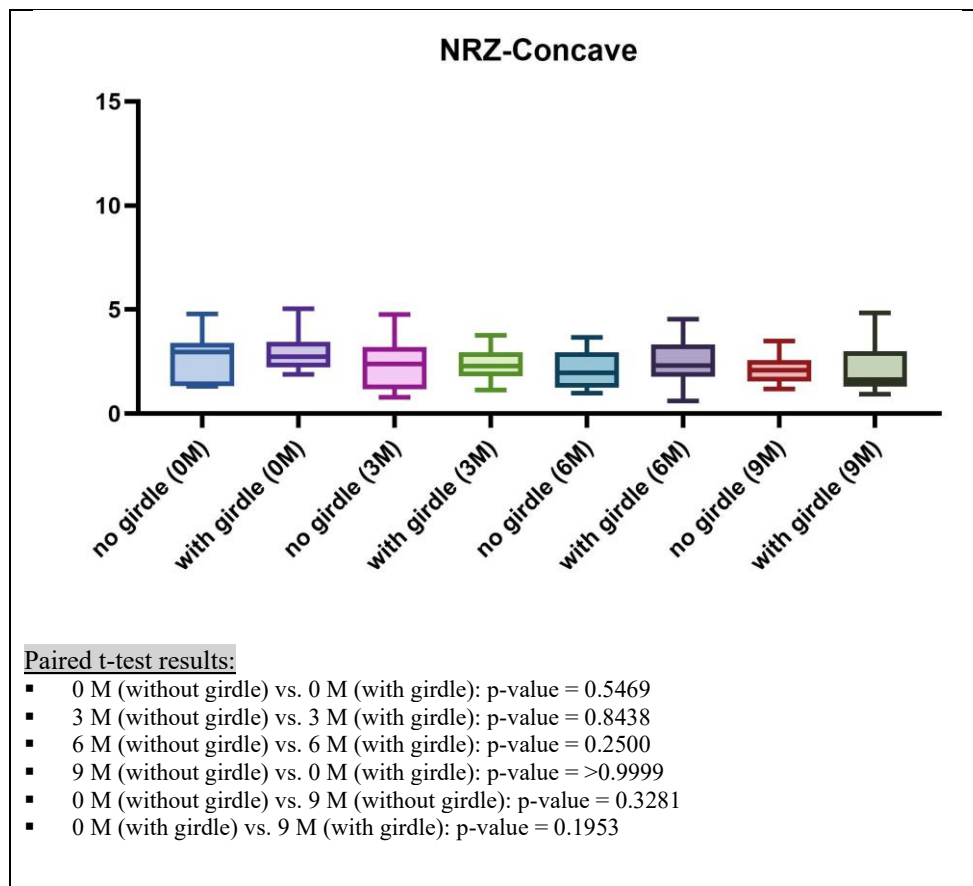


Figure 5.15 Results of NRZ test (concave side)

### NRZ (convex side)

The results of the NRZ test for the convex side are shown in Figure 5.16 (details of the collected data are provided in Appendix X). According to the results, no significant differences are found for the tested items at 0 M, 3 M 6 M and 9 M. In other words, no immediate and significant reduction can be found for proprioception deficit (neck rotation) at all points of time. Also, no long-term significant reduction can be found for proprioception deficit (NRZ) after the completion of the 9-month wear trial when the girdle is donned. However, a significant reduction was found for proprioception deficit (NRZ) after the completion of the 9 month-wear trial when the girdle is doffed ( $p=0.0931$ ).

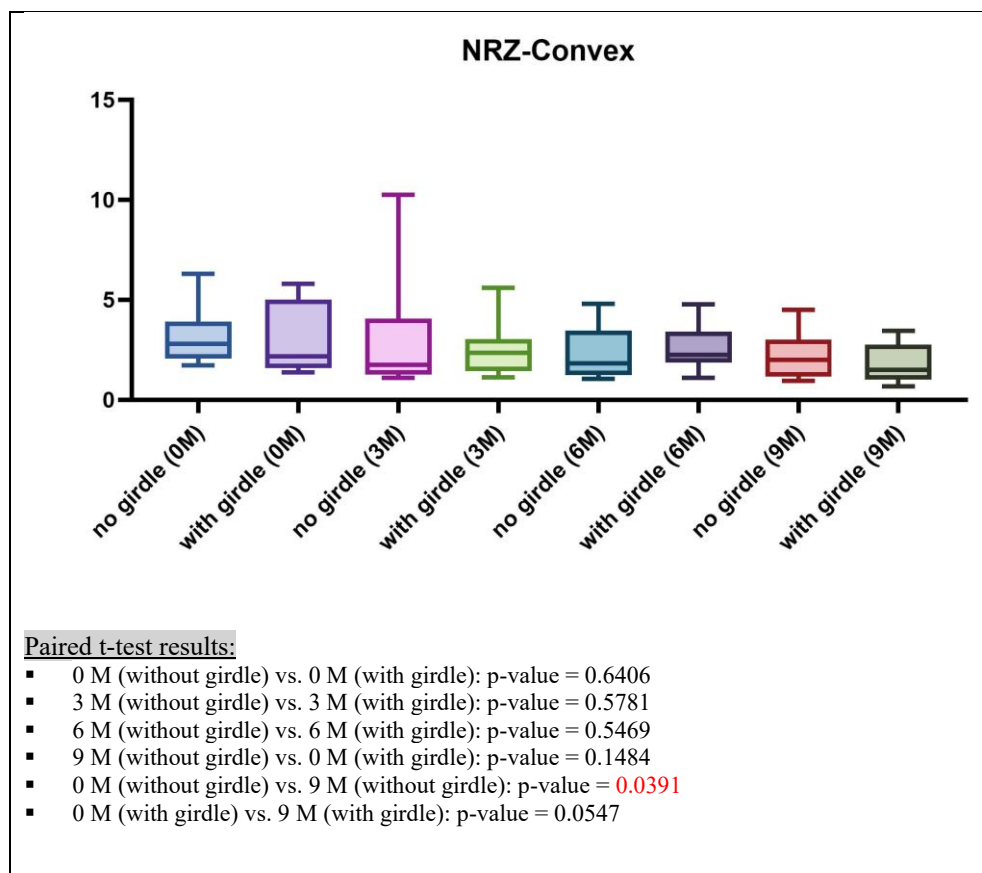


Figure 5.16 Results of NRZ test (convex side)

### 5.7.2 Results of EFY test

#### EFY (dominant side)

The results of the EFY test for the dominant side are shown in Figure 5.17 (details of the collected data are provided in Appendix X). According to the results, no significant differences are found for the tested items at 0 M, 3 M and 6 M. In other words, no immediate and significant reduction can be found for proprioception deficit (EFY) at 0 M, 3 M and 6 M. Also, no long-

term significant reduction can be found for proprioception deficit (EFY) after the completion of the 9 month-wear trial regardless whether the girdle is donned or doffed. However, a significant reduction can be found for proprioception deficit (EFY) at 9 M ( $p=0.0391$ ), which indicates there is an immediate and significant reduction in proprioception deficit (EFY) at this time point.

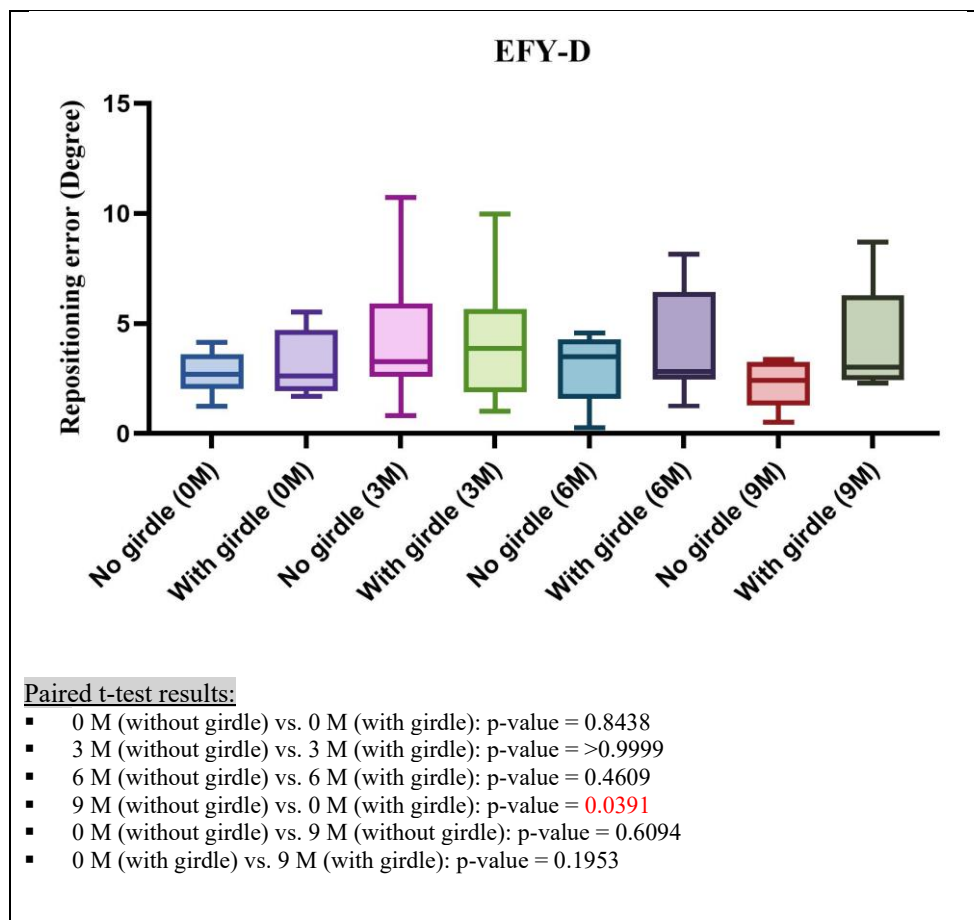


Figure 5.17 Results of EFY test (dominant side)

### **EFY (non-dominant side)**

The results of the EFY test for the non-dominant side are shown in Figure 5.18 (details of the collected data are provided in Appendix X). According to the results, no significant differences are found for the tested items at 0 M, 3 M, 6 M and 9 M. In other words, no immediate and significant reduction can be found for proprioception deficit (EFY) at 0 M, 3 M, 6 M and 9 M. Also, no long-term significant reduction can be found for proprioception deficit (EFY) after the completion of the 9 month-wear trial regardless whether the girdle is donned or doffed.

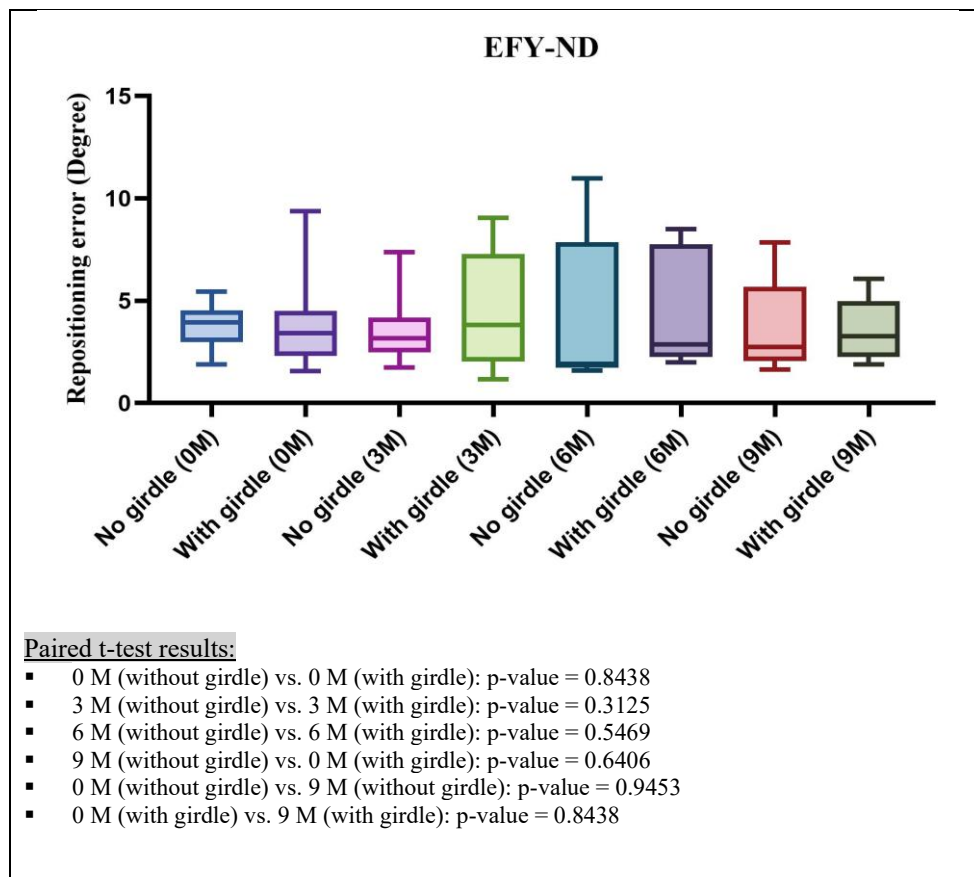


Figure 5.18 Results of EFY test (non-dominant side)

### 5.7.3 Results of KEY test

#### KEY (dominant side)

The results of the KEY test for the dominant side are shown in Figure 5.19 (details of the collected data are provided in Appendix X). According to the results, no significant differences are found for the tested items at 0 M, 3 M, 6 M and 9 M. In other words, no immediate and significant reduction can be found for proprioception deficit (KEY) at 0 M, 3 M, 6 M and 9 M. Also, no long-term significant reduction can be found for proprioception deficit (KEY) after the completion of the 9 month-wear trial regardless whether the girdle is donned or doffed.

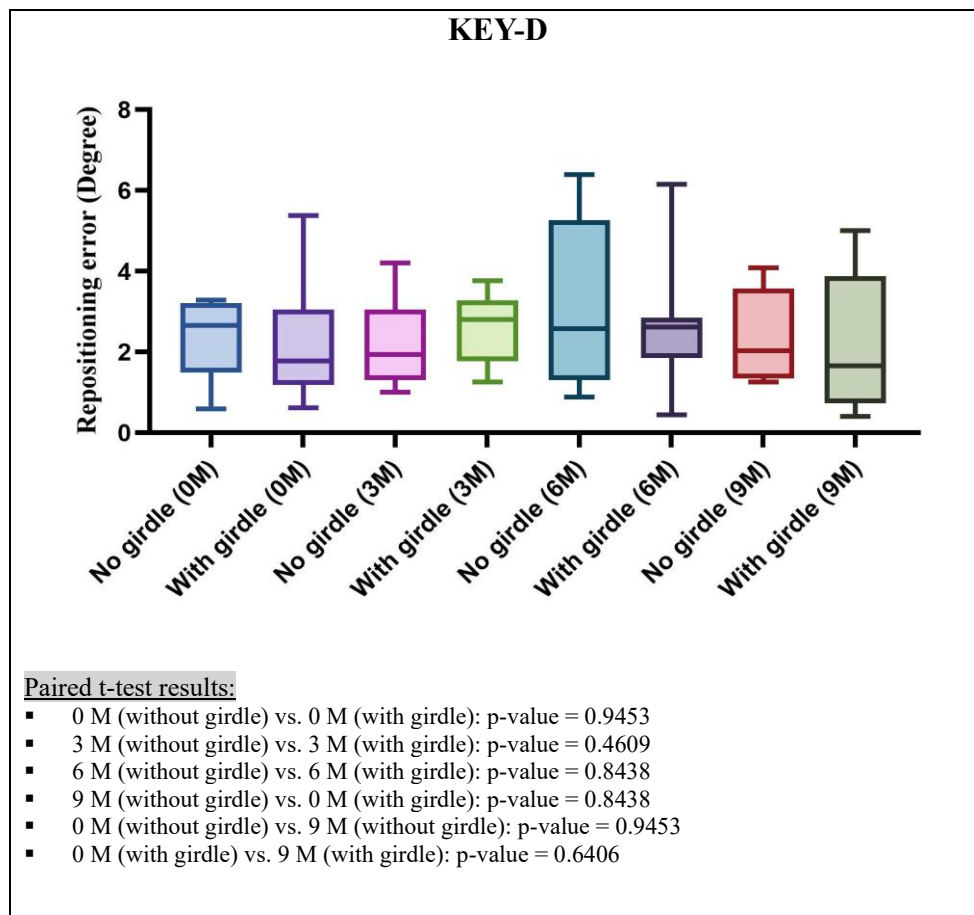


Figure 5.19 Results of KEY test (dominant side)

**KEY (non-dominant side)**

The results of the KEY test for the non-dominant side are shown in Figure 5.20 (details of the collected data are provided in Appendix X). According to the results, no significant differences are found for the tested items at 0 M, 3 M, 6 M and 9 M. In other words, no immediate and significant reduction can be found for proprioception deficit (KEY) at 0 M, 3 M, 6 M and 9 M. Also, no long-term significant reduction can be found for proprioception deficit (KEY) after the completion of the 9 month-wear trial regardless whether the girdle is donned or doffed.

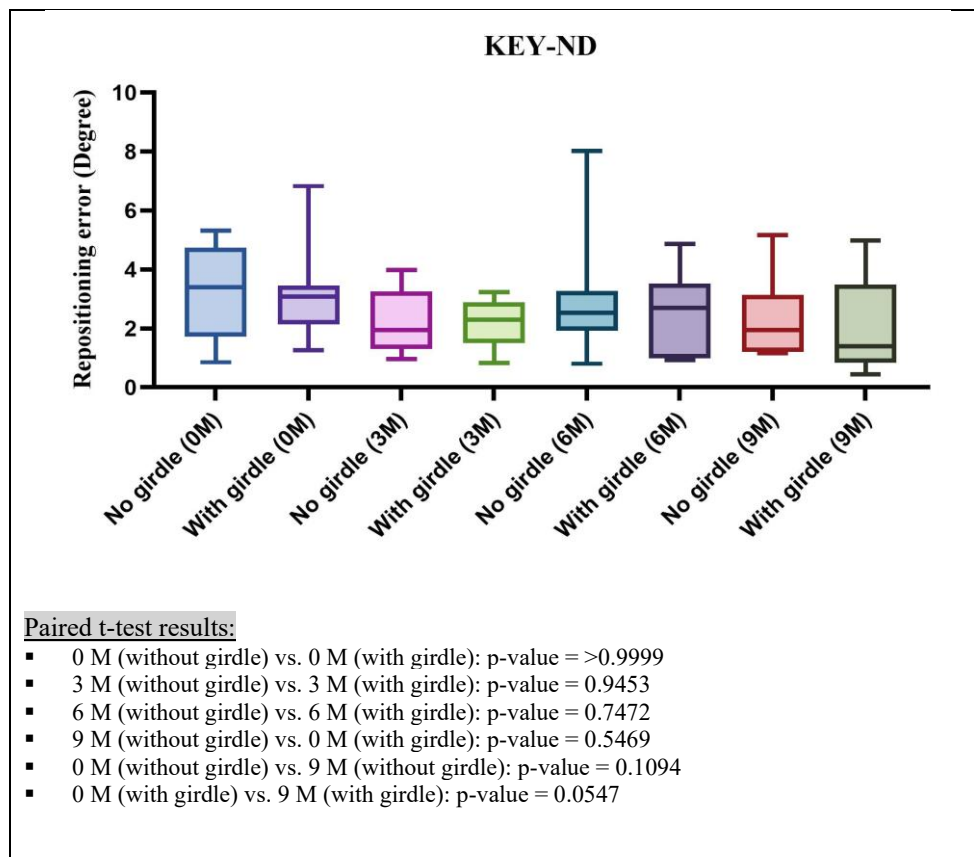


Figure 5.20 Results of KEY test (non-dominant side)

#### 5.7.4 Results of STP test

##### STP (displacement)

The results of the STP test for displacement are shown in Figure 5.21 (details of the collected data are provided in Appendix X). According to the results, no significant differences are found for the tested items at 0 M, 3 M, 6 M and 9 M. In other words, no immediate and significant reduction can be found for proprioception deficit (STP displacement) at 0 M, 3 M, 6 M and 9 M. Also, no long-term significant reduction can be found for proprioception deficit (STP displacement) after the completion of the 9 month-wear trial when the girdle is donned. However, a significant reduction can be found for proprioception deficit (STP displace) after the completion of the 9 month-wear trial when the girdle is doffed (p=0.0469).

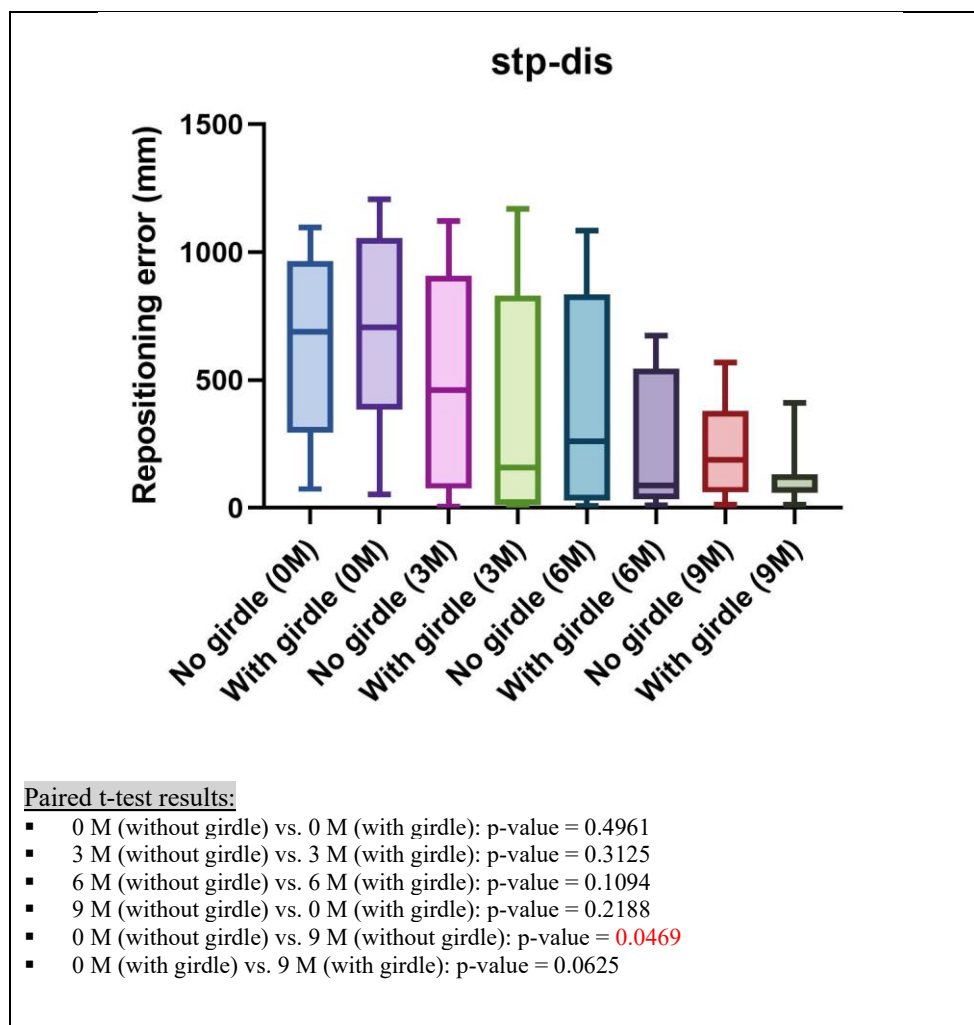


Figure 5.21 Results of STP test (displacement)

### **STP (rotation)**

The results of the STP test for rotation are shown in Figure 5.22 (details of the collected data are provided in Appendix X). According to the results, no significant differences are found for the tested items at 0 M, 3 M, 6 M and 9 M. In other words, no immediate and significant reduction can be found for proprioception deficit (STP rotation) at 0 M, 3 M, 6 M and 9 M. Also, no long-term significant reduction can be found for proprioception deficit (STP rotation) after the completion of the 9 month-wear trial regardless whether the girdle is donned or doffed.

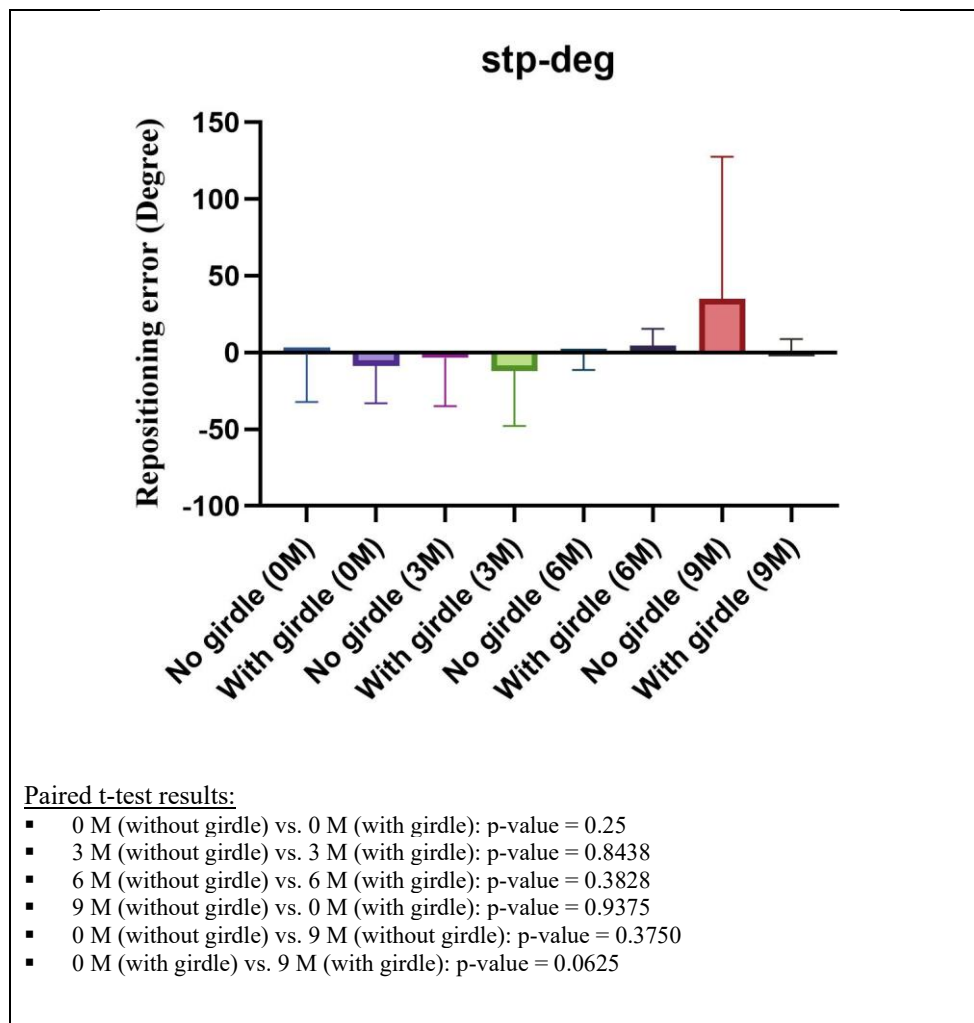


Figure 5.22 Results of STP test (rotation)

### 5.7.5 Discussion of effects on proprioception deficit

Significant improvements in the repositioning error were only found for a few of the tested items (i.e., NRZ - convex side at 0 M vs. 9 M “without the girdle” ( $p=0.0391$ ); EFY – dominant side at 9 M “without the girdle” vs. “with the girdle” ( $p=0.0391$ ); and STP – displacement at 0 M vs. 9 M “without the girdle” ( $p=0.0469$ ). This shows the 9 months of treatment with the mPCG in this study have limits in reducing the proprioception deficit.

Although AIS patients are more prone to proprioceptive deficiencies compared to non-AIS individuals, such as larger repositioning errors and a higher motion detection threshold, Lau et al., (2022) proposed that AIS is caused by, rather than a result of proprioceptive impairment. The level of proprioception dysfunction may not be associated with the severity of the subsequent curvature of the spine if proprioceptive deficiency is the reason for AIS (Lau et al., 2022). In view of this, the reason for the limited effects of the 9 month-wear trial with the

mPCG in reducing proprioception deficits might be explained through this rationale. In other words, even though the spinal curvature is under control or reduced by using the mPCG, the results might not directly enhance the proprioception of the user.

## **5.8 Quality-of-life evaluation**

Three questionnaires including the SRS-22 questionnaire, BrQ, and BSSQ-Brace were given to the recruited subjects to investigate the treatment outcome in terms of their QoL. Since Subjects 3 and 4 withdrew before the evaluation session at 3 M, the questionnaire results were collected from all 10 subjects at 0 M, but only 8 subjects at 3 M, 6 M and 9 M for the analysis.

### **5.8.1 Results of SRS-22 questionnaire**

Haheer et al. (1999) proposed that the SRS-22 questionnaire can be used to evaluate the health-related quality-of-life (HRQoL) of AIS patients. The overall score is between 22 and 110, with a higher score indicating higher quality of life. According to the results, the total overall score at 0 M pre-intervention is 98.5 out of 110, while the total overall score at 9 M is 99 out of 110. These scores are similar to that in Wong (2021) (mean=95, out of a total of 110) which means that the QoL of the recruited subjects are at a satisfactory level and the treatment with the mPCG has only had a minor impact on their daily life.

Figure 5.23 shows the mean scores for the SRS-22 questionnaire in this study. The mean scores for the “pain” and “function/activity” domains gradually increase throughout the 9 month-wear trial (i.e., from 4.4 at 0 M to 4.78 at 9 M for “pain”, from 4.3 at 0 M to 4.88 at 9 M for “function/activity”), which clearly shows increase in satisfaction in these two areas after undergoing treatment with the mPCG. For the “mental health” domain, the mean score is slightly reduced from 4.42 at 0 M to 4.3 and 4.25 at 3 M and 6 M respectively, but eventually increases to 4.48 at 9 M. For the “treatment satisfaction” domain, the mean score slightly declines from 4.45 at 0 M to 4.31 and 4.13 at 3 M and 6 M respectively, but finally increases to 4.25 at 9 M. The results for “mental health” and “treatment satisfaction” show that the subjects might need more time to become accustomed to the mPCG and feel its effectiveness. For the “self-perceived image” domain, the mean score is reduced from 4.8 at 0 M to 4.08 at 9 M, which indicates that the subjects are still concerned about what other people think about them. As the mPCG is still in its experimental stage and has not yet been commercially released, other people might be curious about what the subjects are wearing, which might make them

feel uncomfortable.

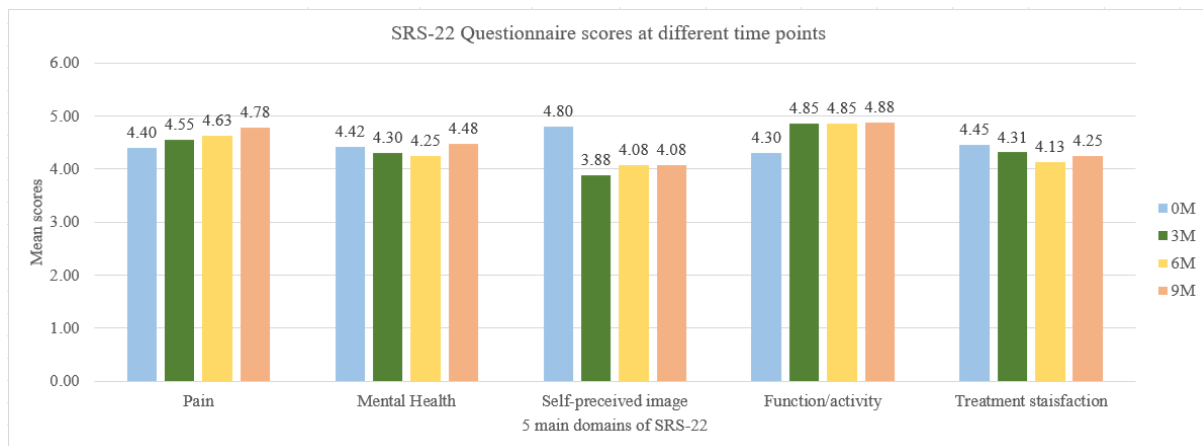


Figure 5.23 Mean scores of SRS-22 questionnaire

### 5.8.2 Results of BrQ

The BrQ is designed to measure the clinical effectiveness of managing AIS patients who wear the mPCG. The questionnaire has eight domains with 34 questions in each area which include: (i) general health perception, (ii) physical functioning, (iii) emotional functioning, (iv) self-esteem and aesthetics, (v) vitality, (vi) school activities, (vii) physical pain, and (viii) social functioning.

All of the subjects were required to complete the BrQ at 0 M (after 2 h), 3 M, 6 M and 9 M. According to the results, the overall mean score is 84.94 (S.D.=5.22) at 0 M and 89.41 (S.D.=8.14) at 9 M. Wong (2021) found that the anisotropic textile brace (ATB), a semi rigid corrective brace for AIS patients, is given an overall BrQ mean score of 83.3 after the preliminary wear trial study. The overall mean score of the BrQ in this study for the mPCG is therefore higher. This higher score shows that the users find that the mPCG does not affect their QoL as much as the ATB.

Figure 5.24 shows the average SRS scores of each domain of the BrQ at different points of time with the mPCG. The “self-esteem and aesthetics” domain has a comparatively low score, mean=3.75 (S.D.=0.39). The score then fluctuates; the score increases to 4.5 at 3 M but declines at 6 M and then increases again at 9 M. This fluctuation might be due to external factors, such as the weather. When the subjects use the mPCG during the summer, they might have a poor wear experience than in other seasons due to the high temperature and humidity. Also, the girdle

cannot be completely obscured under clothing during the summer, which might also affect their self-esteem and aesthetics. Nevertheless, the BrQ also show positive results for the remaining domains, including “general health perception”, “physical functioning”, “vitality”, “school activities”, “physical pain” and social functioning. This might show that the mPCG in general improves QoL after 9 M.

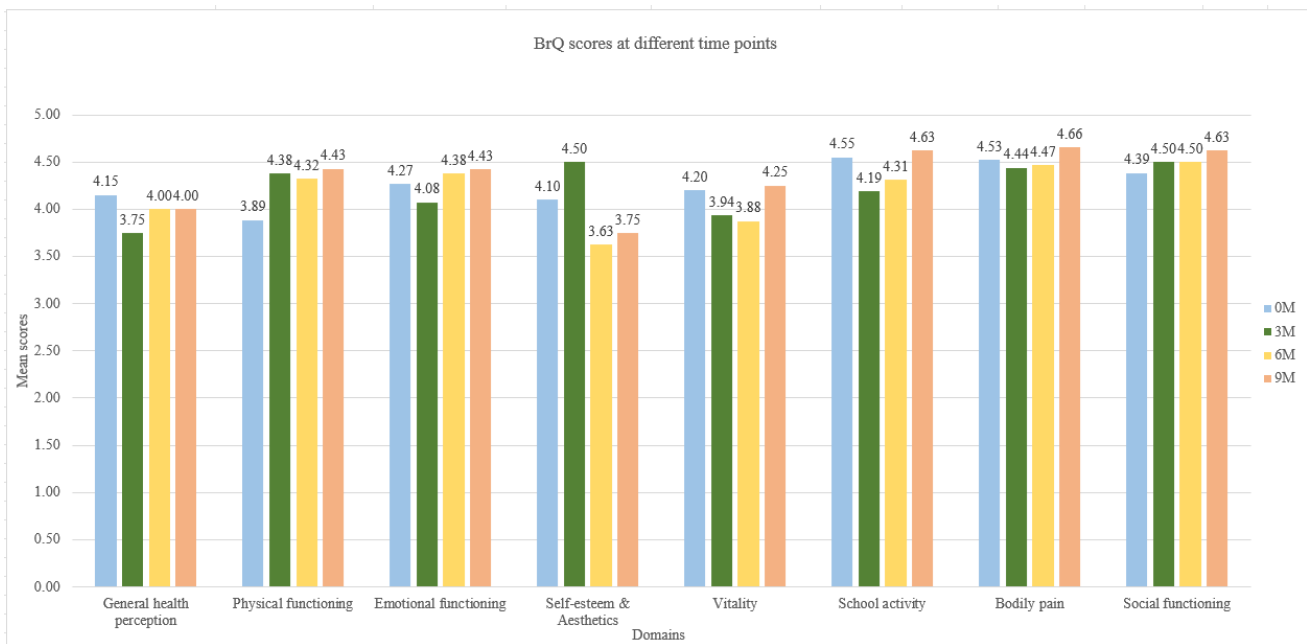


Figure 5.24 Results (mean scores) of BrQ

### 5.8.3 Results of BSSQ-Brace

According to Botens-Helmus et al. (2006), the BSSQ-Brace is used to assess the coping strategies and perceived impairment while patients are wearing an orthosis. The total score ranges from 0 to 24. The stress levels based on final score are classified as follows: 0-8 (high stress), 9-16 (medium stress), and 17-24 (little stress) (Botens-Helmus et al., 2006).

All of the subjects completed the Chinese version of BSSQ-Brace at 0 M (after 2 h), 3 M, 6 M and 9 M. Since Subjects 3 and 4 withdrew before 3 M, they only completed the questionnaire at 0 M.

Figure 5.25 shows the results of the BSSQ-Brace for this study. At 0 M, 4 of the 10 subjects indicated they were experiencing moderate stress (score between 9-16), while the rest indicated that their stress is minimal (score between 17-24). The mean score of the BSSQ-Brace at 0 M

is 18.7. In comparing this mean score to that for the Cheneau brace (i.e., 11.07) in Weiss et al. (2007), the mPCG shows a better performance and causes less stress to the wearer/AIS patient.

After 9 M, 5 of the 8 subjects indicated a low stress level, while the rest have moderate stress levels. The mean score of the BSSQ-Brace at 9 M is 18.5. There is a not a large difference when compared to 0 M (18.7). This can be interpreted to mean that wearing the mPCG for a longer period of time does not significantly affect stress levels. The reason might be because the subjects have already become accustomed to the girdle and adapted to its feeling and tightness, so that they feel less burdened and less inconvenienced.

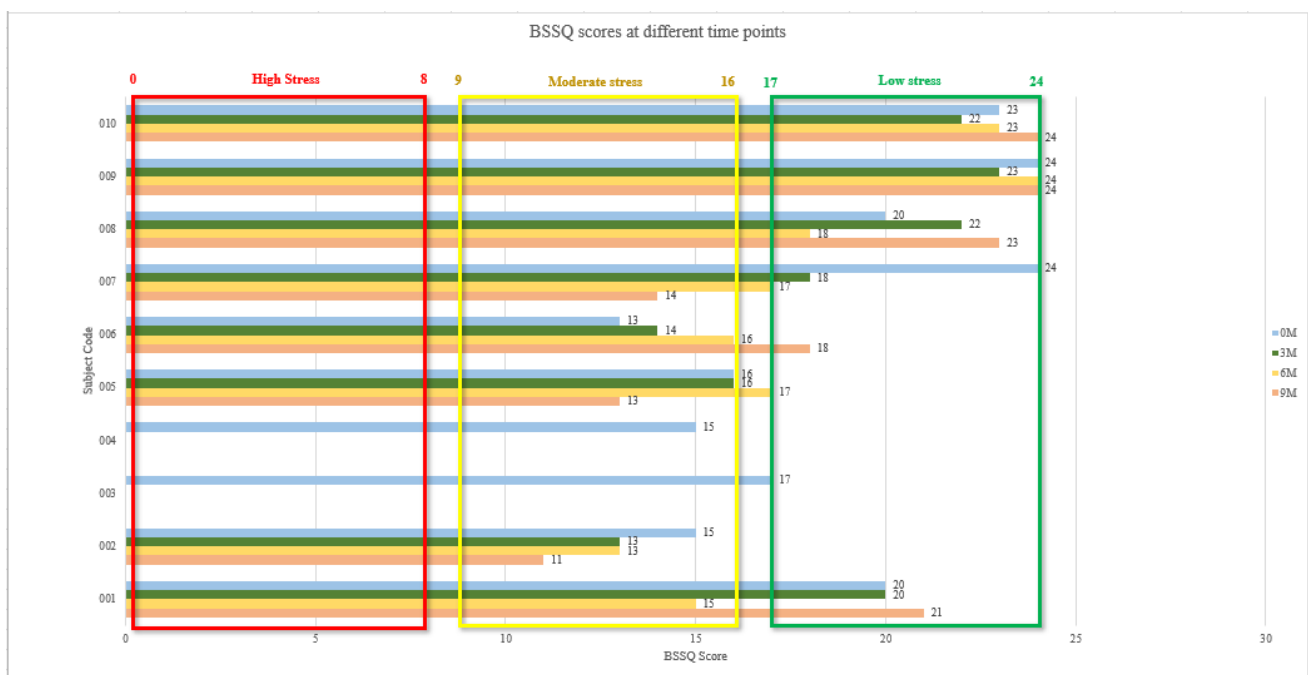


Figure 5.25 Results of BSSQ-Brace

### 5.9 Compliance and thermal comfort monitoring

In order to understand compliance with the mPCG during the 9 month-wear trial, temperature loggers (Hygrochron™ iButton sensors; 16 mm in diameter) were inserted into the pocket lining of the mPCGs to collect information on their wear practices; see Table 5.12, and Figure 5.26. The compliance rate is regarded as 100% if the subjects donned the girdle for 8 hours each day. Since Subjects 3 and 4 withdrew, only the results for 8 of the subjects are presented in the following.

Table 5.12 Wear practices and compliance rate up to 9 M

Subject	Time (mean hours per day)									Mean	SD	Compliance (%)
	1 m	2 m	3 m	4 m	5 m	6 m	7m	8m	9m			
1	5.3	4.1	3.4	5.1	4.6	5.6	3.9	4.9	5	4.66	0.72	58.2
2	6.6	7.1	6.3	7.1	6.9	7.3	8	7.1	7	7.04	0.42	88.1
5	7.3	7.6	7.1	7.2	6.5	7	6.3	7.1	7	7.01	0.40	87.6
6	7.9	8.1	7.7	7.2	7.3	7.9	6.9	7.1	7.2	7.48	0.43	93.5
7	8.5	8	8.2	7.8	8.2	7.9	7.8	7.9	7.7	8.00	0.25	100.0
8	9.4	10.3	10.9	11.2	8.7	10.3	9.7	10.1	10.3	10.10	0.76	126.3
9	8.2	7.8	7.5	8.1	8.3	8.4	7.9	8.1	8	8.03	0.27	100.4
10	8.1	8.3	8.9	9.2	8.5	8.7	8.3	8.2	8.1	8.48	0.38	106.0
<b>Mean</b>	7.66	7.66	7.50	7.86	7.38	7.89	7.35	7.56	7.54	7.60		95 (SD= 19.31)
<b>SD</b>	1.26	1.72	2.15	1.78	1.38	1.37	1.71	1.46	1.48			
<b>Compliance (%)</b>	95.78	95.78	93.75	98.28	92.19	98.59	91.88	94.53	94.22	95 (SD= 2.37)		

\*Notes: Subjects 3 and 4 withdrew in the early stages of the wear trial.

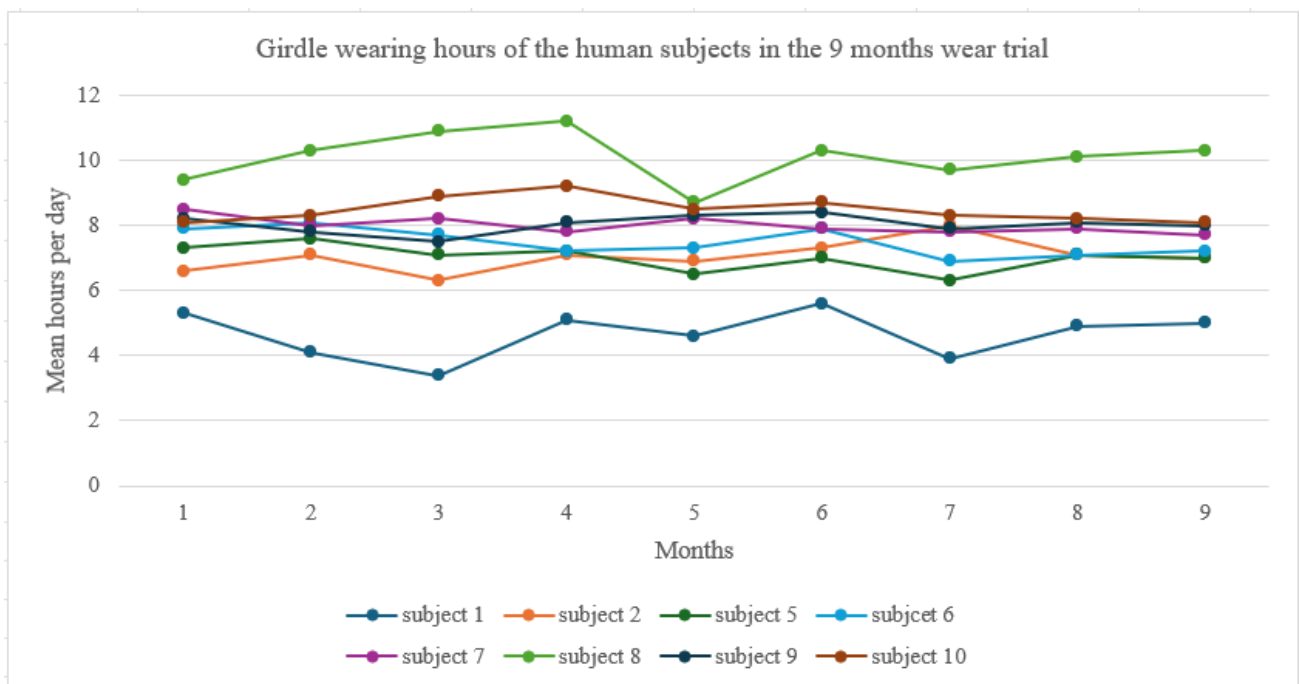


Figure 5.26 Hours mPCG worn throughout 9 month-wear trial

It can be observed that the average rate of compliance with the treatment among the 8 subjects who completed the entire wear trial is 95% (S.D.= 19.31), which is equal to 7.6 hours each day.

That is, the average rate of compliance of these 8 subjects during the 9 months is 95% (S.D. = 2.37). According to Liu (2015), the average rate of compliance with the original PCG among the 9 subjects who completed the entire 6-month wear trial is 93.25% (S.D. = 21.37). That is, the average rate of compliance of the subjects during the 6-month wear trial is 91.33% (S.D. = 7.8). A higher rate of compliance is found in this study which might be due to the refinements to the girdle design and enhancement of the fabric properties/performance.

Specifically, no large difference can be observed for the mean number of hours that the mPCG is worn each day during the 9 months, which range from 7.35 (91.88%) to 7.86 (98.28%) hours each day. However, when the rate of compliance is compared between the subjects, a large difference is observed. For instance, Subject 1 only has a 58.2% mean rate of compliance which is low, while Subject 8 has a 126.3% mean rate of compliance which is much higher than expected/necessary. The difference in compliance between the subjects might be due to their perseverance. According to Zaina et al. (2009) and Hasler et al. (2010), perseverance during treatment might be influenced by personality, psychological aesthetics and understanding of scoliosis. Compliance to treatment might affect its success and effects. Therefore, in this study, the high compliance rate of some of the subjects up to 9 M might be a factor that resulted in a better corrective effect of their spinal curvature and imbalanced posture. Taking the effects on controlling the progression of the spinal curvature after undergoing the 9 month-wear trial (with the mPCG) as an example, Subjects 7, 8, 9 and 10 show a more apparent reduction in their spinal curvature after using the mPCG, likely due to their commitment and high compliance with the treatment. They all have more than a 5° reduction (Table 5.8) and at the same time, all have 100% or higher compliance with the treatment (Table 5.12). Therefore, the suggested time for wearing the mPCG each day (i.e., 8 hours) should be set as the minimum girdling time each day.

Apart from the rate of compliance, the temperature data collected by the temperature loggers were also used to monitor thermal comfort. The results showed that when the mPCG was donned, the recorded temperature ranged from 30°C to 36°C. Arens and Zhang (2006) stated that a comfortable skin temperature for the back is 33.8°C to 35.8°C. Donning clothing increases the thermal resistance of the body, which may lead to an increase in skin temperature (Liu et al., 2011). In this study, the highest temperature collected by the temperature loggers is 36°C, which is 0.2 °C higher than the skin temperature in Arens and Zhang (2006). Since summer in Hong Kong is very hot and humid, thus, the increased temperature after putting on

the mPCG was seen as acceptable. Besides, subjectivity should also be considered when assessing the thermal comfort after donning clothing (Islam et al., 2023). According to the comments of the subjects in this study, although wearing the girdle during the summer feels a bit hot, it is still acceptable, and none of them felt too warm.

### **5.10 Chapter summary**

This chapter has presented the results of the subject recruitment for the study, and the evaluation results of the wear trial experiments. Ten females who are between 10 and 13 years old and diagnosed with early scoliosis (i.e., Cobb angle between  $10^{\circ}$ - $20^{\circ}$ ) are recruited from the school screening programme after a radiographic examination. They and their parents/guardians provided signed informed consent. Seven of them are diagnosed with an S curve while 3 of them with a C curve. Each are prescribed an mPCG in the appropriate size with the corresponding EVA foam padding inserted for the wear trial. Regarding the interface pressure measurement, the mean measurements (corrective points of pressure) range from 4.625 kPa to 8.875 kPa. The highest mean interface pressure measurement is generally found in the mid-level of the spine. Compared with the results from the original PCG, the highest mean pressure value of the mPCG is 3.656 kPa (70%) higher than that of the original design. The higher corrective force might be induced by the modifications made to the girdle.

The wear trial evaluation tests are conducted at 0 M, 3 M, 6 M and 9 M. Subjects 3 and 4 withdrew before the evaluation session at 3 M. Therefore, only the results of the remaining 8 subjects are presented for 3 M, 6 M and 9 M. In terms of the effectiveness in controlling the progression of the spinal curvature, 6 of the 10 subjects show a significant and immediate reduction of their spinal curvature (from  $-5^{\circ}$  to  $-11^{\circ}$ ) after donning the mPCG for 2 hours, while 4 of the 8 subjects show an apparent long-term reduction after 9 M even if the girdle is doffed (reduction ranges from  $-5.2^{\circ}$  to  $-8^{\circ}$ ). As for the result in improving posture imbalance, significant improvements are found for many of the tested items. For instance, lumbar asymmetry in the sagittal plane during habitual standing, asymmetry of the acromion in the frontal plane during habitual standing, pelvis asymmetry in the frontal plane during habitual standing, thoracic asymmetry in the sagittal plane during standing, thoracic asymmetry in the sagittal plane during sitting and lumbar asymmetry in the sagittal plane during sitting are all reduced. However, no significant improvement can be found for the tested areas in the horizontal plane (i.e., acromion, scapula and pelvis rotation). This shows that the corrective

forces exerted by the mPCG work better to reduce imbalances in the posture in the frontal and sagittal planes, rather than the horizontal plane. As for the results of the proprioception tests, although significant effects can be found for a few of the tested items (i.e., NRZ - convex side at 0 M vs. 9 M, EFY – dominant side at 9 M, and STP – displacement at 0 M vs. 9 M), no apparent effect can be found for most of the tested items. This shows that the treatment with the mPCG does not help to reduce proprioception deficits.

Apart from carrying out the tests mentioned above to investigate the effectiveness of the mPCG in controlling the progression of the spinal curvature, correcting posture and reducing proprioception deficit, evaluation of QoL is also done by conducting questionnaire surveys (i.e., SRS-22 questionnaire, BrQ and BSSQ-Brace). The result of SRS-22 indicates that the QoL of the subjects are satisfactory and treatment with the mPCG only has a minor impact on their daily life (e.g. self-perceived image). The result of the BrQ shows that generally, the subjects are doing well. However, in terms of their “self-esteem and aesthetics”, they have a comparatively low score. Finally, the results of BSSQ-Brace show that 4 of the subjects experience moderate stress while the rest experience little stress while using the mPCG. The results of the 3 questionnaire surveys indicate the subjects might need more time to become accustomed to the mPCG. Since the mPCG has not yet been commercially released, others might be curious about the orthosis, which might make the subjects feel uncomfortable. Although the subjects indicated concerns about their “self-perceived image” and “stress level”, the satisfaction with the mPCG in this study is comparable or even higher than that with other orthoses in other studies (Wong, 2021; Weiss et al., 2007).

Finally, according to the data collected by the temperature loggers inserted in the mPCG, it is found that the average rate of compliance with the treatment is 95%, which is higher than that with the original PCG in Liu (2015). The increase of compliance with the treatment might be due to the refinement of the design and replacement of fabric materials, which enhance the aesthetics and function (i.e., wear comfort level, convenience of use, corrective effectiveness). Besides, it is found that the subjects who show a more apparent long-term correction of their spinal curvature have higher compliance. This means that the length of the girdling time each day might affect the effectiveness of the treatment. Furthermore, the data collected by the temperature loggers also show that the level of thermal comfort is acceptable, with no unwell feelings reported by the subjects during the wear trial.

# **CHAPTER 6 – FINITE ELEMENT MODELLING AND DEVELOPMENT OF INTELLIGENT SYSTEM FOR GIRDLE PRESCRIPTION**

## **6.1 Introduction**

FE analysis is a widely used numerical method for solving engineering and physics problems. The method has been increasingly applied to other disciplines, such as biomechanics, to optimise brace designs and simulate the effects of scoliosis braces. In this chapter, a biomechanical FE model of the mPCG for treating AIS is presented. Also, by taking advantage of decision trees and a trained neural network (NN) model, the target patients who are suitable for treatment with the mPCG can be easily identified, while the girdle prescription process based on the different spinal conditions and needs of the patients is facilitated and streamlined. The development of the decision tree and trained NN model in this study is also presented in this chapter. 3 M, 6 M and 9 M for the analysis.

## **6.2 Finite element modelling**

The FE modelling in this study aims to simulate and predict the impact of the mPCG when it is donned. The model combines a numerical stress analysis with thoracic body shape, skeletal structure, and the girdle, as well as the mechanical properties of the tissues and the girdle design. By replicating the wear procedure of the mPCG, the pressure distribution on the skeletal model and the displacement of each vertebral body can be calculated. The modelling can also assess the degree of spinal deformity, which is characterised by the Cobb angle. By modifying the design attributes of the PCG, the efficiency of spinal adjustment while using the mPCG and the pressure distribution on the skeletal model can be obtained. More importantly, this biomechanical model which does not expose subjects to the risk of radiation allows for the investigation of the effectiveness of the mPCG and optimise its design without conducting human wear trials.

### **6.2.1 Construction of finite element model**

A 3D FE model has been developed in this study which consists of the upper body, skeleton, and mPCG. Geometric models of these components were constructed to build the FE model. The structure was then discretised into smaller elements by using a process called meshing.

Next, the boundary conditions were defined to simulate the wearing of the girdle on the body. Finally, a numerical simulation of the girdle being worn on the torso was constructed, and the results were validated against experimental data to ensure the reliability and accuracy of the FE model.

### 6.2.1.1 Geometric model

The data were obtained from a 13-year-old girl with early scoliosis (Subject 1 in this study). The participant had a double scoliotic curvature, with Cobb angles of 14.8° at the thoracic spine and 16.1° at the lumbar spine. Table 6.1 lists her profile details. Initially, the subject underwent a 3D body scan with the Anthroscan body scanning system (Human Solutions GmbH, Germany), to provide the point cloud model. Geomagic Design X (3D Systems, USA) was used to process the point cloud model by repairing the holes and filling in the gaps. The processed model was then meshed and converted into a polygon object, with further processing applied to repair the holes and fill in any missing gaps, reduce noise and ensure point consistency.

Table 6.1 Information of subject for FE model

Subject	Age	Weight (kg)	Height (cm)	BMI	Risser grade	0 M (Pre) Cobb angle	0 M (with girdle) Cobb angle
1	12	45.2	150	20	2	14.8° (T), 16.1° (L)	8° (T), 7° (L)

Spike flattening and hole filling were performed on the polygon object, which was then smoothed and minimised (Fok and Yip, 2021). As a result, contour lines were created on the surface of the object. The boundaries of the patch structure were then formed by using contour and boundary lines, and each patch was given an ordered u-v grid. Finally, a non-uniform rational B-spline (NURBS) surface was constructed on the surface of the object as a function of two parameters mapped to the surface in three dimensions. The geometric models (i.e., upper body, skeleton, and mPCG) used to build the FE model are shown in Figure 6.1. The geometric models of the upper body, skeletal structure (including bones and intervertebral tissues), and the mPCG were imported. The geometric model of the skeleton was built and aligned with the X-ray image, while that of the mPCG was created based on the geometric model of the torso.

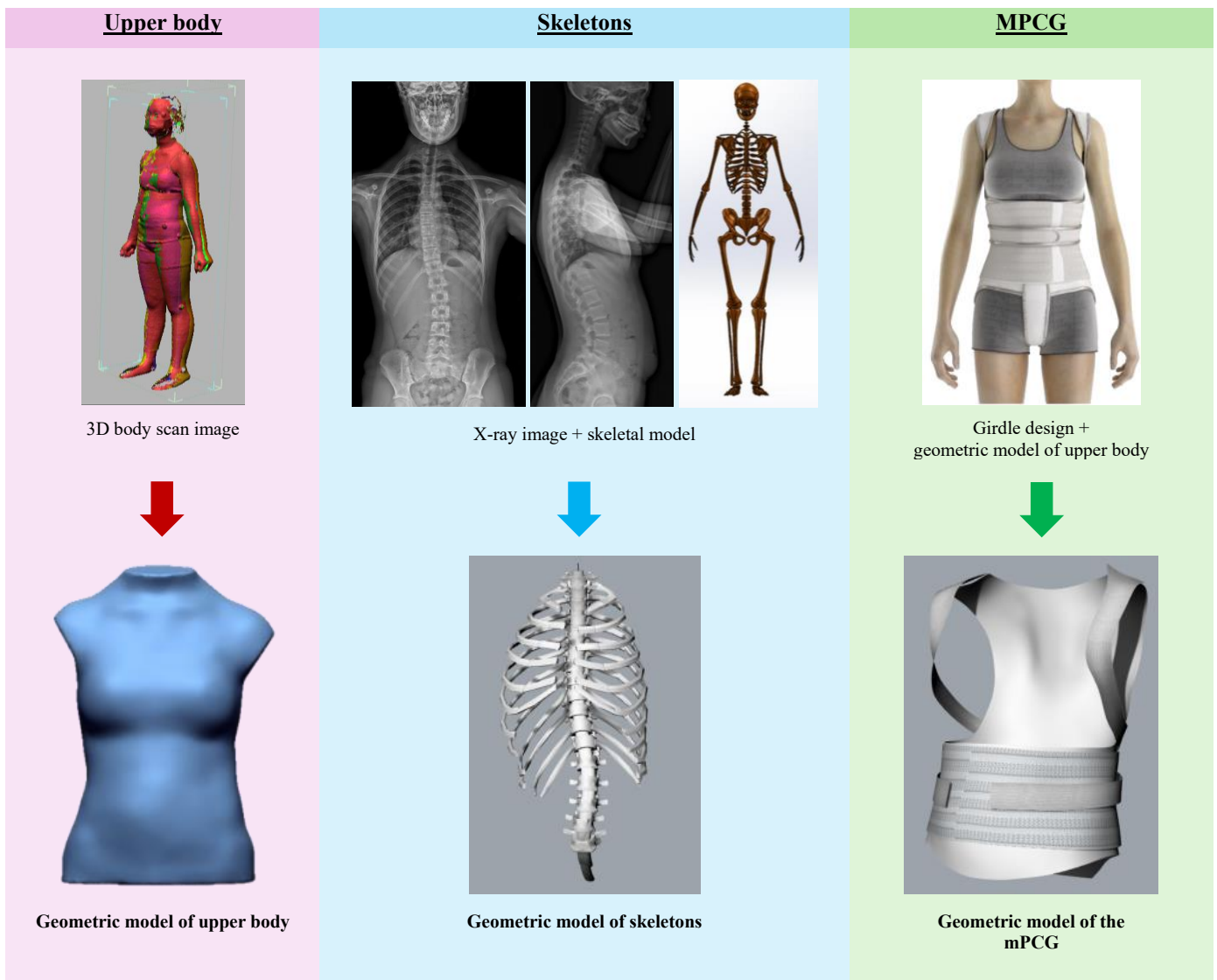


Figure 6.1 Geometric models to build FE model

### 6.2.1.2 Material properties

In earlier studies that focus on the mechanical properties of the upper body, bones, and intervertebral disc tissues, the Young's modulus ( $E$ ) and Poisson's ratio ( $\nu$ ) of the upper body tissues range from 0.01-1 MPa and 0.2-0.45 respectively, while those of the intervertebral disc tissues range from 1-3.59 MPa and 0.3-0.45 respectively, and those of the bone tissues range from 5000-12,000 MPa and 0.2-0.3 respectively (Lohfeld et al., 2012; Cheng et al., 2015; Périé et al., 2004). The stress-strain curve of the textile material of the mPCG was used to calculate the  $E$ , while the  $\nu$  was based on that of previous studies. The  $E$  and  $\nu$  were determined to be 0.59 MPa and 0.4, respectively (Zhou et al., 2010). Table 6.2 lists the material characteristics used to create the upper body, skeletal structure, and girdle models.

Table 6.2. Material properties for different components in FE model

Material properties	Young's modulus (mPa)	Poisson's ratio	Constitutive model
Body	0.05	0.45	Elastic plastic isotropic
Brace body	0.56	0.4	
Padding	300	0.35	
Vertebrae	6300	0.4	
Ribs	5500	0.2~0.4	

### 6.2.1.3 Defining type of mesh element

The mesh elements used for the upper body of the scoliosis patient (Figure 6.2) are 4-node linear quadratic tetrahedral elements with three degrees of freedom at each node (C3D10). The mesh size is at least 40 mm. A total of 36,976 elements made up the upper body, including 4345 for the intervertebral discs, 8827 for the bones, and 23,804 for the upper body. The mesh model of the upper body of the scoliosis patient is shown in Figure 6.3.

The mesh components of the mPCG model are similarly 4-node linear quadratic tetrahedral elements with three degrees of freedom at each node (C3D10, Figure 6.2). The smallest mesh size is 46 mm. The model of the girdle has a total of 2314 elements, including 2041 for the textile material and 273 for the hinge material. The mesh model of the mPCG is shown in Figure 6.3.

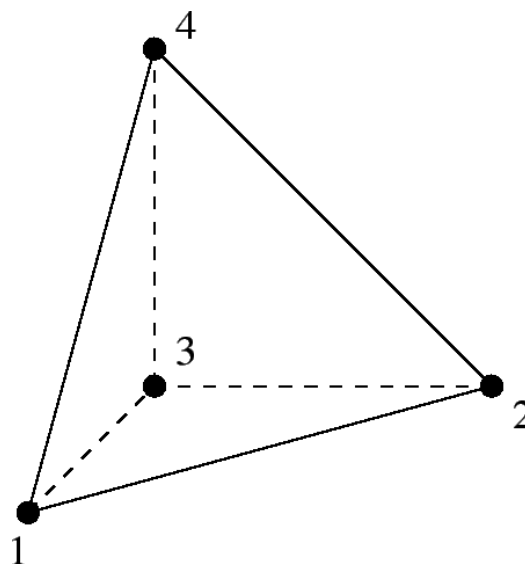


Figure 6.2. 4-node quadratic tetrahedral element

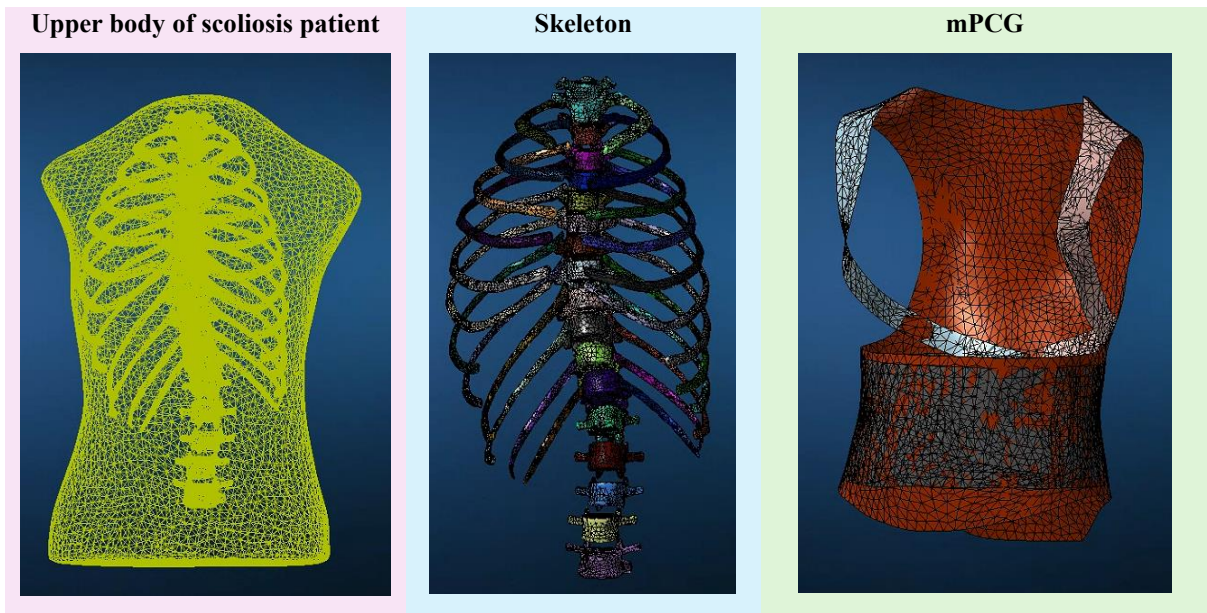


Figure 6.3 Mesh models in this study

#### 6.2.1.4 Boundary conditions

Different boundary conditions were defined on the workpiece to simulate the experimental condition (Figure 6.4). The top and bottom of the body were fixed to prevent any rotation or displacement. The vest part was donned onto the body without applying pressure while the belt was strapped onto the body with compression, and both the left and right shoulder straps were fastened. The inserted padding was defined with 15 mm displacement in the x-direction. The front closure of the mPCG was clasped together and defined with 10 mm displacement in the x-direction.

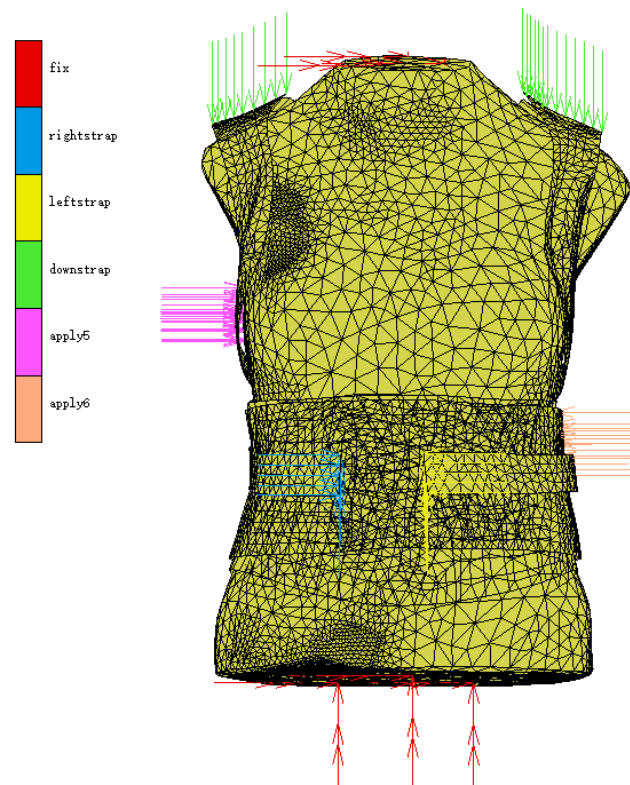


Figure 6.4 Boundary conditions on workpiece to simulate the condition

### 6.2.1.5 Analysis girdle-body interactions

The geometric models for the various parts were imported into FE software (MSC Marc, USA) to analyse the girdle-body interactions under different wear parameters. The model conducted a numerical stress analysis with the thoracic body shape, skeletal structure, girdle, and the mechanical properties of the tissues and the girdle wearing parameters. By simulating the process of wearing the mPCG, the pressure distribution on the skeletal model and the displacement of each vertebral body can be calculated. This analysis helps to evaluate the degree of spinal deformity, characterised by the Cobb angle. Modifications to the attributes of the girdle wearing parameters make it possible to improve the efficiency of spinal adjustment with the use of the mPCG and optimise the pressure distribution on the skeletal model. More importantly, the biomechanical model which does not pose any radiation risk to the user, allows the investigation of the effectiveness of the mPCG and optimisation of its design without conducting human wear trials.

### 6.2.1.6 Effect of the mPCG

The simulated spinal shapes were compared to the spinal shapes of Subject 1 when she was wearing the mPCG. The thoracic and lumbar Cobb angles of Subject 1 in the mPCG are 8° and 7° respectively, while those of Subject 1 with the simulated braces are 10° and 8°, respectively. The effects of the initial status (“without padding”) and pressure exertion status (“with padding”) on the ribs and spine are shown in the Figures 6.5 and 6.6, respectively. The displacement results of the spine and body with the use of different magnitudes of exerted force through the padding and locations of inserted padding are shown in the Figure 6.7.

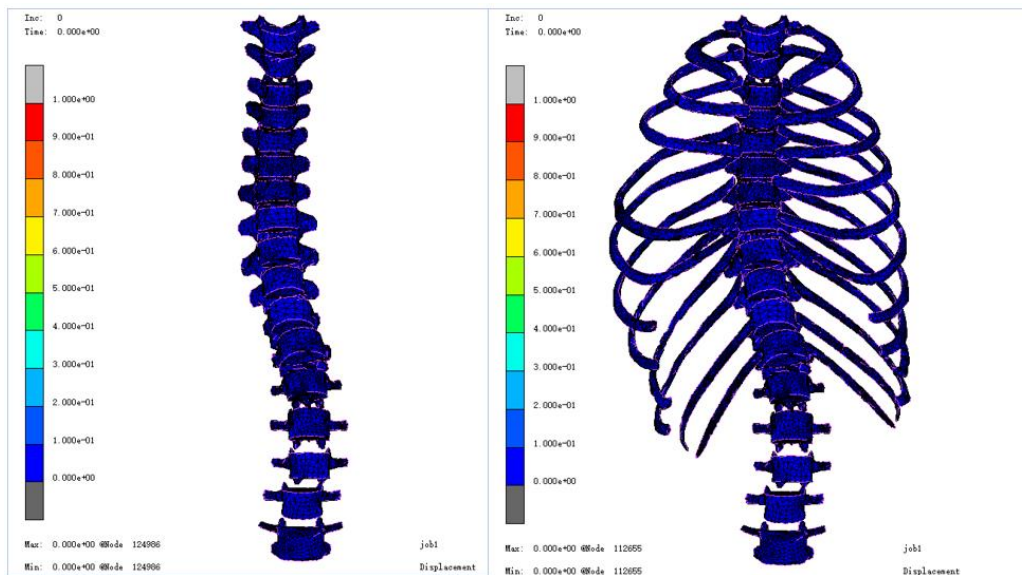


Figure 6.5 Effects of initial status (“without padding”) on ribs and spine

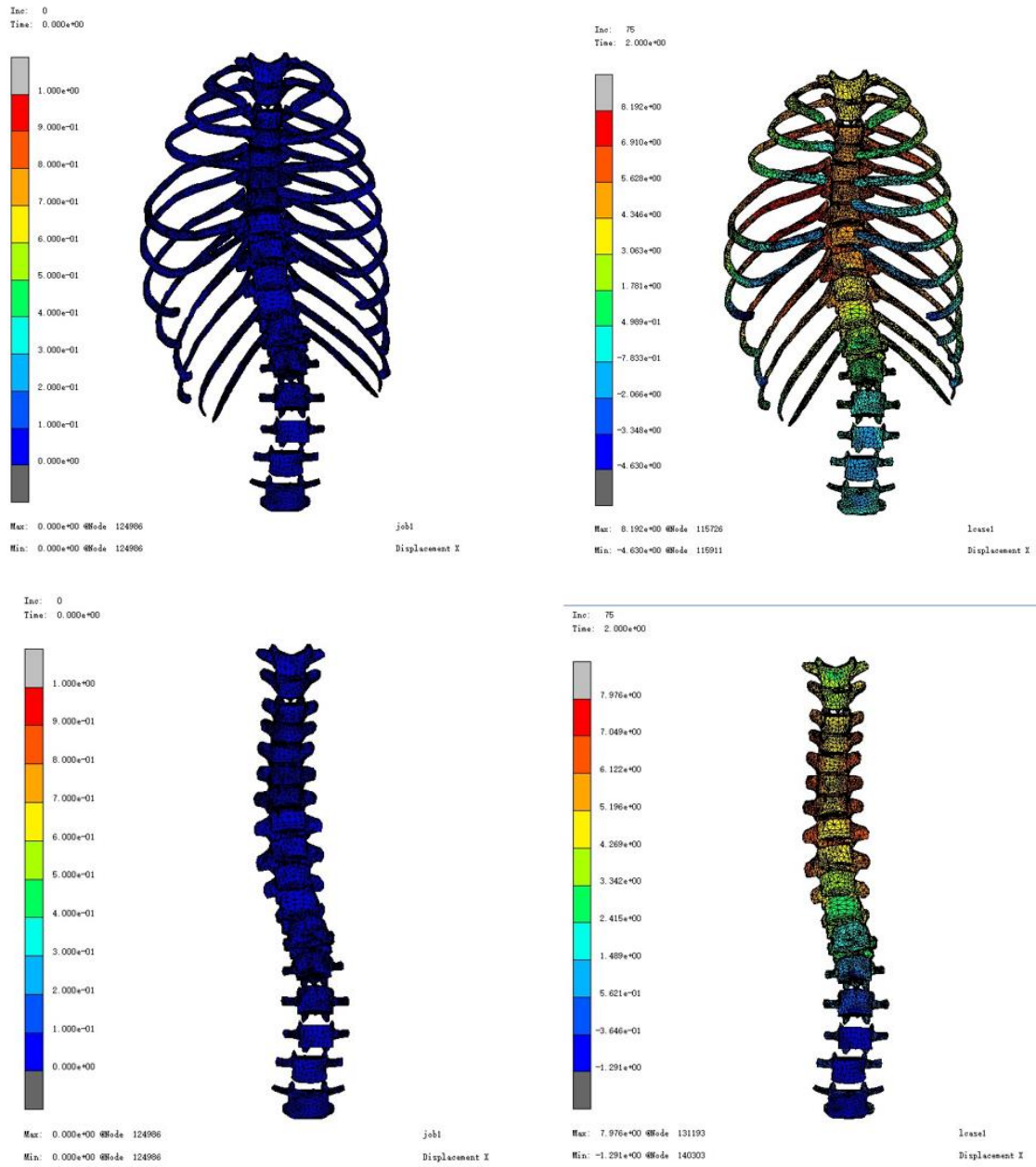


Figure 6.6 Effects of pressure exertion (“with padding”) on ribs and spine

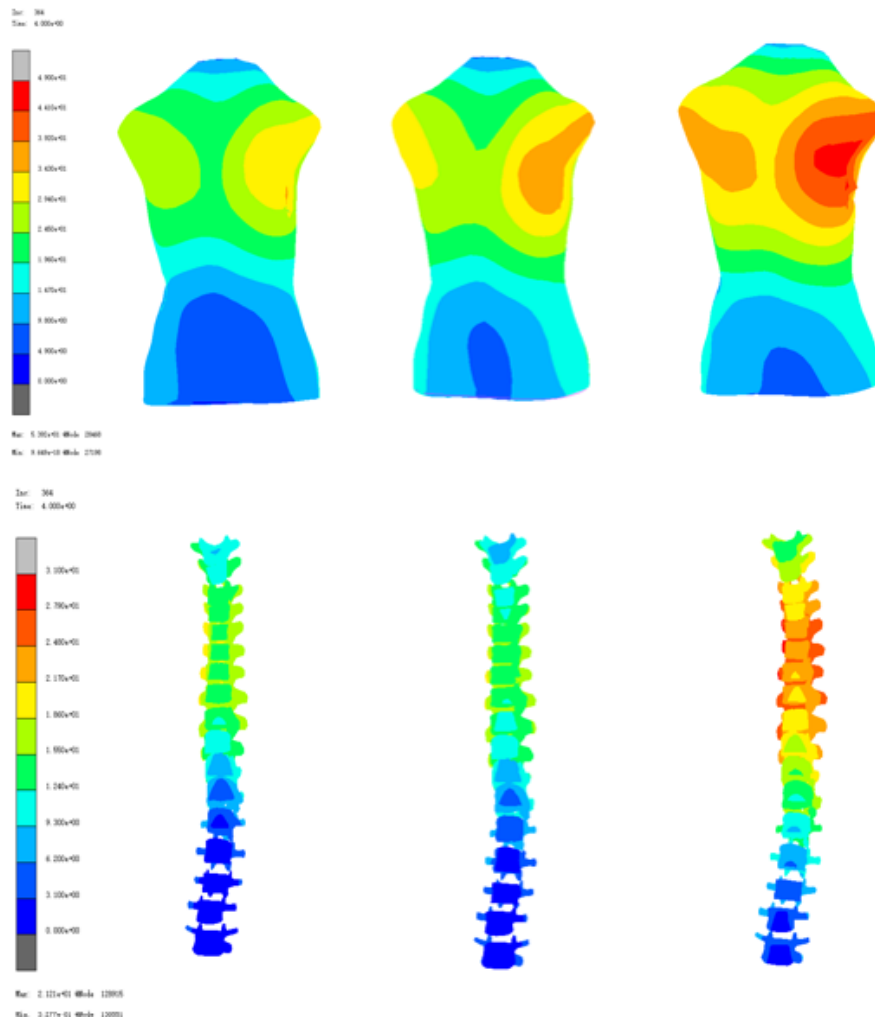


Figure 6.7 Displacement results of spine and body with use of different magnitudes of exerted force through padding and locations of inserted padding

### 6.2.1.7 Validation

Validation is essential in simulation work as the method indicates whether the simulation results reflect the real situation and accuracy of the simulation model. To validate the FE model in this study, the predicted spinal curvature (based on the simulation process) was compared with the actual spinal curvature obtained from the radiographic images. In other words, Cobb angles were measured on the radiographic images of Subject 1 when she donned and doffed the mPGG, and then compared with the predicted results of the FE model. Apart from using Cobb angles measured on the spinal curves in the coronal plane as the parameters for comparison, the position of each vertebral body in the coronal spinal curvature was also compared with the experimentally obtained/actual results. Figure 6.8 illustrates the spinal curvatures obtained from the: (1) simulation of individual “without girdle” in FE model (line in blue), (2) actual X-

rays of the subject in-orthosis (line in orange), (3) simulation of individual “with girdle (1cm padding)” in FE model (line in red) and (4) simulation of individual “with girdle 3cm padding)” in FE model (line in purple).

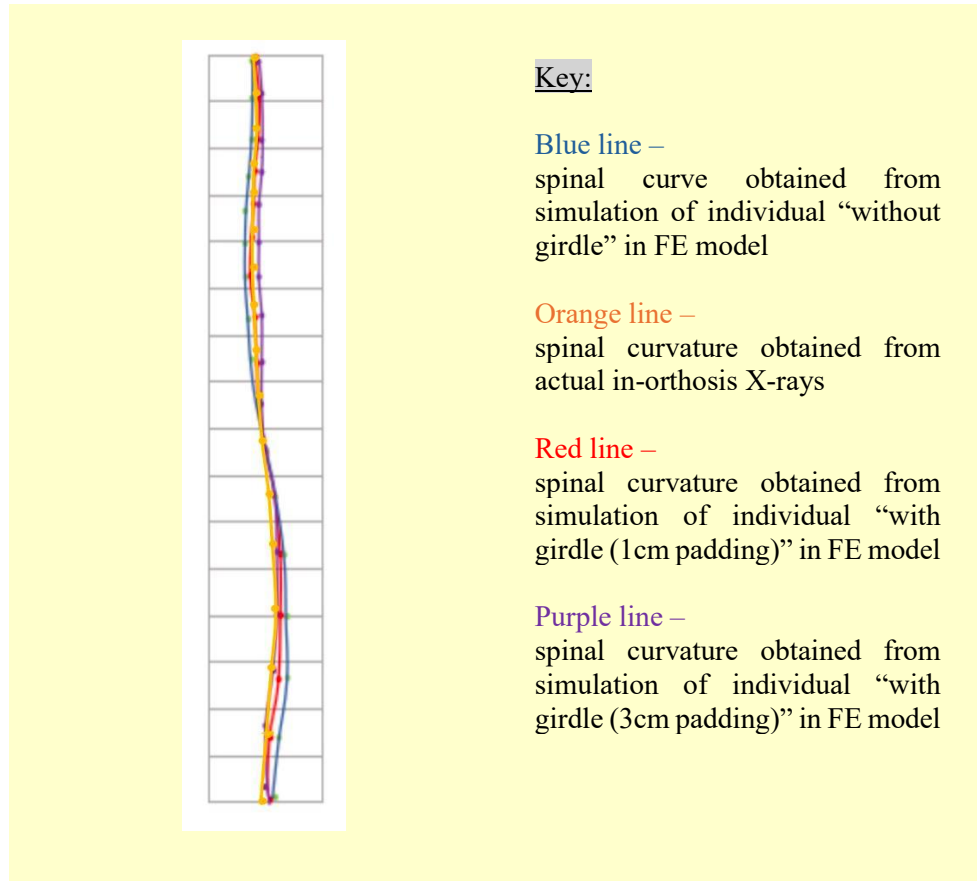


Figure 6.8 Comparison of spinal curvatures between actual and simulated curves

The movement of the simulated spinal curvature obtained with the FE model showed a similar trend as that of the radiographic image when Subject 1 had donned the mPCG. Considering the spinal curvature movement obtained from radiographic image and result estimated by the FE model, the correlation coefficient of the vertebrae position is calculated by using:

$$\text{Correlation coefficient} = \frac{\sum_{i=1}^{17} [(T_i - \bar{T}) \times (E_i - \bar{E})]}{\sqrt{\sum_{i=1}^{17} (T_i - \bar{T})^2} \times \sqrt{\sum_{i=1}^{17} (E_i - \bar{E})^2}} \quad (7)$$

where:

- $T_i$  represents the  $i$ -th value of variable  $T$ ,

- $\bar{T}$  represents the mean of the T values,
- $T_i$  represents the i-th value of variable E,
- $\bar{E}$  represents the mean of the E values, and
- The summations are taken over 17 observations.

The correlation coefficient for the vertebral body displacement is 0.84.

### **6.3 Development of intelligent system for girdle prescription**

In this study, the development of an intelligent system for facilitating the prescription of the mPCG consists of two parts: (1) a decision tree and (2) a neural network model. The former is used to suggest suitable patients for using the mPCG, while the latter after training can be used to suggest appropriate placement of the padding for corrective points of pressure in general according to the different spinal conditions and needs of the users. Their development process is described in the following.

#### **6.3.1 Development of intelligent system for girdle prescription**

##### **6.3.1.1 Using decision tree to group subjects into different treatment groups**

Decision trees are a supervised learning algorithm used for classifications and regressions which leverage unstructured data to derive effective classification rules. The concept behind a decision tree is shown in Figure 6.9. In this study, binary decision trees are used to group adolescents with AIS into different treatment groups. For instance, adolescents who are diagnosed with a Cobb angle below  $10^\circ$  are recommended to undergo examination of their spinal conditions on a periodical basis. Those who are diagnosed with a Cobb angle between  $10^\circ$ - $20^\circ$  are recommended to use the mPCG. Those who are diagnosed with a Cobb angle between  $20^\circ$ - $40^\circ$  should use a more proven effective soft or hard brace. Finally, the adolescents who are diagnosed with a Cobb angle that exceeds  $40^\circ$  would need to consider surgery.

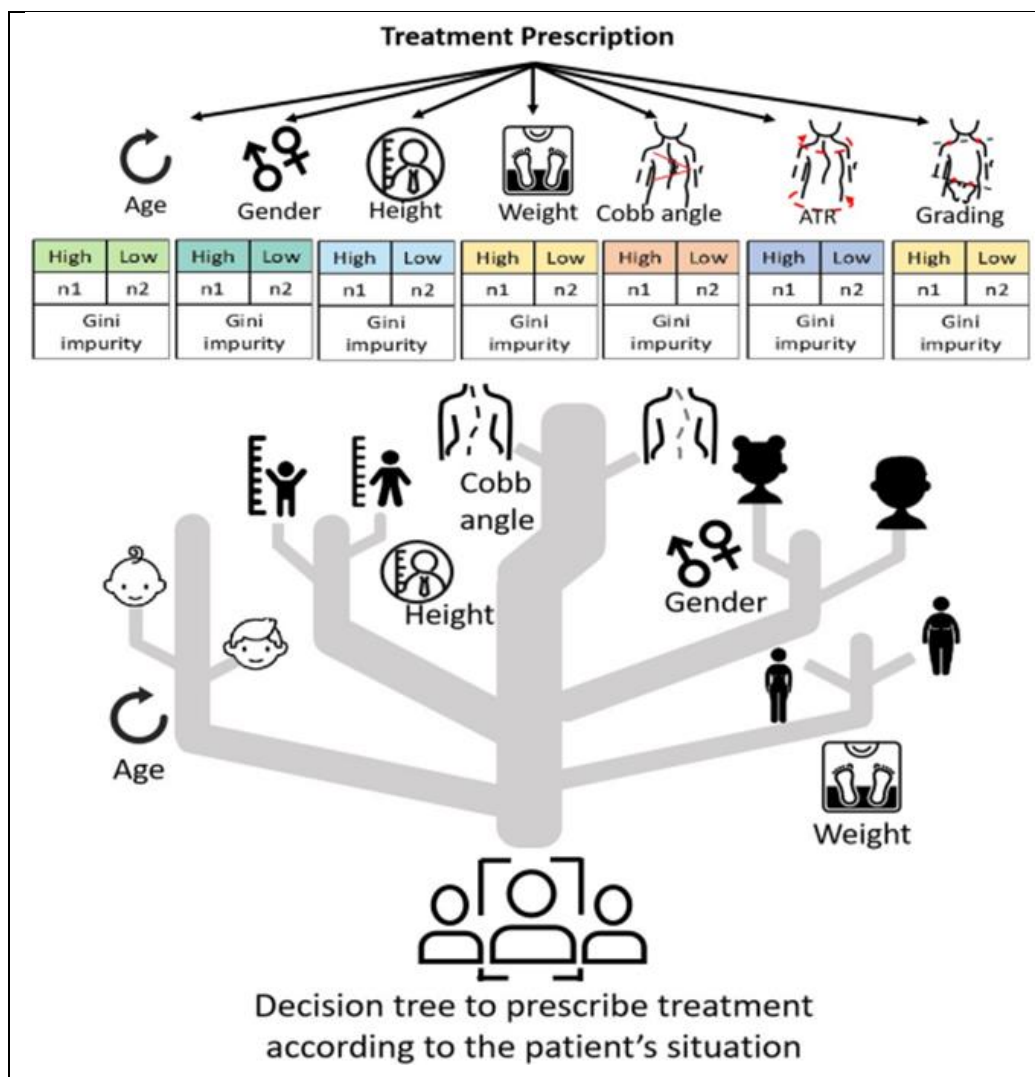


Figure 6.9 Concept behind a decision tree in this study

### 6.3.1.2 Structure and construction of decision tree

The top-down logic of decision trees uses greedy recursive splits to nonparametrically partition the feature space into homogeneous regions. The CART algorithm was selected as the learning algorithm, with Gini impurity as the criterion for selecting optimal split points. Gini impurity quantifies node purity based on the probability of incorrect classification for a random sample, thus enabling the identification of split points that best isolate the different classes. To avoid overfitting and improve the robustness of the decision tree model, cost-complexity pruning was used iteratively. This method removes the leaf nodes where exclusion does not significantly degrade performance on a validation subset, thereby simplifying the tree structure and eliminating extraneous splits. The decision tree model was built by using the scikit-learn Python library.

In the decision tree model, the independent variables are represented as  $X[n]$ , where  $n$  denotes the index of the analysis item. The subject information includes Age ( $X[0]$ ), Height ( $X[1]$ ), Weight ( $X[2]$ ), Risser Sign ( $X[3]$ ), Cobb Angle ( $X[4]$ ), Main Curve Location ( $X[5]$ ), Convexity ( $X[6]$ ), and Spine Length ( $X[7]$ ). Each index corresponds to the order in which the analysis items are placed in the model. For instance,  $X[0]$  refers to the first item (Age) included in the analysis, followed by  $X[1]$  as the second item (Height), and so on.

“If suitable for PCG treatment” is the dependent variable for decision tree modelling. A total of 49 samples are involved in the analysis; see Table 6.3.

Table 6.3 Summary of information for decision tree classification

	<u>Type</u>	<u>Frequency</u>	<u>Percentage</u>
	0.0	29	59.18%
If suitable for PCG treatment	1.0	20	40.82%
	Total	49	100.00%

The structure of the decision tree is shown in Figure 6.10. Each node in each line represents the name of the features and the split criteria. Gini/entropy represents the impurity criteria. "Samples" indicate the sample number under the node. "Value" shows the number of samples for the different categories, with the category having the largest number of samples being the category of this node.

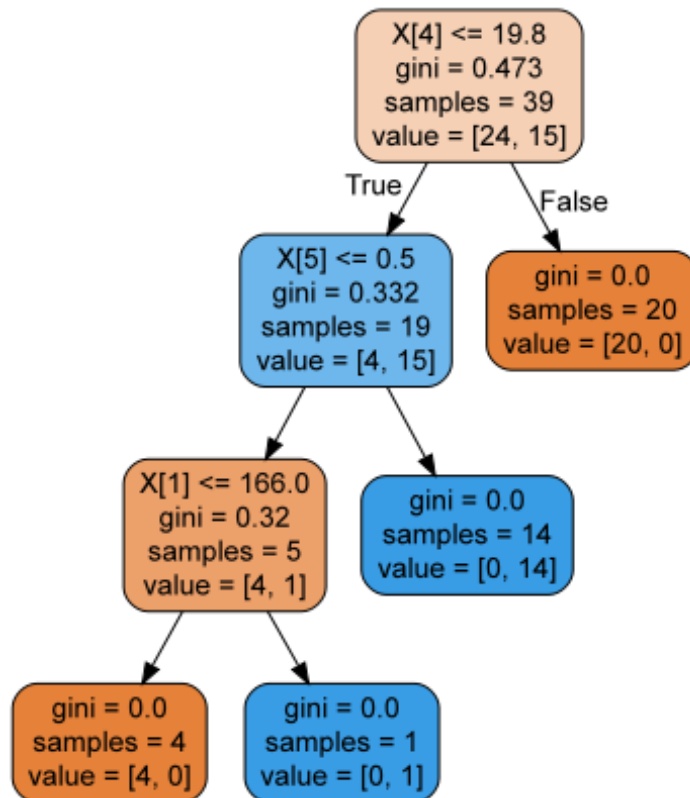


Figure 6.10 Decision tree structure

The feature importance shows the contribution of each variable to the model, with their sum totalling 100%. Figure 6.11 shows that the Cobb angle accounts for 65.79% of the total importance, which has the most weight and plays a critical role in the model construction. Location of the curvature accounts for 25.54% of the importance, is the second most important feature and plays a significant role in model construction. Height accounts for 8.67% of the importance. The combined weight of these three features is 100.00%. The remaining five features, spine length, convexity, Risser sign, weight, and age, each have a weight of 0.00%, which implies that they have no measurable impact on the model's predictive power.

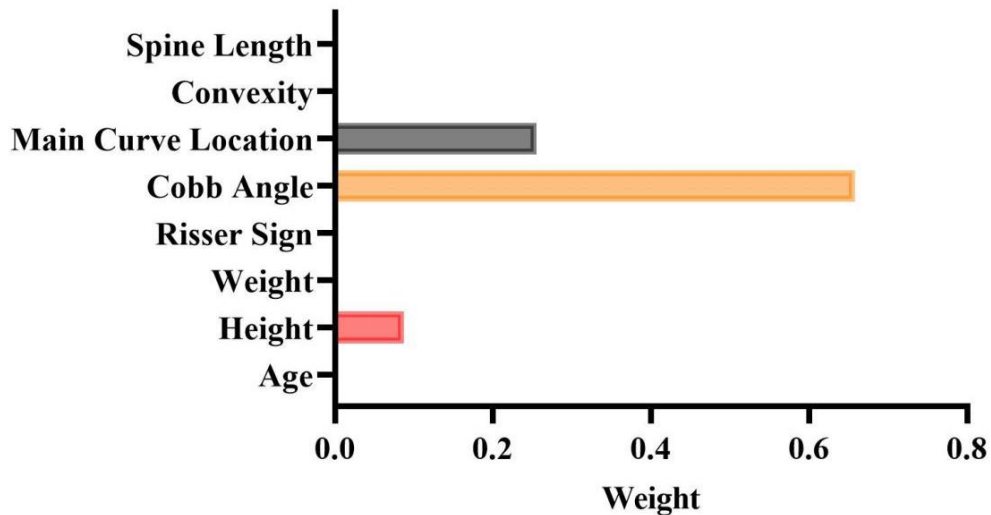


Figure 6.11 Weight of each feature in the decision tree

### 6.3.1.3 Validation of decision tree

Using label as the dependent variable, the training and testing set proportion was set to 0.8:0.2, Gini was used as the node splitting criterion, the node splitting strategy was the best split, and the maximum tree depth was not restricted to perform decision tree modelling. Table 6.11 shows that the final model achieves an accuracy of 100.00% on the test set, accuracy (overall) of 100.00%, recall (overall) of 100.00%, and an f1-score (overall) of 1.00. Therefore, the model has a good performance.

## 6.3.2 Construction of neural network

### 6.3.2.1 Using trained neural network model for suggesting padding placement

NNs are methods that solve machine learning problems, like a computer learning to perform some tasks by doing analysis on training examples (Hardesty, 2017). By taking advantage of a trained NN model to provide recommendations, the placement of the padding insertion in the mPCG to generate the corrective points of pressure in the appropriate locations according to spinal conditions and needs of the users can be easily determined.

### 6.3.2.2 Neural network architecture and model training process

The NN architecture is structured with the input layer, followed by two hidden layers with 512 nodes in each layer. After the hidden layers, the network splits into three branches, each

corresponding to a different configuration of the curvature. These branches ensure that the network can handle and effectively predict the outcomes for the different types of spinal deformities. The database for building a retrospective model to train the NN based on the X-ray results includes a total of 979 X-ray images. Among these, 197 images are missing or unavailable, thus leaving 782 images for the analysis. Within the dataset, 208 images are annotated for grading pathological curvatures, and focus on parameters like the Cobb angle and curve apex locations to assess the spinal conditions, which include information on the placement and effect of padding (for exertion of the corrective forces) used in the mPCG. This dataset provides a comprehensive basis for training the model to analyse and predict spinal conditions based on X-ray images and associated clinical data.

Since the spinal curvature of AIS patients varies, padding of the mPCG should be inserted in the appropriate pocket to exert corrective points of pressure according to the needs of the patients. There are 8 options for the padding placement, which include: (1) Left-Thoracic-1 (L-T-1), (2) Left-Thoracic-2 (L-T-2), (3) Left-Lumbar-3 (L-L-3), (4) Left-Lumbar-4 (L-L-4), (5) Right-Thoracic-1 (R-T-1), (6) Right-Thoracic-2 (R-T-2), (7) Right-Lumbar-3 (R-L-3), and (8) Right-Lumbar-4 (R-L-4). The 8 padding placement options are shown in Figure 6.12. These 8 options can be used in conjunction if necessary, according to the spinal conditions and needs. In most cases, 1 to 3 paddings are inserted into the mPCG for exerting the corrective points of pressure.

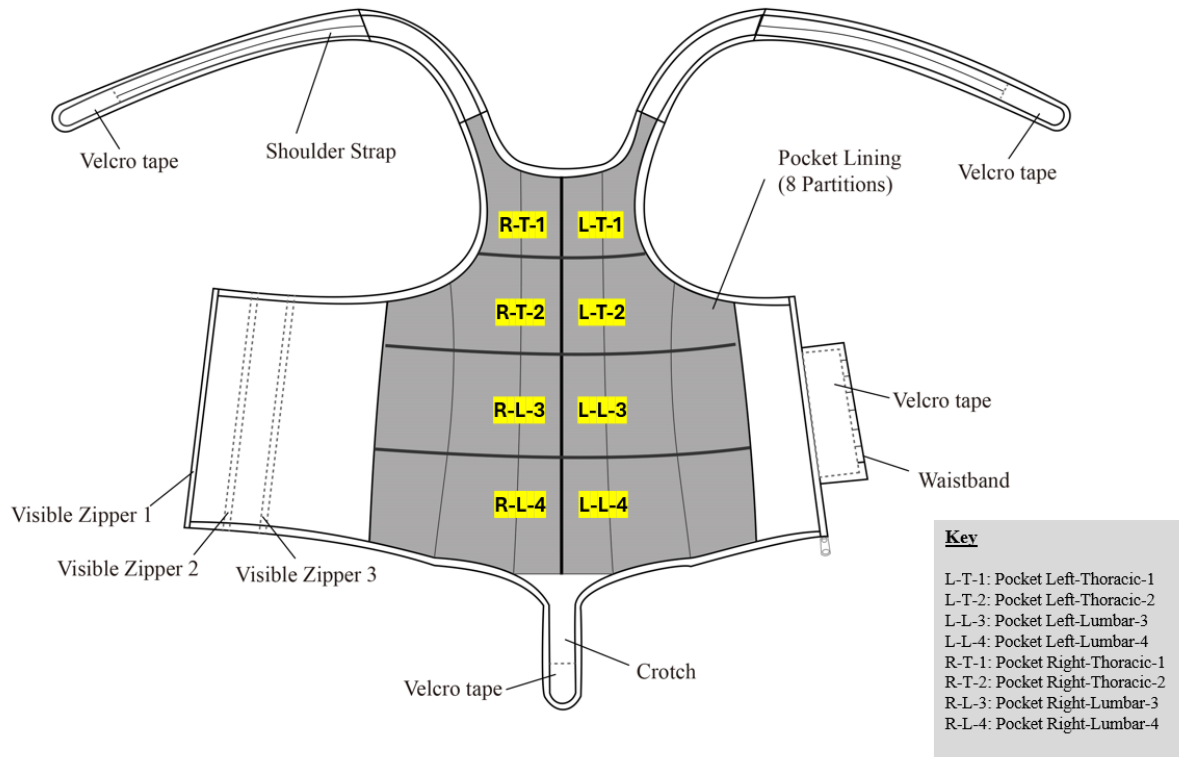


Figure 6.12 Eight padding placement options of mPCG

The NN architecture, as well as the input and output for the model training in this study, are shown in Figures 6.13 and 6.14. The NN architecture begins with an input layer that consists of 12 nodes. This layer processes the initial input data, including features such as curvature conditions (Curve 1 starting vertebrae, Curve 1 apex vertebrae, Curve 1 ending vertebrae, Curve 1 Cobb angle, Curve 2 starting vertebrae, Curve 2 apex vertebrae, Curve 2 ending vertebrae, Curve 2 Cobb angle, Curve 3 starting vertebrae, Curve 3 apex vertebrae, Curve 3 ending vertebrae, and Curve 3 Cobb angle) and padding locations for the mPCG. The network includes two hidden layers, each with 512 nodes, fully connected and utilising the ReLU activation function. The first hidden layer captures complex features from the input data, and identifies non-linear relationships, while the second hidden layer further refines these features, thus enabling the network to understand and extract more intricate patterns. After the hidden layers, the network branches into three distinct configurations, each designed to handle different spinal curvature analyses. The three distinct configurations are:

1. Curve 1 configuration - This configuration has 9 nodes and is tailored to analyse the first type of spinal curve, such as thoracic curves.

2. Curve 2 configuration - With 7 nodes, this configuration focuses on the second type of spinal curve, or lumbar curves.
3. Curve 3 configuration - This configuration has 6 nodes and is intended to analyse more complex or combined spinal curvatures.

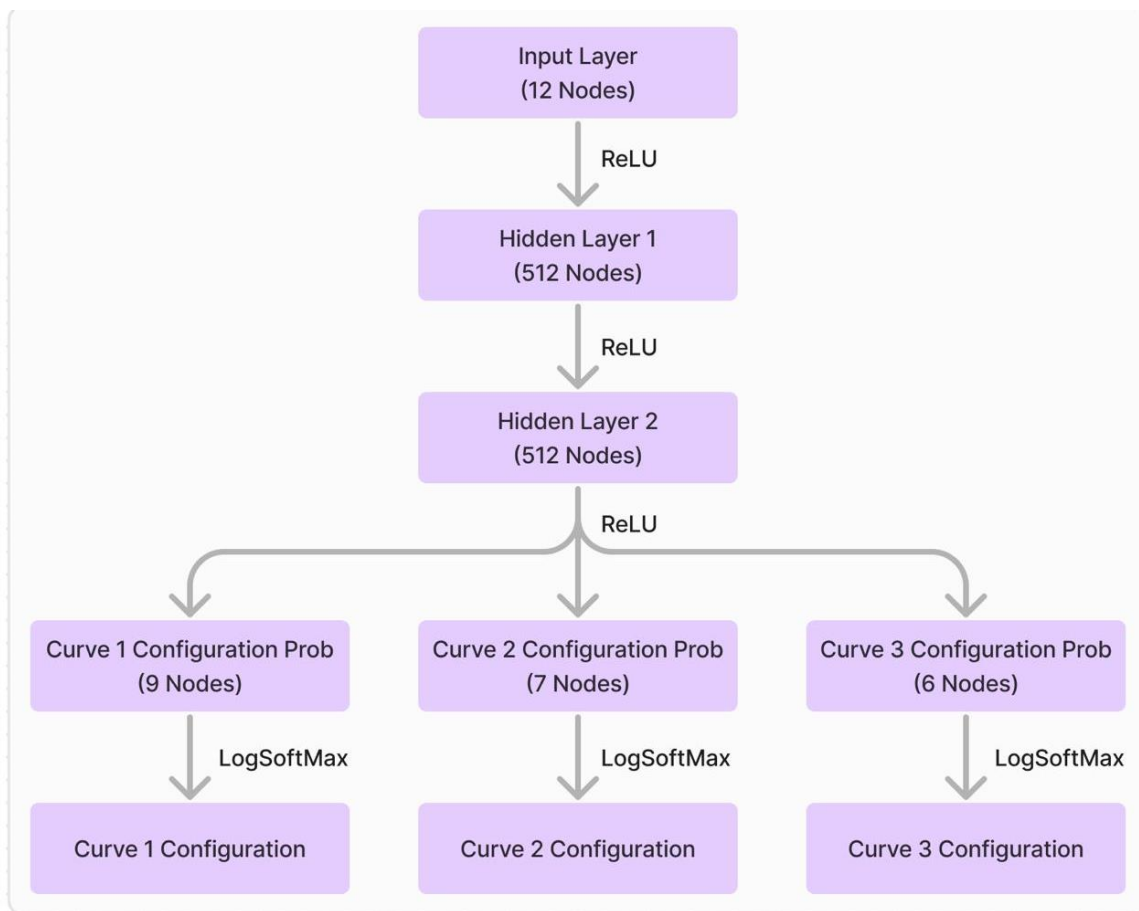


Figure 6.13 Neural network architecture for prescription of mPCG

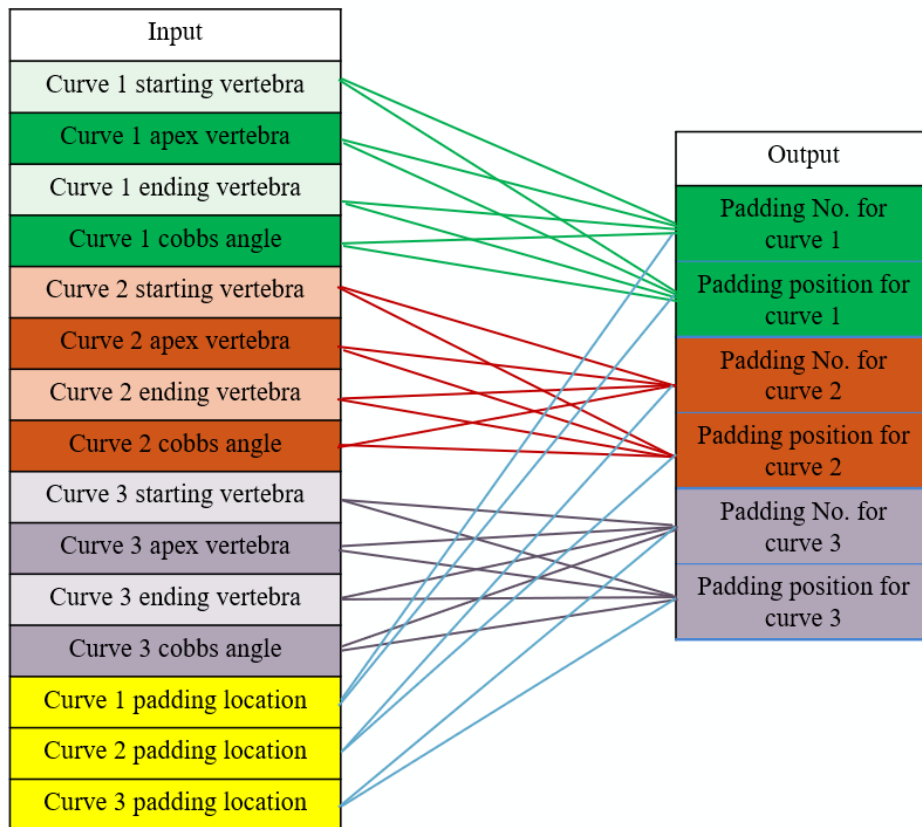


Figure 6.14 Input and output for training neural network

Regarding the data processing, the first step involves normalising the input images so that they have pixel values between 0 and 1, thus ensuring uniformity and ease of processing. Other input features, such as demographic data, are standardised to have a zero mean and unit variance, which helps to produce consistent results. Regarding the model training, the data are split into training and validation sets, typically at an 80:20 ratio. Data augmentation techniques might be used to enhance the diversity of the training set. The model is then trained by using the training data and validated against the validation set. This helps to fine-tune the model and ensures that it generalises well to new data. The cases of the 10 subjects recruited in this study are also used as validation data set to further investigate the prediction accuracy of the model.

The CNN training process follows an iterative and looping approach. Initially, the training and testing datasets are inputted into the NN trainer with a set of initial parameters. The error for each dataset is then calculated by using a weighted cross-entropy loss function. Subsequently, the early stopper evaluates the error of the testing dataset to determine if there has been any improvement compared to the previous iteration. This process continues until there is no further

improvement in the testing error over 20 epochs. At that point, the early stopper terminates the training loop.

### **6.3.2.3 Training result and accuracy of developed neural network model**

In Epoch 231, the performance of the NN for the PCG is detailed through batch losses, curve accuracies, and test error metrics. The batch losses show some variability: Batch 0 (0.021842), Batch 5 (0.099495), Batch 10 (0.022302), Batch 15 (0.323444), Batch 20 (1.053257), and Batch 25 (0.277887). Curve accuracies are notably high, with Curve 1 at 96.36%, Curve 2 at 96.97%, and Curve 3 at 93.94%. The test error shows an average loss of 0.139064. Despite a 13.56% loss improvement from the previous best, this epoch achieves a new best test loss of 0.139064.

## **6.4 Chapter summary**

Traditionally, standard radiographic examination is used to assess the in-orthosis correction of an orthosis/bracing treatment on the spinal curvature. However, radiographic scans should not be done frequently, especially within a short period of time since exposure to radiation may cause damage cancer. With the FE model developed in this study, the impact of the mPCG can be simulated and predicted. The pressure distribution on the skeletal model and the displacement of each vertebral body could also be calculated by simulating the wear process of the girdle. In this way, different girdle wearing parameters can be tested to determine the effect, and the number of radiographic scans during the girdle prescription process can be reduced. Before building the FE model, geometric models of the upper body, skeleton and the mPCG are prepared, while the material properties for the different components are determined. By importing the geometric models and setting the boundary conditions, the FE model for the mPCG is then successfully constructed and validated by comparing the simulated and actual results.

On the other hand, a decision tree and a trained NN are constructed in this study to form an intelligent system to facilitate the process of identifying target patients who are suitable for treatment with the mPCG, as well as choose the appropriate girdle wearing parameters (e.g. placement of padding insertion for generating pressure points) for the patients according to their needs and spinal conditions without being subjected to a trial and error process. Regarding the decision tree development in this study, a top-down logic is used, which divides the feature

space into homogenous sections nonparametrically via greedy recursive splits. The CART algorithm is used as the learning algorithm, with Gini impurity as the criterion for selecting optimal split points. The decision tree is validated and the final model has a 100% accuracy rate. As for the construction of the NN in this study, the NN architecture begins with an input layer that consists of 12 nodes for processing the initial input data, including features such as curvature conditions and padding locations for the mPCG. The network includes two hidden layers, each with 512 nodes, fully connected and utilising the ReLU activation function. The training and testing datasets are inputted into the NN trainer with a set of initial parameters. The error for each dataset is then calculated by using the weighted cross-entropy loss function. Finally, the trained NN is developed for the prescription of the mPCG and validated, in which the accuracy for the curvatures is notably high, with Curve 1 at 96.36%, Curve 2 at 96.97%, and Curve 3 at 93.94%.

The combined approach with the developed FE model, the constructed decision tree and the trained NN forms a comprehensive intelligent system for treating AIS with the mPCG, where the FE model handles the physical simulation, the decision tree screens suitable users and the NN model aids in personalized treatment planning.

## CHAPTER 7 – CONCLUSIONS AND RECOMMENDATIONS FOR FUTURE WORK

### 7.1 Conclusions

AIS, one of the most common spinal conditions associated with adolescent growth, is affecting 2-3 percent of all adolescents in Hong Kong (Student Health Service - Department of Health 2022; Chan, 2019; Lam, 2010). Scoliosis cases of patients who have a lateral curvature that is more than or equal to a Cobb angle of  $10^\circ$  are usually regarded as medical problems, while girls are 3.6 times more likely than boys to experience progression in their spinal curvature (Kubat & Ovadia, 2020; Weinstein, 1994). Patients whose spinal curvature is more than  $25^\circ$  are advised to undergo bracing. If the curvature has progressed to  $40\text{--}50^\circ$ , surgery may be necessary. For individuals whose spinal curvature is less than  $25^\circ$ , the recommended course of action is usually observation with periodic examinations (Spoonamore, 2024, Hresko, 2013). Patients with early scoliosis, particularly those with a Cobb angle between 10 and  $20^\circ$ , have more treatment options (Yip et al., 2016). To address the issue of the lack of appropriate orthosis products for early scoliosis treatment and the problems of hard and flexible braces found in the existing market, Liu et al. (2015) developed a PCG for adolescents with early scoliosis (i.e., Cobb angle  $10\text{--}20^\circ$ ), with the goal of reducing posture imbalance and, consequently, the likelihood of spinal curvature progression.

Changes in posture and body asymmetry may increase the likelihood of scoliosis advancement in patients with AIS (Kouwenhoven and Castelein, 2008; Fortin et al., 2012). As per Wong and Wong (2008) and Chen et al. (1998), patients with spinal deformities may have painful symptoms that intensify due to improper posture and inadequate control over their postural stability. For this reason, a feasible and appropriate approach to assist AIS patients could be making use of a posture training device (Wong and Wong, 2008; Lenssinck et al., 2005). This is also the intention that led Liu et al. (2015) to develop the PCG.

According to the preliminary findings, PCG can control the further progression of spinal curvature and correct posture asymmetry in the frontal, horizontal, and sagittal planes by exerting lateral corrective forces (Liu et al., 2015; Yip et al., 2016). However, the PCG is specifically designed and tailor made for the study participants, which leads to a long production lead time. It also takes time to fit the girdle through a trial-and-error procedure.

Besides, there are certain restrictions of the girdle design that impact the wear comfort and the amount of corrective force exerted. In order to enable mass production and customisation of the girdle, this research project develops a sizing system for the PCG. This might potentially reduce production costs and the waiting time of patients. The girdle design is also modified and refined to work better with the newly developed sizing system, optimise the exertion and effectiveness of the corrective forces, as well as enhance the level of wear comfort. Furthermore, FE modelling is used to study the corrective mechanism and performance of the mPCG, as well as build an intelligent prescription system for the mPCG to facilitate and streamline the girdle prescription and fitting processes. It is anticipated that the mPCG can be personalised as an orthosis treatment to help adolescents with early scoliosis or posture issues. It will also likely enhance the effectiveness of treatment with the mPCG, lower treatment costs, and promote the use of the mPCG in the public to the target group.

The principal objectives of this study include: (1) to understand the theory behind existing orthosis products for AIS treatment and investigate the prevalence of AIS in Hong Kong; (2) to modify the design of the PCG and select suitable materials that optimise its treatment efficacy and level of wear comfort, as well as enhance the garment durability; (3) to develop a specific sizing system for the mPCG for adolescents with early scoliosis to facilitate mass customisation; (4) to recruit subjects who can meet the inclusion criteria for a wear trial in order to evaluate the efficacy of the mPCG scientifically; (5) to study the corrective mechanism of the PCG by using FE modelling; and (6) to construct and validate an intelligent system that facilitates the prescription of the PCG. The objectives listed above have been addressed respectively and the results of this study are summarised as follows.

(1) After gaining an understanding of the background information of scoliosis including the prevalence of AIS in Hong Kong, different types of orthosis products in the market (e.g. traditional hard braces, semi-right braces, and flexible braces) have been reviewed to understand their design features, corrective mechanisms, material applications and target users. Useful information has been consolidated and summarised in Chapter 2. Besides, a school screening programme is also carried out in this study to understand the prevalence of AIS in Hong Kong. The school screening activities have been carried out at 6 primary schools and 3 secondary schools in February 2020, plus 15 screening activities held on PolyU campus. According to the school screening results, 487 (27.88%) of the 1747 participants are suspected to have scoliosis. Only 247 of the 487 suspected scoliosis patients accepted the offer for a

radiographic examination. That is, 6.07%, 5.6% and 2.46% of the school-screened participants are diagnosed with spinal curvature less than 10°, between 10°-20° and more than 20° respectively.

(2) Apart from the existing orthoses for AIS treatment in the market, the original PCG (Liu, 2014; Liu et al. 2015) has also been reviewed. Not only its design features, corrective mechanism, material use and target users, the results of its wear trial, as well as its advantages and limitations are also investigated. The modifications made to the design of the PCG include: i) use of “3 zippers” at the centre front to allow the same size girdle to accommodate a wider range of waist circumferences; ii) elimination of the free-end design of the shoulder straps and waistband to exert degree levels of corrective forces; iii) adding markings on the shoulder straps and waistband to provide more clear references for tension adjustment so as to enable better tension control; iv) increasing the number of pocket lining partitions which more accurately exerts points of pressure to the needed areas with a higher corrective force, and v) elimination of the stitches on the surface and change in colour from nude (beige) to white, which gives the mPCG a cleaner look so that it is more attractive and acceptable to the users. Besides, the shell fabric of the girdle is replaced with a newly selected material, powernet (F4), which improves the dimensional stability, durability, pilling resistance and wear comfort. The newly replaced elastic strap (E5) also performs well in most of the material tests. By modifying the girdle design and changing the material use, the compliance rate with the mPCG should be enhanced. According to the interface pressure measurements, the highest mean pressure value exerted by the mPCG is 3.656 kPa (70%) higher than that of the original design.

(3) A systemic sizing system for the mPCG has been developed based on the body measurement review and investigation, which increases the efficiency of the girdle sizing selection and fitting processes, as well as enables mass customisation. When determining the girdle size for the wearers, their length of spine is a key factor for consideration. There are 3 main sizes in the sizing system that cover different spinal lengths. That is, S covers a spine length of 33.1-38 cm, while M is 38.1 to 43 cm, and L is 43.1 to 48 cm. Each size is further categorised as 2 sub-sizes (i.e., I and II). Sub-size I can accommodate a waist circumference of 50 to 59.9 cm, while sub-size II, 60 to 74 cm.

(4) Ten female subjects between 10 and 13 years old with early scoliosis (i.e., Cobb angle 10-20°) are recruited from the school screening programme for a 9 month-wear trial. Seven of

them are diagnosed with an S curve while 3 of them have a C curve. Two of the subjects (i.e., Subjects 3 and 4) withdrew in the early stages of the study so only 8 subjects completed the 9 month-wear trial. The wear trial took place at 0 M, 3 M, 6 M and 9 M, and examinations are made both with the girdle and without the girdle. The experimental results include change in spinal curvature (radiographic examination and comparison of Cobb angle), improvements in posture balance (3D body scanning and posture angle), and the effects on proprioception deficit (Vicon Nexus 3D motion capture system). Regarding the effectiveness of the mPCG in controlling the progression of the spinal curvature, 6 of the 10 subjects show a significant and immediate curve reduction (a reduction that ranges from 5° to 11°) after putting on the girdle for 2 hours, while 4 of the 8 subjects show an apparent curve reduction for the long-term after the completion of 9 months of treatment with the mPCG even when the girdle is doffed (curve reduction ranges from 5.2° to 8°). Regarding the result on improving the posture imbalance, significant improvements are found for many of the test items. For instance, the lumbar imbalance in the sagittal plane during habitual standing, asymmetry of the acromion in the frontal plane during habitual standing, pelvis asymmetry in the frontal plane during habitual standing, thoracic imbalance in the sagittal plane during standing, thoracic imbalance in the sagittal plane during sitting and lumbar imbalance in the sagittal plane during sitting. However, no significant improvement can be found for the tested areas in the horizontal plane (i.e., acromion, scapula and pelvis rotation). Regarding the results of the proprioception tests, although significant effects are found for a few of the tested items (i.e., NRZ - convex side at 0 M vs. 9 M, EFY – dominant side at 9 M), no apparent effect can be found for most of the tested areas. The results show that treatment with the mPCG is ideal for posture correction except for alignment in the horizontal plane, while reduction in proprioception deficits is not apparent. In regard to controlling the progression of the spinal curvature, the effects are more apparent for those with an S curve. Other than the tests mentioned above the compliance rate of the treatment with the mPCG and the questionnaire results related to the evaluation of the quality-of-life during the wear trial are also included and discussed. It is found that the average compliance rate with the mPCG is 95%, which is 1.75% higher than that with the original version of the PCG in Liu (2015). The increase in compliance might be due to the modified girdle design and use of other fabric materials, which improve the girdle both aesthetically and functionally (i.e. wear comfort, convenience, effectiveness of corrective mechanism). Besides, it is found that the subjects who show apparent reduction in their spinal curvature after the 9-month wear trial tend to comply more with the treatment. This indicates that the length of the girdling time each day might affect the effectiveness of the girdle. In regard to the quality-of-

life questionnaire results, the subjects indicate concerns with their “self-perceived image” and “stress level”, but the level of satisfaction with the girdling treatment in this study is comparable or exceeds that of other studies (Wong, 2021; Weiss et al., 2007). The results show that the subjects might need more time to become accustomed to the girdling treatment. Since the mPCG is not yet commercially available, the general public might be curious about this device, which might cause the subjects in this study to feel uncomfortable.

(5) In this study, an FE model is developed for simulating and predicting the corrective effects of the mPCG on the spinal curvature by obtaining data from Subject 1, importing the prepared geometric models of upper body, skeleton and mPCG, as well as setting the boundary conditions. The pressure distribution on the skeletal model and displacement of each vertebral body are calculated by simulating the wear process of the mPCG. Modifications made to the wear parameters make it possible to improve the efficacy of the mPCG in terms of the spinal adjustment and optimise the pressure distribution on the skeletal model. The corrective mechanism of the mPCG is examined by using the developed FE model. Validation has been done to ensure the reliability of the model by comparing the simulated and actual results. In normal practice, a standard radiographic examination is needed to assess the effects of orthosis/bracing treatment on the spinal curvature. By using the developed FE model, different girdle wearing parameters can be examined to determine the effect and thus the time used for radiographic scanning during the girdle prescription process can be reduced. More importantly, the biomechanical model does not expose the user to radiation, which means that the effectiveness of the mPCG can be examined with ease, and its design optimised without conducting human wear trials, which addresses the problem of the lack of voluntary subjects.

(6) In this study, a decision tree and a trained neural network were constructed to form an intelligent system. This system facilitates the detection of target patients who are suitable for the treatment with the mPCG with the mPCG, as well as choosing appropriate girdle wearing parameters (e.g. placement of padding insertion for generating corrective point pressure) for the patients according to their needs and spinal conditions without the trial-and-error process. The decision tree developed in this study used a top-down logic that divides the feature space into homogenous sections nonparametrically via greedy recursive splits. The Classification and Regression Trees (CART) algorithm was selected as the learning algorithm, with Gini impurity as the criterion for selecting optimal split points. The accuracy rate of the final model in the validation achieved 100%, which means the model is highly reliable. The trained neural

network in this study was constructed with the architecture begins with an input layer consisting of 12 nodes for processing initial input data, including features such as curve conditions and padding locations for the mPCG. The network includes two hidden layers, each with 512 nodes, fully connected and utilizing the ReLU activation function. The input in the training and testing dataset are inputted into the NN trainer with a set of initial parameters. The error for each dataset is then calculated using the weighted cross-entropy loss function. Finally, the trained neural network was developed for the prescription of mPCG with validation, which the curve accuracies are notably high, with Curve 1 at 96.36%, Curve 2 at 96.97%, and Curve 3 at 93.94%.

## **7.2 Limitations and recommendations for future work**

Due to the time constraints, only 10 subjects are successfully recruited for the wear trial in this study, and only 16 schools participated in the school screening procedure. To increase the accuracy of the results, it is recommended that more schools be included for screening and more subjects recruited for the wear trial. A larger sample size might yield even more statistically significant results.

Apart from increasing the number of voluntary subjects for the wear trial, data from more individuals in the target group should be obtained and inputted for FE modelling, decision tree development and neural network training. With more inputted data, the developed and trained models will be more reliable and representable. On the other hand, more girdle wearing parameters can be examined and investigated when building and training the models. For instance, the tension of the straps.

In addition, the wear trial period is only 9 months in this study due to time and resource constraints. A longer wear trial period is recommended to assess the potential impacts of the treatment with the mPCG on spinal deformity control, posture alignment correction and reduction of proprioception deficit. Although the treatment compliance rate among the subjects is high on average, the wear practices and commitment of some of the subjects who have a lower compliance rate could be improved. To increase their awareness of the health repercussions and improve their compliance with the treatment even further, educational workshops are recommended to give them additional information about scoliosis and the negative effects of poor posture.

As for the material selection for the production of the mPCG, only 6 types of fabrics and 5 elastics are sourced for the laboratory testing. More materials should be sourced in order to choose materials with optimal qualities for fabrication of the mPCG and thus a girdle with optimal function and wear comfort. Additionally, aesthetic adjustments to the fabric materials are recommended, such as colour printing, to improve the receptivity to the girdle and enhance compliance by taking psychological needs into consideration.

Although the FE model in this study provides valuable insights into the biomechanical behaviour of the modified posture correction girdle, a few limitations should be acknowledged. The FE model prediction relies on the mechanical properties of biological tissues and girdle materials, which may vary across individuals. Also, the model simplifies certain aspects of the body-girdle interaction by focusing on static conditions, potentially overlooking dynamic factors such as daily activities and long-term use of the girdle. Besides, while the validation process was effective, it was conducted on a single subject. This may limit the generalizability of the results to a larger population of AIS patients. Therefore, more FE models should be developed for a wider range of cases with varying conditions in the future.

Finally, the internal validity of the statistical analysis in this study may be impacted by the absence of a control group, which does not make it possible to attribute the differences or changes to the independent variable. As a result, it is recommended that a control group should be included in future research.

# APPENDICES

## Appendix I

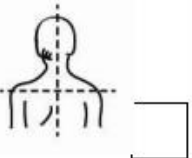
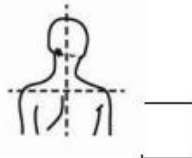
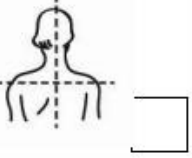
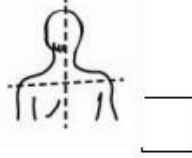
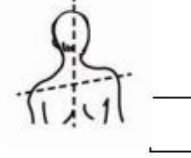
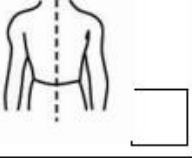
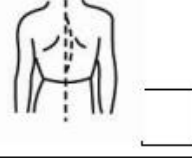
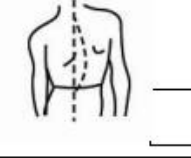
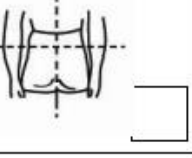
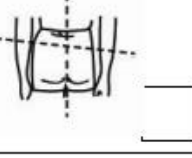
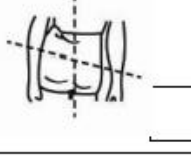
The record form used for the school screening in this study.

Scoliosis Screening Worksheet			
School name:		Date:	
<b>Part I</b>			
<b>Demographic Data</b>			
Student name:		Age:	
Gender: M / F		Tel no. (Parent):	
Birth date: DD / MM / YY			
Height: cm		Weight: Kg/lb	
<b>Scoliometer</b>			
Thoracic:	_____°	Lumbar:	_____°
Difference: _____°			
<b>Result</b>			
<input type="checkbox"/> Normal		<input type="checkbox"/> Follow-up (Please go to Part II)	

**Part II**

(Place an X in the appropriate box to indicate your assessment of the student's condition in each area. If additional comments are necessary, use the space provided at the bottom of this page.)

**Screening Grading**

	GRADING		
	Good	Fair	Poor
Head Tilt Left Right	 <input type="checkbox"/>	 <input type="checkbox"/>	 <input type="checkbox"/>
High Shoulders Left Right	 <input type="checkbox"/>	 <input type="checkbox"/>	 <input type="checkbox"/>
Spinal Curve Left Right	 <input type="checkbox"/>	 <input type="checkbox"/>	 <input type="checkbox"/>
High Hip Left Right	 <input type="checkbox"/>	 <input type="checkbox"/>	 <input type="checkbox"/>

Other comments:

## Appendix II

Information sheet for the participants in the wear trial of this study.

(English version)

### INFORMATION SHEET

#### **Effectiveness of Posture Correction Girdle in Adolescents with Early Scoliosis**

This research study is supervised by Dr. YIP Yiu Wan, Joanne of Institute of Textiles and Clothing, The Hong Kong Polytechnic University and her team members. Please take time to read the following information carefully and discuss it with your parents, relatives and your family doctor if you wish. Ask us if there is anything that is not clear or if you would like to have more information. Take time to decide whether or not you wish to take part.

##### **Purpose of the study**

The purpose of this study is to gain the clinical information necessary for evaluating the efficacy of the Posture Correction Girdle in adolescents with early scoliosis. The Posture Correction Girdle can provide *corrective forces* and *support* to control the poor posture of adolescents, which may help to reduce the possibility of spinal curve progression. Participants' orthopedic conditions, body measurements, posture changes, body asymmetry measurements, infrared thermal images, proprioceptive senses, responses of using the girdle, perception concerning thermal environment and pressure distribution, as well as the clinical procedures will be recorded for analysis.

##### **Who will be invited to participate in this study?**

Adolescents (girls, ages between 10 to 13) who have been screened in primary/secondary schools and diagnosed with a minor spinal curve (Cobb angle is less than 20°) and are at high risk for curve progression will be invited to participate in a thorough evaluation.

##### **What will happen if you decide to take part?**

To begin, participants will be invited for X-ray scans to examine their spinal conditions (e.g. curve patterns and Cobb's angle) at a medical center. Precise body measurements will also be extracted by using a 3D Body Scanner at PolyU and direct measurement by research personnel. All the measurements obtained will be used for girdle preparation, girdle fitting and padding prescription (for generating point-pressure). After the girdle prescription, a preliminary wear trial (for few hours) will be carried out with a post-radiography analysis. Then, participants will be invited to undergo a clinical trial for 6-9 months if positive results are found in the preliminary wear trial.

The 6-9 months clinical trial is a periodical monitoring for participants on their spinal curve condition, posture change, body asymmetry, pressure distribution during sitting, and proprioception (sense of posture), in order to understand the efficacy of the Posture Correction

Girdle. These data will be collected by X-ray scanning, 3D body scanning, pressure mapping, and motion capturing every 2-3 months. In addition, the wearing compliance of participants and interface pressure created by the girdle will be recorded by using temperature logger and pressure sensors respectively. Infrared thermal images of participants will also be captured for the thermographic investigation by using an infrared camera. Furthermore, questionnaires and short interviews will be conducted during the clinical trial for understanding the psychological change of the participants and collecting their valuable feedbacks.

### **What are the benefits of taking part?**

Early management of spinal deformity may prevent the need to prescribe orthotic bracewear and surgery. This study aims to gain the clinical information necessary for evaluating the efficacy of the Posture Correction Girdle in adolescents with early scoliosis, which may help to control their poor posture and reduce the possibility of spinal curve progression.

### **Do you have to take part?**

Your participation in this study is voluntary. If you do decide to take part in this study, please keep this information and sign a consent form. You are free to withdraw at any time without giving a reason during the study. The choice of participation in the study would not affect the standard of care you receive in the clinic. However, if you failed to turn up at appointments, your participation eligibility will be immediately terminated without further notice.

### **Exclusion criteria of subject recruitment**

Any subject who had the history of (1) previous surgical or orthotic treatment for AIS, (2) contraindications for x-ray exposure or pulmonary tests, (3) recent trauma, (4) mental disorder, (5) skin allergy, or (6) fail to compliant to wear the posture correction girdle would not be recruited.

### **Are there any disadvantages and risks of taking part?**

3D body scanning, pressure mapping, motion capturing, infrared thermal image taking, wearing compliance tracking, and interface pressure measuring have no harm for human being. Except the supine X-ray that some of the participants may need to have at the beginning, the rest are low-dose X-ray scans. The frequency of taking low dose X-ray scans will be advised by the professionals. It is believed that the low dose X-ray scan only carries a mild dose of radiation.

As compared with the rigid orthotic bracewear and/or posture correction vests presently being used, the materials and design of the Posture Correction Girdle are safe and comfortable. It may probably cause skin allergy and/or discomfort. However, the Posture Correction Girdles have been tested in subjects for short durations during its design and development periods. In such, there are no special compensation arrangements in this study.

Although the 6-9 months clinical trial will only be arranged for the participants who have achieved body posture/ spinal curve improvement in the preliminary wear trial, it cannot be guaranteed their body posture and spinal curve must be improved after the clinical trial. Further spinal deformity and body asymmetry may also be found. Thus, you are required to consider the risk carefully before deciding the participation.

### **What if something goes wrong?**

There are no special compensation arrangements in this study. If you wish to complain about any aspect of the way you have been approached or treated during this study, you can contact The Secretary of the Subjects Ethics Sub-Committee of The Hong Kong Polytechnic

University in person or writing (c/o M1303, Human Resources Office of the University).

**Will my taking part in this study be kept confidential?**

Yes. If you agree to take part in this study, all personal information and research data collected from participants will only be reviewed and used by the research team as a research aspect. All information collected will be kept confidential.

**What will happen to the collected data and results of the research study?**

The results will be published in referred journals.

**Who is organizing and funding the research?**

The research is organized by the Institute of Textiles and Clothing, The Hong Kong Polytechnic University. This project is funded by Laboratory for Artificial Intelligence in Design.

**Who has reviewed the study?**

The study has been reviewed by the Departmental Research Committee of the Institute of Textiles and Clothing, The Hong Kong Polytechnic University.

Please keep this information sheet for your reference, together with a signed consent form. Should you have any queries, please do not hesitate to contact Dr. Joanne Yip at 2766 4848. Thank you very much in helping us to improve our patients' care. Updates of this study will only be informed, if necessary.

Dr. Yip Yiu Wan, Joanne  
Chief Supervisor  
Tel: +852-27664848  
Email: [joanne.yip@](mailto:joanne.yip@)

## 資料篇

### 姿勢矯正束身衣對早期脊柱側彎青少年的有效性

我們誠意邀請閣下參與一項研究，這項研究由香港理工大學紡織及製衣學系教職員葉曉雲博士及其成員籌劃。請詳細閱讀以下資料，亦可與親友或你的家庭醫生諮詢意見。若有任何不清晰的地方或需要更多資料，請隨時向我們提出。請詳細考慮你是否願意參與。

#### 研究主旨

這項研究的目的是獲得臨床資料，以評估姿勢矯正束身衣對早期脊柱側彎青少年的有效性。姿勢矯正束身衣可提供支撐及矯正力，有助於控制青少年的不良姿勢，從而減低脊柱持續變形的可能性。我們會量度並記錄參加者的脊骨狀況、體形、姿勢變化、身體對稱度、紅外熱像、本體感覺、穿戴束身衣的舒適度（例如熱舒適性和壓力分佈）等資料作出分析。而整個臨床程序及參加者對穿戴束身衣的反饋亦將會被記錄。

#### 誰會被邀請參與這項研究？

此研究會在小學或中學進行篩選，並邀請被診斷患有輕微的脊柱側彎（側彎角度需少於 20°）及很大機會有脊柱持續變形的女童進行徹底的評估。被邀參與的女童年齡需介乎 10 至 13 歲。

#### 受試者招募的排除標準

任何人符合以下其中一項或多於一項，將不會被招募：(1)有 AIS 手術或矯形治療史，(2)不適合進行 X 光掃描或肺部檢查，(3)最近有外傷，(4)有精神障礙，(5)有皮膚過敏，或 (6)不願意按指示進行姿勢矯正束身衣穿著試驗。

#### 決定參加後，你需要做什麼？

一開始，參加者將被邀請在醫療中心進行 X 光掃描，以檢查其脊柱狀況（例如脊柱側彎情況及角度）。研究人員亦將會使用三維人體素描及直接測量的方法來獲取參加者的身形尺寸。獲得的測量結果將用於姿勢矯正束身衣的準備，包括試身及填充襯墊的處方（用於產生點壓力）。完成試身後，參加者會被安排參與數小時的初期穿著試驗。初期穿著試驗完畢後，參加者需再次進行 X 光掃描及評估，以分析穿戴束身衣的初步效果。如束身衣對參加者的情況有正面的改善效果，參加者將被進一步安排參與為期六至九個月的臨床穿著試驗。

在這六至九個月的臨床穿著試驗期間，研究人員會定期為參加者進行脊柱狀況、姿勢變化、身體對稱度、坐姿壓力分佈、本體感覺等方面的監測，以了解姿勢矯正束身衣的有效性。這些數據將會每兩至三個月收集一次，而收集數據時所使用的方法包括 X 光掃描、三維人體掃描、壓力傳感測量及三維動態捕捉等。研究人員亦會使用紅外攝像機拍攝參與者的紅外熱圖像以進行熱舒適性分析。此外，研究人員將會使用溫度記錄器和壓力傳感器，相應地記錄參加者日常穿戴束身衣的頻率和束身衣在參加者身上所產生的界面壓力。參加者還將會被邀請進行問卷調查和簡短訪談，以收集其寶貴反

饋並了解其心理變化。

### **參加是次計劃有什麼好處？**

這項研究旨在為評估姿勢矯正束身衣對早期脊柱側彎青少年的有效性提供必要的臨床信息。與現有的定期觀察、矯形模具及手術相比，我們希望可以為患有輕微脊柱側彎的青少年提供一項較少侵入性的矯形治療，透過貼身舒適及較容易接納的治療方法去改善患者的不良姿勢，從而減低脊柱持續變形的可能性，使其健康成長。

### **您必須參與此研究計劃嗎？**

本計劃全屬自願性質，您可自行選擇是否參加。如果您決定參加，請保存這張詳細資料單張及簽署同意書。在研究過程中，您有權隨時無條件退出本研究計劃。不論任何決定皆不會影響您在診所接受的服務質素。若您在研究期間無故缺席相關的跟進檢查，您的參加資格將被取消，恕不另行通知。

### **參與此研究存在風險嗎？**

三維人體掃描、坐姿壓力分佈檢查、三維動態捕捉、紅外攝像拍攝、日常穿著頻率監測和束身衣界面壓力測量，並不存在任何對人體有害的風險。而除了在計劃開始時部份參加者可能需進行的一次臥位 X 光掃描外，其餘的都是採用低輻射劑量 X 光掃描。低輻射劑量 X 光掃描的拍攝頻率，將參考相關專業人士的建議，相信只會對人體造成輕微的幅射影響。

姿勢矯正束身衣的選料及設計亦安全，舒適。與硬的矯形模具或現有的姿勢矯形背心比較，個別受試者或有輕微皮膚敏感或因物料壓力造成不適。然而，在束身衣的設計及發展過程中，物料已於受試者身上使用及研究了一段短時間。故與此研究有關的創傷均沒有任何意外賠償。

雖然只有在初期穿著試驗獲得正面改善效果的參加者才會被邀請參與為期三至九個月的臨床穿著試驗，但此三至九個月的臨床穿著試驗最終或有機會未能成功改善患者的姿勢及脊柱側彎情況，或有可能出現惡化的機會。故此，閣下需在參與本計劃前仔細考慮並平衡當中涉及的利益及風險項目。

### **如果出現任何事故怎麼辦？**

本研究計劃並沒有設特殊的補償安排。若您欲就本研究提出任何投訴，您可親自或以書面形式聯繫香港理工大學道德評議會秘書 (c/o M1303, 大學人力資源辦公室)。

### **我參與這研究資料是否保密？**

是。如您決定參與此計劃，當中獲得的參加者個人資料及研究數據只會用作研究用途，並由今次的研究人員全權收集及分析。所得的資料一概保密。

### **所得的研究結果將會如何處理？**

研究結果將會被發佈在醫學矯形和紡織設計刊物等。

### **誰統籌及資助此項研究計劃？**

這項研究計劃由香港理工大學紡織及製衣學系統籌，並獲人工智能設計研究所資助。

### 誰曾審核此研究?

這項研究經由香港理工大學紡織及製衣學系研究委員會審批。

請小心保存這份資料和已簽署的同意書作日後參考。

如有疑問請致電 2766 4848 向葉曉雲博士查詢。特此再次感謝您的參與，閣下的支持定能對將來改善醫院病人的服務有很大的幫助。

有關此研究的更新資料或資訊，有需要時將會個別另行通知。

研究組組長

葉曉雲博士

Tel: +852-27664848

Email: [joanne.yip@](mailto:joanne.yip@polyu.edu.hk)

### Appendix III

Inform consent for the wear trial of this study.

(English version)

#### PARTICIPANT CONSENT FORM

### **Title of Project: Effectiveness of Posture Correction Girdle in Adolescents with Early Scoliosis**

Name of Researchers: Ms. LIU Pak Yiu, Dr. YIP Yiu Wan

1. I confirmed that I have read and understand the information sheet dated \_\_\_\_/\_\_\_\_/\_\_\_\_ for the above study and have had the opportunity to ask questions.
2. I understand that my child's participation is voluntary and that I am free to withdraw at any time, without giving any reasons, without my legal rights being affected.
3. I understand that sections of any of my child's medical notes may be looked at by responsible individuals from the researcher's team or from regulatory authorities where it is relevant to my taking part in research. I give permission for these individuals to have access to my records.
4. The results will be published in referred journal. All information collected will be kept confidential.
5. I agree to take part in the above study.

_____	_____	_____
Name of parent/Legal guardian	Date	Signature

_____	_____	_____
Name of witness (if applicable)	Date	Signature

_____	_____	_____
Researcher	Date	Signature

(Chinese version)

## 參與研究項目同意書

研究主題：姿勢矯正束身衣對早期脊柱側彎青少年的有效性

研究人員名稱：廖栢堯小姐, 葉曉雲博士

1. 本人確定已詳細閱讀並了解於\_\_\_\_\_/\_\_\_\_\_/\_\_\_\_\_提供之資料單張,並已有足夠時間發問問題。
2. 本人明白是次參與全是自願性質, 本人有權隨時退出而不必提出任何理由, 而本人法律權利不會有改變。
3. 本人明白及同意本人子女之病歷記錄需要時給與研究員和有關人事作參考。
4. 研究結果將會發報在醫學矯形和紡織設計刊物內。其他收集的資料一概保密
5. 本人同意參與此項研究。

\_\_\_\_\_  
參加者家屬/監護人姓名

\_\_\_\_\_  
日期

\_\_\_\_\_  
簽名

\_\_\_\_\_  
見証人(如適用)

\_\_\_\_\_  
日期

\_\_\_\_\_  
簽名

\_\_\_\_\_  
研究員

\_\_\_\_\_  
日期

\_\_\_\_\_  
簽名

## Appendix IV

Scoliosis Research Society (SRS-22) questionnaire  
(Chinese version)

### SRS-22 Questionnaire SRS-22 病人問卷

姓名: \_\_\_\_\_ 出生日期 (年/月/日): \_\_\_\_\_ 性別: \_\_\_\_\_ M /  
F \_\_\_\_\_  
電話: \_\_\_\_\_ 年齡: \_\_\_\_\_

\*指示: 我們正在小心評估你背部的情況，因此問卷上的每一條問題必須由你親自回答。  
請在每一條問題所提供的選擇中，小心圈出你認為最正確的一個答案。

1. 以下哪一項最能夠準確描述你在過去六個月所感受到痛楚的程度？  
無痛楚 / 輕微 / 中等 / 中等至嚴重 / 嚴重
2. 以下哪一項最能夠準確描述你在過去一個月所感受到痛楚的程度？  
無痛楚 / 輕微 / 中等 / 中等至嚴重 / 嚴重
3. 整體來說，在過去六個月期間你有感到十分焦慮嗎？  
完全沒有 / 小部分時間 / 有時 / 大部分時間 / 全部時間
4. 如果你必須在背部維持現狀不變的情況下繼續生活，你會有甚麼感受？  
十分愉快 / 某程度上愉快 / 沒有愉快或不愉快 / 某程度上不愉快 / 十分不愉快
5. 你現時的活動能力如何？  
只限於床上 / 基本上不能活動 / 些微的運動及勞動 / 有限度的運動及勞動 / 活動不受限制
6. 你在穿上衣服後的外觀如何？  
很好 / 好 / 可以接受 / 差勁 / 十分差勁
7. 在過去六個月期間你曾感到十分沮喪以至於任何事物也不能讓你開懷嗎？  
經常 / 大多數時間 / 有時 / 很少數時間 / 完全沒有

8. 你在休息時背部有感到疼痛嗎？  
經常 / 大多數時間 / 有時 / 很少數時間 / 完全沒有
9. 你現時在工作/學校的活動能力為多少？  
正常的 100% / 正常的 75% / 正常的 50% / 正常的 25% / 正常的 0%
10. 以下哪一項最能夠描述你軀幹的外觀？(軀幹的定義為人的身體除去頭部及四肢)  
很好 / 好 / 可以接受 / 差勁 / 十分差
11. 下例哪一項最能準確地描述你因背部疼痛而所需要服用的藥物？  
無 / 一般止痛藥(每星期服用一次或更少) / 一般止痛藥(天天服用) /  
特效止痛藥(每星期服用一次或更少) / 特效止痛藥(天天服用) /  
其他 [ 藥物名稱：\_\_\_\_\_ 使用程度(每星期或更少或天天):  
\_\_\_\_\_ ]
12. 你的背部疼痛有否影響你做家務的能力？  
沒有 / 少許 / 某程度上有 / 很大程度上有 / 經常有
13. 整體來說，你在過去六個月期間有感到安寧和平靜嗎？  
經常 / 大多數時間 / 有時 / 很少數時間 / 完全沒有
14. 你有否感到你背部的狀況對你的人際關係構成影響？  
沒有 / 少許 / 某程度上有 / 很大程度上有 / 經常有
15. 你以及/或你的家人有否因為你背部的問題而在經濟方面遇到困難？  
極有 / 很大程度上有 / 某程度上有 / 少許 / 沒有
16. 整體來說，在過去六個月期間你有否感到失落和灰心？  
完全沒有 / 很少數時間 / 有時 / 大多數時間 / 經常
17. 在過去三個月期間你有否因背痛而向學校/公司請假？如有，共有多少天？  
零天 / 一天 / 兩天 / 三天 / 四天或以上

18. 你背部的狀況有否阻礙你和家人/朋友外出？  
從來沒有 / 很少數時間 / 有時 / 大多數時間 / 經常
19. 你現時背部的狀況會否讓你覺得自己仍有吸引力？  
會，很有吸引力 / 會，某程度上有吸引力 / 無影響 /  
否，沒有甚麼吸引力 / 否，完全沒有吸引力
20. 整體來說，你在過去的六個月裏感到愉快嗎？  
完全沒有 / 很少數時間 / 有時 / 大多數時間 / 經常
21. 你對你背部治療的成效感到滿意嗎？  
十分滿意 / 滿意 / 不是滿意也不是不滿意 / 不滿意 / 非常不滿意
22. 如果你的背部再次遇到同類的情況你會否接受同樣的治理？  
一定會 / 可能會 / 不清楚 / 可能不會 / 一定不

多謝你的合作，如有任何意見請填寫在以下的空位上。

~問卷完~

## Appendix V

### Brace Questionnaire (BrQ)

(Chinese version)

### Brace Questionnaire (BrQ)

姓名：\_\_\_\_\_ 日期：\_\_\_\_\_

本問卷旨於了解你在佩戴支架時，對自己健康的看法。本問卷並非測驗，答案並無對錯之分。請仔細閱讀每條題目，自行選取你認為最適當的答案，並以✓標示。

#### 個人資料

請填寫你的背景資料。

年齡：\_\_\_\_\_

你從\_\_\_\_\_開始佩戴支架

你每天佩戴支架\_\_\_\_\_小時

在過去3個月...	從不	幾乎不會	有時	大部份時間	經常
1. 支架令你有生病的感覺					
2. 你害怕背部情況會惡化					

在過去3個月，你佩戴支架時...	從不	幾乎不會	有時	大部份時間	經常
3. 你走路時感到疲倦					
4. 你能跑步					
5. 你能在沒有任何協助下佩戴支架					
6. 你能在沒有任何協助下除下支架					
7. 你的胃口不佳					
8. 你睡得不好					
9. 你呼吸不暢順					

在過去3個月...	從不	幾乎不會	有時	大部份時間	經常
10. 你因支架而感到緊張					
11. 你因支架已感到擔心					
12. 你感到快樂					
13. 你相信如果不用佩戴支架的話你會生活得更好					
14. 你相信支架治療是有益處的					

在過去1個月...	從不	幾乎不會	有時	大部份時間	經常
15. 你感到自豪					
16. 你為自己的身體感到滿意					

在過去1個月...	從不	幾乎不會	有時	大部份時間	經常
17. 你感到強壯和充滿力量					
18. 你因支架而感到疲倦乏力					

在過去1個月...	從不	幾乎不會	有時	大部份時間	經常
19. 你上課時遇到困難					
20. 你曾經缺課					
21. 你發覺上課時難以集中精神					

在過去1個月...	從不	幾乎不會	有時	大部份時間	經常
22. 你需服藥止痛					
23. 你晚上有痛楚					
24. 你走路時有痛楚					
25. 你坐着是有痛楚					
26. 你上落樓梯時又痛楚					
27. 你的手臂或大腿有針刺般的					

感覺					
----	--	--	--	--	--

在過去1個月...	從不	幾乎不會	有時	大部份時間	經常
28. 你不能跟朋友外出					
29. 朋友同情你					
30. 你覺得自己有別於同儕（朋友）					
31. 跟家人相處有問題					
32. 你相信如果不用佩戴支架的話，你跟家人或朋友的關係會更好					
33. 因感到羞愧而留在家中					
34. 你穿着特別的衣服					

~問卷完~

## Appendix VI

Bad Sobernheim Stress Questionnaire (BSSQ)-Brace questionnaire  
(Chinese version)

### Bad Sobernheim Stress Questionnaire

#### BSSQ-支具 問卷調查表

以下問題均與您戴矯形支具的感受有關，請認真閱讀問題並以真實的感受作答。以下問題的答案分析，將有助於我們評估出或識別出矯形支具帶給您在心理方面的壓力，在對您進一步的治療中將給予我們很好的建議或指導方向。

[\* 請在所選答案旁的方格中畫上別號]

1. 我身體外觀在姿勢矯正束身衣內，我覺得不舒適。  
完全正確    差不多正確    幾乎不正確    完全不正確
2. 對我來說，我脫下姿勢矯正束身衣是很困難的。  
完全正確    差不多正確    幾乎不正確    完全不正確
3. 當別人能看到我佩戴的姿勢矯正束身衣的情況下，我覺得不舒服。  
完全正確    差不多正確    幾乎不正確    完全不正確
4. 當別人看我佩戴的姿勢矯正束身衣時我不會感到尷尬。  
完全正確    差不多正確    幾乎不正確    完全不正確
5. 我盡量避免身體接觸以至於沒人知道我佩戴姿勢矯正束身衣。  
完全正確    差不多正確    幾乎不正確    完全不正確
6. 當決定穿什麼衣服時或戴假髮時，我試圖確保我的姿勢矯正束身衣隱藏好。  
完全正確    差不多正確    幾乎不正確    完全不正確
7. 在我親近的人面前展現我佩戴的姿勢矯正束身衣我不感到尷尬（例如：父母，朋友，同學）。  
完全正確    差不多正確    幾乎不正確    完全不正確
8. 由於佩戴姿勢矯正束身衣，我避免活動/興趣愛好，即便這些活動是我以前愛做的。  
完全正確    差不多正確    幾乎不正確    完全不正確

~問卷完~

## Appendix VII

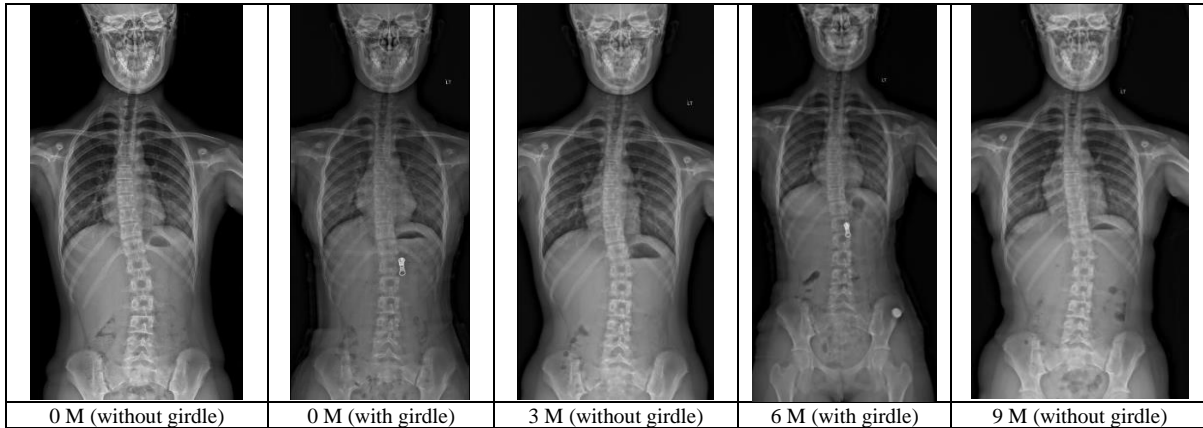
### Body measurements of the recruited subjects

	Measurement items	Measurements of the recruited subjects (cm)									
		Subject 1	Subject 2	Subject 3	Subject 4	Subject 5	Subject 6	Subject 7	Subject 8	Subject 9	Subject 10
1	<b>Over Bust Girth</b>	74	80	82.3	84	78.5	74.5	81	81	73	77
2	<b>Full Bust Girth</b>	75	78.5	81.5	85	79	74.5	78	80.5	71	75
3	<b>Under Bust Girth</b>	65	69	70.5	71	66.5	64	68	68.5	59	64
4	<b>Waist Girth</b>	62	64.5	69	73	65.5	61	62	67	56.5	62
5	<b>Mid Hip Girth</b>	68	69	80.5	84	85	66.5	71	77	69	81
6	<b>Hip Girth</b>	80	85	93	89.5	90	73.5	83	89	83	88
7	<b>Thigh Girth</b>	48.5	50	53	52	56	42	48	52	93.5	47
8	<b>Knee Girth</b>	33	30	33.5	39	37	29	32	36.5	31	36.5
9	<b>Ankle Girth</b>	23.5	21	24	21.5	22	23	21.5	22.5	20	21
10	<b>Bicep Girth</b>	24.5	26	26.4	25.5	24.5	19	22	25	20	21.5
11	<b>Elbow Girth</b>	22	21	23	23	22	19.5	21	23	20	22.5
12	<b>Wrist Girth</b>	15	14	16	16.3	15	14	14.5	16	13.5	15
13	<b>Across Front</b>	29.5	28	28	30	30	29	30	30	26	29
14	<b>Bust Point to Bust Point</b>	15	18	16.5	15.5	18	17	16.5	17	15	16
15	<b>Crotch Depth</b>	20	21	21	26	21	21.2	23	21.5	21.5	22.5
16	<b>Shoulder</b>	20	19	20	19.2	13	14.2	15.5	14	14	15
17	<b>Across Shoulder</b>	40	39.5	40.5	38	38	28	41	39	40	42.5
18	<b>Across Back</b>	33	33	35	30	32	32	32	33	32	32
19	<b>Nape to Armhole depth</b>	16.5	16	14	15.5	17	18.5	15	14.5	14.5	19.5
20	<b>Nape to Waist</b>	34.5	26	25	35.5	35	36	32	33	35.5	36
21	<b>Nape to Ground</b>	127.5	133	135	139.2	135	13.8	136	125	136	141.5
22	<b>Sleeve Length</b>	50	49	26	54.5	50.5	55	53.5	48	51	50.5
23	<b>Waist to High Hip</b>	8	10	9.5	11	11	10.5	10	10	11	11
24	<b>Waist to Hip</b>	14	16.5	16.5	20.5	16	18.5	19	20	21	18
25	<b>Waist to Knee</b>	54	53	56.5	55	57	59.5	53	53	58	59.5
26	<b>Waist to Ankle (out seam)</b>	89	96	91	98	94.5	98.5	98	88	98	99
27	<b>Inseam</b>	72	73.5	75	74.2	74.5	79.5	77	66.5	74.8	81
28	<b>Crotch Length</b>	59	58.5	98	69.5	60.5	56	58	61.5	56	56
29	<b>Spine length (C7 to pelvis level)</b>	40	40.5	44.5	43.5	41	39.5	41.5	40	42.5	45.5

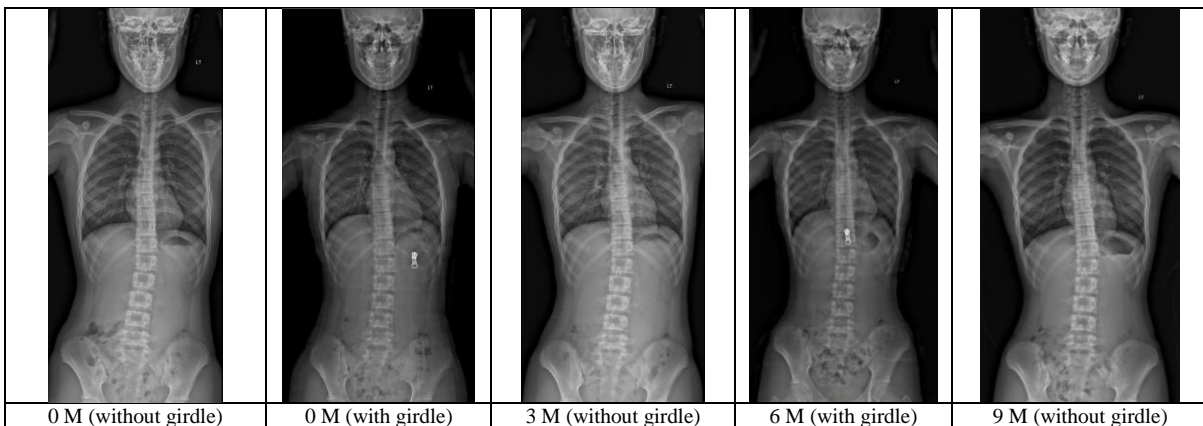
## Appendix VIII

### Radiographic images of the recruited subjects

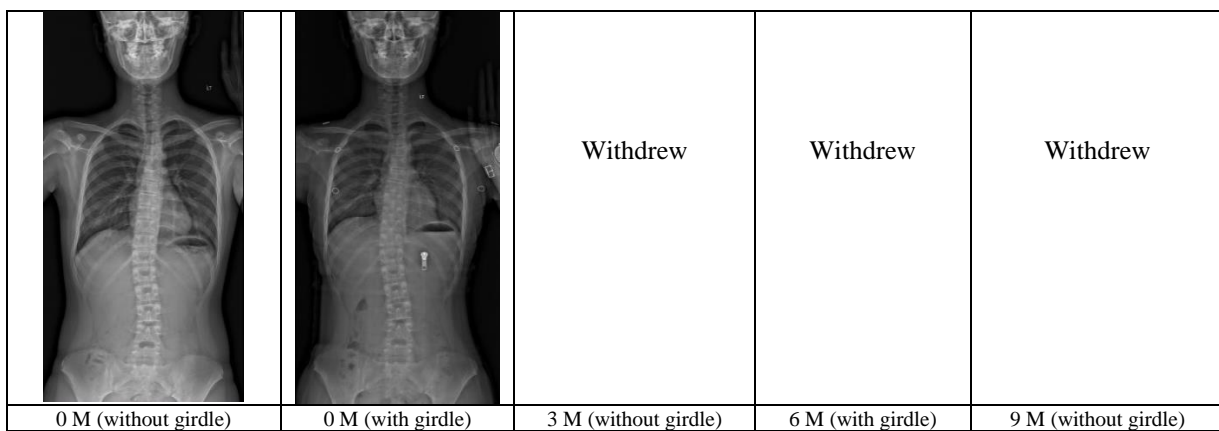
#### Subject 001



#### Subject 002



#### Subject 003



Subject 004

		Withdrew	Withdrew	Withdrew
0 M (without girdle)	0 M (with girdle)	3 M (without girdle)	6 M (with girdle)	9 M (without girdle)

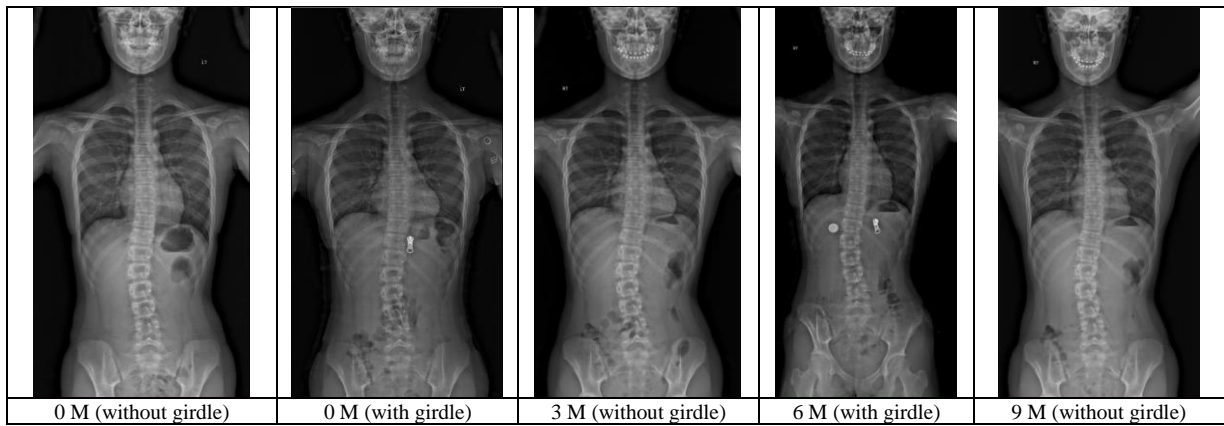
Subject 005

				
0 M (without girdle)	0 M (with girdle)	3 M (without girdle)	6 M (with girdle)	9 M (without girdle)

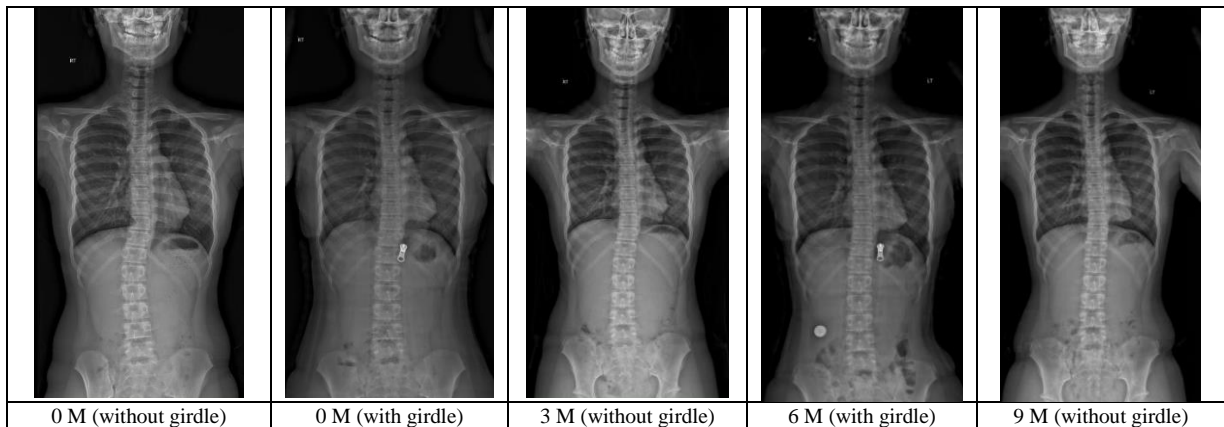
Subject 006

				
0 M (without girdle)	0 M (with girdle)	3 M (without girdle)	6 M (with girdle)	9 M (without girdle)

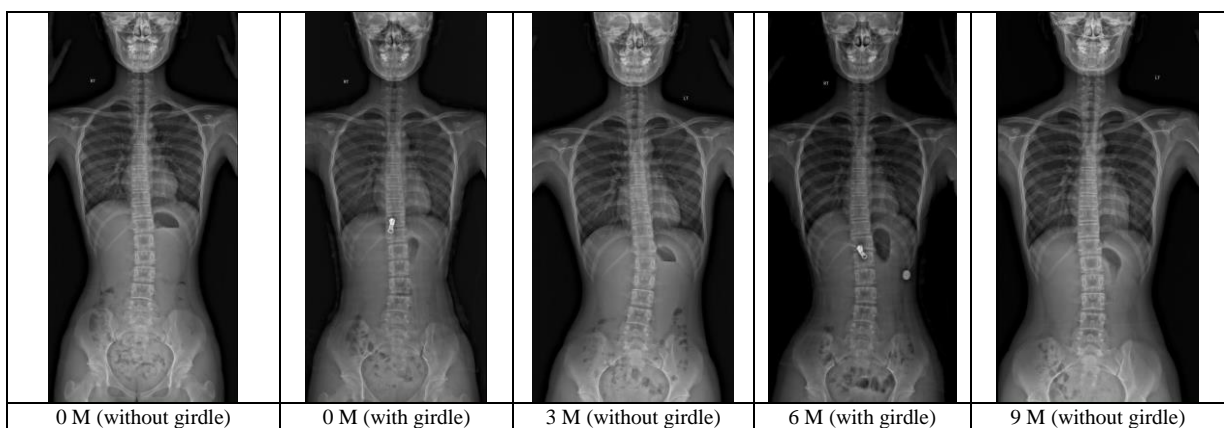
Subject 007



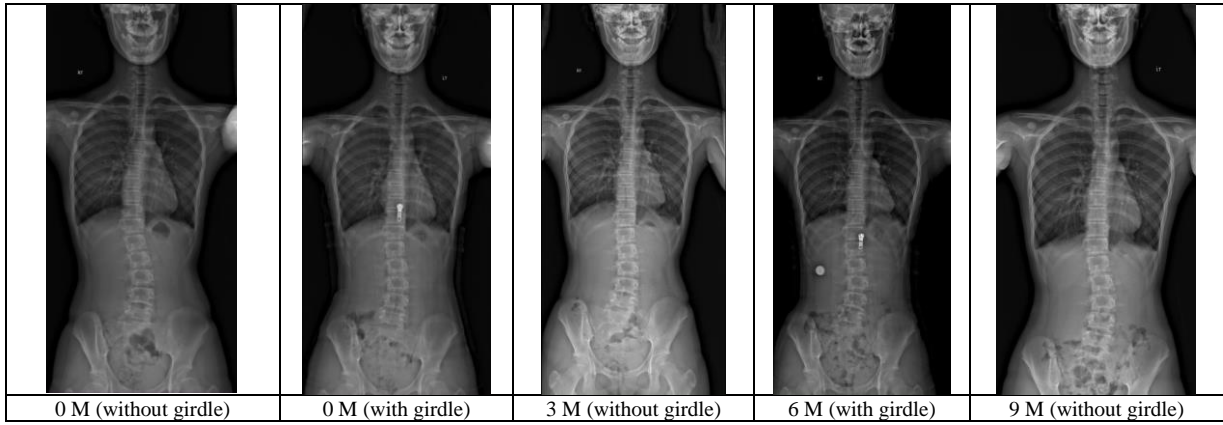
Subject 008



Subject 009



Subject 010



## Appendix IX

Details of the posture angle results at 0 M, 3 M, 6 M and 9 M.

### 1. Posture angles of asymmetry of the acromion in frontal plane during habitual standing (°)

Subject	0 M		3 M		6 M		9 M	
	Without girdle	With girdle						
1	1.2111	0.9827	0.7252	0.8519	1.0185	0.2407	0.2604	0.2274
2	2.9519	1.3904	1.3694	0.2418	1.302	0.5093	0.02	0.4639
3	2.3786	2.2231	Withdrew	Withdrew	Withdrew	Withdrew	Withdrew	Withdrew
4	3.5988	2.3859	Withdrew	Withdrew	Withdrew	Withdrew	Withdrew	Withdrew
5	1.9001	0.8032	1.5009	0.9821	0.2741	0.2768	0.2908	0.5701
6	2.4195	0.6095	1.5275	0.5405	1.3837	0.8032	1.1573	0.8509
7	2.7102	0.8681	1.8476	0.9203	0.2653	0.2634	0.5457	0.217
8	0.6959	0.3031	0.7144	0.1532	0.4918	0.2616	0.1942	0.1969
9	2.3859	0.8263	1.322	0.4658	0.9152	0.7102	0.2285	0.2558
10	2.07	1.5552	0.8343	0.5563	0.5758	0.1785	0.9203	0.7742

### 2. Posture angles of pelvis balance in frontal plane during habitual standing (°)

Subject	0 M		3 M		6 M		9 M	
	Without girdle	With girdle						
1	2.1734	0.971	0.8814	0.1955	1.8111	1.0723	1.6288	0.1614
2	0.8376	0.104	0.8859	1.6273	1.8368	1.2454	0.5968	0.7308
3	2.1535	0.4614	Withdrew	Withdrew	Withdrew	Withdrew	Withdrew	Withdrew
4	1.361	1.2894	Withdrew	Withdrew	Withdrew	Withdrew	Withdrew	Withdrew
5	2.07	0.7417	1.116	0.6228	0.3854	0.2809	0.4324	0.2946
6	0.7742	0.7742	0.8092	0.2731	1.1382	0.8092	0.5927	0.7088
7	1.4411	0.4049	1.1151	0.8628	0.6334	0.1779	0.1596	0.4049
8	0.6031	0.4419	0.7465	0.4683	0.7441	0.5947	0.5631	0.1866
9	1.302	0.9602	1.3603	1.3357	1.2254	0.6338	0.4063	0.312
10	1.6847	1.2364	1.3712	1.0897	1.3804	0.4324	1.4576	0.6821

### 3. Posture angles of acromion/ pelvis balance in frontal plane during habitual standing (°)

Subject	0 M		3 M		6 M		9 M	
	Without girdle	With girdle						
1	0.9623	0.0117	1.6066	1.0475	0.7926	1.313	1.3684	0.3888
2	2.1143	1.2864	2.2553	1.3855	3.1388	1.7547	0.6168	0.2669
3	4.5321	1.7617	Withdrew	Withdrew	Withdrew	Withdrew	Withdrew	Withdrew
4	2.2378	1.0965	Withdrew	Withdrew	Withdrew	Withdrew	Withdrew	Withdrew
5	0.1699	0.0615	2.6169	1.6049	0.6596	0.0041	0.7232	0.2755
6	1.6453	1.3837	0.7183	0.8136	0.2455	0.006	0.5646	1.5597
7	4.1513	0.4631	2.9627	0.0575	0.8987	0.0855	0.3861	0.6219
8	0.0928	0.1387	0.0321	0.3152	1.2359	0.3331	0.3689	0.2901
9	3.6879	0.1339	2.6823	1.8015	2.1406	0.0764	0.6348	0.0562
10	3.7547	0.3188	2.2055	0.5334	1.9562	0.6109	2.3779	1.4563

### 4. Posture angles of asymmetry of the acromion in horizontal plane during habitual standing

(°)

Subject	0 M		3 M		6 M		9 M	
	Without girdle	With girdle						
1	3.1195	1.6563	1.9092	0.2199	0.6987	0.4775	0.2374	0.2283
2	1.9908	2.7501	1.6603	3.2809	1.0178	1.4834	1.688	1.0285
3	4.2157	2.5208	Withdrew	Withdrew	Withdrew	Withdrew	Withdrew	Withdrew
4	3.0448	0.7421	Withdrew	Withdrew	Withdrew	Withdrew	Withdrew	Withdrew
5	1.232	0.7293	0.8283	0.125	1.3211	1.6918	1.6847	1.9886
6	1.8436	1.752	2.6246	1.8337	1.8328	0.5737	0.538	0.2292
7	3.5297	2.447	1.152	1.4934	2.2508	2.5077	0.7457	1.6789
8	6.9245	1.4586	3.0498	2.3191	1.4321	0.6174	0.5752	0.5684
9	5.7354	3.0692	2.9176	0.9414	1.4738	1.1167	1.0374	0.7332

10	0.9454	1.1504	0.7957	0.5055	0.3898	1.273	0.8425	0.958
----	--------	--------	--------	--------	--------	-------	--------	-------

### 5. Posture angles of pelvis balance in horizontal plane during habitual standing (°)

Subject	0 M		3 M		6 M		9 M	
	Without girdle	With girdle						
1	3.6491	6.9811	5.7583	2.1369	3.2262	3.2062	3.4239	1.5154
2	6.1615	0.8088	2.9767	2.51	1.5558	1.2571	1.5637	1.6576
3	0.382	1.3748	Withdrew	Withdrew	Withdrew	Withdrew	Withdrew	Withdrew
4	1.0809	1.1282	Withdrew	Withdrew	Withdrew	Withdrew	Withdrew	Withdrew
5	1.7986	0.674	0.8283	0.4316	0.352	1.5183	2.5125	1.3276
6	3.8587	2.8298	3.0968	2.782	3.8345	1.6239	0.1067	0.5691
7	1.0076	3.8347	0.7902	0.3657	4.5916	5.4142	1.3551	1.7475
8	1.1935	0.6183	1.7843	2.3859	0.958	0.4102	0.6366	0.703
9	1.8779	3.4456	0.8127	1.2212	1.2029	1.2146	0.8425	0.9335
10	1.7062	2.155	1.3946	1.086	1.4688	0.7864	1.6083	1.0521

### 6. Posture angles of scapula asymmetry in horizontal plane during habitual standing (°)

Subject	0 M		3 M		6 M		9 M	
	Without girdle	With girdle						
1	3.2705	2.7065	2.4658	1.9378	1.8813	3.0566	1.8745	1.9481
2	3.9843	0.2558	2.0601	2.6425	1.8087	1.3254	1.5665	1.1573
3	0.4639	0.1936	Withdrew	Withdrew	Withdrew	Withdrew	Withdrew	Withdrew
4	1.6413	1.2018	Withdrew	Withdrew	Withdrew	Withdrew	Withdrew	Withdrew
5	1.727	0.7588	0.7275	1.259	0.1819	1.7127	0.4825	0.7605
6	1.5566	1.3535	1.5208	1.4372	2.1124	0.8831	0.6031	0.8475
7	2.7263	2.5169	0.4571	1.2873	4.648	5.5845	2.0402	1.8183
8	3.9517	3.3019	1.8648	3.2336	0.7598	1.4321	0.439	0.439
9	1.7135	1.4321	2.8986	2.1728	1.6713	1.0813	1.3322	0.7994
10	1.8626	1.0512	1.7776	0.85	1.4548	1.023	0.639	1.2545

### 7. Posture angles of acromion/ scapula asymmetry in horizontal plane during habitual standing (°)

Subject	0 M		3 M		6 M		9 M	
	Without girdle	With girdle						
1	0.5296	4.3628	0.5566	2.3568	2.5275	3.5341	1.6371	2.1764
2	5.9751	3.0059	0.3998	0.7709	2.8265	0.2263	3.1302	0.1288
3	4.6796	2.7144	Withdrew	Withdrew	Withdrew	Withdrew	Withdrew	Withdrew
4	4.6861	1.8703	Withdrew	Withdrew	Withdrew	Withdrew	Withdrew	Withdrew
5	0.0716	0.0295	0.1008	1.384	1.503	0.0209	2.1682	1.2281
6	0.2871	0.3935	1.1038	0.3965	0.2796	0.3094	1.1411	1.0767
7	0.8033	0.0698	0.6949	1.8591	2.3972	3.0768	1.2945	0.1394
8	2.9728	1.8433	1.185	0.9145	0.6723	2.0495	1.0142	0.1294
9	4.0219	1.6371	0.019	1.2314	0.1975	0.0354	0.2948	1.5326
10	0.9172	0.0992	0.9819	0.3445	1.065	0.2	0.2035	2.3066

### 8. Posture angles of acromion/ pelvis balance in horizontal plane during habitual standing (°)

Subject	0 M		3 M		6 M		9 M	
	Without girdle	With girdle						
1	6.39	8.6374	3.8491	1.917	1.1826	3.6836	3.1865	1.7437
2	4.1707	1.9413	4.637	0.6384	2.5736	2.7405	0.1243	0.6291
3	4.5977	1.146	Withdrew	Withdrew	Withdrew	Withdrew	Withdrew	Withdrew
4	1.9639	0.4597	Withdrew	Withdrew	Withdrew	Withdrew	Withdrew	Withdrew
5	0.5666	0.553	1.6566	0.5566	1.6731	0.1735	0.8278	3.3162
6	2.015	4.5818	0.4722	0.9483	2.0017	1.0502	0.4313	0.7983
7	4.5373	1.3877	1.9422	0.2061	2.3408	2.9065	0.6094	0.0686
8	5.731	0.8403	1.2655	0.0668	2.3901	0.2072	0.0614	0.1346
9	7.6133	0.3764	2.1049	0.2798	0.2709	0.0979	0.1949	1.6667
10	0.7608	1.0046	2.5733	0.5805	1.079	2.0594	0.7658	0.0941

**9. Posture angles of thoracic curve in sagittal plane during habitual standing (°)**

Subject	0 M		3 M		6 M		9 M	
	Without girdle	With girdle						
1	152.4133	160.8844	156.4167	159.1431	158.9977	161.4533	158.2196	158.272
2	147.5641	159.9615	154.7259	157.0051	156.176	157.2384	156.8358	156.0219
3	155.1825	157.0304	Withdrew	Withdrew	Withdrew	Withdrew	Withdrew	Withdrew
4	153.7856	156.5946	Withdrew	Withdrew	Withdrew	Withdrew	Withdrew	Withdrew
5	147.1814	156.4768	152.3189	159.6398	157.4331	158.9584	161.4061	161.9427
6	151.6272	157.0755	154.961	161.8391	154.8789	164.534	156.5302	161.8152
7	155.3479	156.9436	162.4747	164.486	160.0699	162.6176	159.8112	161.0877
8	150.0929	162.3932	157.0377	161.736	164.6569	164.6635	167.6798	165.0948
9	152.1726	168.2211	164.5363	165.2856	164.2474	167.002	166.5887	166.1073
10	158.9487	166.9379	166.7489	166.9047	167.0169	171.5111	164.9053	169.7349

**10. Posture angles of lumbar curve in sagittal plane during habitual standing (°)**

Subject	0 M		3 M		6 M		9 M	
	Without girdle	With girdle						
1	144.1837	151.6575	148.8465	158.1303	144.8156	159.0491	145.1904	157.4826
2	153.1744	155.8471	143.0272	159.915	152.5209	170.6424	154.2782	163.6066
3	154.0435	159.1432	Withdrew	Withdrew	Withdrew	Withdrew	Withdrew	Withdrew
4	147.6464	157.2672	Withdrew	Withdrew	Withdrew	Withdrew	Withdrew	Withdrew
5	146.8164	156.4768	147.6688	160.8655	148.8377	158.6147	156.5737	160.3337
6	147.0592	156.9446	160.1418	164.8527	162.2144	167.5461	154.1501	165.0591
7	149.6849	154.5456	156.1285	157.5957	160.484	164.5674	158.9142	170.5806
8	147.4774	154.6097	149.4708	158.6626	156.2099	163.0759	156.9582	163.5247
9	148.4946	165.3811	148.6343	166.0915	159.553	163.0011	152.0426	162.3114
10	166.3788	166.4622	167.3285	170.4897	170.6412	173.30598	167.5738	176.9471

**11. Posture angles of thoracic curve in sagittal plane during habitual sitting (°)**

Subject	0 M		3 M		6 M		9 M	
	Without girdle	With girdle						
1	163.6442	166.435	162.679	163.1524	171.6136	165.9382	169.2287	167.9821
2	156.0902	159.4094	149.1	160.7742	158.5	156.5209	163.2378	163.6434
3	152.0999	156.4757	Withdrew	Withdrew	Withdrew	Withdrew	Withdrew	Withdrew
4	160.3753	159.8962	Withdrew	Withdrew	Withdrew	Withdrew	Withdrew	Withdrew
5	147.8358	159.563	161.1963	162.5114	161.3007	162.955	160.1876	161.5192
6	142.1161	151.0555	154.6604	159.5618	160.9405	161.5533	158.724	159.3499
7	161.2812	164.1029	162.8771	163.2089	165.6258	166.6889	165.5943	163.9011
8	163.3865	163.9237	165.6208	166.0647	167.5345	168.3256	172.3138	172.6292
9	159.5537	161.529	160.2865	164.6237	168.165	169.0064	163.4248	165.566
10	165.2004	165.9527	167.7903	167.5392	168.6379	168.0427	172.1086	172.4834

**12. Posture angles of lumbar curve in sagittal plane during habitual sitting (°)**

Subject	0 M		3 M		6 M		9 M	
	Without girdle	With girdle						
1	186.8428	178.8032	162.0981	167.64	167.1769	169.1445	165.2747	171.9676
2	163.8663	170.5417	152.9	167.2369	164.2	169.0361	164.7794	171.2838
3	174.7404	177.1343	Withdrew	Withdrew	Withdrew	Withdrew	Withdrew	Withdrew
4	167.1718	169.7757	Withdrew	Withdrew	Withdrew	Withdrew	Withdrew	Withdrew
5	152.0052	174.0047	161.1963	171.554	167.5829	168.4825	162.7744	164.4613
6	157.419	167.2988	163.2327	168.8316	170.9994	172.7633	168.644	170.8304
7	163.8874	169.9555	169.9521	170.9494	166.1362	166.4189	169.839	173.3952
8	168.147	168.376	173.7509	174.3262	174.8153	174.9269	174.7706	174.9554
9	166.2408	172.8841	167.4155	176.4677	166.0382	174.6459	164.1912	169.2589
10	174.8056	175.4428	177.1187	177.0446	177.5954	176.2558	174.744	177.3091

# Appendix X

Details of the proprioception test results at 0 M, 3 M, 6 M and 9 M.

## Neck rotation

Subject code	Time of the test	0 month				3 month				6 month				9 month			
		Neck rotation - Concave		Neck rotation - Convex		Neck rotation - Concave		Neck rotation - Convex		Neck rotation - Concave		Neck rotation - Convex		Neck rotation - Concave		Neck rotation - Convex	
		no girdle	with girdle	no girdle	with girdle	no girdle	with girdle	no girdle	with girdle	no girdle	with girdle	no girdle	with girdle	no girdle	with girdle	no girdle	with girdle
Subject 1	3	3.42	2.57	4.07	1.82	2.21	2.33	1.09	2.48	2.07	2.73	1.73	3.61	2.11	1.44	2.30	1.18
Subject 2	3	1.31	2.29	6.29	5.69	3.28	1.85	4.50	5.60	3.66	4.53	4.80	4.78	3.49	4.83	4.51	3.44
Subject 3	3	3.50	4.17	3.67	4.12												
Subject 4	3	1.56	2.31	4.82	1.44												
Subject 5	3	3.31	2.89	3.32	2.55	0.78	3.76	1.26	2.32	1.22	1.91	1.85	2.34	1.43	0.93	0.95	0.68
Subject 6	3	3.30	2.21	2.27	1.80	2.92	1.15	1.58	3.22	3.02	3.51	2.65	2.15	2.42	1.42	3.18	2.33
Subject 7	3	1.30	1.89	2.23	1.38	2.56	1.78	2.74	1.85	1.36	0.61	1.06	1.10	2.08	1.27	1.19	0.97
Subject 8	3	4.80	5.05	3.48	5.80	4.75	3.15	10.25	2.36	2.74	2.71	3.74	2.81	2.62	3.08	2.52	2.90
Subject 9	3	2.64	3.61	2.01	1.52	1.08	2.40	1.29	1.29	0.99	1.78	1.05	1.75	1.90	2.72	1.72	1.67
Subject 10	3	1.38	2.95	1.72	2.96	1.41	2.24	1.92	1.12	1.87	1.79	1.79	2.15	1.20	1.84	1.14	1.34
P value of no girdle		0.5469		0.6406		0.8438		0.5781		0.2500		0.5469		>0.9999		0.1484	

Concave - 0 vs 9 month no girdle p value = 0.3281  
 Concave - 0 vs 9 month with girdle p value = 0.1953  
 Convex - 0 vs 9 month no girdle p value = 0.0391 \*  
 Convex - 0 vs 9 month with girdle p value = 0.0547

## Elbow flexion

Subject code	Time of the test	0 month				3 month				6 month				9 month			
		Elbow (dominant)		Elbow (non-dominant)		Elbow (dominant)		Elbow (non-dominant)		Elbow (dominant)		Elbow (non-dominant)		Elbow (dominant)		Elbow (non-dominant)	
		no girdle	with girdle	no girdle	with girdle	no girdle	with girdle	no girdle	with girdle	no girdle	with girdle	no girdle	with girdle	no girdle	with girdle	no girdle	with girdle
Subject 1	3	1.24	4.10	4.17	4.56	10.74	5.11	7.37	9.05	3.71	6.59	10.98	8.32	1.67	8.69	4.95	2.70
Subject 2	3	1.93	5.53	4.27	9.37	6.47	9.98	3.56	3.31	3.27	8.15	4.99	6.07	2.54	2.63	1.66	3.87
Subject 3	3	5.80	5.75	7.36	5.85												
Subject 4	3	5.37	7.21	5.58	13.89												
Subject 5	3	2.55	2.31	5.46	3.73	3.31	5.12	2.45	4.35	4.57	2.77	1.73	2.21	3.37	6.39	2.46	2.13
Subject 6	3	4.15	1.71	3.72	2.29	0.80	5.83	4.40	6.55	1.45	5.93	1.93	2.70	0.50	3.34	5.94	5.34
Subject 7	3	2.38	1.80	4.63	3.13	3.24	1.83	3.44	1.80	0.26	1.25	1.90	2.44	1.15	2.30	2.93	1.91
Subject 8	3	2.85	4.90	2.89	4.42	4.27	2.65	1.74	7.53	4.13	2.77	8.82	2.01	3.28	5.95	7.86	6.07
Subject 9	3	3.48	2.69	3.28	1.57	3.12	2.06	2.55	2.72	4.35	2.87	1.59	8.50	3.22	2.70	2.55	2.70
Subject 10	3	3.64	2.55	1.91	2.37	2.41	1.01	2.92	1.17	2.03	2.36	1.78	3.07	2.29	2.38	1.93	3.94
P value of no girdle		0.8438		0.8438		>0.9999		0.3125		0.4609		0.5469		0.0391*		0.6406	

Dominant - 0 vs 9 month no girdle p value = 0.6094  
 Dominant - 0 vs 9 month with girdle p value = 0.1953  
 Non-dominant - 0 vs 9 month no girdle p value = 0.9453  
 Non-dominant - 0 vs 9 month with girdle p value = 0.8438

## Knee extension

Subject code	Time of the test	0 month				3 month				6 month				9 month			
		Knee (dominant)		Knee (non-dominant)		Knee (dominant)		Knee (non-dominant)		Knee (dominant)		Knee (non-dominant)		Knee (dominant)		Knee (non-dominant)	
		no girdle	with girdle	no girdle	with girdle	no girdle	with girdle	no girdle	with girdle	no girdle	with girdle	no girdle	with girdle	no girdle	with girdle	no girdle	with girdle
Subject 1	3	1.40	1.48	4.89	2.92	4.20	3.77	1.76	3.23	3.41	2.47	1.75	4.86	1.97	1.70	5.17	2.37
Subject 2	3	3.04	3.31	3.02	3.58	2.99	1.26	3.59	1.54	3.00	0.45	2.94	2.82	2.09	2.25	1.33	0.44
Subject 3	3	1.38	2.12	4.88	2.92												
Subject 4	3	2.14	0.87	5.00	3.59												
Subject 5	3	3.23	2.26	4.31	3.12	1.22	2.87	2.28	2.72	6.39	2.86	3.39	3.45	4.09	5.01	3.27	3.87
Subject 6	3	1.75	0.62	2.40	3.06	1.01	3.12	0.97	2.53	1.82	2.78	2.46	2.59	1.59	0.90	1.59	0.90
Subject 7	3	0.60	2.09	0.85	3.11	1.62	2.75	3.98	2.95	1.14	2.85	2.47	1.06	3.26	0.67	2.30	0.83
Subject 8	3	3.29	5.38	5.31	6.83	3.07	3.33	2.13	0.83	5.89	6.15	8.02	3.55	3.68	4.42	2.74	4.99
Subject 9	3	2.29	1.22	3.77	1.27	1.57	1.62	1.78	2.07	0.88	2.33	0.80	0.96	1.26	0.40	1.17	1.21
Subject 10	3	3.18	1.18	1.51	1.88	2.27	2.23	1.15	1.49	2.16	1.69	2.61	0.93	1.26	1.61	1.17	1.59
P value of no girdle		0.9453		>0.9999		0.4609		0.9453		0.8438		0.7422		0.8438		0.5469	

Dominant - 0 vs 9 month no girdle p value = 0.9453  
 Dominant - 0 vs 9 month with girdle p value = 0.6406  
 Non-dominant - 0 vs 9 month no girdle p value = 0.1094  
 Non-dominant - 0 vs 9 month with girdle p value = 0.0547

## Unterberger stepping

Subject code	Time of the test	0 month				3 month				6 month				9 month			
		Stepping - displacement		Stepping - rotation		Stepping - displacement		Stepping - rotation		Stepping - displacement		Stepping - rotation		Stepping - displacement		Stepping - rotation	
		no girdle	with girdle	no girdle	with girdle	no girdle	with girdle	no girdle	with girdle	no girdle	with girdle	no girdle	with girdle	no girdle	with girdle	no girdle	with girdle
Subject 1	3	882.66	706.14	-33.11	-49.15	598.03	25.70	21.19	18.57	295.92	189.22	11.30	-7.55	417.53	109.25	19.19	0.81
Subject 2	3	1097.67	1061.38	7.91	4.88	1123.60	883.66	-17.41	27.28	939.58	672.98	-5.47	6.96	181.78	64.22	7.26	3.53
Subject 3	3	167.63	371.15	-39.59	7.65												
Subject 4	3	770.98	1051.69	40.51	32.78												
Subject 5	3	671.43	397.52	-25.75	-25.82	407.87	169.78	38.14	-70.49	80.13	81.40	1.80	6.69	122.16	132.04	-4.44	-4.74
Subject 6	3	424.66	657.41	-23.72	-14.29	512.22	664.49	-5.56	-51.18	1084.60	662.96	0.54	-4.12	567.67	411.86	-17.26	-9.34
Subject 7	3	687.95	745.30	44.55	-13.12	161.45	147.88	-68.27	-36.44	228.53	82.14	-19.39	26.48	196.26	60.81	-2.04	2.63
Subject 8	3	1046.95	1206.52	19.19	6.81	1010.65	1169.03	-6.51	7.41	516.55	93.94	-9.40	-4.73	267.33	#DIV/0!	262.33	#DIV/0!
Subject 9	3	73.98	53.40	4.58	-28.09	46.24	7.00	5.22	1.23	12.76	17.52	1.60	1.38	39.88	68.94	2.17	0.83
Subject 10	3	#DIV/0!	#DIV/0!	#DIV/0!	#DIV/0!	4.00	5.00	6.00	7.00	8.00	9.00	10.00	11.00	12.00	13.00	14.00	15.00
	P value of no girdle	0.4961		0.25		0.3125		0.8438		0.1094		0.3828		0.2188		0.9375	
		Displacement - 0 vs 9 month no girdle p value = 0.0469 *															
		Displacement - 0 vs 9 month with girdle p value = 0.0625															
		Rotation - 0 vs 9 month no girdle p value = 0.3750															
		Rotation - 0 vs 9 month with girdle p value = 0.0625															

## BIBLIOGRAPHY

- Adair, I., Van, M. W., & Armstrong, G. (1977). Moiré topography in scoliosis screening. *Clinical Orthopaedics and Related Research* (129), 165-171.
- Adams, W. (1882). Lectures on the pathology and treatment of lateral and other forms of curvature of the spine. *Churchill. Am*, 66(7): 1061-1071.
- Ahmed, M. U., Begum, S., Funk, P., Xiong, N., & von Scheele, B. (2011). A multi-module case-based biofeedback system for stress treatment. *Artificial Intelligence in Medicine*, 51(2), 107-115.
- Akuthota, V., & Nadler, S. F. (2004). Core strengthening. *Archives of Physical Medicine and Rehabilitation*, 85, 86-92.
- Alam, M., Newton, P. O., Yaszay, B., & Bastrom, T. P. (2013). Are Thoracic Curves With a Low Apex (T11 or T11/T12) Really Thoracic Curves? *Spine Deformity*, 1(2), 139-143. <https://doi.org/10.1016/j.jspd.2012.12.004>
- An, H., & Lee, I. (2015). A conceptual framework for Asian women's emotional needs in fashion design. *International Journal of Fashion Design, Technology and Education*, 8(3), 206-213. Retrieved from <https://doi.org/10.1080/17543266.2015.1053421>. doi:10.1080/17543266.2015.1053421
- Anitha, H., & Prabhu, G. (2012). Identification of Apical Vertebra for Grading of Idiopathic Scoliosis using Image Processing. *The Journal of the Society for Computer Applications in Radiology*, 25(1), 155-161. <https://doi.org/10.1007/s10278-011-9394-x>
- Arens, E. A., & Zhang, H. (2006). The skin's role in human thermoregulation and comfort.
- Ascani, E., Bartolozzi, P., Logroscino, C., Marchetti, P., Ponte, A., Savini, R., Travaglini, F., Binazzi, R., & Di, M. S. (1986). Natural history of untreated idiopathic scoliosis after skeletal maturity. *Spine*, 11(8), 784-789.

- Asher MA, Burton DC. Adolescent idiopathic scoliosis: natural history and long term treatment effects. *Scoliosis*. 2006;1(1):2.
- Aulisa, A. G., Guzzanti, V., Falciglia, F., Giordano, M., Marzetti, E., & Aulisa, L. (2015). Lyon bracing in adolescent females with thoracic idiopathic scoliosis: a prospective study based on SRS and SOSORT criteria. (Research article)(Clinical report). *BMC Musculoskeletal Disorders*, 16, 316.
- Aulisa, A.G., Guzzanti, V., Marzetti, E., Giordano, M., Falciglia, F. & Aulisa, L. (2014) ‘Brace treatment in juvenile idiopathic scoliosis: a prospective study in accordance with the SRS criteria for bracing studies-SOSORT award 2013 winner’, *Scoliosis*, 9(3).
- Aulisa, A. G., Guzzanti, V., Perisano, C., Marzetti, E., Specchia, A., Galli, M., ... & Aulisa, L. (2010). Determination of quality of life in adolescents with idiopathic scoliosis subjected to conservative treatment. *Scoliosis*, 5, 1-7.
- Ayhan, C., Unal, E., & Yakut, Y. (2014). Core stabilisation reduces compensatory movement patterns in patients with injury to the arm: a randomized controlled trial. *Clinical Rehabilitation*, 28(1), 36-47.
- Babaka. (2020). About Babaka. Babaka. Retrieved from [https://bebejia-cn.translate.google/?\\_x\\_tr\\_sch=http&\\_x\\_tr\\_sl=zh-CN&\\_x\\_tr\\_tl=zh-TW&\\_x\\_tr\\_hl=zh-TW&\\_x\\_tr\\_pto=sc](https://bebejia-cn.translate.google/?_x_tr_sch=http&_x_tr_sl=zh-CN&_x_tr_tl=zh-TW&_x_tr_hl=zh-TW&_x_tr_pto=sc)
- Bago, J., Climent, J. M., Pineda, S., & Gilperez, C. (2007). Further evaluation of the Walter Reed Visual Assessment Scale: correlation with curve pattern and radiological deformity. *Scoliosis*, 2(1), 12.
- Bathe, K. J. (2008). *Finite element method*. John Wiley & Sons, Inc.
- Benedict, F. G., Miles, W. R., & Johnson, A. (1919). The temperature of the human skin. *Proceedings of the National Academy of Sciences of the United States of America*, 5(6), 218.

- Berdishevsky, H., Lebel, V. A., Bettany-Saltikov, J., Rigo, M., Lebel, A., Hennes, A., Romano, M., BiaAek, M., M'Hango, A., Betts, T., de Mauroy, J. C., & Durmala, J. (2016). Physiotherapy scoliosis-specific exercises - a comprehensive review of seven major schools. (Report). *Scoliosis*, 11(1). <https://doi.org/10.1186/s13013-016-0076-9>
- Berger, N., Edelsten, J., Fishman, S., Krebs, D. & Springer, W. (1983). *Spinal Orthotics: Prosthetics and Orthotics*. New York: New York University, Post-Graduate Medical School.
- Berteau, J. P., Pithioux, M., Mesure, S., Bollini, G., & Chabrand, P. (2011). Beyond the classic correction system: a numerical nonrigid approach to the scoliosis brace. *The Spine Journal*, 11(5), 424-431.
- Bessette, A. & Rousseau, C. M. (2012) *Human Anatomy and Physiology: Scoliosis: Causes, Symptoms and Treatment*. Nova Science Publishers, Inc.p.121-136
- Bettijane, E. (1999). *Coping with scoliosis*. New York: The Rosen Publishing Group, INC.
- Bettany-Saltikov, J., Campo, A., M'hango, A., Colliard, C., Durmala, J., De Mauroy, J. C., Rigo, M., Bialek, M., Romano, M., & Negrini, S. (2012). Physical Therapy for Adolescents with Idiopathic Scoliosis. *INTECH Open Access Publisher*, 227 <https://books.google.com.hk/books?id=ZbLvoAEACAAJ>
- Birbaumer, N., Flor, H., Cevey, B., Dworkin, B. & Miller, N. E. (1994). Behavioral treatment of scoliosis and kyphosis. *Journal of psychosomatic research*, 38(6), 623-628.
- Blecher, R., Krief, S., Galili, T., Biton, I. E., Stern, T., Assaraf, E., ... & Zelzer, E. (2017). The proprioceptive system masterminds spinal alignment: insight into the mechanism of scoliosis. *Developmental cell*, 42(4), 388-399.
- Blount, W. P., & Moe, J. H. (1973). *The Milwaukee Brace: Williams & Wilkins*. Bella J. May, Ed.D. Oxford Academic.

- Borysov, M., Borysov, A., & Weiss, H.-R. (2013). Bracing according to best practice standards—Are the results repeatable? *Orthopedic & Muscular System: Current Research*, 1-4.
- Botens-Helmus, C., Klein, R., & Stephan, C. (2006). The reliability of the Bad Sobernheim Stress Questionnaire (BSSQbrace) in adolescents with scoliosis during brace treatment. *Scoliosis*, 1, 1-5.
- Brand, R. A. (2008). 50 years ago in CORR: the iliac apophysis: an invaluable sign in the management of scoliosis Joseph C. *Clinical Orthopaedics and Related Research®*, 466(6), 1516-1517.
- Branthwaite MA. Cardiorespiratory consequences of unfused idiopathic scoliosis. *British journal of diseases of the chest*. Oct 1986;80(4):360-369.
- Bray, D. (1998). Biofeedback. *Complementary Therapies in Nursing and Midwifery*, (1), 22-24.
- Brooks H. L., Azen S. P., Gerberg E., Brooks R. & Chan L. (1975). Scoliosis: A prospective epidemiological study. *J Bone Joint Surg Am*. 57:968–72.
- Botens-Helmus, C., Klein, R., & Stephan, C. (2006). The reliability of the Bad Sobernheim Stress Questionnaire (BSSQbrace) in adolescents with scoliosis during brace treatment. *Scoliosis*, 1, 1-5.
- Bulthuis, G.J., Veldhuizen, A.G. & Nijenbanning, G. (2008). Clinical effect of continuous corrective force delivery in the non-operative treatment of idiopathic scoliosis: a prospective cohort study of the TriaC-brace. *European Spine Journal*, 17(2), pp.231-239.
- Bunge, E. M., de Bekker-grob, E. W., van Biezen, F. C. & Essink-bot, M. L. & de Konig, H. J. (2009). Patients' preferences for scoliosis brace treatment. A discrete choice experiment. *Spine*, 35 57-63.

- Bunnell, W. P. (1984). An objective criterion for scoliosis screening. *The Journal of Bone & Joint Surgery*, 66(9), 1381-1387.
- California Department of Education. (2007). *Standards for Scoliosis Screening in California Public Schools (2007 ed.)*. CDE Press
- Canavese F. & Kaelin A. (2011). Adolescent idiopathic scoliosis: indications and efficacy of nonoperative treatment. *Indian J Orthopaedics*, 45: 7–14.
- CareAllies. (2007) *Medical Necessity Guidelines*. Scoliosis Treatments, Idiopathic. <https://www.careallies.com/resources>
- Chan, A., Lou, E., & Hill, D. (2013). Review of current technologies and methods supplementing brace treatment in adolescent idiopathic scoliosis. *Journal of children's orthopaedics*, 7(4), 309-316.
- Chan, C.H.Y. (2019). *Department of Health Annual Report 2018/2019, Hong Kong*. [https://www.dh.gov.hk/english/pub\\_rec/pub\\_rec\\_ar/pdf/1819/ADR\\_2018\\_19\\_e.pdf](https://www.dh.gov.hk/english/pub_rec/pub_rec_ar/pdf/1819/ADR_2018_19_e.pdf) Accessed 1 May 2023.
- Chan, S. L. (2014). *A correlation study among the orthotic treatment effectiveness, compliance to spinal orthosis and health-related quality of life of the patients with adolescent idiopathic scoliosis (AIS) in the initial treatment period*. [Doctoral dissertation.] Faculty of Health and Social Sciences, The Hong Kong Polytechnic University. <https://theses.lib.polyu.edu.hk/handle/200/7620>
- Chan, W. Y., Yip, J., Yick, K. L., Ng, S. P., Lu, L., Cheung, K. M. C., ... & Tse, C. Y. (2018). Mechanical and clinical evaluation of a shape memory alloy and conventional struts in a flexible scoliotic brace. *Annals of Biomedical Engineering*, 46(8), 1194-1205.
- Charles, Y. P., Daures, J. P., de Rosa, V., & Dimeglio, A. (2006). Progression risk of idiopathic juvenile scoliosis during pubertal growth. *Spine (Phila Pa 1976)*, 31(17), 1933-1942. Retrieved from <https://insights.ovid.com/pubmed?pmid=16924210>. doi: 10.1097/01.brs.0000229230.68870.97

- Chase, A. P., Bader, D. L., & Houghton, G. R. (1989). The biomechanical effectiveness of the Boston brace in the management of adolescent idiopathic scoliosis. *Spine*, 14(6), 636-642. doi:10.1097/00007632-198906000-00018
- Chen, P. Q., Wang, J. L., Tsuang, Y. H., Liao, T. L., Huang, P. I., and Hang, Y. S. (1998). The postural stability control and gait pattern of idiopathic scoliosis adolescents. *Clinical biomechanics*, 13(1), pp.S52-S58.
- Cheng, J. C., Castelein, R. M., Chu, W. C., Danielsson, A. J., Dobbs, M. B., Grivas, T. B., Gurnett, C. A., Luk, K. D., Moreau, A., & Newton, P. O. (2015). Adolescent idiopathic scoliosis. *Nature reviews disease primers*, 1(1), 1-21.
- Cheng, J. C., Guo, X., & Sher, A. H. (1998). Posterior tibial nerve somatosensory cortical evoked potentials in adolescent idiopathic scoliosis. *Spine*, 23(3), 332-337.
- Cheng, L., & Hannaford, B. (2015). Finite element analysis for evaluating liver tissue damage due to mechanical compression. *Journal of biomechanics*, 48(6), 948-955.
- Chesler, A. T., Szczot, M., Bharucha-Goebel, D., Čeko, M., Donkervoort, S., Laubacher, C., ... & Bönnemann, C. G. (2016). *The role of PIEZO2 in human mechanosensation*. *New England Journal of Medicine*, 375(14), 1355-1364.
- Cheung, H. Y. (2024). *Evaluation and enhancement of the performance of anisotropic textile brace for moderate Adolescent Idiopathic Scoliosis*. [Master's dissertation.] School of Fashion and Textiles, The Hong Kong Polytechnic University.  
<https://theses.lib.polyu.edu.hk/handle/200/12972>
- Cheung, K. M., Senkoylu, A., Alanay, A., Genc, Y., Lau, S., & Luk, K. D. (2007). Reliability and concurrent validity of the adapted Chinese version of Scoliosis Research Society-22 (SRS-22) questionnaire. *Spine*, 32(10), 1141-1145.
- Chow, D. H., Kwok, M. L., Cheng, J. C., Lao, M. L., Holmes, A. D., Au-Yang, A., ... & Wong,

- M. S. (2006). The effect of backpack weight on the standing posture and balance of schoolgirls with adolescent idiopathic scoliosis and normal controls. *Gait & posture*, 24(2), 173-181.
- Climent, J. M. & Sánchez, J. (1999). Impact of the type of brace on the quality of life of adolescents with spine deformities. *Spine*, 24(18): 1903
- Clin, J., Aubin, C.-E., Parent, S., Sangole, A., & Labelle, H. (2010). Comparison of the biomechanical 3D efficiency of different brace designs for the treatment of scoliosis using a finite element model. *European Spine Journal*, 19(7), 1169-1178. <https://doi.org/10.1007/s00586-009-1268-2>
- Cobb, J. R. (1948). Outline for the study of scoliosis. *Instructional course lecture*. Ann Arbor.
- Coillard, C., Circo, A., & Rivard, C. H. (2008). A new concept for the non-invasive treatment of Adolescent Idiopathic Scoliosis: The Corrective Movement © principle integrated in the SpineCor System. *Disability and Rehabilitation: Assistive Technology*, 3(3), 112-119. <https://doi.org/10.1080/17483100801903913>
- Coillard, C., Leroux, M. A., Badeaux, J., & Rivard, C. H. (2002). SPINECOR: a new therapeutic approach for idiopathic scoliosis. *Studies in health technology and informatics*, 215-217.
- Coillard, C., Leroux, M., Zabjek, K., & Rivard, C. (2003). SpineCor – a non-rigid brace for the treatment of idiopathic scoliosis: post-treatment results. *European Spine Journal*, 12(2), 141-148. <https://doi.org/10.1007/s00586-002-0467-x>
- Cole, A. K. (2008). The Spine and Scapula Stabilizing (S3) Brace Has an Effect on Posture and Muscle Activity in Overhead Athletes with Poor Posture. ProQuest.
- Cooke, E., Carter, L., & Pilcher, M. (1980). Identifying scoliosis in the adolescent with thermography: A preliminary study. *Clinical Orthopaedics and Related Research*, (148), 172-6.

- Costa, L., Schlosser, T. P., Jimale, H., Homans, J. F., Kruyt, M. C., & Castelein, R. M. (2021). The effectiveness of different concepts of bracing in Adolescent Idiopathic Scoliosis (AIS): A systematic review and meta-analysis. *Journal of Clinical Medicine*, 10(10), 2145.
- Cummings, R. J., Loveless, E. A., Campbell, J., SAMELSON, S., & Mazur, J. M. (1998). Interobserver Reliability and Intraobserver Reproducibility of the System of King et al. for the Classification of Adolescent Idiopathic Scoliosis\*. *The Journal of Bone & Joint Surgery*, 80(8), 1107-11.
- de Mauroy, J. C., Lecante, C., & Barral, F. (2011). "Brace Technology" Thematic Series – The Lyon approach to the conservative treatment of scoliosis [journal article]. *Scoliosis*, 6(1), 4. <https://doi.org/10.1186/1748-7161-6-4>
- Dietz, V. (2002). Proprioception and locomotor disorders. *Nature Reviews Neuroscience*, 3(10), 781-790.
- Department of Health. (2019). *Department of Health Annual Report 2018/2019, Hong Kong*. Accessed 1 May 2023. [https://www.dh.gov.hk/english/pub\\_rec/pub\\_rec\\_ar/pdf/1819/ADR\\_2018\\_19\\_e.pdf](https://www.dh.gov.hk/english/pub_rec/pub_rec_ar/pdf/1819/ADR_2018_19_e.pdf)
- Department of Health. (2014). *Department of Health Annual Report 2013/2014, Hong Kong*. Accessed 13 June 2022. [https://www.dh.gov.hk/english/pub\\_rec/pub\\_rec\\_ar/pdf/1314/ADR2013\\_14\\_e.pdf](https://www.dh.gov.hk/english/pub_rec/pub_rec_ar/pdf/1314/ADR2013_14_e.pdf)
- Department of Health. (2010). *Department of Health Annual Report 2009/2010, Hong Kong*. Accessed 13 June 2022. [https://www.dh.gov.hk/english/pub\\_rec/pub\\_rec\\_ar/pdf/0910/ADR\\_2009\\_10\\_full.pdf](https://www.dh.gov.hk/english/pub_rec/pub_rec_ar/pdf/0910/ADR_2009_10_full.pdf)
- Dimeglio, A. (2001). Growth in Pediatric Orthopaedics. *Journal of Pediatric Orthopaedics*, 21(4), 549-555.
- DiRocco P, Vaccaro P. Cardiopulmonary functioning in adolescent patients with mild idiopathic

scoliosis. *Archives of physical medicine and rehabilitation*. 1988;69(3 Pt 1):198-201.

DJO Global (2023). DONJOY BACK BRACE II TLSO. Accessed July 25, 2023.

[https://enovis.com/sites/default/files/3512%20Donjoy%20Brace%20II%20-%20Family%20Brochure%20REV%20E\\_r16-DOMESTIC\\_No%20Postural.pdf](https://enovis.com/sites/default/files/3512%20Donjoy%20Brace%20II%20-%20Family%20Brochure%20REV%20E_r16-DOMESTIC_No%20Postural.pdf)

DMO Orthotics. (2023). DMO postural scoliosis suit. Accessed July 25, 2023.

<https://www.dmorthotics.com/products-and-services/product/dm34-postural-scoliosis-suit/>

Dj Orthopedics, Llc. (2023). DONJOY BACK BRACE II TLSO. Accessed: July 25, 2023.

[https://enovis.com/sites/default/files/3512%20Donjoy%20Brace%20II%20-%20Family%20Brochure%20REV%20E\\_r16-DOMESTIC\\_No%20Postural.pdf](https://enovis.com/sites/default/files/3512%20Donjoy%20Brace%20II%20-%20Family%20Brochure%20REV%20E_r16-DOMESTIC_No%20Postural.pdf)

Dmo Orthotics. (2023). DMO postural scoliosis suit. Retrieved from

<https://www.dmorthotics.com/products-and-services/product/dm34-postural-scoliosis-suit/>

Dobbs, M. B., & Weinstein, S. L. (1999). Infantile and juvenile scoliosis. *Orthopedic Clinics of North America*, 30(3): 331-341

Dolan, L. A., Donnelly, M. J., Spratt, K. F. & Weinstein, S. L. (2007). Professional opinion concerning the effectiveness of bracing relative to observation in adolescent idiopathic scoliosis. *Journal of Pediatric Orthopaedics*, 27(3): 270-276.

Dhatt, G., Lefrançois, E., & Touzot, G. (2012). *Finite element method*. John Wiley & Sons.

D'Oswaldo, F., Schierano, S., Iannis, M., & Righini, E. (2000). The level protractor: A new simple instrument to measure Cobb angle and back hump: A validation study. *European Journal of Physical and Rehabilitation Medicine*, 36(4), 191.

Dopico-González, C., New, A. M., & Browne, M. (2010). Probabilistic finite element analysis of the uncemented hip replacement—effect of femur characteristics and implant design geometry. *Journal of Biomechanics*, 43(3), 512-520.

- Dubousset, J., Charpak, G., Dorion, I., Skalli, W., Lavaste, F., De Guise, J., Kalifa, G., & Ferey, S. (2005). Le systeme EOS. Nouvelle imagerie osteo-articulaire basse dose en position debout. *e-Mémoires de l'Académie Nationale de chirurgie*, 4(4), 22-27.
- Dworkin, B., Miller, N., Dworkin, S., Birbaumer, N., Brines, M.L., Jonas, S., Schwentker, E.P. & Graham, J.J. (1985). Behavioral Method for the Treatment of Idiopathic Scoliosis. *Medical Sciences*, 82 (8), 2493-2497.
- Edgar, M. (2002). A new classification of adolescent idiopathic scoliosis. *The Lancet*, 360(9329), 270-271. [https://doi.org/10.1016/S0140-6736\(02\)09562-4](https://doi.org/10.1016/S0140-6736(02)09562-4)
- Emery, K., De Serres, S. J., McMillan, A., & Côté, J. N. (2010). The effects of a Pilates training program on arm–trunk posture and movement. *Clinical Biomechanics*, 25(2), 124-130.
- EOS imaging. (2020). EOS System- Low dose imaging system. Retrieved from <https://www.eos-imaging.com/professionals/eos/eos>.
- Eston, R. & Reilly, T. (2008). *Kinanthropometry and exercise physiology laboratory manual: Tests, procedures and data*. Volume 1: Anthropometry (3rd Edition). Routledge.
- Fan, J., Newton, E., Au, R. and Chan, S. C. F. (2001). ‘Predicting Garment Drapewith a Fuzzyneural Network’, *Textile Research Journal*, 71(7), 605.
- Fayssoux, R. S., Cho, R. H., & Herman, M. J. (2010). A history of bracing for idiopathic scoliosis in North America. *Clinical Orthopaedics and Related Research®*, 468(3), 654-664.
- Federico, C., & André, K. (2011). Adolescent idiopathic scoliosis: Indications and efficacy of nonoperative treatment. *Indian Journal of Orthopaedics*, 45(1), 7-14. <https://doi.org/10.4103/0019-5413.73655>
- Ferraro, C., Venturin, A., Ferraro, M., Fabris, M. D., & Masiero, S. (2016). Hump height in idiopathic scoliosis measured using a humpmeter in growing subjects: the relationship

between the hump height and the Cobb angle and the effect of age on the hump height. *European journal of physical and rehabilitation medicine*.

Fok, L. H. (2020). Functional intimate apparel for adolescents with scoliosis. [Doctoral dissertation] Institute of Textiles and Clothing, Hong Kong Polytechnic University. <https://theses.lib.polyu.edu.hk/handle/200/10816>

Fok, Q., Yip, J., Yick, K., & Ng, S. (2021). Design and fabrication of anisotropic textile brace for exerting corrective forces on spinal curvature. *Journal of Industrial Textiles*. <https://doi.org/10.1177/15280837211032619>

Fok, Q., & Yip, J. (2021, June). Applying numerical simulation to predict effect of brace wear for scoliosis. In *International Conference on Applied Human Factors and Ergonomics* (pp. 217-223). Cham: Springer International Publishing.

Fok Q., Yip J., Yick K. L., Ng S. P., and Tse C. Y. (2018). Effectiveness of Posture Correction Girdle as Conservative Treatment for Adolescent Idiopathic Scoliosis: a Preliminary Study. *Ortho. Res. Online J*, 1, 1-3.

Fortin, C., Feldman, D. E., Cheriet, F., Gravel, D., Gauthier, F., & Labelle, H. (2012). Reliability of a quantitative clinical posture assessment tool among persons with idiopathic scoliosis. *Physiotherapy*, 98(1), 64-75.

Fortin, C., Ehrmann Feldman, D., Cheriet, F., & Labelle, H. (2011). Clinical methods for quantifying body segment posture: a literature review. *Disability and rehabilitation*, 33(5), 367-383.

Frontera, W. R., Silver, J. K. & Rizzo, T. D. (2008). *Essentials of physical medicine and rehabilitation: musculoskeletal disorders, pain and rehabilitation: 2nd edn*. Philadelphia: Saunders Elsevier Inc.

Fung, H. Y. (2020). Ergonomic brace wear for adolescent idiopathic scoliosis (AIS). [M.Phil. dissertation, The Hong Kong Polytechnic University].

<http://hdl.handle.net/10397/81419>

Fung, H. Y., O., Yip, J., Cheung, M. C., Yick, K. L., Yat-Hong Kwan, K., Man-Chee Cheung, K., ... & Tse, C. Y. (2020). Exploring mass customization and textile application in medical products: re-designing scoliosis brace for shorter production lead time and better quality of life. *Textile Research Journal*, 90(19-20), 2304-2321.

Gatchel, R. J., Price, K. P. (1979) Clinical Applications of Biofeedback: Appraisal and Status. New York: Pergamon Press. St. George T, Vlahos P, Harner T, et al. A rapidly equilibrating, thin film, passive water sampler for organic contaminants; characterization and field testing. *Environ Pollut* 2011; 159: 481–486.

George, M., Catalin, R. Z., Simona, P., & Gilda, R. Z. (2011). Assessment condition degradation of the EVA compound used as cable jacket. In *2011 7<sup>th</sup> International Symposium on Advanced Topics in Electrical Engineering (ATEE)*, (pp. 1-4). IEEE.

Giorgi, S., Piazzolla, A., Tafuri, S., Borracci, C., Martucci, A., & Giorgi, G. (2013). Chêneau brace for adolescent idiopathic scoliosis: long-term results. Can it prevent surgery? *European Spine Journal*, 22(6), 815-822. <https://doi.org/10.1007/s00586-013-3020-1>

Goldberg, C. J., Kaliszer, M., Moore, D. P., Fogarty, E. E. & Dowling, F. E. (2001). Surface topography, Cobb angles, and cosmetic change in scoliosis. *Spine*, 26(4), E55- E63.

Gong, R. H. and Chen, Y. (1999). ‘Predicting the Performance of Fabrics in Garment Manufacturing with Artificial Neural Networks’, *Textile Research Journal*, 69(7), 477.

Grivas, T. B., Bountis, A., Vrasami, I., & Bardakos, N. V. (2010). Brace technology thematic series: the dynamic derotation brace. *Scoliosis*, 5, 20-20. <https://doi.org/10.1186/1748-7161-5-20>

Grivas, T.B., Vasiliadis, E., Mouzakis, V., Mihas, C. & Koufopoulos, G. (2006) ‘Association between adolescent idiopathic scoliosis prevalence and age at menarche 274 in different

geographic latitudes’, *Scoliosis*, 1(9), pp.1-12.

Grivas, T.B., Vasiliadis, E., Mouzakis, V., Mihas, C. & Koufopoulos, G. (2006) ‘Association between adolescent idiopathic scoliosis prevalence and age at menarche 274 in different geographic latitudes’, *Scoliosis*, 1(9), pp.1-12.

Gutman, G., Benoit, M., Joncas, J., Beauséjour, M., Barchi, S., Labelle, H., ... & Mac-Thiong, J. M. (2016). The effectiveness of the SpineCor brace for the conservative treatment of adolescent idiopathic scoliosis. Comparison with the Boston brace. *The Spine Journal*, 16(5), 626-631.

Guyot, M.-A., Agnani, O., Peyrodie, L., Samantha, D., Donze, C., & Catanzariti, J.-F. (2016). Cervicocephalic relocation test to evaluate cervical proprioception in adolescent idiopathic scoliosis. *European spine journal*, 25(10), 3130-3136.

Haheer, T. R., Gorup, J. M., Shin, T. M., Homel, P., Merola, A. A., Grogan, D. P., ... & Murray, M. (1999). Results of the Scoliosis Research Society instrument for evaluation of surgical outcome in adolescent idiopathic scoliosis: a multicenter study of 244 patients. *Spine*, 24(14), 1435.

Hardesty, L. (2017). Ballyhooed artificial-intelligence technique known as “deep learning” revives 70-year-old idea. *MIT News Office, Massachusetts Institute of Technology*.

Harvard Medical School. (2023). Harvard Medical School Health Topics A-Z. Harvard Health Publications. Retrieved from [https://www.health.harvard.edu/a\\_to\\_z/scoliosis-a-to-z](https://www.health.harvard.edu/a_to_z/scoliosis-a-to-z)

Hasler, C. C., Wietlisbach, S. & Büchler, P. (2010). Objective compliance of adolescent girls with idiopathic scoliosis in a dynamic SpineCor brace. *J Child Orthop*, 4 211-218.

Helenius I, Remes V, Yrjönen T, et al. Comparison of Long-Term Functional and Radiologic Outcomes After Harrington Instrumentation and Spondylodesis in Adolescent Idiopathic Scoliosis: A Review of 78 Patients. *Spine*. 2002;27(2):176 -180.

- Hannes, B., Karlmeinrad, G., Michael, O., & Martin, K. (2002). Multisurgeon assessment of coronal pattern classification systems for adolescent idiopathic scoliosis: reliability and error analysis. *Spine*, 27(7), 762-767.
- Hillier, S., Immink, M., & Thewlis, D. (2015). Assessing proprioception: a systematic review of possibilities. *Neurorehabilitation and neural repair*, 29(10), 933-949.
- Hresko, M. T. (2013). Idiopathic scoliosis in adolescents. *New England Journal of Medicine*, 368(9), 834-841.
- Hewitt, J. (2011). *Scoliosis: Causes, tests and treatments*. Charleston, SC: CreateSpace.
- Hresko, M. T. (2013). Idiopathic scoliosis in adolescents. *New England Journal of Medicine*, 368(9), 834-841.
- Hong, Y., Fong, D. T. P., & Li, J. X. (2011). The effect of school bag design and load on spinal posture during stair use by children. *Ergonomics*, 54(12), 1207-1213.
- Horne, J. P., Flannery, R., & Usman, S. (2014). Adolescent idiopathic scoliosis: diagnosis and management. *American family physician*, 89(3), 193.
- Horng, M. H., Kuok, C. P., Fu, M. J., Lin, C. J., & Sun, Y. N. (2019). Cobb angle measurement of spine from X-ray images using convolutional neural network. *Computational and mathematical methods in medicine*, 2019.
- Huang S. J., Huo H. J., Yang X. J., Xiao Y. L., Xing Z. Y., Zhu Y., Xin D. Q. & Huang S. Q. (2016). Three-dimensional finite element investigation of posterior surgical correction of PUMC type d1 adolescent idiopathic scoliosis. *International Journal of Orthopaedics*, 37(1), 46-52.
- Illés, T., & Somoskeöy, S. (2012). The EOS™ imaging system and its uses in daily orthopaedic practice. *International Orthopaedics*, 36(7), 1325-1331.
- Islam, M. R., Golovin, K., & Dolez, P. I. (2023). Clothing thermophysiological comfort: A

textile science perspective. *Textiles*, 3(4), 353-407.

Issuu Inc. (2023). Prototyp des Spinealite®. Retrieved from

[https://issuu.com/fischfell/docs/002\\_pt\\_buch\\_schroth\\_best\\_practice\\_1\\_buch\\_leseprob/s/17726063](https://issuu.com/fischfell/docs/002_pt_buch_schroth_best_practice_1_buch_leseprob/s/17726063)

Janicki, J. A., & Alman, B. (2007, Nov). Scoliosis: Review of diagnosis and treatment. *Paediatr Child Health*, 12(9), 771-776. <https://doi.org/10.1093/pch/12.9.771>

Juskeliene, V., Magnus, P., Bakketeig, L. S., Dailidiene, N., & Jurkuvenas, V. (1996). Prevalence and risk factors for asymmetric posture in preschool children aged 6–7 years. *International journal of epidemiology*, 25(5), 1053-1059.

Kalender, W. A. (2011). *Computed tomography: fundamentals, system technology, image quality, applications*. John Wiley & Sons.

Kane W. J. (1997). Scoliosis prevalence: a call for a statement of terms. *Clin Orthop*. 126:43–6.

Kappes B. (2008), Biofeedback therapy: Training or treatment. *Applied psychophysiology and biofeedback*, 33, 173–9

Karachalios, T., Sofianos, J., Roidis, N., Sapkas, G., Korres, D., & Nikolopoulos, K. (1999). Ten-year follow-up evaluation of a school screening program for scoliosis: Is the forward-bending test an accurate diagnostic criterion for the screening of scoliosis? *Spine*, 24(22), 2318

Katz, E. D., & Durrani, A. A. (2001). Factors That Influence Outcome in Bracing Large Curves in Patients With Adolescent Idiopathic Scoliosis. *Spine*, 26(21), 2354-2361. <https://doi.org/10.1097/00007632-200111010-00012>

Katz, D. E., Herring, J. A., Browne, R. H., Kelly, D. M., & Birch, J. G. (2010). Brace wear control of curve progression in adolescent idiopathic scoliosis. *Journal of Bone and Joint Surgery*, 92(6), 1343. <https://doi.org/10.2106/JBJS.I.01142>

- Kesling, K. L., & Reinker, K. A. (1997). Scoliosis in twins: a meta-analysis of the literature and report of six cases. *Spine*, 22(17), 2009-2014.
- Kilinc-Balci, F. S. (2011). Testing, analyzing and predicting the comfort properties of textiles. In *Improving comfort in clothing* (pp. 138-162). Woodhead Publishing.
- Kim HJ, Blanco JS, Widmann RF. Update on the management of idiopathic scoliosis. *Current Opinion in Pediatrics*. 2009;21(1):55-64.
- Kim, M.-J., & Park, D.-S. (2017). The effect of Schroth's three-dimensional exercises in combination with respiratory muscle exercise on Cobb's angle and pulmonary function in patients with idiopathic scoliosis. *Physical Therapy Rehabilitation Science*, 6(3), 113-119.
- Kim, S. H., Pyun, J. K., & Choi, H. Y. (2010). Digital human body model for seat comfort simulation. *International Journal of Automotive Technology*, 11(2), 239-244.
- King, H. A., Moe, J. H., Bradford, D. S., & Winter, R. B. (1983). The selection of fusion levels in thoracic idiopathic scoliosis. *The Journal of Bone & Joint Surgery*, 65(9), 1302-1313.
- Knott, P., Pappo, E., Cameron, M., Rivard, C., Kotwicki, T., Zaina, F., Wynne, J., Stikeleather, L., Bettany-Saltikov, J., & Grivas, T. B. (2014). SOSORT 2012 consensus paper: reducing x-ray exposure in pediatric patients with scoliosis. *Scoliosis*, 9(1), 4.
- Kotwicki, T. (2008). Evaluation of scoliosis today: Examination, X-rays and beyond. *Disability & Rehabilitation*, 2008, Vol.30(10), p.742-751, 30(10), 742-751.
- Kotwicki T, Cheneau J. Biomechanical action of a corrective brace on thoracic idiopathic scoliosis: Cheneau 2000 orthosis. *Disability and Rehabilitation: Assistive Technology*. 2008/01/01 2008;3(3):146-153.
- Kouwenhoven, J. W. M., & Castelein, R. M. (2008). The pathogenesis of adolescent idiopathic scoliosis: review of the literature. *Spine*, 33(26), 2898-2908.

- Kubat, O., & Ovadia, D. (2020). Frontal and sagittal imbalance in patients with adolescent idiopathic deformity. *Annals of translational medicine*, 8(2).
- Kwok, H. C. G. (2017). Development of posture correction tank-top synchronized with biofeedback muscle training for adolescents with early scoliosis. [Master's dissertation.] Institute of Textiles and Clothing, The Hong Kong Polytechnic University]. <https://theses.lib.polyu.edu.hk/bitstream/200/9144/1/991021965754103411.pdf>
- Lam, P.Y. (2010). *Department of Health Annual Report 2009/2010, Hong Kong*. [https://www.dh.gov.hk/english/pub\\_rec/pub\\_rec\\_ar/pdf/0910/ADR\\_2009\\_10\\_full.pdf](https://www.dh.gov.hk/english/pub_rec/pub_rec_ar/pdf/0910/ADR_2009_10_full.pdf)  
Accessed 13 June 2022.
- Landauer, F., Wimmer, C., & Behensky, H. (2003). Estimating the final outcome of brace treatment for idiopathic thoracic scoliosis at 6-month follow-up. *Pediatric rehabilitation*, 6(3-4), 201-207.
- Lao, M. L., Chow, D. H., Guo, X., Cheng, J. C., & Holmes, A. D. (2008). Impaired dynamic balance control in adolescents with idiopathic scoliosis and abnormal somatosensory evoked potentials. *Journal of Pediatric Orthopaedics*, 28(8), 846-849.
- Lau, K. (2011). Health in your hands: Your plan for natural scoliosis prevention and treatment (2nd ed.). *Singapore: Health in Your Hands Pte.*
- Lau, K. K., Law, K. K., Kwan, K. Y., Cheung, J. P., Cheung, K. M., & Wong, A. Y. (2022). Timely revisit of proprioceptive deficits in adolescent idiopathic scoliosis: a systematic review and meta-analysis. *Global Spine Journal*, 12(8), 1852-1861.
- Le Berre, M., Guyot, M.-A., Agnani, O., Bourdeauducq, I., Versyp, M.-C., Donze, C., Thévenon, A., & Catanzariti, J.-F. (2017). Clinical balance tests, proprioceptive system and adolescent idiopathic scoliosis. *European spine journal*, 26(6), 1638-1644.
- LeBlanc, R., Labelle, H., Rivard, C. H., & Poitras, B. (1997). Relation between adolescent idiopathic scoliosis and morphologic somatotypes. *Spine*, 22(21), 2532-2536.

- Lee, C. F., Fong, D. Y., Cheung, K. M., Cheng, J. C., Ng, B. K., Lam, T. P., ... & Luk, K. D. (2010). Costs of school scoliosis screening: a large, population-based study. *Spine*, 35(26), 2266-2272.
- Lehnert-Schroth, C. (1979). Schroth's three dimensional treatment of scoliosis. *ZFA. Zeitschrift fur Allgemeinmedizin*, 55(34), 1969-1976.
- Lehrer, P., Smetankin A., Potapova T. (2000). Respiratory Sinus Arrhythmia Biofeedback Therapy for Asthma: A Report of 20 Unmedicated Pediatric Cases Using the Smetankin Method. *Applied Psychophysiology and Biofeedback*, (3), 193-200.
- Lenke, L. G., BETZ, R. R., Bridwell, K. H., Clements, D. H., Harms, J., Lowe, T. G., & SHUFFLEBARGER, H. L. (1998). Intraobserver and Interobserver Reliability of the Classification of Thoracic Adolescent Idiopathic Scoliosis. *The Journal of Bone & Joint Surgery*, 80(8), 1097-1106.
- Lenke, L. G., Betz, R. R., Harms, J., Bridwell, K. H., Clements, D. H., Lowe, T. G., & Blanke, K. (2001). Adolescent idiopathic scoliosis: a new classification to determine extent of spinal arthrodesis. *The Journal of bone and joint surgery. American volume*, 83-A(8), 1169.
- Lenzen M.L.B., Frijlink A.C., Berger M.Y., Bierma-Zeinstra S. MA, Verkerk K., and Verhagen A.P. Effect of bracing and other conservative interventions in the treatment of idiopathic scoliosis in adolescents: A systematic review of clinical trials. *Physical Therapy* 2005, 85(12), pp.1329-39.
- Leonisa Inc. (2017). Posture Corrector Wireless Back Support Bra  
<http://www.leonisa.com/en/products/posture-corrector-wireless-back-support-bra/>
- Li, M., Wong, M. S., Luk, K. D., Wong, K. W., and Cheung, K. M. C. (2014). Time-dependent response of scoliotic curvature to orthotic intervention: when should a radiograph be obtained after putting on or taking off a spinal orthosis?. *Spine*, 39: 1408-1416, 2014.

- Lin, S., Wang, X. S., Wu, Z. H., Zhai, J. L., & Li, S. G. (2009). Three-dimensional finite element analysis of adolescent idiopathic scoliosis correction by different correction methods. *Journal of Clinical Rehabilitative Tissue Engineering Research*, 13(30), 5972-5976.
- Lin, Y., Cheung, J. P. Y., Chan, C. K., Wong, S. W. F., Cheung, K. M. C., Wong, M., Wong, W. C., Cheung, P. W. H., & Wong, M. S. (2022). A Randomized Controlled Trial to Evaluate the Clinical Effectiveness of 3D-Printed Orthosis in the Management of Adolescent Idiopathic Scoliosis. *Spine*, 47(1), 13-20.
- Little, J. P., Izatt, M. T., Labrom, R. D., Askin, G. N., & Adam, C. J. (2013). An FE investigation simulating intra-operative corrective forces applied to correct scoliosis deformity. *Scoliosis*, 8(1), 9.
- Liu, F., Fan, J. and Lau, L. (2006). 'Perceived Body Size Affected by Garment and Body Mass Index', *Perceptual and Motor Skills*, 103(1), 253.
- Liu, P. Y., Yip, J., Chen, B., He, L. F., Cheung, J. P. Y., Yick, K. L., & Ng, S. P. (2022). Immediate effects of posture correction girdle on adolescents with early scoliosis. *In 13th International Conference on Applied Human Factors and Ergonomics (AHFE 2022)*.
- Liu, P. Y. (2015). Development of posture correction girdle for adolescents with early scoliosis. [Master's dissertation.] Institute of Textiles and Clothing, The Hong Kong Polytechnic University]. <https://theses.lib.polyu.edu.hk/handle/200/7926>
- Liu, P.-Y., Yip, J., Yick, K.-L., Yuen, C.-W. M., Ng, S.-P., Tse, C.-Y., & Lawa, D. (2014). An Ergonomic Flexible Girdle Design for Preteen and Teenage Girls with Early Scoliosis. *Journal of Fiber Bioengineering and Informatics*, 7(2), 233-246. <https://doi.org/10.3993/jfbi06201410>

- Liu, P.-Y., Yip, J., Yick, K.-L., Yuen, C.-W. M., Tse, C.-Y., Ng, S.-P., & Law, D. (2015). Effects of a tailor-made girdle on posture of adolescents with early scoliosis. *Textile Research Journal*, 85(12), 1234-1246. <https://doi.org/10.1177/0040517514561928>
- Liu, R. R., & McClure, P. (2001). Recognizing cross-cultural differences in consumer complaint behavior and intentions: an empirical examination. *Journal of Consumer Marketing*, 18(1), 54-75. Retrieved from <https://doi.org/10.1108/07363760110365813>. doi:10.1108/07363760110365813
- Liu, W., Lian, Z., Deng, Q., & Liu, Y. (2011). Evaluation of calculation methods of mean skin temperature for use in thermal comfort study. *Building and Environment*, 46(2), 478-488.
- Logithasan, V., Wong, J., Reformat, M., & Lou, E. (2022). Using machine learning to automatically measure axial vertebral rotation on radiographs in adolescents with idiopathic scoliosis. *Medical Engineering & Physics*, 107, 103848.
- Lohfeld, S., Cahill, S., Doyle, H., & McHugh, P. E. (2015). Improving the finite element model accuracy of tissue engineering scaffolds produced by selective laser sintering. *Journal of Materials Science: Materials in Medicine*, 26, 1-12.
- Lonstein, J. E. (2006). Scoliosis: surgical versus nonsurgical treatment. *Clin Orthop Relat Res*, 443, 248-259. Retrieved from <https://insights.ovid.com/pubmed?pmid=16462448>. doi:10.1097/01.blo.0000198725.54891.73
- Lonstein, J. E. (2003). Milwaukee brace treatment of scoliosis. *Scoliosis Research Society Bracing Manual*  
[https://www.srs.org/Files/Research/Manuals-and-Publications/SRS\\_Milwaukee\\_Brace.2003.pdf](https://www.srs.org/Files/Research/Manuals-and-Publications/SRS_Milwaukee_Brace.2003.pdf)
- Lonstein, J. E., & Carlson, J. M. (1984). The prediction of curve progression in untreated idiopathic scoliosis during growth. *The Journal of bone and joint surgery. American volume*, 66(7), 1061-1071.

- Luk, K. D., Lee, C. F., Cheung, K. M., Cheng, J. C., Ng, B. K., Lam, T. P., ... & Fong, D. Y. (2010). Clinical effectiveness of school screening for adolescent idiopathic scoliosis: a large population-based retrospective cohort study. *Spine*, 35(17), 1607-1614.
- Lau, K. K., Law, K. K., Kwan, K. Y., Cheung, J. P., Cheung, K. M., & Wong, A. Y. (2022). Timely revisit of proprioceptive deficits in adolescent idiopathic scoliosis: a systematic review and meta-analysis. *Global Spine Journal*, 12(8), 1852-1861.
- Lyons, G. M., Sharma, P., Baker, M., O'Malley, S., & Shanahan, A. (2003, September). A computer game-based EMG biofeedback system for muscle rehabilitation. In Engineering in Medicine and Biology Society, 2003. *Proceedings of the 25th Annual International Conference of the IEEE 2*, 1625-1628). IEEE.
- McCarthy, R. E. (2001). Evaluation of the patient with deformity. Evaluation of the patient with deformity. Weinstein S, red. *The Pediatric Spine*, 185-224.
- MacDonald, N. E. (2003). Adolescent access to healthcare. *Paediatrics & child health*, 8(9), 551-552.
- Mackenzie F. A. (1922). The Operative Treatment of Scoliosis. *The Journal of Bone & Joint Surgery*, 4(3): 446-452.
- Manuel D., Monica V. & Dino G. (2010). A specific scoliosis classification correlating with brace treatment: description and reliability. *Scoliosis*, 5(1), 179-186
- Mac-Thiong, J. M., Petit, Y., Aubin, C. É., Delorme, S., Dansereau, J., & Labelle, H. (2004). Biomechanical evaluation of the Boston brace system for the treatment of adolescent idiopathic scoliosis: relationship between strap tension and brace interface forces. *Spine*, 29(1), 26-32.

- Mair, S., Lattermann, C., & Malone, T. R. (2013). Glenohumeral instability and glenoid bone loss in a throwing athlete. *International Journal of Sports Physical Therapy*, 8(2), 205.
- Malfair, D., Flemming, A. K., Dvorak, M. F., Munk, P. L., Vertinsky, A. T., Heran, M. K., & Graeb, D. A. (2010). Radiographic evaluation of scoliosis: review. *AJR. American journal of roentgenology*, 194(3 Suppl), S8. <https://doi.org/10.2214/AJR.07.7145>
- Marschall, M., Harrington, A. C., & Steele, J. R. (1995). Effect of work station design on sitting posture in young children. *Ergonomics*, 38(9), 1932-1940.
- Maruyama, T., Takeshita, K., & Kitagawa, T. (2008). Milwaukee brace today. *Disability & Rehabilitation: Assistive Technology*, 2008, Vol.3(3), p.136-138, 3(3), 136-138. <https://doi.org/10.1080/17483100801904036>
- Maruyama, T., Takesita, K., Kitagawa, T., & Nakao, Y. (2011). Milwaukee brace. *Physiotherapy theory and practice*, 27(1), 43-46.
- Masso, P. D. & Gorton III, G. E. (2000). Quantifying changes in standing body segment alignment following spinal instrumentation and fusion in idiopathic scoliosis using an optoelectronic measurement system. *Spine*, 25(4), 457-462.
- Matthew, M. (2017). Orthotic device (N.Z. Patent No. 709234B2). New Zealand patent application. <https://patentimages.storage.googleapis.com/54/df/79/3498ed48179e45/NZ709234B2.pdf>
- McKenzie, R., & Van Wijmen, P. (1988). *Treat your own back* (p. 80). Spinal Publications.
- Medical Expo. (2023). Thoraco-lumbo-sacral support corset. Accessed June 10, 2023. <https://www.medicalexpo.com/prod/optec-usa/product-80454-633217.html>
- Miller NH. Genetics of Familial Idiopathic Scoliosis. *Clinical orthopaedics and related*

research. 2007; 462:6-10.

Morgan, T. H., & Scott, J. C. (1956). Treatment of infantile idiopathic scoliosis. *The Journal of Bone & Joint Surgery British Volume*, 38(2), 450-457.

Mukhopadhyay, A., Ishtiaque, S. M., & Uttam, D. (2011). Impact of structural variations in hollow yarn on heat and moisture transport properties of fabrics. *Journal of the Textile Institute*, 102(8), 700-712.

Mungo, T. A. (1952). Posture-corrective brassiere [United States Patents].

<https://www.google.com.hk/patents/US2591462>

Muthukrishnan, R., Shenoy, S. D., Jaspal, S. S., Nellikunja, S., & Fernandes, S. (2010). The differential effects of core stabilization exercise regime and conventional physiotherapy regime on postural control parameters during perturbation in patients with movement and control impairment chronic low back pain. *BMC Sports Science, Medicine and Rehabilitation*, 2(1), 13.

Nault, M. L., Allard, P., Hinse, S., Le Blanc, R., Caron, O., Labelle, H., and Sadeghi, H. (2002). Relations between standing stability and body posture parameters in adolescent idiopathic scoliosis. *Spine*, 27(17), pp.1911-1917.

Nebel, J. C. (2001). *Soft tissue modelling from 3D scanned data*. In *Deformable 279 avatars* (pp. 85-97). Springer, Boston, MA.

Negrini, S., Aulisa, A. G., Aulisa, L., Circo, A. B., de Mauroy, J. C., Durmala, J., Grivas, T. B., Knott, P., Kotwicki, T., Maruyama, T., Minozzi, S., O'Brien, J. P., Papadopoulos, D., Rigo, M., Rivard, C. H., Romano, M., Wynne, J. H., Villagrasa, M., Weiss, H.-R., & Zaina, F. (2012). 2011 SOSORT guidelines: Orthopaedic and Rehabilitation treatment 235 of idiopathic scoliosis during growth. *Scoliosis*, 7, 3-3.

<https://doi.org/10.1186/1748-7161-7-3>

Negrini, S., Donzelli, S., Aulisa, A. G., Czaprowski, D., Schreiber, S., de Mauroy, J. C., Zaina,

- F. (2018). 2016 SOSORT guidelines: orthopaedic and rehabilitation treatment of idiopathic scoliosis during growth. *Scoliosis and Spinal Disorders*, 13, 3.
- Negrini, S., Minozzi, S., Bettany-Saltikov, J., Chockalingam, N., Grivas, T.B., Kotwicki, T., Maruyama, T., Romano, M. & Zaina, F. (2015). Braces for idiopathic scoliosis in adolescents, *Cochrane Database of Systematic Reviews*, (6).
- Negrini, S., Marchini, G., & Tomaello, L. (2006). The Sforzesco brace and SPoRT concept (Symmetric, Patient-oriented, Rigid, Three-dimensional) versus the Lyon brace and 3-point systems for bracing idiopathic scoliosis. *Studies in health technology and informatics*, 123, pp.245.
- Negrini, S., Minozzi, S., Bettany-Saltikov, J., Zaina, F., Chockalingam, N., Grivas, T. B., ... & Vasiliadis, E. S. (2010). Braces for Idiopathic Scoliosis in Adolescents-A Cochrane Review. *The Spine Journal*, 10(9), S130-S131.
- Nestoriuc, Y., Martin, A., Rief, W., & Andrasik, F. (2008). Biofeedback treatment for headache disorders: a comprehensive efficacy review. *Applied psychophysiology and biofeedback*, 33(3), 125-140.
- Newton, R. U., & Neal, R. J. (1994). Three-dimensional quantification of human standing posture. *Gait & Posture*, 2(4), 205-212.
- Oates, S., Evans, G. W., & Hedge, A. (1999). An anthropometric and postural risk assessment of children's school computer work environments. *Computers in the Schools*, 14(3-4), 55-63.
- Ogon, M., Giesinger, K., Behensky, H., Wimmer, C., Nogler, M., Bach, C. M., & Krismer, M. (2002). Interobserver and intraobserver reliability of Lenke's new scoliosis classification system. *Spine*, 27(8), 858-862.
- Ólafasson, Y., Saraste, H. & Ahlgren, R. M. (1999). Does bracing affect self-image? A prospective study on 54 patients with adolescent idiopathic scoliosis. *Eur Spine J*, 12 141-148.

Optec USA. (2020). Custom CTLSO. Accessed Sep 10, 2022.  
<http://www.optecusa.com/product/custom-ctlso>

Otman, S., Kose, N., & Yakut, Y. (2005). The efficacy of Schroth's 3-dimensional exercise therapy in the treatment of adolescent idiopathic scoliosis in Turkey. *Neurosciences Journal*, 10(4), 277-283.

Padua R, Padua S, Aulisa L, et al. Patient Outcomes After Harrington Instrumentation for Idiopathic Scoliosis: A 15- to 28-Year Evaluation. *Spine*. 2001;26(11):1268-1273.

Parent, S., Newton, P. O., & Wenger, D. R. (2005). Adolescent idiopathic scoliosis: etiology, anatomy, natural history, and bracing. *Instr Course Lect*, 54, 529-536.

Parent, S., Newton, P. O., & Wenger, D. R. (2004). Adolescent idiopathic scoliosis: etiology, anatomy, natural history, and bracing. *Instructional course lectures*, 54, 529-536.

Park, J. H., Jeon, H. S., & Park, H. W. (2018, Jun). Effects of the Schroth exercise on idiopathic scoliosis: a meta-analysis. *Eur J Phys Rehabil Med*, 54(3), 440-449.  
<https://doi.org/10.23736/s1973-9087.17.04461-6>

Patias, P., Grivas, T. B., Kaspiris, A., Aggouris, C., & Drakoutos, E. (2010). A review of the trunk surface metrics used as Scoliosis and other deformities evaluation indices. *Scoliosis*, 5(12), 1748-7161.

Pearsall, D., Reid, J., & Hedden, D. (1992). Comparison of three noninvasive methods for measuring scoliosis. *Physical Therapy*, 72(9), 648-57.

Pehresson A., Danielsson A. & Nachemson A. (2001). Pulmonary function in adolescent idiopathic scoliosis: a 25 year follow up after surgery or start of brace treatment. *Thorax* 56:388-393.

Pehrsson, K., Larsson, S., Oden, A. & Nachemson, A. (1992). Long-term follow-up of patients with untreated scoliosis A study of mortality, causes of death, and symptoms. *Spine*,

17(9), 1091-1096.

- Peltonen, J., Poussa, M., & Ylikoski, M. (1988). Three-year results of bracing in scoliosis. *Acta orthopaedica Scandinavica*, 59(5), 487-490.
- Penha, P. J., Baldini, M. & João, S. M. A. (2009). Spinal postural alignment variance according to sex and age in 7-and 8-year-old children. *Journal of manipulative and physiological therapeutics*, 32(2), 154-159.
- Penha, P. J., João, S. M. A., Casarotto, R. A., Amino, C. J., & Penteado, D. C. (2005). Postural assessment of girls between 7 and 10 years of age. *Clinics*,60(1), 9-16.
- Penha, P. J., Penha, N. L. J., De Carvalho, B. K. G., Andrade, R. M., Schmitt, A. C. B., & João, S. M. A. (2017). Posture alignment of adolescent idiopathic scoliosis: photogrammetry in scoliosis school screening. *Journal of manipulative and physiological therapeutics*, 40(6), 441-451.
- Perie, D., De Gauzy, J. S., & Hobatho, M. C. (2002). Biomechanical evaluation of Cheneau-Toulouse-Munster brace in the treatment of scoliosis using optimisation approach and finite element method. *Medical and Biological Engineering and Computing*, 40(3), 296-301.
- Périé, D., Aubin, C. E., Petit, Y., Labelle, H., & Dansereau, J. (2004). Personalized biomechanical simulations of orthotic treatment in idiopathic scoliosis. *Clinical Biomechanics*, 19(2), 190-195.
- Pham, V. M., Houilliez, A., Schill, A., Carpentier, A., Herbaux, B., & Thevenon, A. (2008). Study of the pressures applied by a Chêneau brace for correction of adolescent idiopathic scoliosis. *Prosthetics and Orthotics International*, 32(3), 345-355.  
<https://doi.org/10.1080/03093640802016092>
- Phan, P., Mezghani, N., Nault, M. L., Aubin, C. É., Parent, S., de Guise, J., & Labelle, H. (2010). A decision tree can increase accuracy when assessing curve types according to Lenke classification of adolescent idiopathic scoliosis. *Spine*, 35(10), 1054-1059.

- Pineda, S., Bago, J., Gilperez, C., & Climent, J. M. (2006). Validity of the Walter Reed Visual Assessment Scale to measure subjective perception of spine deformity in patients with idiopathic scoliosis. *Scoliosis*, 1(1), 18.
- Pittsburgh Physical Medicine. (2023). Scoliosis and Chiropractic Care: Exploring Non-Surgical Treatment Options. Retrieved from <https://www.pittsburghphysmed.com/blog/scoliosis-and-chiropractic-care-exploring-non-surgical-treatment-options>
- Poelert, S., Valstar, E., Weinans, H., & Zadpoor, A. A. (2013). Patient-specific finite element modeling of bones. Proceedings of the Institution of Mechanical Engineers, Part H: *Journal of Engineering in Medicine*, 227(4), 464-478.
- Price, C. T., Scott, D. S., Reed JR, F. E., & Riddick, M. (1990). Nighttime Bracing for Adolescent Idiopathic Scoliosis with the Charleston Bending Brace: Preliminary Report. *Spine*, 15(12), 1294-1299.
- Puno, R. M., An, K. C., Puno, R. L., Jacob, A., & Chung, S. S. (2003). Treatment recommendations for idiopathic scoliosis: an assessment of the Lenke classification. *Spine*, 28(18), 2102-2114.
- Qian, B., Zhao, Q., Mao, S., Qiu, Y., Jiang, J., & Zhu, F. (2010). The influence of elastic orthotic belt on sagittal profile in adolescent idiopathic thoracic scoliosis: a comparative radiographic study with Milwaukee brace. *BMC Musculoskeletal Disorders*, 11(1), 219. <https://doi.org/10.1186/1471-2474-11-219>
- Qiu, G., Li, Q., Wang, Y., Yu, B., Qian, J., Yu, K. & Lu, W. W. (2008). Comparison of reliability between the PUMC and Lenke classification systems for classifying adolescent idiopathic scoliosis. *Spine*, 33(22), E836-E842.
- Qiu G, Zhang J, Wang Y, et al. A New Operative Classification of Idiopathic Scoliosis: A Peking Union Medical College Method. *Spine*. 2005;30(12):1419-1426  
1410.1097/1401.brs.0000166531.0000152232.0000166530c.

- Qiu, G. X., Zhang, J. G., & Wang, Y. P. (2003). The PUMC operative classification system for idiopathic scoliosis. *Chinese Journal of Orthopaedics*, 1, 000.
- Raine, S. & Twomey, L. (1994). Attributes and qualities of human posture and their relationship to dysfunction or musculoskeletal pain. *Critical Reviews in Physical and Rehabilitation Medicine*, 6, 409-409.
- Raggio, C. L. (2006). Sexual dimorphism in adolescent idiopathic scoliosis. *Orthopedic Clinics*, 37(4), 555-558.
- Ramirez, N., Johnston, C. E., & Browne, R. H. (1997). The prevalence of back pain in children who have idiopathic scoliosis. *J Bone Joint Surg Am*, 79(3), 364-368. Retrieved from <https://insights.ovid.com/pubmed?pmid=9070524>.
- Reamy B. V. & Slakey, J. B. (2001). Adolescent Idiopathic Scoliosis: review and current concepts. *American Family Physician*, 64 (1): 111-116.
- Refsum, H., Næss-Andresen, C.F. & Lange, J. E. (1990). Pulmonary Function and Gas Exchange at Rest and Exercise in Adolescent Girls with Mild Idiopathic Scoliosis during Treatment with Boston Thoracic Brace, *Spine*. 15(5):420-423.
- Richards, S. & Vitale, M. (2008). Screening for Idiopathic Scoliosis in Adolescents. *The Journal of Bone and Joint Surgery American Edition*, 90: 195–198.
- Rigo, M. D., Villagrasa, M., & Gallo, D. (2010). A specific scoliosis classification correlating with brace treatment: description and reliability. *Scoliosis*, 5(1), 1-1. doi:10.1186/1748-7161-5-1
- Rigo, M., Villagrasa, M., & Gallo, D. (2009). A specific scoliosis classification correlating with brace treatment: description and reliability. *Scoliosis*, 4(Suppl 2), O23-O23. Retrieved from <http://www.ncbi.nlm.nih.gov/pmc/articles/PMC2793449/>. doi:10.1186/1748-7161-4-S2-O23

- Risser, J. C. (1957). The Iliac apophysis; an invaluable sign in the management of scoliosis. *Clinical orthopaedics*, 11, 111-119.
- Roach, J. W. (1999). Adolescent idiopathic scoliosis. *Orthopedic Clinics of North America*, 30(3): 353-365.
- Rogala E. J., Drummond D. S. & Gurr J. (1978). Scoliosis incidence and natural history: a prospective epidemiological study. *The Journal of Bone and Joint Surgery. American volume*. 60:173–6
- Ron, E. (2003). Cancer risks from medical radiation. *Health Physics*, 85(1), 47-59.
- Richards, B. S., Bernstein, R. M., D'Amato, C. R., & Thompson, G. H. (2005). Standardization of criteria for adolescent idiopathic scoliosis brace studies: SRS Committee on Bracing and Nonoperative Management. *Spine*, 30(18), 2068-2075.
- Sanders, J. O., Polly Jr, D. W., Cats-Baril, W., Jones, J., Lenke, L. G., O'Brien, M. F. & AIS Section of the Spinal Deformity Study Group. (2003). Analysis of patient and parent assessment of deformity in idiopathic scoliosis using the Walter Reed Visual Assessment Scale. *Spine*, 28(18), 2158-2163.
- Sapountzi-Krepia, D. S., Valavanis, J., Panteleakis, G. P., Zangana, D. T., Vlachogiannis, P. C., & Sapkas, G. S. (2001). Perceptions of body image, happiness and satisfaction in adolescents wearing a Boston brace for scoliosis treatment. *Journal of Advanced Nursing*, 35(5), 683-690. doi:10.1046/j.1365-2648.2001.01900.x
- Saville, B. P. (1999). *Physical testing of textiles*. Elsevier.
- Schleenbaker, R. E., & Muinous III, A. G. (1993). Electromyographic biofeedback for neuromuscular reeducation in the hemiplegic stroke patient: a metaanalysis. *Medicine*, 40536, 0284.
- ScoliCare. (2023). Scoliosis Treatments. ScoliCare Australia. Accessed July 21, 2023. <http://www.scolicare.com.au/treatments>

Scoliosis Research Society (SRS). (2023). Early onset scoliosis - treatment. Accessed Nov 25, 2023.

<https://www.srs.org/Patients/Conditions/Scoliosis/Early-Onset-Scoliosis>

Sevastik JA and Diab KM (eds). Research Into Spinal Deformities 1 (Vol.1). IOS Press, Netherlands, 1997, pp.293–296.

Seymour, R. (2002). *Prosthetics and orthotics: lower limb and spinal*. Lippincott Williams & Wilkins.

Smith, J. S., Shaffrey, C. I., Kuntz IV, C., & Mummaneni, P. V. (2008). Classification systems for adolescent and adult scoliosis. *Neurosurgery*, 63(3), A16-A24.

Spoonamore, M.J. (2024). *Scoliosis, Children's spine surgery*. USC Center for Spinal Surgery. <http://www.uscspine.com/conditions/childrens-scoliosis.cfm> Accessed 13 June 2023

Soucacos, P N, Soucacos, P K, Zacharis, K C, Beris, A E, & Xenakis, T A. (1997). Schoolscreening for scoliosis. A prospective epidemiological study in northwestern and central Greece. *The Journal of Bone and Joint Surgery. American Volume*, 79(10), 1498-503.

Student Health Service - Department of Health | The Government of the Hong Kong Special Administrative Region (2022). *Bone and Spinal Health - Scoliosis*. Accessed Jun 22, 2022.  
[https://www.studenthealth.gov.hk/english/resources/resources\\_bl/files/bl\\_scoliosis.pdf](https://www.studenthealth.gov.hk/english/resources/resources_bl/files/bl_scoliosis.pdf)

Student Health Service - Department of Health (2022). *Scoliosis* [Brochure].  
[https://www.studenthealth.gov.hk/english/resources/resources\\_bl/files/bl\\_scoliosis.pdf](https://www.studenthealth.gov.hk/english/resources/resources_bl/files/bl_scoliosis.pdf)  
Accessed Jun 22, 2022.

- Sun, X., Wu, T., Liu, Z., Zhu, Z., Qian, B., Zhu, F., Ma, W., Yu, Y., Wang, B., & Qiu, Y. (2013). Osteopenia Predicts Curve Progression of Adolescent Idiopathic Scoliosis in Girls Treated With Brace Treatment. *Journal of Pediatric Orthopaedics*, 33(4), 366-371. <https://doi.org/10.1097/BPO.0b013e31827b7b5f>
- Sung, R. Y., So, H. K., Choi, K. C., Nelson, E. A., Li, A. M., Yin, J. A., ... & Fok, T. F. (2008). Waist circumference and waist-to-height ratio of Hong Kong Chinese children. *BMC public health*, 8(1), 1-10.
- Szeinberg A, Canny GJ, Rashed N, Veneruso G, Levison H. Forced vital capacity and maximal respiratory pressures in patients with mild and moderate scoliosis. *Pediatric Pulmonology*. 1988;4(1):8-12.
- Tainfu Morning Post, (2006). Babaka: Does it work on kyphosis correction? Accessed October 30, 2019. <http://morning.scol.com.cn/2006/10/27/20061027510524444562.htm> (Tianfu Morning Post was founded on June 1, 1999. On January 1, 2020, it ceased publication. The article is no longer available.)
- Tajima, N., Watanabe, T., Takeuchi, H., Yamaguchi, I., & Fukazawa, T. (1981). New Hump Meter for measurement of the height and angle of hump in initial screening for the early detection of scoliosis. *Orthopedics & Traumatology*, 30(1), 213-217.
- The SpineCorporation Limited. (2018). SpineCor Dynamic Corrective Brace Retrieved from [www.spinecor.com](http://www.spinecor.com)
- The University of Hong Kong Faculty of Medicine. (2012). Scoliosis and its Treatment. Press Info. Accessed Aug 10 2023. <https://www.med.hku.hk/healthedu/issue7/e-issue7.pdf>
- Trobisch, P., Suess, O., & Schwab, F. (2010). Idiopathic scoliosis. *Deutsches Ärzteblatt International*, 107(49), 875.
- Ueno, M., Takaso, M., Nakazawa, T., Imura, T., Saito, W., Shintani, R., Uchida K., Fukuda M., Takahashi K., Ohtori S., Kotani T., Minami, S. (2011). A 5-year epidemiological study on the prevalence rate of idiopathic scoliosis in Tokyo: School screening of more than

250,000 children. *Journal of Orthopaedic Science*, 16(1), 1-6.

Underworks®. (2024). The details of Women's Posture Corrector and Trainer. Retrieved from <https://www.underworks.com/womens-posture-corrector-and-trainer>

Upadhyay, S. S., Nelson, I. W., Ho, E. K. W., Hsu, L. C. S., & Leong, J. C. Y. (1995). New Prognostic Factors to Predict the Final Outcome of Brace Treatment in Adolescent Idiopathic Scoliosis. *Spine*, 20(5), 537-545. <https://doi.org/10.1097/00007632-199503010-00006>

USC Center for Spinal Surgery. (2005). *Scoliosis, Children's spine surgery*. USC Center for Spinal Surgery. Accessed 13 June 2023. <http://www.uscspine.com/conditions/childrens-scoliosis.cfm>

Veldhuizen, A.G., Cheung, J., Bulthuis, G.J. & Nijenbanning, G. (2002). A new orthotic device in the non-operative treatment of idiopathic scoliosis. *Medical engineering & physics*, 24(3), pp.209-218.

Vergari, C., Ribes, G., Aubert, B., Adam, C., Miladi, L., Ilharreborde, B., Abelin-Genevois K., Rouch P. & Skalli, W. (2015). Evaluation of a patient-specific finite-element model to simulate conservative treatment in adolescent idiopathic scoliosis. *Spine Deformity*, 3(1), 4-11.

Vrtovec, T., Pernuš, F., & Likar, B. (2009). A review of methods for quantitative evaluation of spinal curvature. *European Spine Journal*, 18(5), 593-607.

Wan, J., Steele, B., Spicer, S. A., Strohsband, S., Feijó'o, G. R., Hughes, T. J., & Taylor, C. A. (2002). A one-dimensional finite element method for simulation-based medical planning for cardiovascular disease. *Computer Methods in Biomechanics & Biomedical Engineering*, 5(3), 195-206.

Wang, H. J. (2013). Posture-correcting garment [China patent]. <https://www.google.com.hk/patents/CN203303208U?cl=en>

- Wang, Z., Liu, Z., Wang, Z. & Wang, C. (2008). Development of the Personalized Finite Element Model of the Adolescent Idiopathic Scoliosis and Its Significance. *Journal of Biomedical Engineering*, 25(5), 1084-1088.
- Ward, W. T., Rihn, J. A., Solic, J. & Lee, J. Y. (2008). A comparison of the Lenke and King classification systems in the surgical treatment of idiopathic thoracic scoliosis. *Spine*, 33(1): 52-60.
- Weinstein, S. L. (1994). Adolescent idiopathic scoliosis: prevalence and natural history. *The pediatric spine: principles and practice*.
- Weinstein, S. L., Dolan, L. A., Wright, J. G., & Dobbs, M. B. (2013). Design of the Bracing in Adolescent Idiopathic Scoliosis Trial (BrAIST). *Spine*, 38(21), 1832. <https://doi.org/10.1097/01.brs.0000435048.23726.3e>
- Weiss, H. R., & Goodall, D. (2008). The treatment of adolescent idiopathic scoliosis (AIS) according to present evidence. A systematic review. *European Journal of Physical and Rehabilitation Medicine*, 44(2): 177-193.
- Weiss, H. R., & Werkmann, M. (2012). Soft braces in the treatment of Adolescent Idiopathic Scoliosis (AIS)—Review of the literature and description of a new approach. *Scoliosis*, 7(1), 1-11.
- Weiss HR, Werkmann M. (2010). ""Brace Technology"" Thematic Series – The ScoliOlogiC(R) Cheneau light brace in the treatment of scoliosis. *Scoliosis*. 5:19.
- Weiss, H. R., Werkmann, M., & Stephan, C. (2007). Brace related stress in scoliosis patients—Comparison of different concepts of bracing. *Scoliosis*, 2, 1-6.
- Wiley, J. W., Thomson, J. D., Mitchell, T. M., Smith, B. G., & Banta, J. V. (2000). Effectiveness of the Boston brace in treatment of large curves in adolescent idiopathic scoliosis. *Spine*, 25(18), 2326-2332.

- Willner, S. (1979). Moire topography for the diagnosis and documentation of scoliosis. *Acta Orthopaedica Scandinavica*, 50(3), 295-302.
- Wong, H., Hui, J., Rajan, U., & Chia, H. (2005). Idiopathic scoliosis in Singapore schoolchildren: A prevalence study 15 years into the screening program. *Spine*, 30(10), 1188-96.
- Wong, H. K., & Tan, K. J. (2010). The natural history of adolescent idiopathic scoliosis. *Indian journal of orthopaedics*, 44(1), 9.
- Wong, M. S., Cheng, C. Y., Lam, T. P., Ng, K. W., Sin, S. W., Lee-Shum, L.F., Chow, H. K. & Tam, Y.P. (2008). The Effect of Rigid Versus Flexible Spinal Orthosis on the Clinical Efficacy and Acceptance of the Patients With Adolescent Idiopathic Scoliosis. *SPINE*, 33 (12), 1360-1365.
- Wong, M. S., Mak, A. F., Luk, K. D., Evans, J. H. & Brown, B. (2001). Effectiveness of audio-biofeedback in postural training for adolescent idiopathic scoliosis patients. *Prosthetics and Orthotics International*, 25, 60-70.
- Wong, M. S., Mak, A. F. T., Luk, K. D. K., Evans, J. H., & Brown, B. (2000, 2000/08/01). Effectiveness and biomechanics of spinal orthoses in the treatment of adolescent idiopathic scoliosis (AIS). *Prosthetics and Orthotics International*, 24(2), 148-162. <https://doi.org/10.1080/03093640008726538>
- Wong, M. S., Cheng, J. C. Y., Lam, T. P., Ng, B. K. W., Sin, S. W., Lee-Shum, S. L. F., Chow, D. H. K., & Tam, S. Y. P. (2008). The effect of rigid versus flexible spinal orthosis on the clinical efficacy and acceptance of the patients with adolescent idiopathic scoliosis. *Spine*, 33(12), 1360. <https://doi.org/10.1097/BRS.0b013e31817329d9>
- Wong, S. H. (2021). *Design and development of anisotropic textile brace for adolescent idiopathic scoliosis (AIS)*. [Master's dissertation.] Institute of Textiles and Clothing, The Hong Kong Polytechnic University. <https://theses.lib.polyu.edu.hk/handle/200/11299>

- Wong, W. Y., & Wong, M. S. (2008). Smart garment for trunk posture monitoring: A preliminary study. *Scoliosis*, 3(7), 1-9.
- Wybier, M., & Bossard, P. (2013). Musculoskeletal imaging in progress: the EOS imaging system. *Joint Bone Spine*, 80(3), 238-243.
- Xiong, Y., & Tao, X. (2018). Compression garments for medical therapy and sports. *Polymers*, 10(6), 663.
- Yamada, K., Yamamoto, H. I. R. O. S. H. I., Nakagawa, Y., Tezuka, A., Tamura, T., & Kawata, S. (1984). Etiology of idiopathic scoliosis. *Clinical orthopaedics and related research*, (184), 50-57.
- Yang, X., Zhang, X., Song, M. (2011). Establishment of 3-D finite element model of scoliosis and mechanical analysis. *Journal of Gansu College of Traditional Chinese Medicine*, 5, 021.
- Yip, J., Liu, P. Y., Yick, K. L., Cheung, M. C., Tse, C. Y., & Ng, S. P. (2016). Effect of a Functional Garment on Postural Control for Adolescents with Early Scoliosis: A Six-Month Wear Trial Study. In *Advances in Physical Ergonomics and Human Factors* (pp. 143-154). Springer, Cham.
- Yip, J., & Ng, S. P. (2008). Study of three-dimensional spacer fabrics: Physical and mechanical properties. *Journal of materials processing technology*, 206(1-3), 359-364.
- Yu, A., Yick, K. L., Ng, S. P., Yip, J., & Chan, Y. F. (2016). Numerical simulation of pressure therapy glove by using Finite Element Method. *Burns*, 42(1), 141-151.
- Yu, H. Q., Gu, S. X., Li, M., Ding, Z. Q., Yang, X. M., & Fang, X. T. (2008). Three-dimensional finite element model of the scoliotic spine for biomechanical study of scoliosis. *Journal of Medical Biomechanics*, 23(2), 136-139.
- Yu, W. W. (Ed.). (2016). *Advances in women's intimate apparel technology*. Woodhead

- Zabjek, K. F., Leroux, M. A., Coillard, C., Prince, F., & Rivard, C. H. (2008). Postural characteristics of adolescents with idiopathic scoliosis. *Journal of Pediatric Orthopaedics*, 28(2), 218-224.
- Zacharkow, D. (1988). Posture: sitting, standing, chair design, and exercise. (*No Title*).
- Zaina, F., Negrini, S., Atanasio, S., Fusco, C., Romano, M., & Negrini, A. (2009, 2009/04/07). Specific exercises performed in the period of brace weaning can avoid loss of correction in Adolescent Idiopathic Scoliosis (AIS) patients: Winner of SOSORT's 2008 Award for Best Clinical Paper. *Scoliosis*, 4(1), 8. <https://doi.org/10.1186/1748-7161-4-8>
- Zhang, J., Shi, X., Liang, L., Wang, X., Zhang, Y., & Guo, F. (2013). Computerized Lenke classification of scoliotic spine. 35th Annual International Conference of the IEEE EMBS, Japan.
- Zhang, J., Lou, E., Shi, X., Wang, Y., Hill, D. L., Raso, J. V., ... & Lv, L. (2010). A computer-aided Cobb angle measurement method and its reliability. *Journal of spinal disorders & techniques*, 23(6), 383-387.
- Zheng, Y. P., Mak, A. F., & Leung, A. K. (2001). State-of-the-art methods for geometric and biomechanical assessments of residual limbs: a review. *Journal of rehabilitation research and development*.
- Zhou, S. H., Guo, P., & Stolle, D. F. (2018). Interaction model for “shelled particles” and small-strain modulus of granular materials. *Journal of Applied Mechanics*, 85(10), 101001.